PB 184652

STUDY OF THE APPLICABILITY OF PHYSICAL METHODS OF SEPARATION TO THE DEVELOPMENT OF NEW PROCESSES FOR THE CONTROL OF SULFUR DIOXIDE POLLUTION

J. R. Hamm, et al

National Center for Air Pollution Control
Public Health Service
Department of Health, Education, and Welfare

Final Report
Period Ending January 31, 1969
Contract No. PH-22-68-34

January 31, 1969

Reproduced by the
CLEARINGHOUSE
for Federal Scientific & Technical
Information Springfield Va. 22151

277

STUDY OF THE APPLICABILITY OF PHYSICAL METHODS OF SEPARATION TO THE DEVELOPMENT OF NEW PROCESSES FOR THE CONTROL OF SULFUR DIOXIDE POLLUTION

J. R. Hamm, et al

National Center for Air Pollution Control
Public Health Service
Department of Health, Education, and Welfare

Final Report
Period Ending January 31, 1969
Contract No. PH-22-68-34

January 31, 1969

TABLE OF CONTENTS

Page

1. Summary 1-1

2. Introduction 2-1

3. Feasibility Analyses of Physical Methods of Separating SO_2 from Flue Gas 3-1

   3.1 Gaseous Diffusion 3-1

      3.1.1 Porous Barrier 3-1
      3.1.2 Mass Diffusion 3-15

   3.2 Membrane Separation 3-19

      3.2.1 Silicone Rubber Membrane 3-19
      3.2.2 Immobilized Liquid Film 3-28

   3.3 Centrifugation 3-30

   3.4 Condensation 3-86

   3.5 Mass Spectrometry 3-95

   3.6 Magnetic Effects 3-98

   3.7 Electromagnetic Excitation 3-108

   3.8 Electrical Excitation 3-124

   3.9 Nuclear Radiation Excitation 3-129

   3.10 Vortex Tube 3-132

4. Conclusions 4-1

5. Recommendations 5-1

6. Appendices

   6.1 Bibliographies 6-1

   6.2 Theory of Cascade Design Modified for SO_2 Removal Application 6-26

   6.3 Mechanical Design of High Speed Centrifuges 6-55

   6.4 Properties of Materials 6-62

      6.4.1 Data on Glass Fibers & Resins 6-62
      6.4.2 Data on Titanium Alloys 6-64
      6.4.3 Data on Maraging Steel 6-65

Page

6.5 Cost Estimates of Components for Centrifuge Cascade System 6-75

6.5.1 Derivation of Centrifuge Bearing Power Loss Equation 6-75
6.5.2 Estimate of the Cost of Materials used in Fabricating Centrifuges 6-83
6.5.3 Estimates of the Cost of Bearings for Gas Separation Centrifuges 6-85
6.5.4 Estimate of Vacuum Chamber Costs 6-89

6.6 Survey of Methods of Recovery of Sulfur as a By-Product 6-93

6.7 Communication from Oak Ridge National Laboratory 6-108

6.8 Saturation Properties for SO_2 and CO_2 6-111

LIST OF TABLES

Table		Page
3.1	Design and Cost Data for Porous Barrier Separation	3-13
3.2	Design and Cost Data for Silicone Rubber Membrane Separation	3-25
3.3	Flue Gas Composition Used in Centrifugation Analysis	3-33
3.4	Molecular Structure and Rotational g_J Factors for Some Effluent Gases	3-106
3.5	Absorption Regions of Flue Gas Components	3-121
3.6	Some Characteristics of Spectral Sources	3-122
6.1	Market Prices of Sulfur Compounds	6-93

LIST OF FIGURES

Figure		Page
3.1	Gaseous Diffusion Cascade	3-10
3.2	Separative Duty vs % SO_2 in Product Stream	3-11
3.3	Separative Duty vs SO_2 in Waste Stream	3-12
3.4	Mass Diffusion Cascade	3-18
3.5	Process Depicting the Use of Steam in Membrane Separation of SO_2 from Flue Gas	3-26
3.6	Equilibrium Separation Factor vs Centrifuge Peripheral Velocity	3-57
3.7	Minimum Number of Stages in a Cascade of Centrifuges	3-58
3.8	Maximum Separative Capacity Per Foot Length of Centrifuge vs Peripheral Velocity	3-59
3.9	The Martin Profile Used to Calculate the Flow Pattern Efficiency	3-60
3.10	Flow Pattern Efficiency for the Martin Profile vs Peripheral Velocity	3-61
3.11	Separative Efficiency vs Peripheral Velocity	3-62
3.12	Actual Separative Capacity Per Foot Length of Centrifuge vs Peripheral Velocity	3-63
3.13	Total Length of Centrifuges vs Product Concentration	3-64
3.14	Total Length of Centrifuges vs Peripheral Velocity	3-65
3.15	Tangential Stress in Centrifuge vs Peripheral Velocity	3-66
3.16	Bearing Power Requirements, CS Glass Centrifuge	3-67
3.17	Capital Cost Equivalent of Bearing Energy Losses, CS Glass Centrifuge	3-68

Figure Page

3.18 Bearing Costs, CS Glass Centrifuge Cascade 3-69

3.19 Material Costs, CS Glass Centrifuge Cascade 3-70

3.20 Vacuum Chamber Costs, CS Glass Centrifuge Cascade 3-71

3.21 Partial Costs of Centrifuge Cascade System, CS Glass 3-72

3.22 Bearing Power Requirements, S Glass Centrifuge 3-73

3.23 Capital Cost Equivalent of Bearing Energy Losses, S Glass Centrifuge 3-74

3.24 Bearing Costs, S Glass Centrifuge Cascade 3-75

3.25 Material Costs, S Glass Centrifuge Cascade 3-76

3.26 Vacuum Chamber Costs, S Glass Centrifuge Cascade 3-77

3.27 Partial Costs of Centrifuge Cascade System, S Glass 3-78

3.28 Bearing Power Requirement for a Cascade of Centrifuges Made of Titanium 3-79

3.29 Partial Cost of Centrifuge Cascade System, Ti-3Al-13V-11 Cr 3-80

3.30 Partial Cost of Centrifuge Cascade System, Ti-6Al-4V 3-81

3.31 Bearing Power Requirements for a Cascade of Centrifuges Made of 18% Ni Maraging Steel 3-82

3.32 Partial Cost of Centrifuge Cascade System, 18% Ni Maraging Steel 3-83

3.33 Flow Diagram for SO_2 Removal by Condensation Using Cryogenic Refrigeration 3-92

3.34 Flow Diagram for SO_2 Removal by Condensation Using the Joule-Thompson Effect 3-93

3.35 Flow Diagram for SO_2 Removal by Condensation Using an Expansion Turbine 3-94

3.36 Chemical Kinetics of Vibrationally Excited Molecules 3-112

3.37 Relaxation Path for SO_2 Vibrational Energy 3-115

Figure		Page
3.38	Vortex Tube Model for Cooling	3-138
3.39	Ratio of Peripheral to Core Pressure in Vortex Tube	3-139
3.40	Ratio of Temperature Change in Vortex Tube to Inlet Gas Temperature	3-140
3.41	Vortex Tube Model for Separation	3-141
6.1	Heads Flow Rate vs Stage Number in an Ideal Cascade	6-40
6.2	Separation Potential in Cascade Design Theory	6-49
6.3	Virgin Glass Filament Tensile Strength at Various Temperatures	6-69
6.4	Single Glass Fiber Modulus of Elasticity	6-70
6.5	Effect of Soaking at Elevated Temperature on the Strength of Glass Filament Reinforced Plastic Composite Material	6-71
6.6	Strength Characteristics of Titanium Alloy Ti-13V-11Cr-3Al Heat Treated	6-72
6.7	Strength Characteristics of Titanium Alloy Ti-6Al-4V	6-73
6.8	Tensile Modulus of Titanium Alloys vs Temperature	6-74
6.9	Ratio of Centrifuge Diameter to Length for Titanium Alloys	6-75
6.10	Tensile Strength of 18% Ni Maraging Steel vs Temperature	6-76
6.11	Ratio of Centrifuge Diameter to Length for 18% Ni Maraging Steel	6-77
6.12	Ratio of Flow to Length vs Peripheral Velocity for a Centrifuge with a Martin Profile	6-84
6.13	Estimated Cost of Tilting Pad Journal Bearings	6-90
6.14	Estimated Cost of Bearings for Centrifuges for 500 mw Power Plant	6-91
6.15	Estimated Cost of Cylindrical Vacuum Chamber for Centrifuges	6-95
6.16	Flow Sheet of Sulphidine Process	6-106
6.17	Flow Sheet of ASARCO Process	6-106

Figure		Page
6.18	Flow Sheet of COMINCO Process	6-107
6.19	Flow Sheet of Original Chamber Process	6-107
6.20	Flow Sheet of American Type Badische Contact Unit	6-108
6.21	Simplified Flow Diagram of ASARCO Process	6-109
6.22	Flow Sheet of Alkalized Alumina Process	6-109
6.23	Saturation Pressure vs Temperature for SO_2	6-114
6.24	Saturation Pressure vs Temperature for CO_2	6-115

1. SUMMARY

The Westinghouse Electric Corporation Research Laboratories ~~has completed~~ a feasibility study was made of the use of physical methods for separating SO_2 from flue gas. Thi~~s~~e study included both direct removal techniques and physical techniques for converting SO_2 to a more easily removable form such as SO_3.

It was found to be technically feasible to directly separate SO_2 from flue gas by gaseous diffusion, permeation, centrifugation, mass spectrometry, vortex tube, and Joule-Thompson condensation. Condensation by surface heat exchangers or by the use of an expansion turbine does not appear to be technically feasible because of operating problems.

The conversion of SO_2 to SO_3 by electrical excitation ~~has been~~ was demonstrated to be technically feasible and there are indications that such conversion could also be accomplished by electromagnetic excitation and nuclear radiation excitation.

It was found that a magnetic field selectively affects the molecular diffusivity of different molecular species. However, at the pressures considered for this application, extremely strong magnetic fields would be required to get a slight effect.

All of the processes for direct separation of SO_2 which were found to be technically feasible were found not to be economically feasible by a substantial margin, and the physical processes for conversion of SO_2 to SO_3 were shown to have minimum (theoretical) energy requirements which were excessive.

It is recommended that no further work be done in the area of physical separation of SO_2 from flue gas

2. INTRODUCTION

The Westinghouse Electric Corporation Research Laboratories has completed a technical and economic feasibility study of the use of physical methods for removing SO_2 from flue gas under Contract PH-22-68-34. The work statement for this study included evaluation of both direct removal processes and processes for converting the SO_2 to more easily removable forms and a survey of by-product recovery processes.

The specifications for this study were that the concentration of SO_2 in the flue gas should be 3000 ppm and that the sulfur removal should be 90% for moderate sized plants and 95% for large sized plants. The flue gas pressure was assumed to be 1 atmosphere and the temperature 300-400°F.

The study team at the Westinghouse Research Laboratories was as follows:

Selective Diffusion and Permeation	Dr. W. J. Rebello
Centrifugation and Vortex Tube	Mr. J. R. Hamm Mr. A. Hagg Mr. J. Akey
Condensation	Dr. W. J. Rebello Mr. Norman Farquhar*
Mass Spectrometry	Mr. W. M. Hickam
Magnetic Field Effects	Dr. J. D. Feichtner
Electrical Excitation	Dr. Martin Nahemow
Electromagnetic Excitation	Dr. J. D. Feichtner
Nuclear Radiation Excitation	Dr. K. H. Sun

Assistance in the analysis of porous barrier gaseous diffusion and separation by permselective membranes was given by the Oak Ridge National Laboratory at Oak Ridge, Tennessee. Consultation on the mechanical design of filament wound glass-resin composite materials was obtained from the Brunswick Corporation of Lincoln, Nebraska. Data on materials of construction were obtained from the following companies.

---

* Waltz Mills

Owens Corning Fiberglas Corp.
Dow Chemical Co.
Dow Corning Corp.
Union Carbide Corp.
Koppers Company, Inc.

3. FEASIBILITY ANALYSIS OF THE PHYSICAL METHODS OF SEPARATING SULFUR DIOXIDE FROM FLUE GAS

3.1. Gaseous Diffusion

3.1.1. Porous Barrier

Gaseous diffusion is a separation process which depends on the phenomenon of molecular effusion through a porous barrier and is usually performed in a large number of stages called a cascade. In each stage the feed gas, a mixture of two or more gases, is forced through a porous barrier with pore sizes of the order of the mean free path of molecules. Thus bulk flow through the barrier is prevented, though individual molecules may escape through the barrier. The kinetic energy of the molecules being independent of the molecular masses, the average velocity of the lighter molecules will be higher resulting in a preferential flow of the lighter molecules through the barrier. The enriched or heads fraction is fed to the stage above while the stripped or tails fraction is fed to the stage below. Hence the feed for each stage consists of the heads and tails fraction from its neighboring stages. A gaseous diffusion cascade is depicted in Figure 3.1. The entire theory of Cascade Design has been presented in Section 6.3 of this report and will not be detailed here.

The most important successful application of gaseous diffusion to date is the separation of isotopes of uranium, and plants are in operation in the U. S., Britain, France, and the U.S.S.R. The only other large-scale operation using a metallic barrier is in hydrogen purification[1] where hydrogen diffuses through a palladium foil in a one-step separation process. The main reason for the lack of gaseous diffusion plants on a commercial scale is the unfavorable economics especially when a large number of stages are necessary. In this evaluation of a gaseous diffusion plant for the separation of SO_2 from the flue gas, the assumptions and important design parameters will be discussed briefly before the results are presented.

Flue Gas Composition

The flue gas flow rate selected for the design calculations is 10^6 SCFM which corresponds approximately to a 500 MW power plant. As the effect of water vapor present in the flue gas on the permeability of the barrier is not known, it is assumed that the flue gas is dry with the following volumetric analysis: N_2 - 80.8%, CO_2 - 15.9%, O_2 - 3.0%, and SO_2 - 0.3%. The flue gas is assumed to be devoid of particulate matter. Room temperature is assumed throughout the cascade.

Flow Mechanism Through the Barrier

In the ideal case, if the barrier pores are small compared to the mean free path of the gas molecules, the flow is by effusion only. In the case of Knudsen flow, the controlling factor is the molecular weights of the component gases. In practice, because of the non-uniformity of the pore sizes, all the flow is not molecular and a non-separative Poiseuille flow occurs. In addition, adsorptive or surface flow is of importance. It has been demonstrated experimentally[2] that carbon dioxide and propane can be effectively separated in flow through porous Vycor glass even though they have essentially the same molecular weight. Propane passed through the barrier at a faster rate because of adsorptive flow. In general, components with a higher critical temperature exhibit a greater amount of surface flow. In isotope separation, since both molecules have similar physicochemical properties, there will be negligible differences in surface flow characteristics even though the separation is inhibited. However, in this case, the SO_2 with a higher molecular weight and critical temperature will flow preferentially through the barrier, due to surface flow counteracting the effect of Knudsen flow. Since surface flow properties for the gases and barrier materials concerned are not readily available, surface flow will be neglected in this analysis. In any event, this assumption will result in an optimistic design.

Choice of Operating Pressures

The operating pressures have an effect on the separation effectiveness, power consumption and capital costs. An increase in the upstream pressure reduces the proportion of Knudsen flow across the barrier and hence decreases the separation effectiveness. An increase in the downstream pressure has a likewise effect by increasing the back diffusion. On the other hand, an increase in the upstream pressure reduces the size of the equipment and reduces the capital cost. The total electric power is directly proportional to the pressures via the compression ratio and indirectly via the separation factor. It has been shown(3) that, for a constant upstream pressure, the pumping power per unit separative power passes through a minimum at a compression ratio of about 3 and slowly increases with increasing compression ratio. The pressure ratio chosen in practice is usually greater than this minimum value because of pressure drops in the stage cooler and pipework and also because of the fewer stages and hence lower capital costs associated with larger compression ratios.

For this study, an upstream pressure of 1 atm. and a compression ratio of 5 have been selected.

Barrier Characteristics

The most important component of a gaseous diffusion stage is the porous barrier. For successful operation, the barrier must be fine-pored with an extremely small thickness and yet possess mechanical strength. The pore diameters should be at least of the order of the mean free path of the gas molecules, and the number of pores per unit area should be large so as to reduce the total barrier area required. Information on barrier design and properties is relatively scarce because of the sensitive nature of their application. Several papers on barrier characteristics have been presented at the Second United Nations International Conference on the Peaceful Uses of Atomic Energy, Geneva, 1958.(4-7)

Barriers are characterized by their mean pore radius, r, in Å and by their permeability G, which is usually expressed in terms of the number of moles of air passing through 1 cm^2 of surface per minute and per cm Hg of pressure difference under conditions of molecular flow. Other characteristics of importance are the lifetime and mechanical resistance which are more difficult to evaluate quantitatively. The permeability G is very nearly inversely proportional to the thickness while the upstream pressure is roughly inversely proportional to r. The quantity G/r is in practice limited by the physical conditions of maximum porosity and minimum thickness and thus it is advantageous to choose a barrier with as large a value of G/r as its mechanical strength allows. Operation at higher upstream pressures would reduce the equipment size and capital costs but would require a smaller pore radius. In practice the minimum mean pore radius is fixed at about 100 Å.

Barriers can be classified as 'simple barriers,' characterized by a structure independent of the thickness or 'composite barriers,' composed of a very permeable support without separative action, and a thin layer having a small pore radius. The two principal methods of preparation of porous barriers are: a) treatment of an originally non-porous barrier; b) agglomeration or fritting of submicronic grains. An example of a barrier of type 'a' is the anodic oxidation of an aluminum foil in a bath containing sulfuric or oxalic acid. Barriers prepared in this way, while they can withstand only weak bending, can be used with pressure differences of more than an atmosphere if properly supported. Barriers of type 'b' may be obtained by fritting finely powdered alumina or nickel at high temperatures or by rolling a teflon emulsion on a metal mesh. The choice of barrier materials for isotope separation is based primarily on their resistance to the corrosive action of UF_6.

For the purpose of design calculations for the SO_2 Removal Problem, a Fritted Alumina Barrier No. 1864 has been selected from the publication of Massignon.(4) The pore diameter of this barrier is 0.06μ which is approximately the mean free path of nitrogen at 60 F and one atmosphere. Other properties of interest are the Permeability,G = 220 x 10^{-7} g moles/cm^2min(CmHg) and the Porosity of 0.55.

The Stage Separation Factor

The ideal point separation factor, α^*, is a measure of the degree of separation obtained when a binary mixture flows through an ideal barrier with zero back pressure and can be shown to be equal to the square root of the molecular weights:

$$\text{In this case } \alpha^* = \sqrt{M_{SO_2}/M_{AVE.}} = \sqrt{\frac{64}{29.5}} = 1.475 \quad . \qquad (3.1)$$

The actual stage separation factor, α, differs from this because of the following factors:

1. The Barrier Efficiency Factor - This factor takes into account Poiseuille Flow which is not separative and the finite pressure of operation at which the Knudsen flow is not ideal.

2. The Back Pressure Efficiency Factor - With a finite back pressure the lighter component would also effuse back through the barrier. In this analysis the pressures on both sides of the barrier are 1 atm. and 0.2 atm. respectively.

3. The Mixing Efficiency Factor - During the flow of gas on the high pressure side of the barrier, the gas next to the barrier surface becomes depleted in the lighter component. This results in a concentration gradient perpendicular to the barrier so that the effective enrichment coefficient is smaller than that obtained by considering the average concentration of lighter component in the gas stream. This factor can be calculated by considering diffusion through an effective film representing the resistance to diffusion.

4. The Cut Correction Factor - The cut correction takes into account the fact that the concentrations of the desired component on either side of the barrier are changing as the gas flows through the stage. In this case, the exit or stream concentration of the stage upflow is equal to the average concentration of the effused gas, while the exit or stream concentration of the down flow is equal to the terminal concentration of the uneffused gas which is at maximum and not average

depletion. Therefore, the stage separation factor relating to the exit concentration is greater than the point separation factor and the cut correction factor exceeds unity.

The cut correction $E_c = \frac{1}{\theta} \ln \frac{1}{1-\theta}$

where θ is the cut.

For the SO_2 separation problem, θ has been selected as 0.5, resulting in a cut correction factor of 1.386.

The Barrier Separation Efficiency, S, which takes into account the first three of the above factors, has been determined for the Fritted Alumina Barrier No. 1864 by the method of Massignon.(4)

An approximate expression for the separation effectiveness has been developed by Massignon(8) and given below

$$S(P_F, KP_F) = (1-K)2^{-(1-0.95K)P_F/P_o} \tag{3.2}$$

where K = ratio of the back and high pressures P_B/P_F

P_o = reference pressure given by

$$P_o = \left(\frac{2 \log 2}{A + B}\right)\frac{1}{r_{sep}} \tag{3.3}$$

where r_{sep} = effective separation radius of a real barrier

$$A = \frac{3}{16\eta} \left(\frac{\pi M_2}{8 RT}\right)^{1/2} \tag{3.4}$$

$$B = \frac{8}{3} \left(\frac{1}{2\pi RT}\right)^{1/2} \frac{RT}{PD_{12}} \left(\frac{1}{M_1 M_2}\right)^{1/2} x$$

$$[N(M_1)^{1/2} + (1-N)(M_2^{1/2})] \tag{3.5}$$

The parameters A and B are expressed in terms of the masses M_1 and M_2 ($>M_1$) of the two gases in a binary mixture, their concentrations N and (1-N), their mutual diffusion coefficient D_{12} and their viscosity η.

From Equations (3.2) and (3.3), for the case of a measurement of S with zero back pressure,

$$r_{sep} = \frac{-2 \log S(P_F,0)}{(A + B)P_F} \qquad (3.6)$$

The separation radius is defined in terms of the slope of the straight line which represents the behavior of log S as a function of P_F. In order to account for the noncircular cross section and crookedness of the pores, the terms A and B in Equation (3.6) may be replaced by

A by $A\ k_K/k_P$

B by B/k_K

where k_K and k_P are shape factors determined experimentally.

In this analysis, the values of r_{sep}, k_K and k_P for the Fritted Alumina Barrier No. 1864 were taken from Massignon,$^{(4)}$ and computations made using the above equations assuming a binary mixture of N_2 and SO_2. The computations resulted in a value of S(1 atm., 0.2 atm.) = 0.407.

$$\begin{aligned} \therefore\ (\alpha-1) &= SE_c(\alpha^*-1) \\ &= 0.407 \times 1.368 \times 0.475 \\ &= 0.268 \\ \therefore\ \alpha &= 1.268 \end{aligned}$$

Thus the actual stage separation factor, α, is 1.268.

Results

The design calculations have been performed for an ideal close-separation cascade since $\alpha - 1 < 1$. The equations used may be referred to in Section 6.2, and the results are depicted in Figures 3.2 , 3.3 and Table 3.1 . It may be mentioned here that in the separation of SO_2 from flue gas, the enriched stream may logically be called the waste and the depleted stream the product. However, in this case, convention will be followed and the stream enriched in SO_2 will be called the product.

Figure 3.2 is a plot of the Separative Duty (D) and the percentage of SO_2 in the product. The separative duty is a measure of the magnitude of the separation job. In the case of the ideal cascade, the total flow rate, the total pump capacity, the total power demand, and the total barrier area are all proportional to the separative duty. It is therefore interesting to note from Figure 3.2 that the separative duty is not a strong function of the SO_2% in the product and increases by only about 12% for an increase in the SO_2 concentration in the product from 5% to 90%. The curve is based on a 95% removal of SO_2 from the flue gas. (i.e. $x_w = 0.00015$)

Figure 3.3 is a plot of the Separative Duty versus the % Removal of SO_2 from the flue gas and indicates that the cost of separative work depends strongly on the waste composition or % of SO_2 removal. As the SO_2 concentration in the waste approaches zero, i.e., for 100% Removal of SO_2, the cost of separative work increases without limit. In fact, the increase in SO_2 removal from flue gas from 90% to 95%, results in a 23% increase in the cost of separative work.

The results of the design calculations are listed in Table 3.1. In column 1 are values for 95% removal of SO_2 from the flue gas with an SO_2 concentration in the product of 20%. The value of x_P of 0.20 was chosen arbitrarily since most commercial processes for the recovery of sulfur require an SO_2 concentration from 5% to 20%. In Column 3 are the design and costs calculations made by Mr. S. Blumkin of the Oak Ridge Gaseous Diffusion Plant using existing computer programs. A copy of the preliminary design and cost calculations performed by Oak Ridge National Laboratory is attached in the Appendix 6.7. Column 2 represents the results for the Fritted Alumina Barrier with parameters chosen so as to provide a ready comparison between these calculations and the Oak Ridge results.

It may be observed from Columns 1 and 2 that an increase in percent SO_2 removal from 88.7% to 95% results in a substantial increase in barrier area and Compressor Power. With power requirements of about 20 million H.P., compressor costs alone would be several times the capital costs of a 500 MW fossil-fuel fired power plant. No attempt was made to ascribe a value for the barrier costs as accurate cost data was not available. In comparing these calculations with the Oak Ridge values, the differences in Barrier area between Columns 2 and 3 are due partly to the chosen value of the cut. The Oak Ridge design estimates capital costs of $\$ 390 \times 10^6$ or about $650 per KW.

Any process for SO_2 separation from flue gases must have favorable economics. These preliminary investigations indicate that the costs would be prohibitive. The only commercial application of gaseous diffusion process is the one step hydrogen-diffusion process through a palladium barrier. Even with barriers of high permeabilities, a large reduction in the number of stages and barrier area cannot be expected. With the large flow rates involved compressor power costs could not be appreciably reduced. Therefore it may be concluded that, with these unfavorable economics, the gaseous diffusion process can be eliminated from consideration for the removal of SO_2 from the flue gas.

Dwg. 858A357

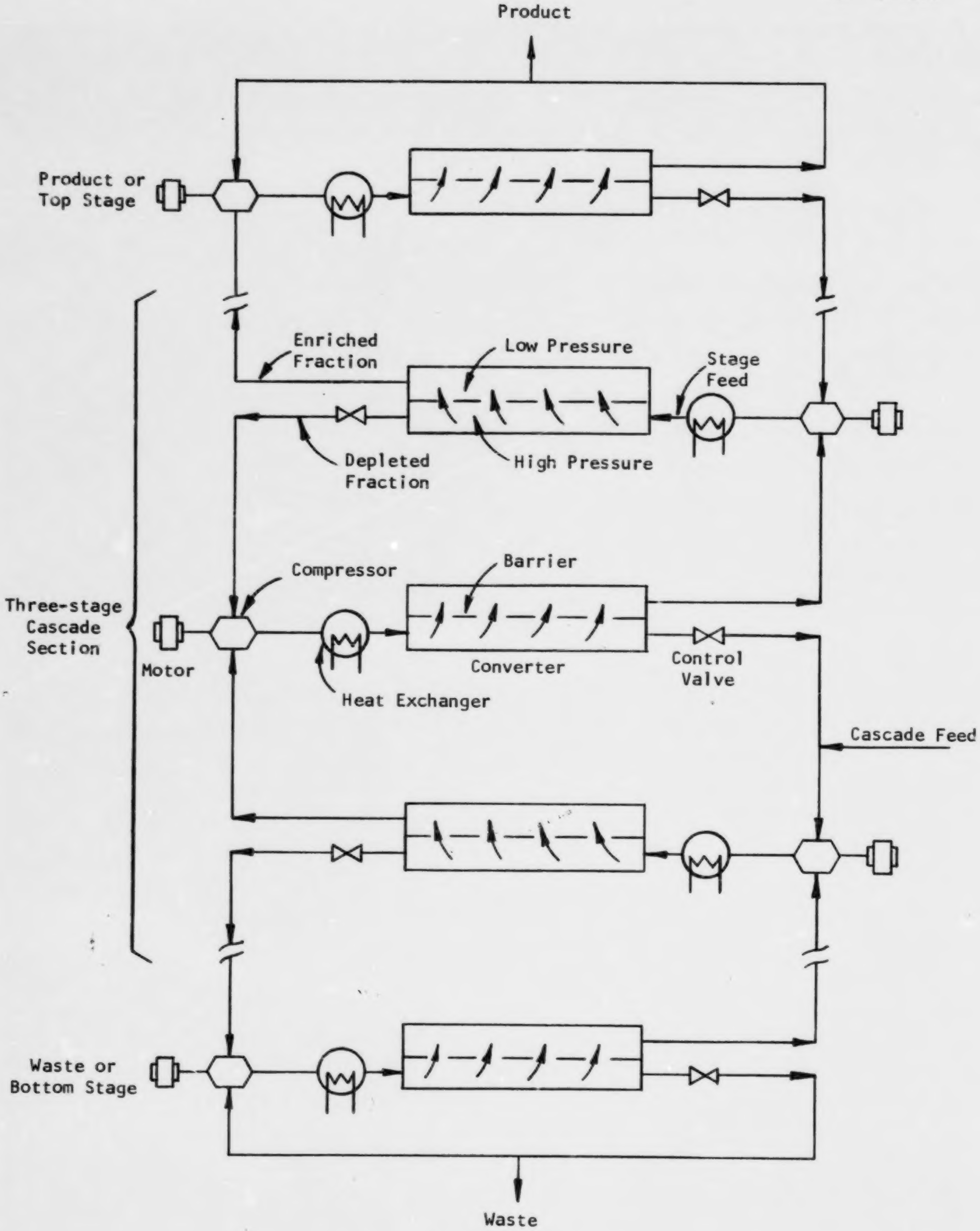
Product
Product or Top Stage
Three-stage Cascade Section
Enriched Fraction
Low Pressure
Stage Feed
Depleted Fraction
High Pressure
Compressor
Barrier
Motor
Converter
Control Valve
Heat Exchanger
Cascade Feed
Waste or Bottom Stage
Waste

Fig. 3.1—A gaseous diffusion cascade

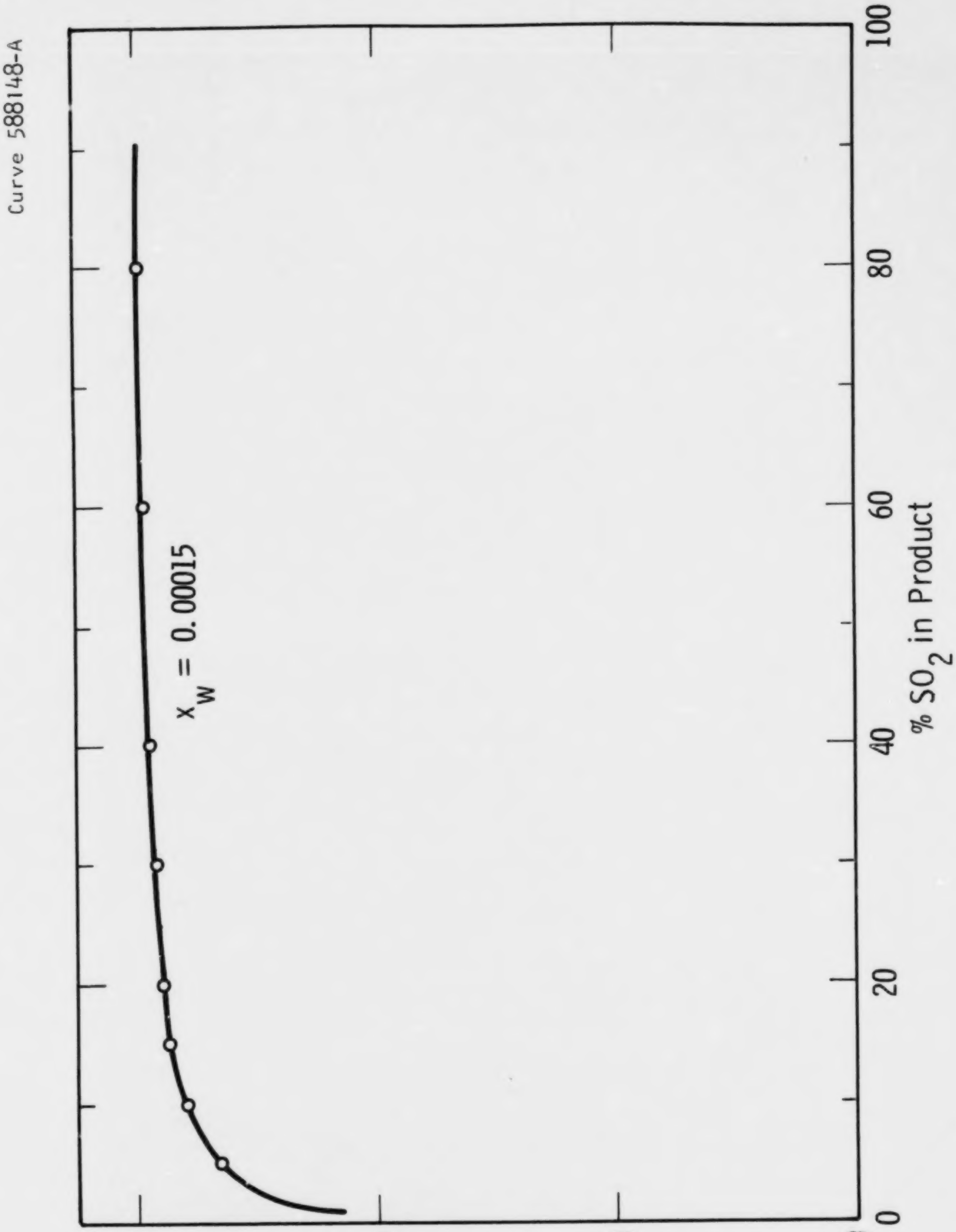

Fig. 3.2—Separative duty vs % SO_2 in product

Curve 588149-A

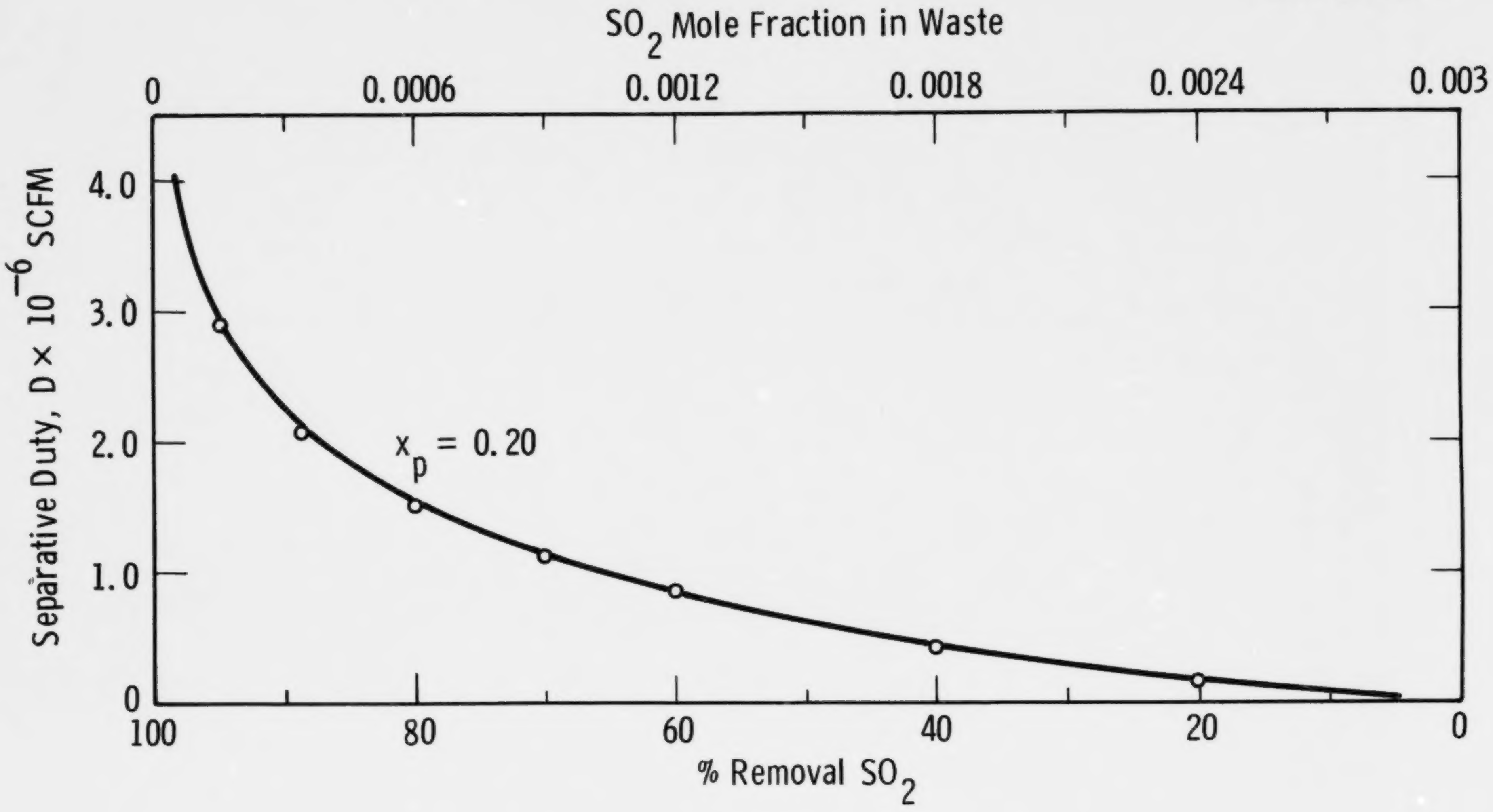

Fig. 3.3—Separative duty vs SO_2 in waste

TABLE 3.1 - DESIGN AND COST DATA

		1	2	3
		Fritted Alumina Barrier (Ref.3)	Fritted Alumina Barrier (Ref.3)	Oak Ridge Design
Barrier Properties				
Pore Radius μ		0.03	0.03	Unknown
Porosity		0.55	0.55	Unknown
Permeability G	$\frac{\text{moles}}{\text{cm}^2\text{min(cmHg)}}$	220×10^{-7}	220×10^{-7}	Unknown
Ideal Separation Factor α^*		1.475	1.475	1.475
Actual Separation Factor α		1.268	1.268	Unknown
Feed Rate	SCFM	10^6	10^6	10^6
Product Rate (Stream Enriched in SO_2)	SCFM	14,300	5,400	5,400
Cut θ		0.50	0.50	0.47
SO_2 Fraction In Feed		0.003	0.003	0.003
SO_2 Fraction In Waste		(95% Removal) 0.00015	88.7% Removal 0.00034	88.7% Removal 0.00034
SO_2 Fraction Product		0.20	0.49	0.49
Separative Duty - SCFM		2.886×10^6	2.124×10^6	2.124×10^6
Number of Stages		56	60	53
Total Upflow	SCFM	160.0×10^6	118×10^6	106×10^6
Barrier Area	Ft^2	149.3×10^6	110×10^6	94×10^6
Upstream Pressure	Atm	1.0	1.0	1.0
Downstream Pressure	Atm	0.2	0.2	0.2
Compression Ratio		5	5	5
Compressor Power (Efficiency) 85%	HP MW	19.5×10^6 14,600	14.4×10^6 10,750	
Power Requirements	MW			12300
Estimated Costs				
Capital Costs	\$ \$/kW			390×10^6 650
Power	\$/Year			490×10^6

References

(1) Engelhard Industries Technical Bulletin 7, No. 1/2 (June/Sept. 1966).

(2) Kammermayer and Wyrick, Industrial & Engineering Chemistry v 50 n 9 Sept. 1958.

(3) Kronberger and Geoghegan, Proc. Int. Symp. on Isotope Separation, Amsterdam, pp. 513 (1957).

(4) Massignon, D., "Characteristics of Barriers that Can be Used for Isotope Separation by Gaseous Diffusion," 2nd. U.N. Conference on Peaceful Uses of Atomic Energy, Geneva, 1958.

(5) Charpin, J., et al., "Application of General Methods of Study of Porous Barriers to the Determination of the Characteristics of Barriers," 2nd. U.N. Conference on Peaceful Uses of Atomic Energy, Geneva (1958).

(6) Martensson, et al., "Some Types of Membranes for Isotope Separation by Gaseous Diffusion," 2nd. U.N. Conference on Peaceful Uses of Atomic Energy, Geneva (1958).

(7) Bilous, O. and Counas, G., "Determination of the Separation Factor of Uranium Isotopes Produced by Gaseous Diffusion," 2nd. U.N. Conference on Peaceful Uses of Atomic Energy, Geneva (1958).

(8) Massignon, D., Communication to the Amsterdam Symposium on Isotope Separation (1957), Report ESU, 185 (1957).

3.1.2. Mass Diffusion

A mixture of two gases may be separated by allowing them to diffuse through a third gas or vapor if the diffusion coefficients of the two gases with respect to the third gas or vapor differ. This process is referred to as sweep diffusion. A porous screen is sometimes used, though it is unlike the gaseous diffusion barrier and not essential to the process, and is referred to as mass diffusion. Both mass and sweep diffusion have been investigated for use in isotope separation(1,2).

The process of mass diffusion, which may be carried out in stages similar to a gaseous diffusion cascade, usually employs a condensible vapor such as steam as the sweep vapor. Each stage consists of a chamber divided by a mass diffusion screen. Steam is fed at one end of the chamber above the screen and the product enriched in the lighter of the component gases is removed at the other end. A schematic of a mass diffusion cascade is shown in Figure 3.4. The gas mixture is fed at the product end of the lower chamber and the waste, depleted in lighter component, is removed at the other end of the lower chamber. After the product and waste streams leave the diffusion stage, they are cooled to separate out the sweep vapor. This involves a condenser and separator for each stage in addition to a circulating pump for the feed. The light and heavy fractions of the gas mixture are then fed to the neighboring stages as in the case of gaseous diffusion. Requirements of the diffusion screen are not as severe as in the case of gaseous diffusion although relatively small holes are preferred in order to obtain better control of pressure differences across the screen. Various materials have been used for the screen such as 1/64 inch perforated plates, fine-mesh wire screen, and porous metal sheets. As regards the operating pressures, it has been found that the most efficient operation occurs when both streams are at approximately the same pressure.

---

(1) Benedict and Pigford, "Nuclear Chemical Engineering," McGraw-Hill, New York, 1957, p. 473.

(2) Kirk-Othmer, "Encyclopedia of Chemical Technology," 2nd. Edition, Vol. 7, p. 119.

In order to obtain a quantitative idea of the steam requirements for a mass diffusion cascade for SO_2 separation from flue gas, a design calculation was performed with the following assumptions:

(1) Pressures on both sides of the screen are equal to an atmosphere.

(2) The ratio of molar rate of flow of steam to process gas for each stage is unity.

(3) The process gas consists of a binary mixture of 0.3% by volume of SO_2 with the remainder N_2. The gas flow rate was chosen as 10^6 SCFM corresponding approximately to a 500 MW power plant.

(4) The process gas is not soluble in the condensed steam.

(5) The interstage flow rates are given by the equations for an ideal cascade as reported in Appendix 6.2.

(6) An ideal stage separation factor α is given by the following equation:

$$\alpha-1 = \frac{2(D_1-D_2)}{D_1+D_2} \tag{3.7}$$

where D_1 is the diffusion coefficient of N_2 in steam and D_2 that of SO_2 in steam.

The results indicate that for a 500 MW power plant with 95% removal of SO_2, the steam requirements would be of the order of 20×10^6 lbm/hr, which is far in excess of the steam flow rate of the power plant. The cascade would consist of 19 stages with a total screen area of about 15×10^6 ft^2. While the process is relatively simple and the equipment easy to construct, there are two important problems which could reduce the separation effectiveness; namely, the solubility of process gas in the condensed vapor and the thermodynamic irreversibility of the process itself. The steam is vaporized at the operating pressure of the stage and then condensed at a lower partial pressure, resulting in an irreversible flow of heat. Thus a large size mass diffusion plant would consume large amounts of power. Besides increased capital costs due to the auxiliary equipment like condensers and separators, it must be noted that condensing a mixture of steam and non-condensible gases results in a lower condensing coefficient and increases the surface area and costs of the condenser.

There are no known industrial applications of the mass diffusion process, though experiments have been conducted on the separation of some isotopic mixtures. However in view of the large steam requirements, it is concluded that the mass diffusion process does not show much promise in the case of SO_2 separation from flue gas.

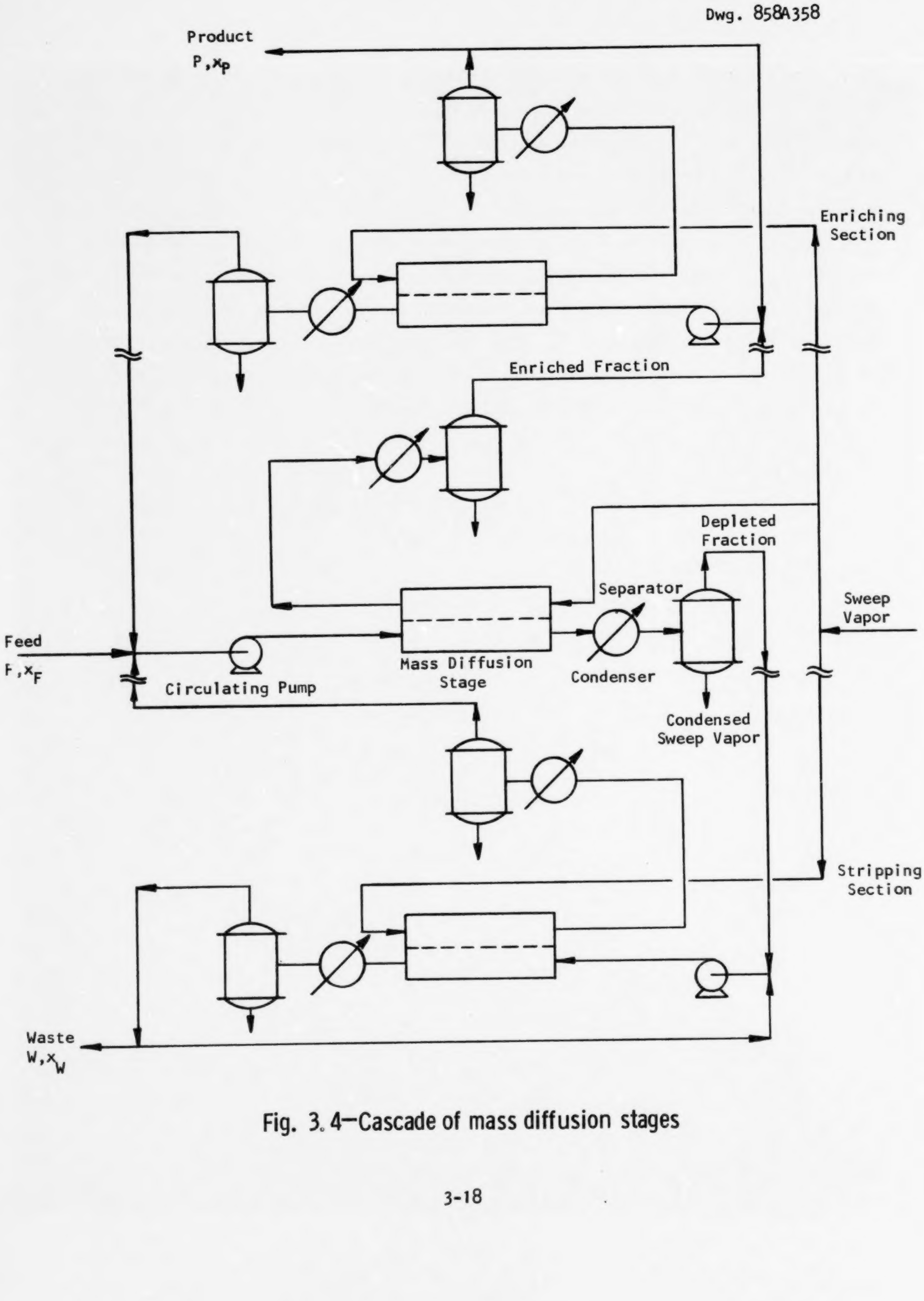
Dwg. 858A358
Product
P, x_P
Enriching Section
Enriched Fraction
Depleted Fraction
Separator
Sweep Vapor
Feed
F, x_F
Circulating Pump
Mass Diffusion Stage
Condenser
Condensed Sweep Vapor
Stripping Section
Waste
W, x_W

Fig. 3.4—Cascade of mass diffusion stages

3.2. Membrane Separation

3.2.1. Silicone Rubber Membrane

Separation of gases by membrane transport processes are based on the difference in the solubility of the gases in the membrane and the ability of the membrane to pass one component more rapidly than another despite equality of driving potential. The latter characteristic distinguishes membrane separations from other common separation processes. Unlike barriers used in gaseous diffusion, most permselective membranes are homogeneous solids without any pores and are polymeric in their molecular structure. The gas molecules must enter the solid phase and pass through by a process of molecular diffusion. With the development of extremely thin and highly permeable synthetic polymers, commercial separation of gases is now possible. Silicon rubber[(1-3)] has a higher permeability to SO_2 than other materials tested and with the development of a silicone rubber membrane bonded between sheets of Dacron by the General Electric Research and Development Center at Schenectady, New York, the feasibility of using it for SO_2 separation from flue gases has been investigated.

Theory

The transport process basically consists of 1) dissolution of the gas in the membrane and 2) diffusion of the gas through the membrane. The solubility of a gas in the membrane is directly proportional to its activity, i.e. partial pressure in the gas phase, which is Henry's Law of Solubility.

$$C_i = k_i p_i \tag{3.8}$$

where C_i = concentration of component i in the membrane
k_i = the solubility constant
p_i = partial pressure of component i

Using Ficks first law of diffusion for the component i

$$J_i = -D_i \frac{dC_i}{dx} \tag{3.9}$$

where J_i = mass flux
D_i = the diffusivity of gas i in the membrane
C_i = concentration of the gas in the membrane
x = distance into the membrane

If the diffusivity is constant throughout the membrane

$$J_i = D_i[(C_{i_1} - C_{i_2})/\ell] \tag{3.10}$$

where ℓ = thickness of the membrane and the subscripts refer to the two sides of the membrane. Combining equations (3.3) and (3.10)

$$J_i = k_i D_i \; (p_{i_1} - p_{i_2})/\ell \tag{3.11}$$

where $P_i = k_i D_i$ = the permeability of the membrane to i. For two gaseous permeants i and j

$$\frac{J_i}{J_j} = \frac{k_i}{k_j} \cdot \frac{D_i}{D_j} \cdot \frac{p_{i_1} - p_{i_2}}{p_{j_i} - p_{j_2}} \tag{3.12}$$

Permselectivity of the membrane to i with respect to j may be defined as

$$\alpha_{ij} = \left(\frac{p_{i_2}}{p_{j_2}}\right)\left(\frac{p_{j_1}}{p_{i_1}}\right) \tag{3.13}$$

Since for ideal gases, the partial pressure ratio is equal to the mole fraction ratio, α_{ij} represents the enrichment factor or separation factor for the membrane. Combining equations (3.12) and (3.13) yields

$$\alpha_{ij} = \frac{k_i D_i}{k_j D_j} \quad \frac{1-\alpha_{ij}(P_{j_2}/P_{j_1})}{1-(P_{i_2}/P_{i_1})} \tag{3.14}$$

In the limit that the downstream gas pressure tends to zero,

$$\alpha_o = \frac{k_i D_i}{k_j D_j} = \frac{P_i}{P_j} \tag{3.15}$$

where α_o = the stage separation factor for zero back pressure. Correction for finite back pressure is given by Rainey et al.(4)

$$\alpha^* = \frac{\alpha_o}{1 + R(\alpha_o - 1)} \tag{3.16}$$

where R = ratio of low to high pressure.

Membrane Characteristics

The Silicone Rubber membrane is composed of thin sheets of methylphenyl polymer bonded between two thin sheets of Dacron mat for support. For the purpose of this analysis the membrane thickness was taken as 0.002 inches. Its permeabilities are given below:

SO_2 - 0.795 Ft.^{3}Mil/Min Yd^2 (atm ΔP)
CO_2 - 0.172 Ft.^{3}Mil/Min Yd^2 (atm ΔP)
O_2 - 0.0318 Ft.^{3}Mil/Min Yd^2 (atm ΔP)
N_2 - 0.0148 Ft.^{3}Mil/Min Yd^2 (atm ΔP)

Assuming the gas comprises only of SO_2 and N_2, the ideal separation factor, α_o, is 53.7. Applying the correction for finite back pressure and the cut correction of 1.12 for a cut of 0.22, which is the same as for gaseous diffusion, the actual separation factor, α, is 10.26.

Results

The flue gas has been assumed to be completely dry with the same composition as in the case of gaseous diffusion. The cascade equations are similar except that this cannot be considered a close separation cascade as the actual stage separation factor is much larger than unity. The results of the design and cost calculations are shown in Table 3.2. In column 1 are values for 95% removal of SO_2 from the flue gas with an SO_2 product concentration of 20%. Column 3 represents the design and cost evaluation performed by Mr. S. Blumkin of the Oak Ridge Gaseous Diffusion Plant using computer programs developed for treating similar stagewise operations. Column 2 represents the results of computations with parameters chosen so as to provide a ready comparison with the Oak Ridge evaluation. For 95% SO_2 removal from the flue gases, the number of stages, membrane area, and compressor power are greatly reduced when compared with the gaseous diffusion cascade. The estimated capital costs for the Oak Ridge Design are about $80 million for a 600 MW plant which is somewhat higher than the base cost of the power plant. It is felt that the membrane separation plant cannot complete favorably with present day processes for SO_2 removal and hence may be ruled out.

Use of Sweep Vapor in Membrane Separation

In most processes dealing with the separation of gases by membrane permeation, the permeate is usually delivered at low absolute pressure leading to extremely high volumetric flow rates for small mass flow rates. The low permeate pressure is necessary because of the fact that the mass flow rate of a particular gas through the membrane is a function of the gas partial pressure difference on either side of the membrane. The attendant large pressure drops in the permeate channels of a membrane module, make it difficult ot sustain the low pressure, near the membrane surface, required for efficient permeation. In view, of the above, the use of an easily condensed sweep vapor, such as steam, on the permeate side of the membrane has been investigated. Such a membrane module is depicted in Figure 3.5.

Consider the steam leaving the membrane module. The partial pressure of the SO_2 in the steam is given by

$$x_{SO_2} \simeq \frac{N_{SO_2}}{N_{steam}} \simeq \frac{p_{SO_2}}{p_{steam}} \qquad (3.17)$$

where N = number of moles

p = partial pressure

The number of moles of SO_2 is a constant depending upon the percent SO_2 removed from the flue gas. For any given steam pressure, the partial pressure of SO_2 in the steam may be decreased only if the number of moles of steam is increased to satisfy the above equation. The analysis of the membrane module may be performed in the same way as that for a counterflow heat exchanger with the exception that the driving force is not a temperature difference but a partial pressure difference. Proceeding in the above manner it was determined that the minimum steam flow rate required, for the flue gas conditions shown in Figure 3.5 and for a steam pressure of 1 atm, was 2.8×10^6 lb_m/hr. This amounts to 0.6 lb of steam per lb of flue gas. If low pressure steam is worth $0.10/1000 lb, the cost of steam would be about $1.45 per ton of coal. To reduce the steam costs to an acceptable level, a steam loop pressure of about 0.1 atmosphere would be required. Besides the steam costs, the condenser and refrigerant costs, and SO_2 compressor costs must also be considered. It may be noted that an SO_2 compressor will be a necessity for the steam pressures considered. The above considerations should apply to any type of membrane used if the SO_2 flow across the membrane is a function of the SO_2 partial pressures across the membrane. It should be mentioned here that the effect of water vapor on the permeability of the membrane to SO_2 was not considered.

From thermodynamic considerations alone, it is evident that mixing the SO_2 permeate with steam increases the irreversibilities of the process, thus increasing the overall costs of separating the SO_2

from steam as opposed to compressing the SO_2 if no steam sweep were employed. It is also obvious that the steam does not serve any useful purpose as in the case of a pervaporative membrane stage. In a pervaporative process, which involves the volatilization of a liquid on the membrane-permeate vapor interface, it is necessary to supply the enthalpy of vaporization of the liquid. Thus, by using steam sweep, partial condensation occurs, thereby supplying the necessary enthalpy of vaporization of the permeate liquid. This condition does not apply in the case of gas permeation.

In view of the above, it may be concluded that steam sweep techniques, in membrane permeation of gases, are uneconomical and need not be considered further.

TABLE 3.2

DESIGN AND COST DATA FOR SILICONE RUBBER MEMBRANE

	1	2	Oak Ridge Design
Ideal Stage Separation Factor - α_o	53.7	53.7	
Actual Stage Separation Factor α	10.26	10.26	
Feed Rate SCFM	10^6	10^6	10^6
Product Rate SCFM	14300	5400	5400
Cut θ	0.22	0.22	0.22
SO_2 Fraction in Feed	0.003	0.003	0.003
SO_2 Fraction in Waste	95% Removal	96% Removal	96% Removal
	0.00015	0.00012	0.00012
SO_2 Fraction in Product	0.20	0.53	0.53
Separation Duty SCFM	2.886×10^6	3.154×10^6	3.164×10^6
Number of Stages	6	7	5
Total Upflow SCFM	1.161×10^6	1.248×10^6	0.75×10^6
Membrane Area $Ft.^2$	49.0×10^6	52.7×10^6	45×10^6
Upstream Pressure-atm.	11	11	11
Downstream Pressure-atm.	1.0	1.0	1.0
Compressor Power MW	292	303.5	321
Barrier Costs at $\$10/yd^2$ \$	54.5×10^6	58.6×10^6	50.0×10^6
Estimated Costs (600 MW Plant)			
Capital \$			80×10^6
\$/KW			133.00
Power \$/Year			13×10^6

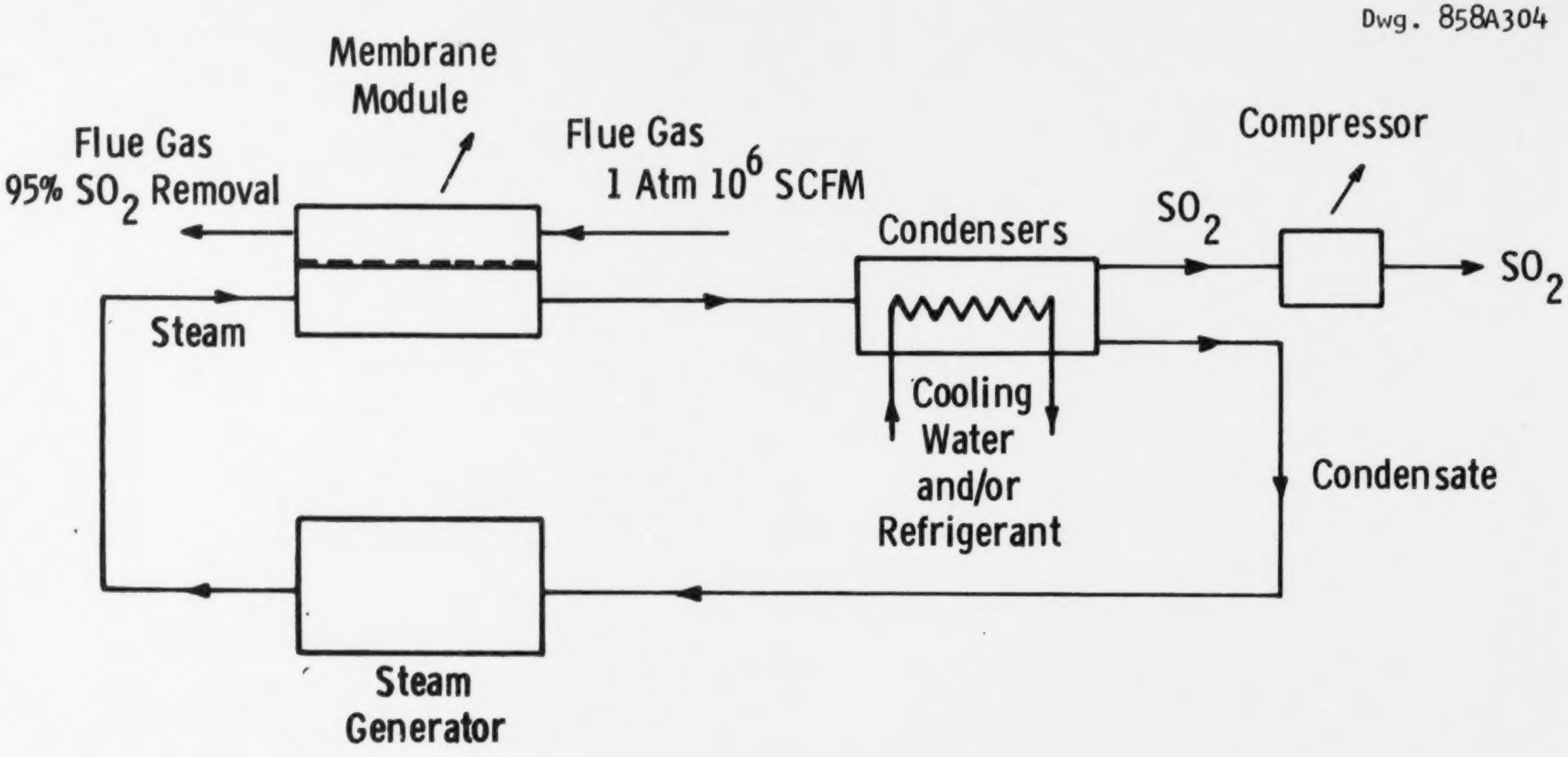
Dwg. 858A304
Membrane Module
Flue Gas 95% SO2 Removal
Flue Gas 1 Atm 10^6 SCFM
Steam
Condensers
Cooling Water and/or Refrigerant
SO2
Compressor
SO2
Condensate
Steam Generator

Fig. 3.5—Process depicting use of steam in membrane separation of SO_2 from flue gas

References

(1) Robb, W. L., General Electric Co., Report No. 65-C-031, (Oct. 1966).

(2) Barrer, R. M. and Chio, H. T., Journal of Polymer Science C, 10, 11 (1965).

(3) Tock, R. W., M. S. Thesis, University of Iowa (1964).

(4) Rainey, R. H. et. al., "Separation of Radioactive Xenon and Krypton from Gases by Use of Permselective Membranes", Oak Ridge National Laboratory, Oak Ridge, Tennessee.

3.2.2. Immobilized Liquid Membrane

The Immobilized Liquid Membrane[1,2] was developed by the General Electric Company for separating CO_2 from gas mixtures. Essentially a porous cellulose acetate membrane impregnated with an aqueous bicarbonate-carbonate solution, the material is characterized by chemical reactions at the gas-liquid interface and within the membrane. The reactions can be catalized to achieve still higher separation factors. Films impregnated with saturated cesium bicarbonate solutions gave separation factors in the order of 1500. The three principal reactions occurring in the film are given below

$$CO_2 + H_2O \rightleftarrows H^+ + HCO_3^- \qquad (3.18)$$

$$CO_2 + OH^- \rightleftarrows HCO_3^- \qquad (3.19)$$

$$HCO_3^- \rightleftarrows H^+ + CO_3^{--} \qquad (3.20)$$

On the high pressure side of the film reactions (3.18) and (3.19) tend to go to the right and (3.20) to the left. Thus CO_2 is consumed near the surface of the film. The above reactions tend to occur in reverse direction on the other side of the film exposed to a low partial pressure of CO_2. Therefore, the CO_2 transport across the film is augmented by the diffusion of bicarbonate.

A quantitative evaluation of the separation of SO_2 from flue gas was not performed in this case because of the lack of permeability data. If permeability data were available, the calculation procedure would be similar to that of Section (3.2.1). Though it is conceivable that catalysts could be found to give the high separation factors for SO_2, the following factors would have to be considered in the application of the immobilized liquid films to the separation of SO_2 from flue gases.

1. Carbon dioxide is highly soluble in water and would also flow preferentially through the film. With the large concentrations of CO_2 in the flue gas, the problem of separating the CO_2 and SO_2 in the permeate would still exist if the number of stages are to be minimized.

2. The films should be backed up by a membrane such as silicone rubber to avoid forcing the solution out of the cellulose acetate matrix. The membrane should be highly permeable to SO_2.

3. The film should be sufficiently hygroscopic to resist dehydration when exposed to normal flue gas temperatures of 300 to 400 F. It is possible that the flue gas would have to be cooled prior to separation.

4. The cellulose acetate matrix could be hydrolyzed by the solution.

It is felt that the immobilized liquid membrane would not have any advantage over a standard scrubbing process using the same solution. In view of this, it may be concluded that the process could not compete favorably with current processes for SO_2 removal from flue gases. The use of steam sweep techniques with the immobilized liquid film process would be governed by the same considerations as enumerated in Section (3.2.1).

References

(1) Robb, W.L. and Ward, W.J., Ind. Res. 8, No. 12, 81 (December 1966).

(2) Ward, W.J. and Robb, W.L., Science 156, No. 3781, 1481 (1967).

3.3 Feasibility Analysis of Centrifugation

History of Centrifuge Development

The use of centrifuges for liquid-liquid separation dates back to the introduction of the cream separator over a century ago. Since that time there have been numerous commercial applications of centrifugation for liquid-solid and liquid-liquid separations. The possibility of separating isotopes by centrifugation of gases was first suggested in 1919 by Federmann and Aston(1) who also worked out the equilibrium theory for the separation in an ideal gas and in an incompressible liquid. This theory was improved and extended by Mulliken,(2) Harkens,(3) Chapman,(4) and others;(5) but, all of the experimental work during this period was unsuccessful.(2,5) However, after the development of the vacuum type ultracentrifuge at the University of Virginia in 1934, the method was tried again and was successful.(6,7,8,9,10)

In the first successful gas isotope separation experiments, the so-called evaporative centrifuge method which is a batch method was used. In 1939, after the discovery of nuclear fission, the evaporative centrifuge method was successfully applied to the separation of uranium isotopes as UF_6 and it was demonstrated that the method could be cascaded. Due to the fact that the evaporative centrifuge method is a batch method and, therefore, inconvenient for large scale production, the development of other methods which could be made continuous was started at the University of Virginia. The first method tried was the concurrent or "flow through method" which was first used successfully in the separation of these isotopes in ethyl chloride.

At this time an organization was formed under the Manhattan project to develop and build a pilot plant centrifuge system for the separation of uranium isotopes. This organization consisted of a group from Columbia University under Professor Urey, a group at the Westinghouse Research Laboratory in Pittsburgh, and a group under E.V. Murphee at the Standard Oil Development Company in addition to the group at the

University of Virginia under J. W. Brans. The Columbia group was to do the theory and coordinate the over-all operation, the Virginia group was to test the theory and investigate various centrifuge configurations, Westinghouse was to design and build the centrifuges for the pilot plant, and Standard Oil Development was to operate the pilot plant.

Professor Urey suggested the counter-current flow type of centrifuge and Cohen of Columbia developed a theory which showed that the counter-current flow method is superior to the concurrent method. Experimental results were in good agreement with the Cohen theory.

Westinghouse designed a centrifuge with bowls which were 42 in. in length and 8 in. in diameter with a rated speed of 28,000 rpm. Two of these were built and delivered to Standard Oil Development for pilot tests in 1943. One of these centrifuges was operated for a total of 99 days before the centrifuge program was terminated because a decision had been made to go with gaseous diffusion. In addition, Westinghouse developed a dynamic model of a centrifuge with a bowl 132 in. long and 8 in. in diameter. Although this machine was wrecked in tests, the experience indicated that a production centrifuge of this length could be operated successfully at 28,000 rpm.

Starting at about the same time in Germany, Beyerle and Groth carried out extensive development work on centrifuges. More recently Beyerle and Groth and Kistermaker and Los have done extensive work on the development of centrifuges for isotope separation.(11,12) Other Europeans who have been active in this field are Hertz, Nann, and Zippe.(13,14)

Centrifugation Theory for Binary Systems

The equation for radial variation of the partial pressure of a gas under a centrifugal field according to the Boltzmann distribution law is[15]:

$$p_i(r) = p_i(o) \exp \frac{Mi(\omega r)^2}{2g\underline{R}T} \tag{3.21}$$

For two gases of different molecular weights under equilibrium conditions this becomes[15]:

$$\frac{p_A(r)}{p_B(r)} = \frac{p_A(o)}{p_B(o)} \exp \frac{(M_A - M_B)(\omega r)^2}{2g\underline{R}T} \tag{3.22}$$

In a binary system

$$p_A + p_B = p \tag{3.23}$$

If x is the mole fraction of the gas having molecular weight M_A,

$$x_A = p_{A/p} \tag{3.24}$$

$$x_B = 1 - x_A = p_{B/p} \tag{3.25}$$

Substituting (3.24) and (3.25) into (3.22) gives:

$$\left(\frac{x_A}{x_B}\right)_r = \left(\frac{x_A}{x_B}\right)_o \exp \frac{(M_A - M_B)(\omega r)^2}{2g\underline{R}T} \tag{3.26}$$

The equilibrium separation factor between gas at the axis of the centrifuge and gas at the periphery is therefore[16]

$$\alpha_o \equiv \frac{(x_A/x_B)_o}{(x_A/x_B)_{r_2}} = \exp \frac{(M_B-M_A)(\omega r)^2}{2g\underline{R}T} \qquad (3.27)$$

This shows that the separation factor for the centrifuge process is a function of the difference in molecular weights of the components being separated, the square of the peripheral velocity, and the reciprocal of the temperature.

Application to Flue Gas Purification

The flue gas composition specified for use in this study is listed in Table 3.3.

TABLE 3.3

Component	% by Volume
N_2	74.9
CO_2	14.7
H_2O	7.25
O_2	2.8
SO_2	0.3
NO_x	0.005
	99.955

To reduce this to a binary stream the gases other than SO_2 will be lumped with an average molecular weight of 29.74. The difference in molecular weights for SO_2 and the composite gas is therefore

$$M_B - \overline{M}_A = 64-29.74 = 34.26 \tag{3.28}$$

The equilibrium separation factor for this flue gas composition is plotted as a function of peripheral velocity in Figure 3.6. This shows that the equilibrium separation factor for SO_2 in flue gas is significantly greater than 1 at rather modest peripheral velocities. At a peripheral velocity of 300 M/sec.which is commonly used[17], the value of α_o is 1.8. This contrasts with the equilibrium separation factor for uranium isotopes at a peripheral velocity of 350 M/sec. which is only 1.0686.[16]

Assuming the equilibrium separation factor is analogous to a total reflux condition, the minimum number of stages can be calculated using the expression

$$n = \frac{\ln \dfrac{x_p(1-x_w)}{(1-x_p)x_w}}{\ln \alpha_o} \tag{3.29}$$

For flue gas having 3000 ppm of SO_2, 90% reduction in SO_2, and an enriched stream concentration of 20%, the minimum number of stages as a function of peripheral velocity is given in Figure 3.7. This shows that the minimum number of stages at commonly used peripheral speeds is of the order of 10.

In centrifuges which have flow and therefore are not in equilibrium, the separation factor is substantially different from the equilibrium value. In fact, the separative efficiency is better defined in terms of separative work δU than in terms of separation factor. Thus, the separative efficiency, E, is defined by[18]

$$E = \frac{\delta U \text{ (experimental)}}{\delta U \text{ (max)}} \tag{3.30}$$

where δU (experimental) is the actual separative work done by a specific centrifuge design and δU (max) is the maximum theoretical separative capacity of the machine. The expression derived by Cohen for the maximum separative work is

$$\delta U_{(\max)} = \frac{\pi Z c D_{AB}}{2} \left[\frac{(M_B - M_A)(\omega r_2)^2}{2 g R T} \right]^2 \qquad (3.31)$$

The value of $(\delta U)_{\max}$ is a function of peripheral velocity to the fourth power, proportional to the length, and independent of the radius. Note that the expression in the brackets is $\ln \alpha_o$.

Reference 19 gives diffusivities of binary gas mixtures for nitrogen-sulfur dioxide and carbon dioxide-sulfur dioxide at one atmosphere as follows:

	D_{AB} - cm^2/sec
N_2-SO_2	0.104 @ -10°C
CO_2-SO_2	0.108 @ 70°C

No data were found for water vapor-sulfur dioxide.

Diffusion coefficients of gases at low pressure are nearly independent of composition, increase with temperature approximately as $T^{1.8}$, and vary inversely with total pressure[30]. For a flue gas at a temperature of 300°F and a pressure of 1 atmosphere, the diffusivities of these pairs become

	D_{AB} @ 300°F - cm^2/sec
N_2-SO_2	0.243
CO_2-SO_2	0.157

Weighting these values for composition gives a composite value of 0.23 cm^2/sec. or 2.5×10^{-4} ft^2/sec.

The total molar concentrations of the flue gas at one atmosphere pressure and 300°F is

$$c = \frac{\rho}{M} = \frac{P}{MRT} = \frac{P}{\underline{R}T} = \frac{144 \times 14.7}{1545 \times 760} = 0.018 \text{ lb.mole/ft}^3$$

Substituting these values in (11) gives

$$\frac{\delta U_{(max)}}{Z} = \frac{\pi \times 0.018 \times 2.5 \times 10^{-4}}{2} \left[\frac{34.26 \ (\omega r_2)^2}{2 \times 32.2 \times 1545 \times 760} \right]^2$$

$$= 1.451 \times 10^{-6} \ (\omega r_2)^4 \qquad (3.32)$$

Figure 3.8 shows the quantity $\delta U_{(max)}/Z$ plotted as a function of (ωr_2).

Separative Efficiency

Cohen[15] has shown theoretically that the maximum separative work can be produced by a centrifuge of the countercurrent type. The separative efficiency, E, of a countercurrent gas centrifuge may be considered to be the product of four factors, all but one of which can be evaluated on a theoretical basis. This efficiency is formulated as[18]

$$E = e_C e_I e_F e_E \qquad (3.33)$$

where

e_C = circulation efficiency
e_I = ideality efficiency
e_F = flow pattern efficiency
e_E = experimental efficiency and includes all phenomena such as turbulence and end effects not taken into account by the other efficiency factors.

The circulating efficiency for a countercurrent gas centrifuge is given by

$$e_C = m^2/(1 + m^2) \qquad (3.34)$$

where m is the ratio at which gas flows upwards in the centrifuge to the quantity L_o. L_o in turn is a function of the configuration of the bowl, the physical properties of the gas, and the flow pattern. Thus, m is directly proportional to the flow through the centrifuge, and the value of e_C approaches unity as the value of m increases.

The ideality efficiency takes into account the difference between the shape of a centrifuge which may be regarded as a square cascade and that of an ideal cascade. The square cascade can meet the conditions for the ideal cascade at only a single point in the enricher and stripper sections. Thus, an efficiency can be associated with each point in the cascade which is a function of the departure of the actual flow from the ideal flow. The ideality efficiency is effectively the overall average of these point efficiencies. Analysis of the gradient equations for a countercurrent gas centrifuge shows that, when flow rates are optimized, the ideality efficiency has a maximum value of 81%.

The flow pattern efficiency, e_F, is a function solely of the shape of the velocity profile in the circulating gas and can be obtained by integrating the velocity gradient equation. Flow pattern efficiencies have been evaluated for a number of assumed velocity profiles. Cohen[15] has shown that there is an optimum velocity profile which gives an e_F value of 1.0. The two-shell velocity profile was also analyzed by Cohen. In this case the flow consists of two thin streams, one a radius r flowing upwards and the other flowing downwards at the wall. For the optimum position of the upflowing stream, the value of flow pattern efficiency is 0.8145. In 1950 Martin[21] derived an equation for the velocity profile in a countercurrent gas centrifuge by considering the flow along a heated plate in a strong gravitational field. Coriolis forces and resistance to the axial flow were neglected. Martin's equation was used to calculate the flow pattern efficiency shown in Figure 3.9 as a function of a dimensionless parameter A. The maximum flow pattern efficiency attainable is 0.956.

The separative efficiency for the separation of SO_2 from flue gas at 300°F is estimated as follows:

Assume $m = 3$

$$e_C = m^2/(1 + m^2) = 0.9$$

Assume maximum value for E_I

i.e. $e_I = 0.81$

$$\begin{aligned} e_F &= e_F(A) \\ A &= [M(\omega r_w)^2/2\underline{gR}T]^{1/2} \\ &= [29.83(\omega r_2)^2/2 \times 32.2 \times 1545 \times 760]^{1/2} \qquad (3.35) \\ &= (39.448 \times 10^{-8})^{1/2} \; (\omega r_2) \\ &= 6.281 \times 10^{-4}(\omega r_2) \end{aligned}$$

Equation 3.25 is used to calculate e_F as a function of ωr_2 and this is shown plotted in Figure 3.10.

Assume $e_E = 0.9$

Thus

$$E = 0.9 \times 0.81 \times e_F(\omega r_2) \times 0.9$$

Figure 3.11 is a plot of E vs. ωr_2 for the specified flue gas at 300°F. From Equation 3.30

$$E = \frac{\delta U(\text{exp.})/Z}{\delta U(\text{max.})/Z} \qquad (3.36)$$

Thus

$$\delta U_{(\text{exp.})}/Z = E \times \delta U_{(\text{max.})}/Z \qquad (3.37)$$

Combining Figures 3.8 and 3.11 gives $\delta U_{(exp.)}/Z$ as a function of ωr_2. This is shown plotted in Figure 3.12.

Separative Duty

The separative duty of a gas separation process is shown in Appendix 6.2 to be

$$D = W\ \phi(x)_w + P\ \phi(x)_P - F\ \phi(x)_F \qquad (3.38)$$

For a 500 MW power plant with the specified flue gas composition

$F = 0.9 \times 10^6$ SCFM = 38.2 lb.mole/sec.

$x_F = 0.003$ by volume

$\phi(x_F) = 5.77^{(22)}$

$x_w = (1-\eta_R)\ x_F$

η_R = 90% for small plants
95% for large plants

$(x_w)_{0.9} = 0.0003$

$\phi(x_w)_{0.9} = 8.15^{(22)}$

$(x_w)_{0.95} = 20.00015$

$\phi(x_w)_{0.95} = 8.81^{(22)}$

Values of separative duty can be computed for specific values of product concentration using the following equations for product and waste flow rates.

$$P = \frac{F(x_F-x_w)}{(x_P\ x_w)} \qquad (3.39)$$

and

$$W = \frac{F(x_P-x_F)}{(x_P-x_w)} \qquad (3.40)$$

Total Length of Centrifuges Required

So far in this analysis the separative capacity of centrifuges has been expressed in terms of unit length. Thus, the total number of feet of centrifuge required for a given separative duty is

$$\ell = \frac{D}{\delta U_{(\text{exp.})}/Z} = n\ Z \tag{3.41}$$

Figure 3.13 is a plot of the total length of centrifuges required for the 500 MW plant with the specified flue gas composition and 90% removal as a function of product concentration and peripheral veloctiy. This shows that the length of centrifuges required for a 99% SO_2 product concentration is only about 5% greater than that for 20% product concentration and 15% greater than that for 5% product concentration.

Figure 3.14 is a plot of total length of centrifuges as a function of peripheral velocity and percent recovery. This shows that increasing the percent recovery from 90 to 95 increases the total length of centrifuges by about 30 percent.

The section on the recovery of sulfur as a by-product shows that the various processes available for the production of by-product sulfur from relatively concentrated gas streams are adapted to the following gas stream concentrations.

By Product	Concentration - % Vol.
SO_2	10-20
H_2SO_4	8-11
Elemental S	5-8

These values can therefore be used as the interface concentrations between the centrifuge cascade and the subsequent sulfur recovery process. Figure 3.13 shows that the total length of centrifuges increases only about 10% over the range of product concentration from 5 to 20%.

Transient Characteristics of Centrifuge System for SO_2 Removal

As described in Appendix 6.2, the equilibrium time of an ideal cascade is

$$t_{eq} = \frac{\text{N.D.M.H.}}{\text{average net transport time}}$$

The equilibrium time of a cascade of centrifuges was computed using α_o which gives a pessimistic result since the effective α in a countercurrent centrifuge is substantially greater than α_o. The following assumptions were made for the centrifuge unit

Rotor length - 4 ft.
Rotor length/diameter ratio - 5
ω r = 600 meters/sec.

The number of stages was calculated using the equations for the number of stages in an ideal cascade given in Appendix 6.2. For a product concentration of 5% and 90% sulfur removal, the total number of stages is 5 with 3 in the enriching section and 2 in the stripping section.

The distribution of centrifuges among the stages was determined on the basis of the stage feed quantities. The net desired material holdup (N.D.M.H.) was then calculated from the volume of centrifuges in enriching section and the concentration in each stage. The results of these computations are summarized below

Stage	$\Sigma \ell$s-ft.	N s	Vs-ft^3	N.D.M.H.-lb.moles
3	110,880	27,720	55,420	2.27
4	33,600	8,400	16,800	1.80
5	10,080	2,520	5,040	1.27
			TOTAL	5.34

The average net transport time for an ideal cascade is equal to $P(x_p - x_P)$. For x_P = 0.05 and x_F = 0.003 the quantity of product P is 2.08 lb.moles/sec. Therefore, the equilibrium time for this centrifuge cascade design is

$$t_{eq} = \frac{5.34}{2.08(0.05-0.003)} = 55 \text{ seconds.}$$

This contrasts with gaseous diffusion cascades for uranium isotope separation where the equilibrium time runs into weeks, and indicates that a centrifuge cascade for removing SO_2 from flue gases would have satisfactory transient characteristics.

Selection of Materials for Centrifuge Construction

As shown in the preceding sections, the separative power of a centrifuge is proportionate to the fourth power of its peripheral velocity (ωr). Appendix 6.3 shows that the maximum operating peripheral velocity for a thin-walled cylinder is

$$(\omega r)_{max} = (g\ \sigma_{H\ design}/1.05\rho)^{1/2} \qquad (3.42)$$

or that the limitation on the performance of a centrifuge is a function of the strength to density ratio of the material of construction. Figure 3.15 shows a correlation of tangential or hoop stress in the cylinder wall and the peripheral velocity of a centrifuge for a number of materials. The parameters for this plot are the density values for the specific materials. Values of maximum published ambient temperature yield or ultimate stresses are plotted for each type of material from which corresponding values of maximum obtainable peripheral velocities can be obtained. Comparison of these values shows that the most promising materials are filament wound glass-resin composite materials, titanium, and steel-nickel alloys. Economic analyses were made for centrifuge cascade systems for each of these candidate materials.

Economic Analysis of Centrifuge Cascade Systems

A prime consideration in the mechanical design of a gas separation centrifuge is the relationship between the operating speed of the centrifuge rotor and its critical speed or frequency. As described in Appendix 6.3 the most applicable formula for the critical speed of a light weight thin-walled cylinder supported by tilting pad journal bearing is the one for free-free vibration. While centrifuges have been operated successfully at speeds greater than the first critical, this is not considered to be practical for this application because of the higher construction costs and probable operating problems. Therefore, a ratio of operating critical speeds of 0.75 was used in the design of the centrifuge with all of the candidate materials of construction.

Filament Wound Glass Resin Composites

There are three basic types of glass filaments commercially available. These types are designated as E, S, and CS glass by Dow Corning Corporation who is the principal manufacturer of glass filaments. The properties of single filaments of these glasses are summarized as follows.

Glass Filament Data at Room Temperature

	E	S	CS
Density - lb/in^3	0.092	0.090	0.090
Tensile Modulus - psi	10.5x10^6	12.4x10^6	12.4 x 10^6
Ultimate Strength - psi	500,000	665,000	665,000
Cost - $/lb	0.35-0.40	8.00	1.50

Source: Owens Corning Fiberglass Corporation

Complete physical properties of these glasses are given in Appendix 6-4.

E glass is widely used commercially while S glass is primarily used in the aerospace field. CS glass is a recent development which has properties nearly the same as those of S glass and is nearly as cheap as E glass.

The three types of glass filaments can be used in combination with a wide variety of resin materials. In this application it was assumed that separation would have to be done at normal flue gas temperatures of 300-400°F, i.e. cooling and reheating would not be economic. Therefore, the chief criteria for selection of resin candidates was that they be capable of operation at temperatures up to 400°F. Literature surveys indicates that the 400°F requirement could be met with the following four resin types: silicone, epoxy novalac, polyester and phenolic.

When the glass filaments are combined with the resin matrix to give a filament wound composite material, the ultimate strength of the glass filaments is reduced to about 50% of the single filament values due to a deleterious effect of the resin on the surface of the glass filament. This effect can be minimized by the use of a surface treatment on the glass filament. The ultimate glass strengths of filament wound glass-resin composite materials do not vary significantly with the type of resin used as long as the resin and the surface treatment are compatible. Ultimate glass strengths realistically attainable in composites using the three different types of glass are:

Type	Ultimate Glass Strength at (23) Room Temperature - psi
E	260,000
S	360,000
CS	330,000

Glass fibers are subject to a deterioration in strength with time under steady load which is known as static fatigue. This fatigue is a strong function of the ratio of the ultimate glass strength to the design glass stress

$$t_{FATIGUE} = C(\sigma_{ult}/\sigma_{design})^{45}$$

and

$$t_{FATIGUE} \approx 5 \text{ years for } \sigma_{ult}/\sigma_{design} \text{ of } 2.0$$

Therefore

$$\frac{\sigma \text{ ultimate}}{\sigma \text{ design}} \approx 2\left(\frac{t_{fatigue}}{5}\right)^{1/45} \qquad (3.43)$$

For an indefinite fatigue life this ratio approaches a value of 2.15.

The above ratio of ultimate glass strength to design stress is a rational basis for the design of these composite materials. One constraint which may take precedence over this criterion is the amount of strain which can be tolerated without crazing of the resin matrix. In composite materials the amount of strain under load is dependent upon the properties of the filament material.

The strain obtained in composites made of E glass, at a glass stress level which would give an indefinite static fatigue life, is

$$e = \frac{\sigma_{design}}{E} = \frac{260{,}000/2.15}{10.5\text{x}10^6} = 1.16\%$$

For S glass and CS glass, the corresponding values of strain are 1.56 and 1.43% respectively. This shows that the maximum percent elongation for any of the glass filaments with an ultimate to design glass stress ratio of 2.15 is about 1.6%.

The properties of three resins which were recommended for this application are

Resin	Specific Gravity	Tensile Elongation - %
Dow Corning R-5071 Silicone	1.22	< 1.0
Dow D.E.N. 439 Epoxy Novalac	1.20	1.61
Koppers Co. M7000-15 Polyester	1.13	0.70-0.80

This comparison indicates that the silicone and polyester resins are relatively brittle and that the epoxy novalac resin is the only resin type which is elastic enough to accommodate the strains of all of the filament types for an ultimate to design stress ratio of 2.15. In view of this the Dow D.E.N. 439 epoxy novalac resin was used in the economic analysis of centrifuges constructed of filament wound glass-resin composites, and a static fatigue factor of 2.2 was used in designing with these materials.

A typical resin bulk factor for filament wound composite materials is 1.7.(23) Combining the 2.2 static fatigue factor and this bulk factor gives a ratio of composite material design stress to ultimate glass stress of

$$(\sigma_C)_{design}/(\sigma_g)_{ultimate} = 0.267$$

The relationship between hoop or tangential stress and stress in the direction of the glass filaments in a composite material is shown in Appendix 6.3 to be

$$\sigma_H = (\sigma_C)_{design} \times \sin^2 \alpha \qquad (3.44)$$

The total hoop stress in the thin walled cylinder is made of two components

$$\sigma_H = \sigma_{CF} + \sigma_P \qquad (3.45)$$

The stress due to the internal pressure in the centrifuge is assumed to be 5% of that due to centrifugal force. Therefore,

$$\sigma_H = 1.05\ \sigma_{CF} \qquad (3.46)$$

and

$$\sigma_{CF} = 0.267\ (\sigma_g)_{ult} \times \sin^2 \alpha/1.05 \qquad (3.47)$$

Combining this with (3.44) gives

$$(\omega r)_{design} = \left[(0.267\ (\sigma_g)_{ult} \times \sin^2 \alpha \times g)/(1.05 \times \rho_C)\right]^{1/2} \quad (3.48)$$

Appendix 6.5.1 shows that the expression for the total centrifuge bearing power requirements of a centrifuge cascade is

$$P_B' = \frac{1.693 \times 10^{-2} \times \ell(D,\omega r) \times \left(\frac{L}{Z}(\omega r)\right)^{3/2} \times (\omega r)^2 \times \left(\frac{Z}{d}\right)^2}{Z^{3/2}} \quad (3.49)$$

In filament wound composite materials the elastic modulus is a function of the winding pattern of the filament since the elastic modulus of the filament and the resin differ greatly. The relationship between the composite material hoop and longitudinal moduli for the centrifuge rotor is shown in Appendix 6.3 to be

$$(E_C)_{long} = E_C \times \cos^2 \alpha \quad (3.50)$$

and

$$E_C = \frac{E_f}{B} = E_f/1.7 \quad (3.51)$$

Therefore

$$(E_C)_{long} = (E_f \times \cos^2 \alpha)/1.7 \quad (3.52)$$

Appendix 6.5.1 shows that the ratio of centrifuge length to radius is

$$\frac{Z}{d} = 2.015 \left[\frac{N}{N_{s\ crit}}\right] \left(\frac{(E_C)_{long}}{\sigma_{CF}}\right)^{1/4} \quad (3.53)$$

For $(N_s/N_{s\ crit})_{design} = 0.75$ this becomes

$$\frac{Z}{d} = 1.745\ ((E_C)_{long}/\sigma_{CF})^{1/4} \tag{3.54}$$

Substituting for $(E_C)_{long}$ and σ_{CF} in this equation gives

$$\begin{aligned} \frac{Z}{d} &= 1.745 \left[\frac{E_f \times \cos^2 \alpha/1.7}{0.267\ (\sigma_g)_{ult} \times \sin^2 \alpha/1.05}\right]^{1/4} \\ &= 2.15\ (E_f/(\sigma_g)_{ult})^{1/4}\ (1/\tan \alpha)^{1/2} \end{aligned} \tag{3.55}$$

Appendix 6.5.1 contains the development of

$$\frac{L}{Z} = \frac{L}{Z}(\omega r)$$

and this function is plotted in Figure 6.12.

The function $\ell(D,\omega r)$ is plotted in Figure 3.14 for two values of η_R.

Appendix 6.5.2 contains the development of the formula for the total volume of material in a cascade of centrifuges.

$$V_T = \pi \times \ell(\omega r) \times d^2\ (\frac{t_w}{d})\ (1 + 0.625(\frac{d}{Z})) \tag{3.56}$$

where

$$\left(\frac{t_w}{d}\right) = \frac{g \times p_{(o)}\ \exp \bar{M}(\omega r)^2/2g\underline{R}T}{2 \times \rho(\omega r)^2\ (\sigma_P/\sigma_{CF})_{design}} \tag{3.57}$$

Equation (3.57) is used to calculate the approximate cost of material in the centrifuge system.

Appendix 6.5.3 contains a development of an equation for the number and size of bearings for the centrifuges in a cascade system. Figure 6.13 is a correlation of the cost of tilting pad journal bearings as a function of size and Figure 6.14 is a plot of the specific cost of the centrifuge bearings in a 500 MW power plant with $x_p = 0.20$ and $\eta_R = 0.95$.

The high speed gas centrifuge must be operated in a vacuum environment to avoid extreme windage losses. Pressure levels of the order of 5 mm of Hg are typical. Therefore, each of the centrifuge units would be enclosed in a vacuum chamber. Appendix 6.5.4 contains the development of a procedure for estimating the cost of these vacuum chambers.

Cost Estimates for Composite Materials

CS Glass and Dow D.E.N. 439 Resin

The most promising glass filament candidate is CS glass since it has properties which approach those of S glass and a cost which approaches that of E glass.

Input Data

$$(\sigma_g)_{ult} \text{ @ } 70°F = 330{,}000 \text{ psi}$$

Temperature correction factor (from Figure 6.3)

$$\frac{630{,}000}{665{,}000} = 0.95$$

High temperature aging correction factor (from Figure 6.5). Assume 15% for 400°F. Static fatigue factor - 2.2.

$$(\sigma_g)_{des} \text{ @ } 400°F = 121{,}500 \text{ psi}$$

$$E_f = 12.2 \times 10^6 \text{ psi (from Figure 6.4)}$$

$$\rho_c = 122.3 \text{ lb/ft}^3$$

$x_P = 0.20$

$\eta_R = 0.95$

$P = 1$ atmos

$T = 860°R$

Cost of CS glass - \$1.50/lb
Cost of D.E.N. 439 resin - \$0.71/lb

Results

	Figure
Centrifuge bearing power requirements	3.16
capital cost equivalent of bearing energy losses*	3.17
bearing costs	3.18
Cost of material of construction of centrifuges	3.19
Vacuum chamber purchase costs	3.20
Sum of partial costs of cascade system	3.21

Discussion

Figure 3.21 shows that the sum of the bearing loss equivalent, the centrifuge bearing costs, the centrifuge material costs, and the vacuum chambers costs for this material combination has a minimum value of about \$120 installed KW. Since the cost of several major system components, such as driving motors, vacuum system, piping, and sulfur recovery systems, and the cost of fabricating the centrifuges are not included, it is clear that a centrifuge system made of these materials is not economic.

---

*It should be pointed that the net plant output remains at 500 MW. The capital cost equivalent of the bearing power requirement is in effect the cost of the larger plant required to maintain a net output of 500 MW.

S Glass and Dow D.E.N. 439 Resin

Input Data

Resin bulk factor 1.7

(σ_g) with @ 70°F = 360,000 psi

Temperature correction factor (from Figure 6.3)

$$\frac{630{,}000}{665{,}000} = 0.95$$

With temperature aging correction factor
(from Figure 6.5).
Assume 15% for 400°F

Static fatigue factor - 22

(σ_g) design @ 400°F - 132,000 psi

$E_f = 12.2 \times 10^6$ psi (from Figure 6.4)

$\rho_c = 122.3$ lb/ft^3

$x_p = 0.20$

$\eta_R = 0.95$

$p = 1$ atmos

$T = 860°R$

Cost of S glass - \$8.25/lb

Cost of D. E. N. 439 resin - 0.71/lb

Results

	Figure
Centrifuge bearing power requirements	3.22
Capital cost equivalent of bearing energy losses	3.23
Bearing costs	3.24
Cost of material of construction for centrifuges	3.25
Vacuum chamber purchase costs	3.26
Sum of partial costs of cascade system	3.27

Discussion of Results

Comparison of Figures 3.21 and 3.27 shows that the minimum value of the sum of these four cost components is essentially the same for S glass as for CS glass. This indicates that this sum is a weak function of the cost of the material of construction of the centrifuges

E Glass and Dow D. E. N. 439 Resin

The use of the cheapest glass, i.e. E glass, would not lower since it is a weak function of material costs minimum values for this sum. More likely these values would increase due to the substantially lower strength of E glass compared to CS and S glass.

Cost Estimates For Titanium Alloys

A prime consideration in the selection of a titanium alloy for this application is weldability since the most reasonable method for fabricating a centrifuge rotor from metal is welding. Of those commercially available titanium alloys which are classified as weldable, the type which has the highest yield strength is Ti-3Al-13V-11Cx. The tensile strength of this alloy over a range of temperatures is given in Figure 6.6 of Appendix 6.4.2. While this alloy is classified as weldable, it is weldable only in the annealed condition and the weld joint efficiency tends to be low. This is so because the weld metal ages at different rates than the bare metal and large grain size and microsegregation of alloying constituents develop at weld-metal grain boundaries during the fission process. The high potential of this alloy might be attained by welding in a relatively thick ring with subsequent cold rolling to reduce the grain size.

The next strongest titanium alloy which is weldable is Ti-6 Al-4V. This alloy has a weld joint efficiency of nearly 100% and its yield strength over a temperature range is shown in Figure 6.7.

Design data

Factor of safety - 1.5

$x_P = 0.20$

$\eta_R = 0.95$

$T = 860°R$

$p = 1$ atmos.

Ti-3Al-13V-11Cr

$E = 14.8 \times 10^6$

$\sigma_{0.2\%\ \text{yield}}$ @ 400°F = 178,000 psi

$\rho = 302.4$ lb/ft

Cost = \$6.00/lb

Ti-6Al-4V

$E = 16.5 \times 10^6$ psi

$\sigma_{0.2\%\ \text{yield}}$ @ 400°F = 140,000 psi

$\rho = 276.5$ lb/ft^3

Cost = \$5.00/lb

Results

Figure 3.28 shows the bearing power requirements as a function of centrifuge length for both of the titanium alloys being considered. These power requirements were converted to equivalent capital cost values and are plotted on Figures 3.29 and 3.30 along with the estimated cost of the material of construction for the centrifuges. These two quantities are added and the minimum sums are \$118/KW for Ti-3Al-13V-11Cr and \$121/KW for Ti-6Al-4V. Since these two costs are only a fraction of the total cost of a centrifuge system, it is clear that a centrifuge system made of titanium would be uneconomic for this application.

Cost Estimates for Steel Alloys

The strongest available steel alloy which would meet the fabrication requirements of this application is 18% Ni managing steel. Figure 6.10 is a plot of the ultimate and 0.2% yield strength of a typical steel of this type as a function of temperature.

Design Data

Factor of safety - 1.5

$E = 26.5 \times 10^6$ psi

$\sigma_{0.2\% \text{ yield}}$ @ 400°F = 251,000 psi

$\rho = 501.0$ lb/ft^3

Cost - \$2.50/lb.

$x_P = 0.20$

$\eta_R = 0.95$

$T = 860°R$

$p = 1$ atmos.

Results

The power requirements for the centrifuges bearings are shown plotted in Figure 3.31. The power requirements were counted to equivalent capital cost and are shown plotted on Figure 3.32 along with the cost of the material of construction of the centrifuges. The sum of these two costs has a minimum value of \$115/KW which shows that a centrifuge system constructed of 18% Ni marging steel is also uneconomic for this application.

Cost Estimate for Aluminum Alloys

Aluminum alloys have been widely used in experimental centrifuges and they have relatively low costs. In view of this, a brief economic analysis of aluminum alloys was included. Aluminum alloy 7178 has the following properties:

$\sigma_{0.2\% \text{ yield}}$ @ RT = 78,000 psi

$E = 10.5 \times 10^6$

$\rho = 176$ lb/ft^3

Cost = \$0.80 - 0.90/lb.

and with a 1.5 factor of safety the design operating peripheral velocity would be 360 meters/sec which is somewhat less than those for 18% Ni marging steel and Ti-6Al-4V which are 380 and 382 meters/sec, respectively. For this reason the power requirements for aluminum centrifuges would be at least as large as for the steel and titanium centrifuges. In addition the cost of the vacuum chambers shown in the section on composite materials for $\alpha = 60°$ would apply. These values and their sum are as follows:

Z-ft	5	10	20	30	40
Bearing Loss Equiv. \$/kW	392	154	54	30	20
Vacuum Chamber - \$/kW	50	70	104	133	159
Sum	442	224	158	163	179

This indicates that the cost of a centrifuge system using aluminum alloys is also excessive.

Conclusions

Feasibility analysis have been made of centrifuge cascade systems for the removal of SO_2 from flue gas for a number of both composite and isotropic materials of construction. The use of gas centrifuges constructed of these materials was found to be technically feasible. However, it was found that the cost of such a gas separation system with all candidate materials was in excess of \$100/KW. Therefore, it is concluded that the use of gas centrifuges for this purpose is not economically feasible.

LIST OF SYMBOLS

c - molar density

D - separative duty

D_{AB} - diffusivity of gases A and B

E - overall separative efficiency

e - efficiency factor

F - feed

g - gravitational constant

M - molecular weight

n - number of stages

P - product

p - partial pressure

$\underline{R}$ - universal gas constant

r - radius - feet

T - temperature - °R

t_{eq} - equilibrium time of cascade

δU - separative work capacity

V_s - volume of centrifuges in a stage

W - waste

x - mole fraction

$\phi(x)$ - separation potential

Z - height of centrifuge

α - separation factor

η_r - removal efficiency

ρ - density

ω - angular velocity - radians/sec

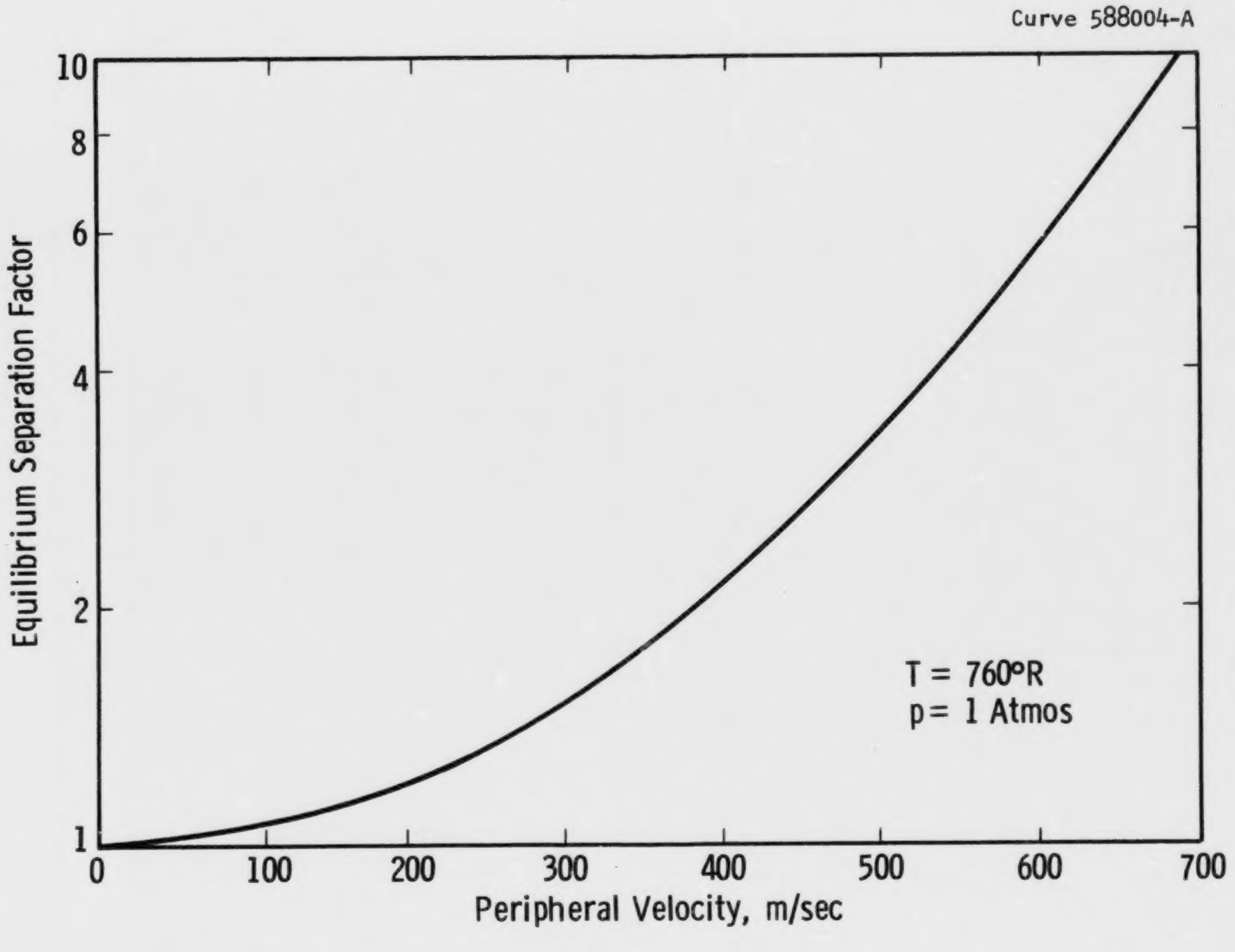

Fig. 3.6—Equilibrium separation factor vs centrifuge peripheral velocity for separation of SO_2 from flue gas

Curve 588018-B

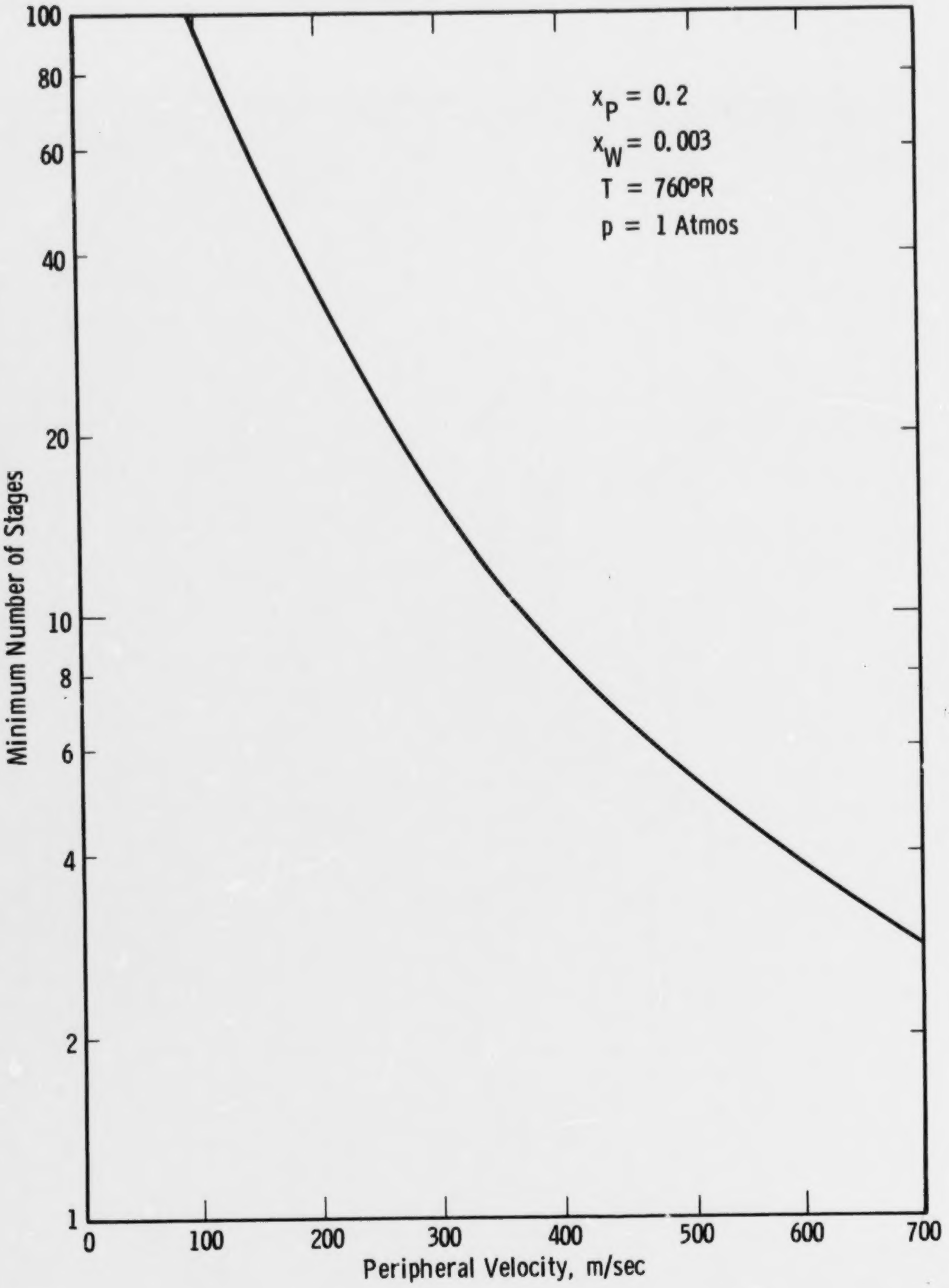

Fig. 3.7 —Minimum number of stages in a cascade of centrifuges for separation of SO_2 from flue gas

Curve 588019-B

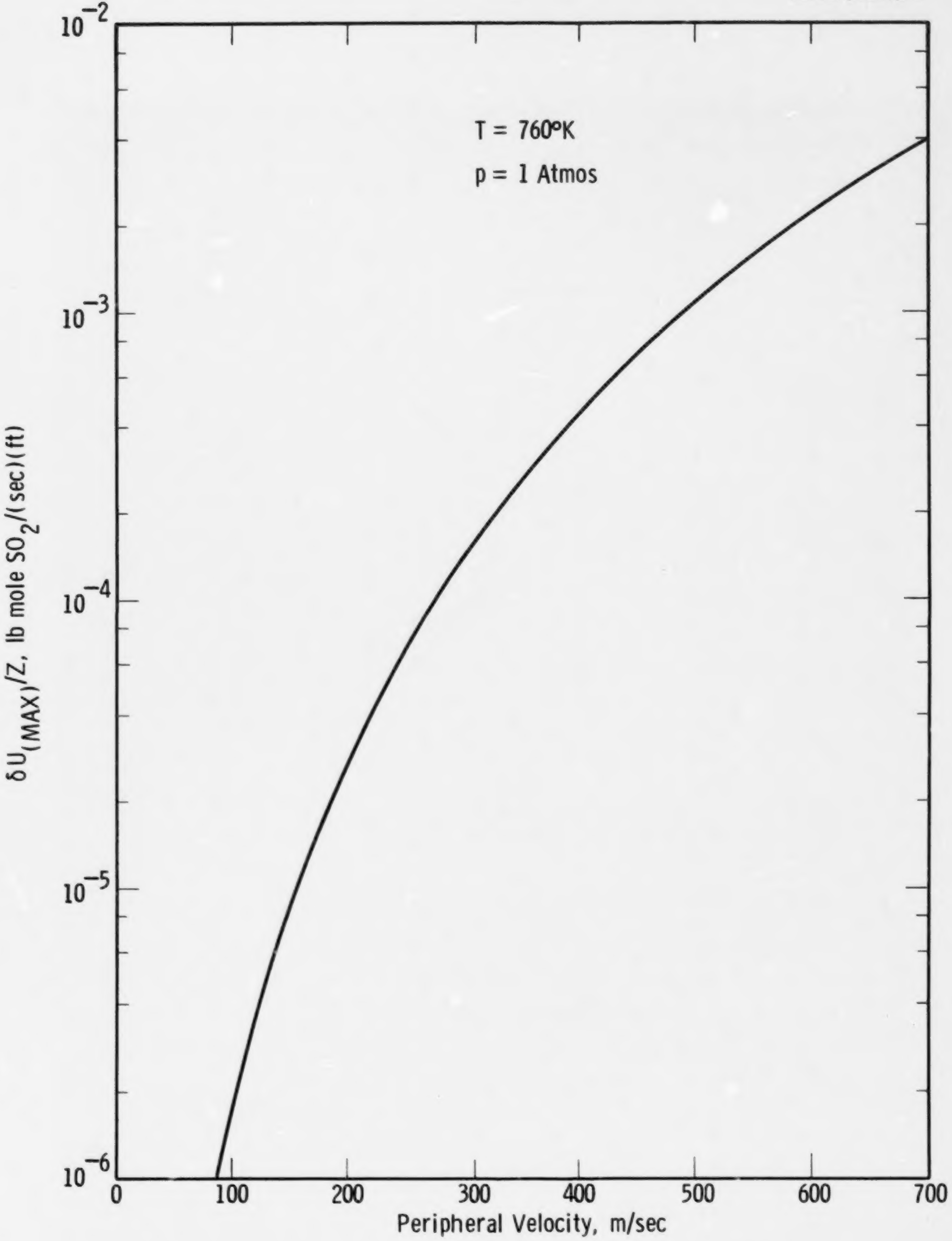

Fig. 3.8—Maximum separative capacity for sulphur dioxide per foot of length vs peripheral velocity

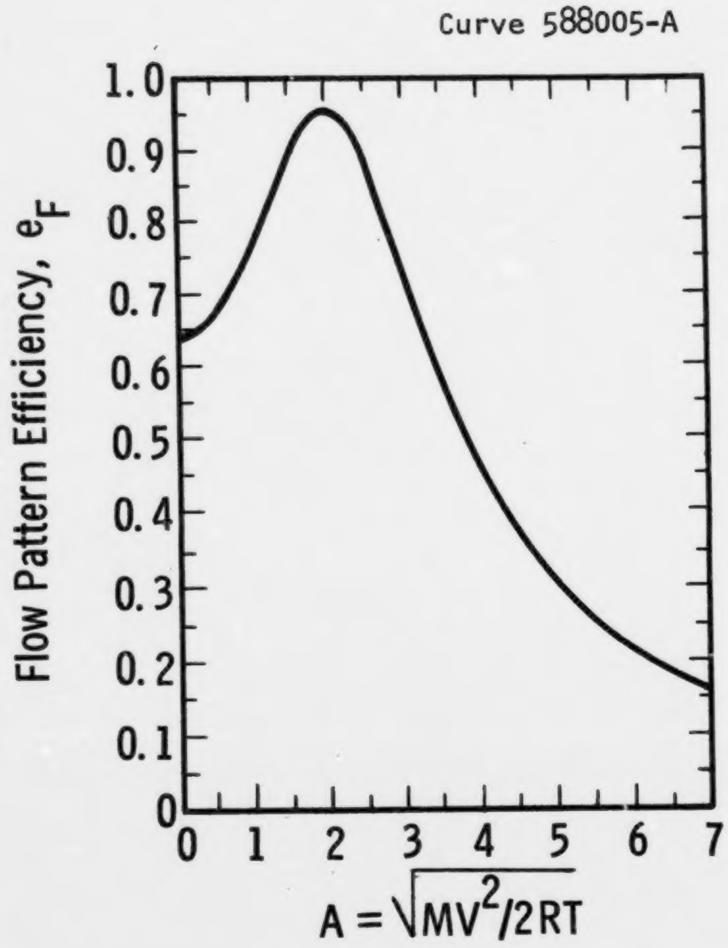

Fig. 3.9 —The dependence of the flow-pattern efficiency on the dimensionless parameter, A, for the Martin profile

Curve 588006-A

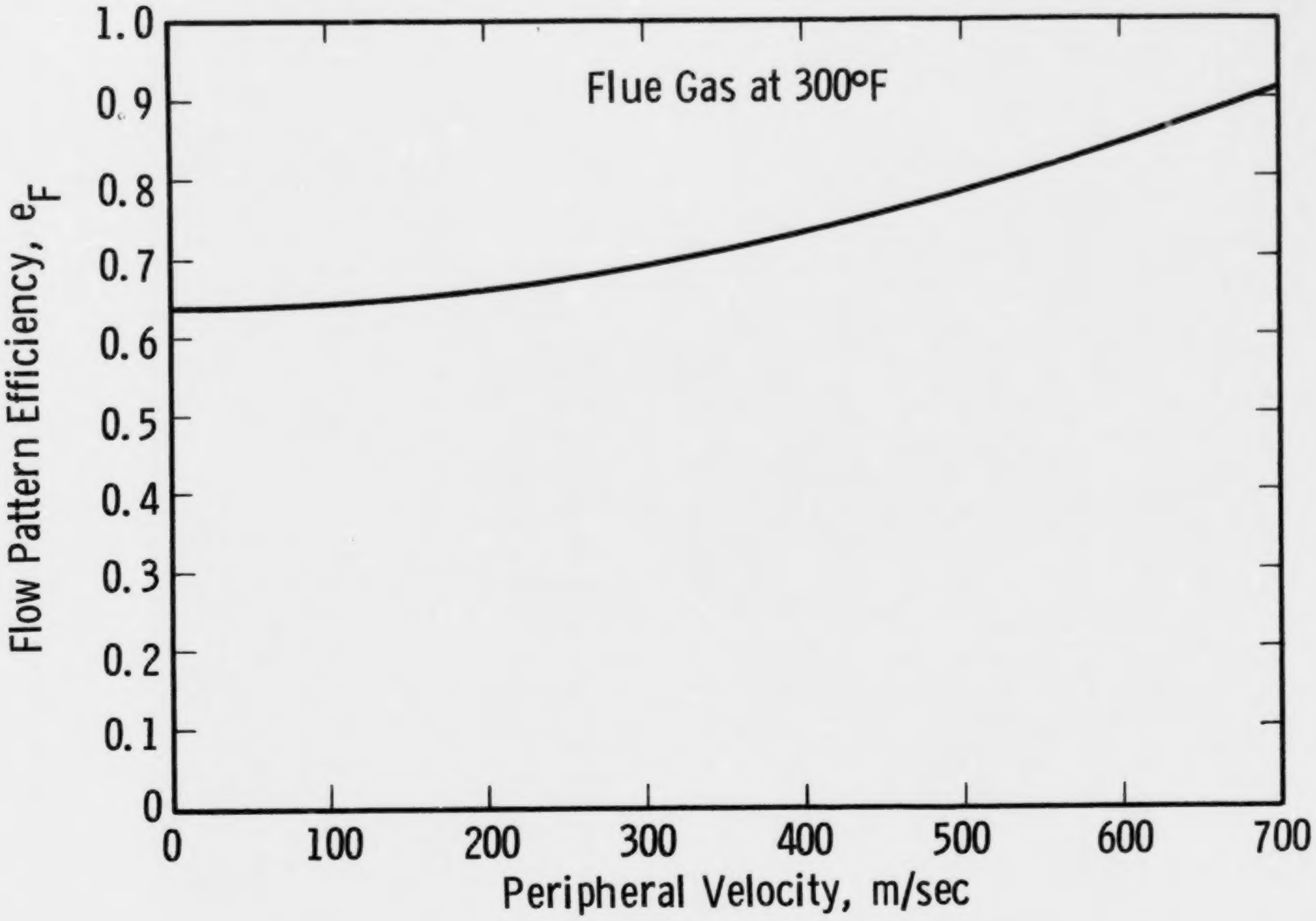

Fig. 3.10 —Flow pattern efficiency for Martin profile vs peripheral velocity

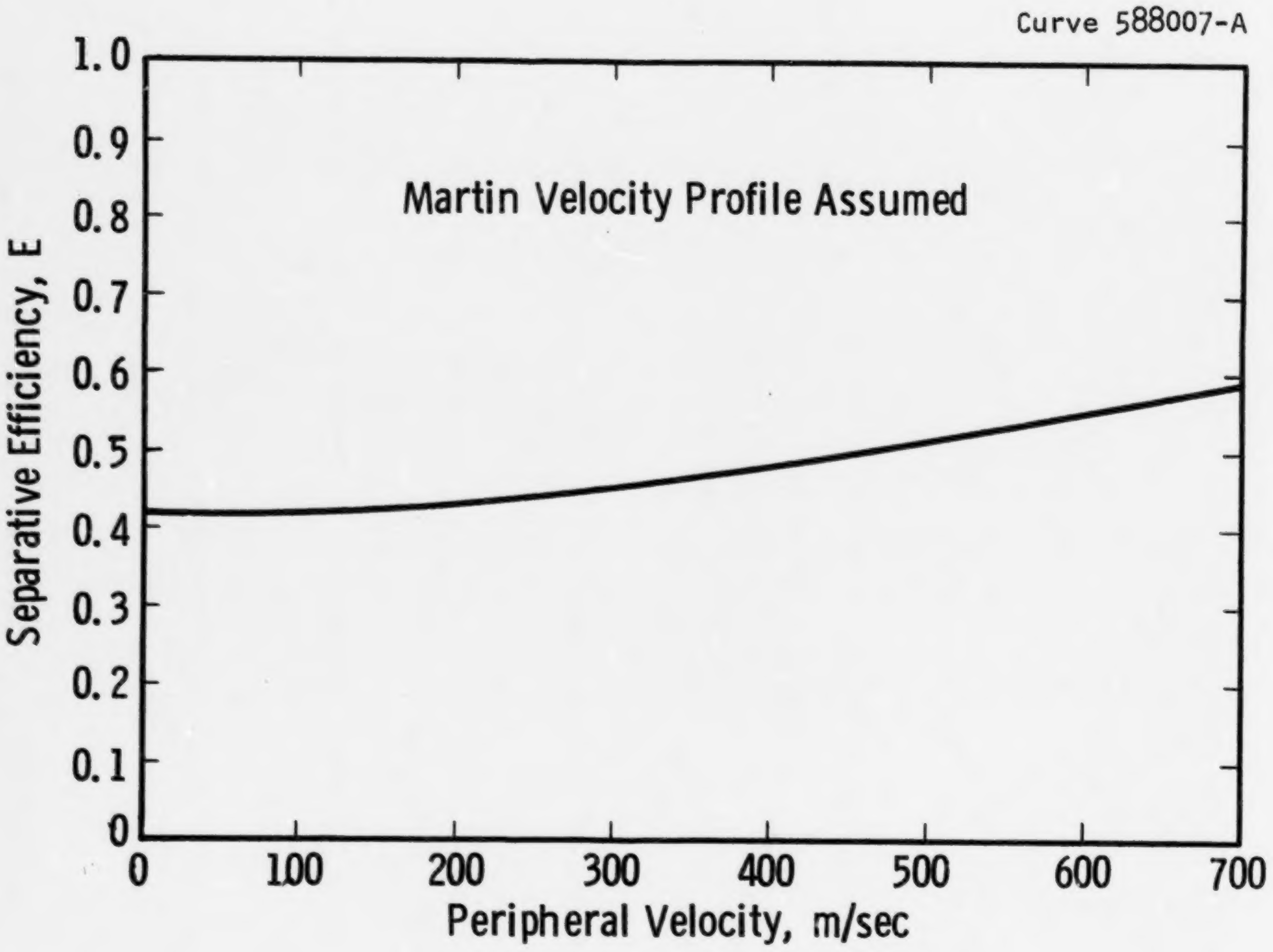

Fig. 3.11 —Separative efficiency vs peripheral velocity for specified flue gas at 300°F

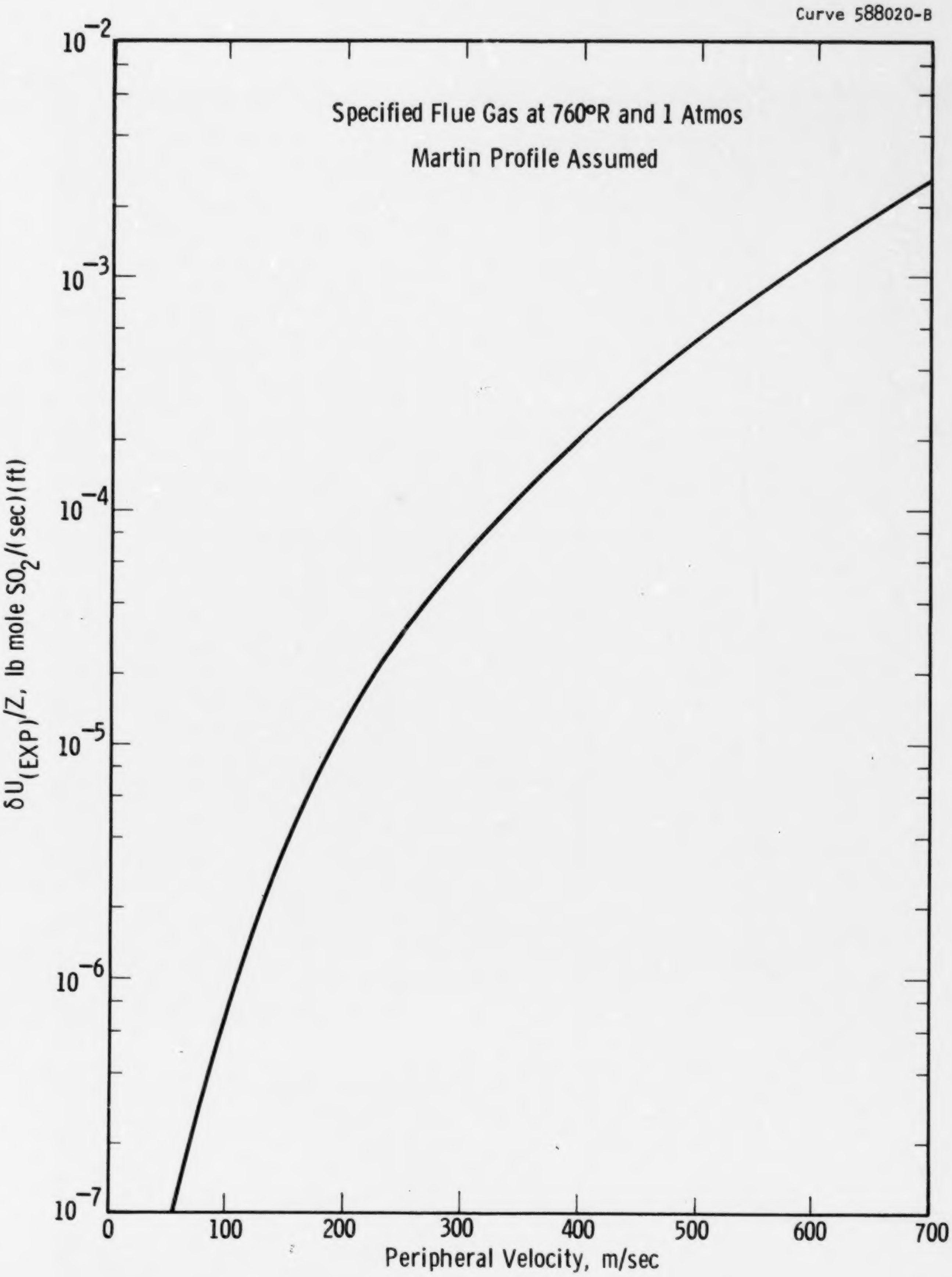

Fig. 3.12 — Actual separative capacity for sulfur dioxide per foot of length vs peripheral velocity

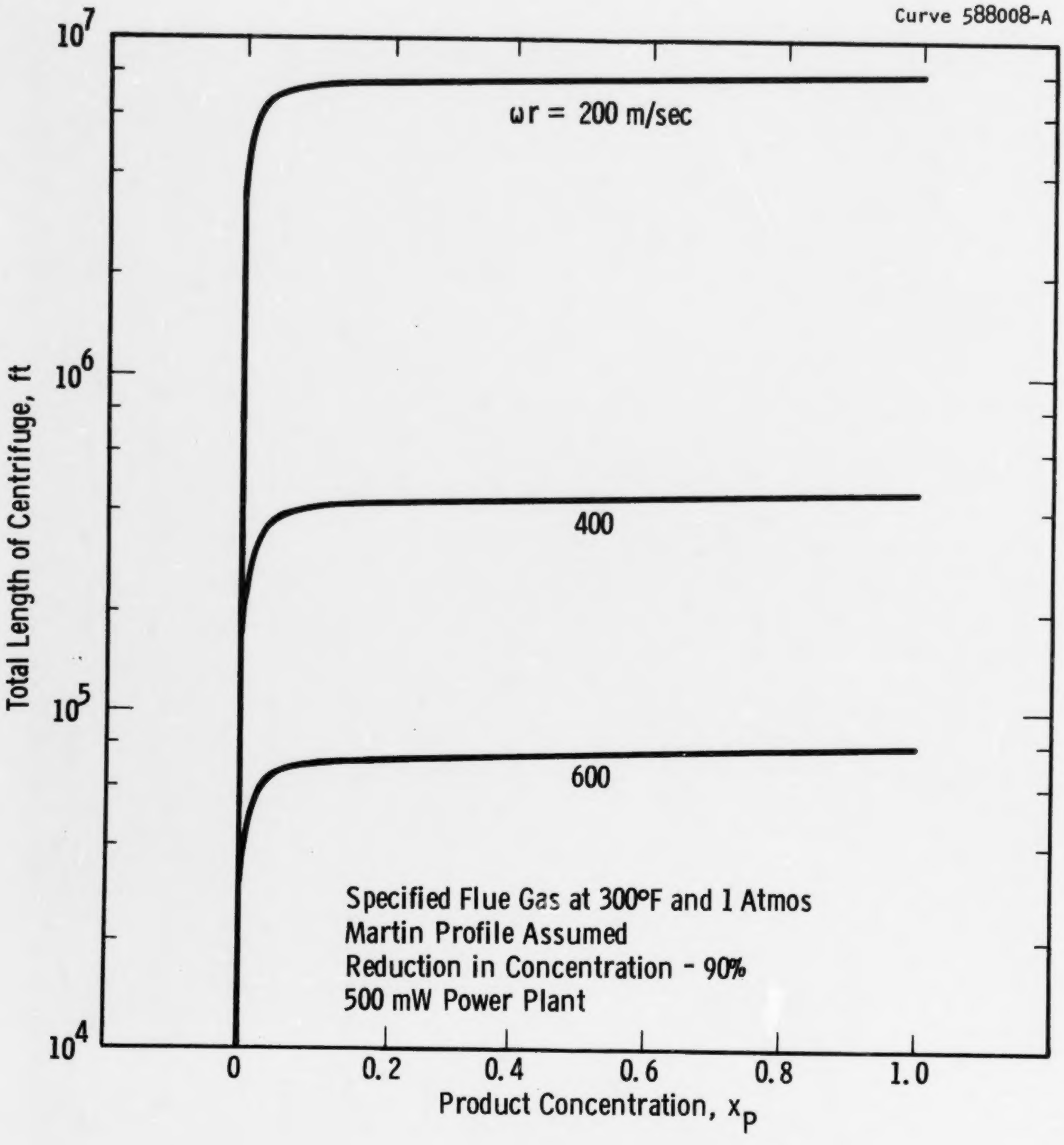

Fig. 3.13 —Total length of centrifuges vs product concentration

Curve 588021-B

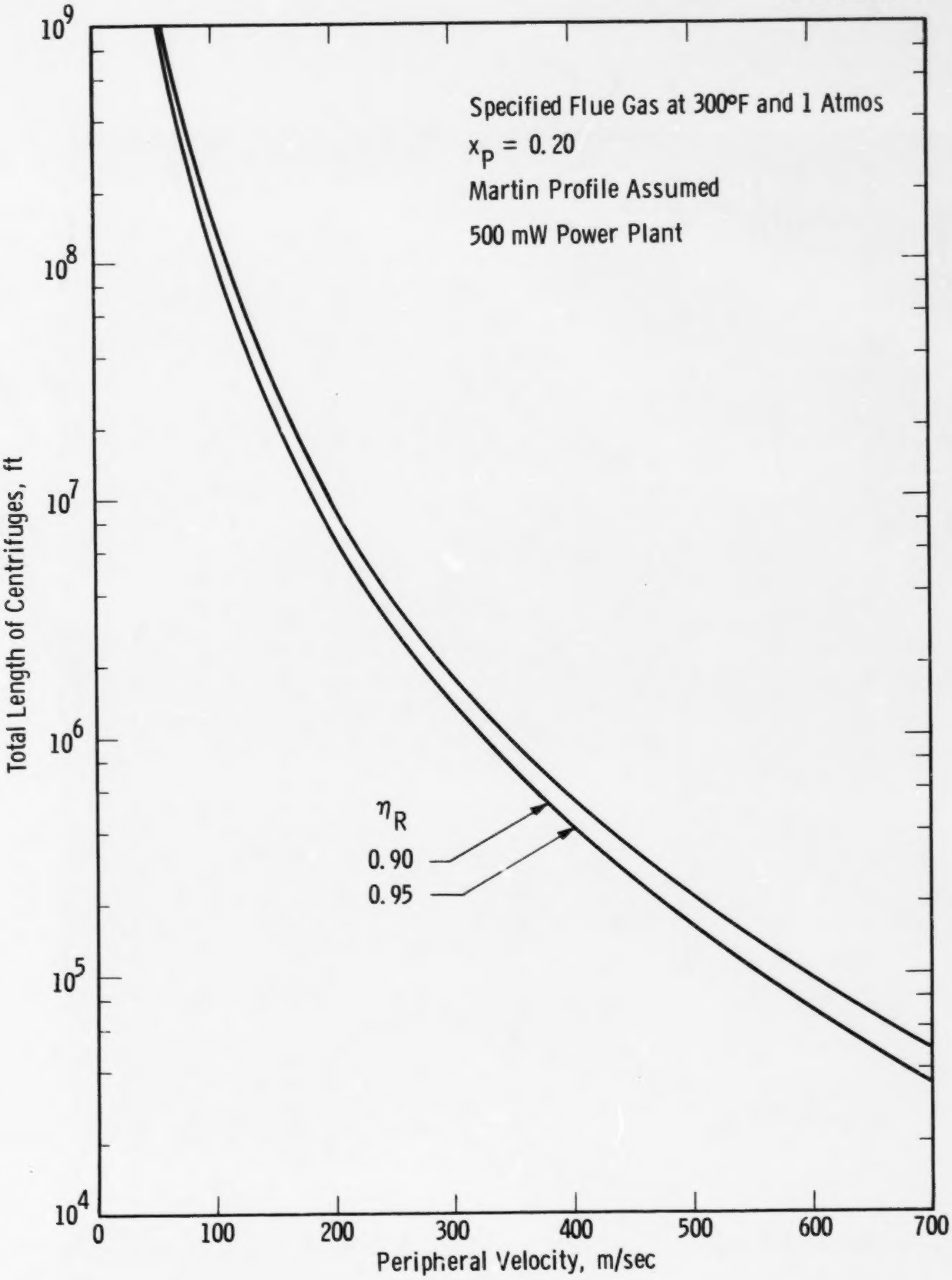

Fig. 3.14—Total length of centrifuges vs peripheral velocity

Curve 588022-B

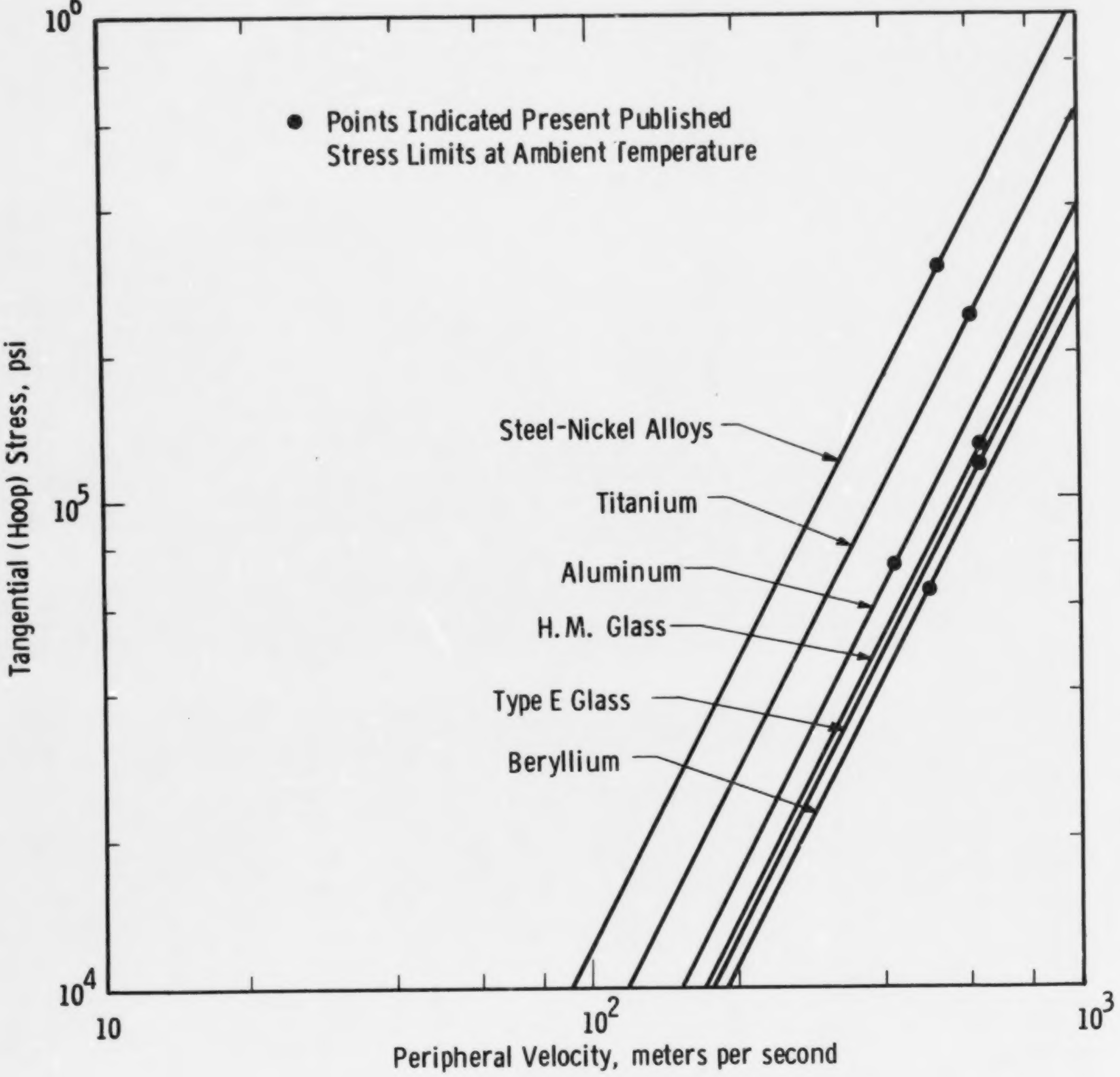

Fig. 3.15—Tangential stress in centrifuge vs peripheral velocity

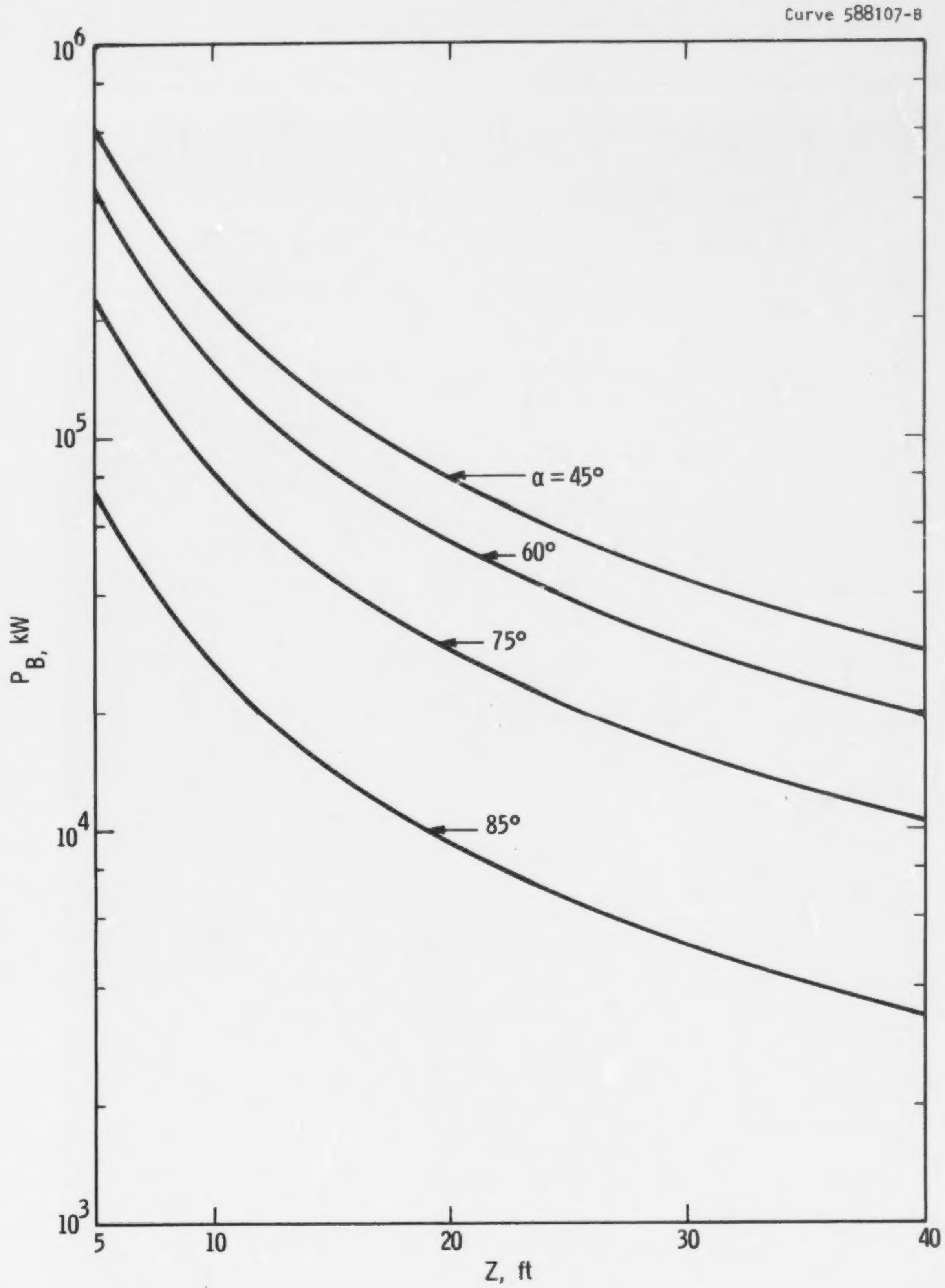

Fig. 3.16—Centrifuge bearing power requirement for cascade of centrifuges made of CS glass and D.E.N. resin

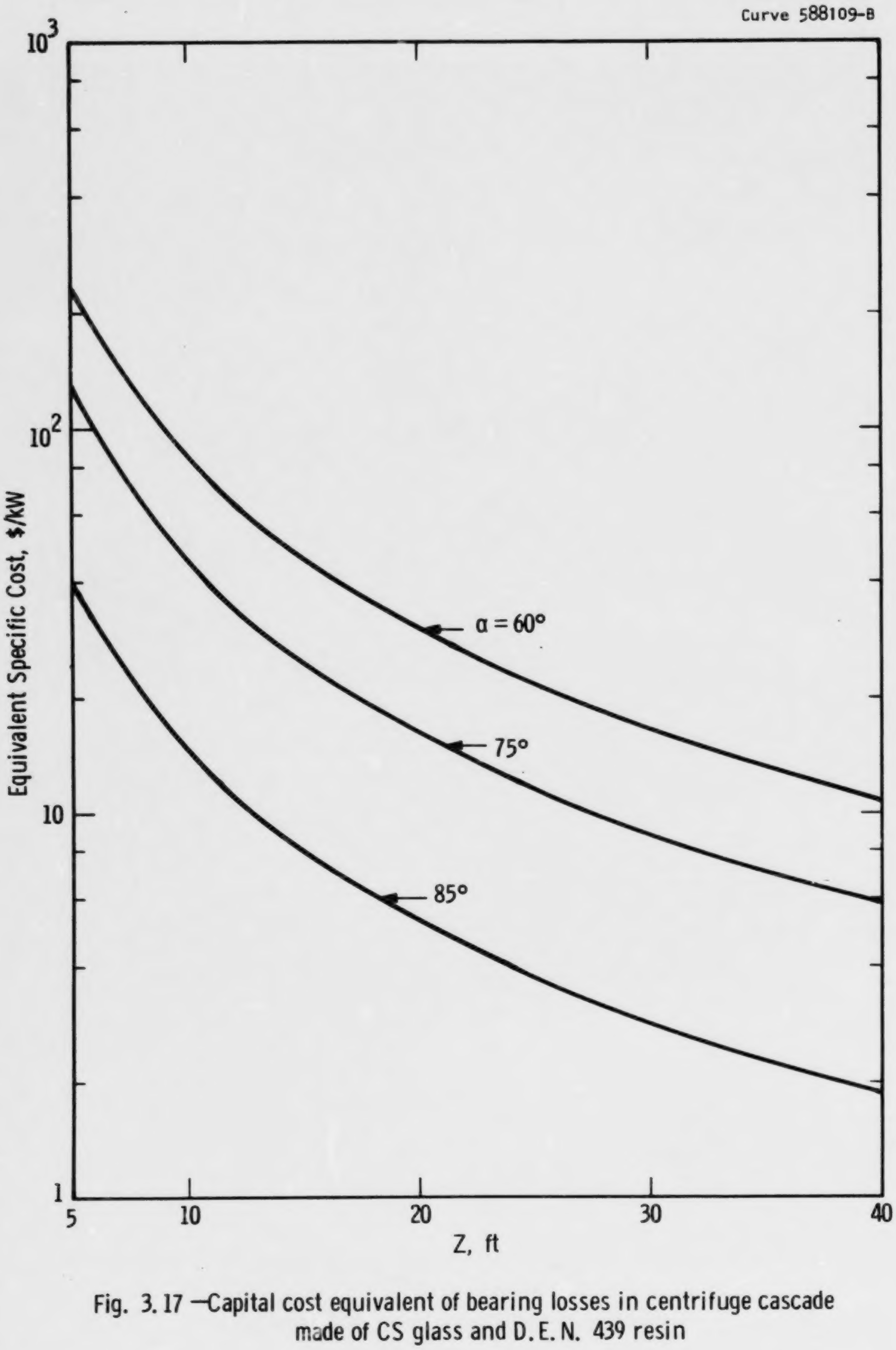

Fig. 3.17 —Capital cost equivalent of bearing losses in centrifuge cascade made of CS glass and D.E.N. 439 resin

Curve 588101-A

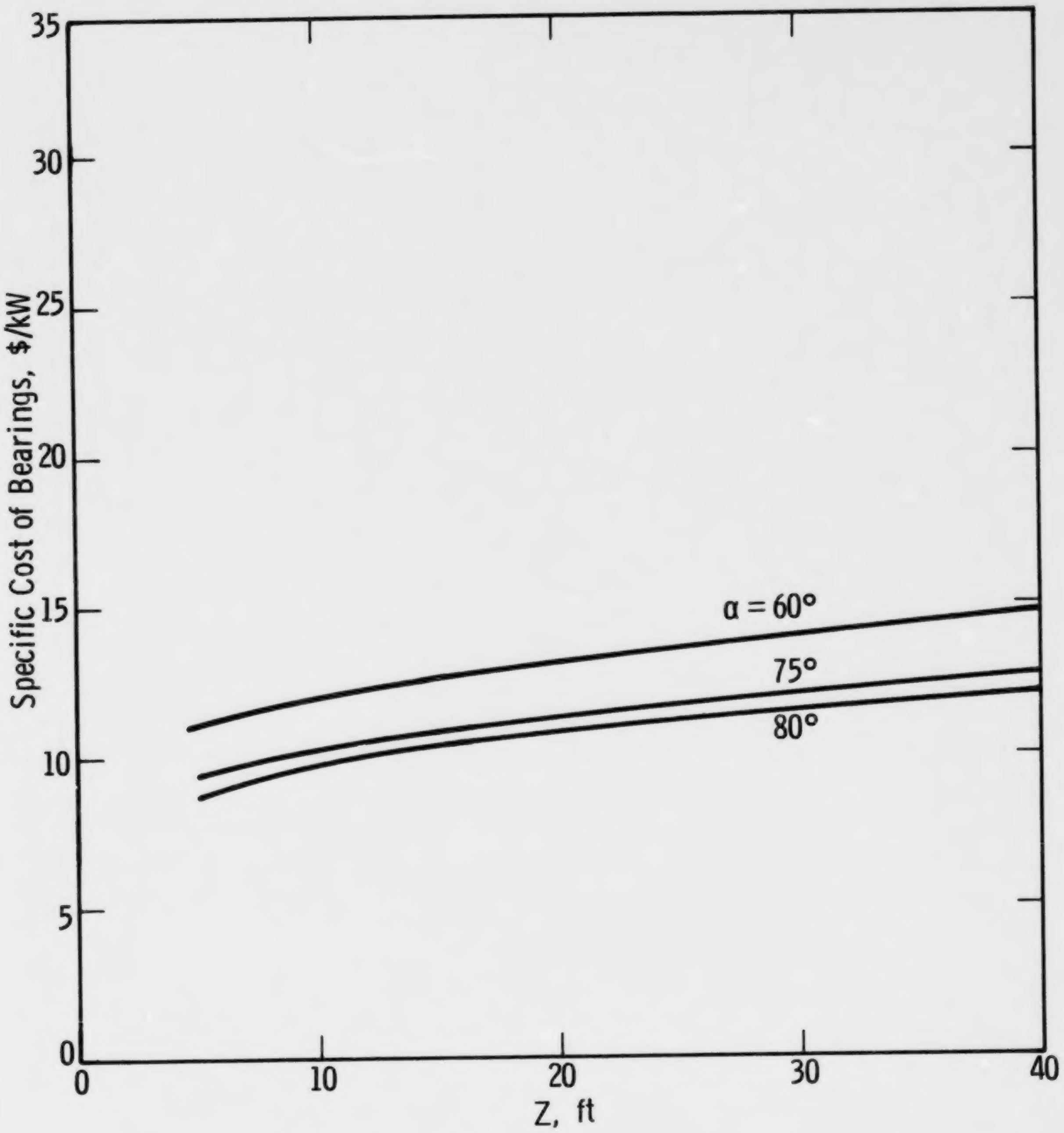

Fig. 3.18—Estimated cost of bearings for centrifuge cascade made of CS glass and D.E.N. 439 resin

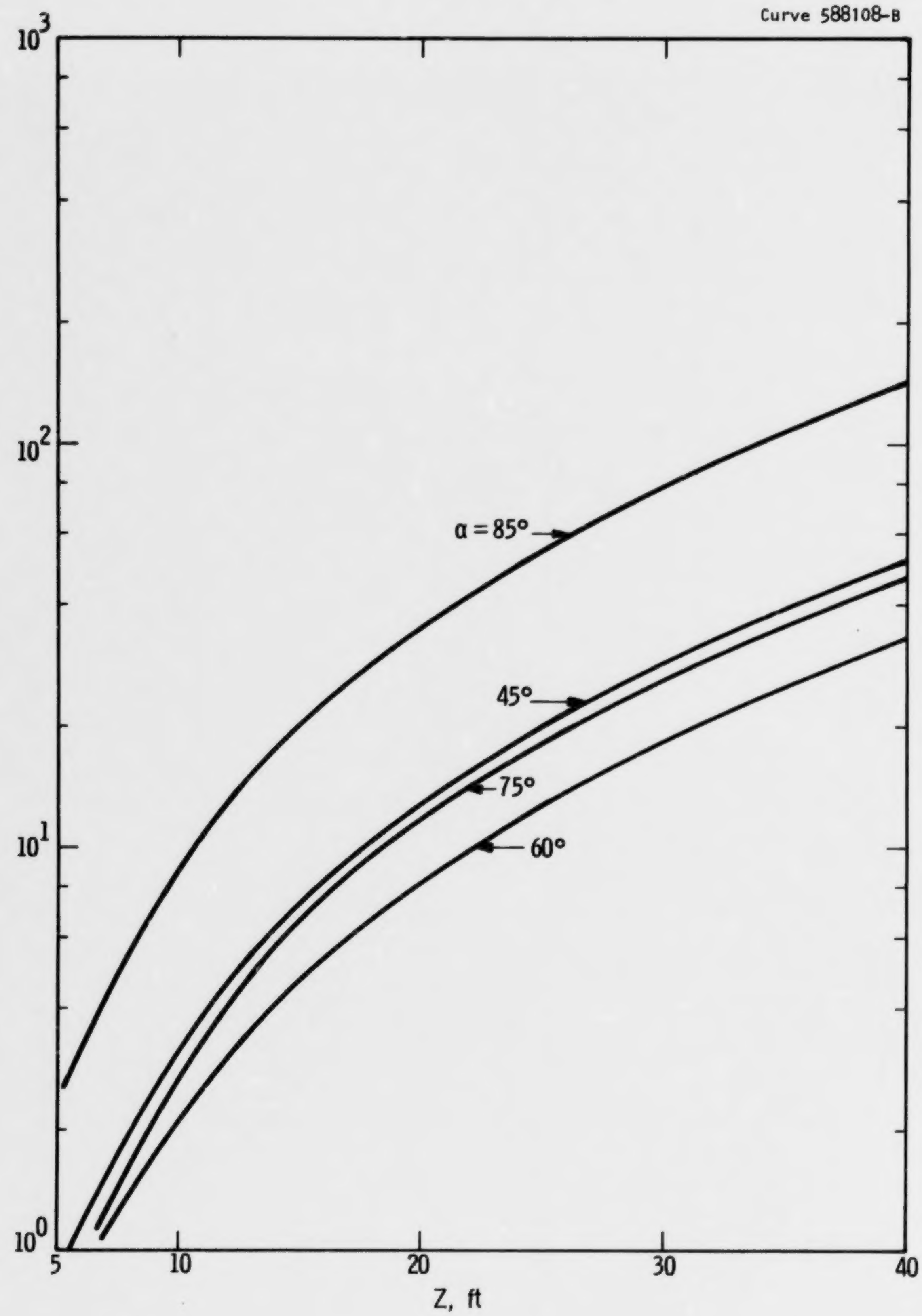

Fig. 3.19 —Estimated cost of material in centrifuges made of CS glass and D.E.N. 439 resin

Curve 588102-A

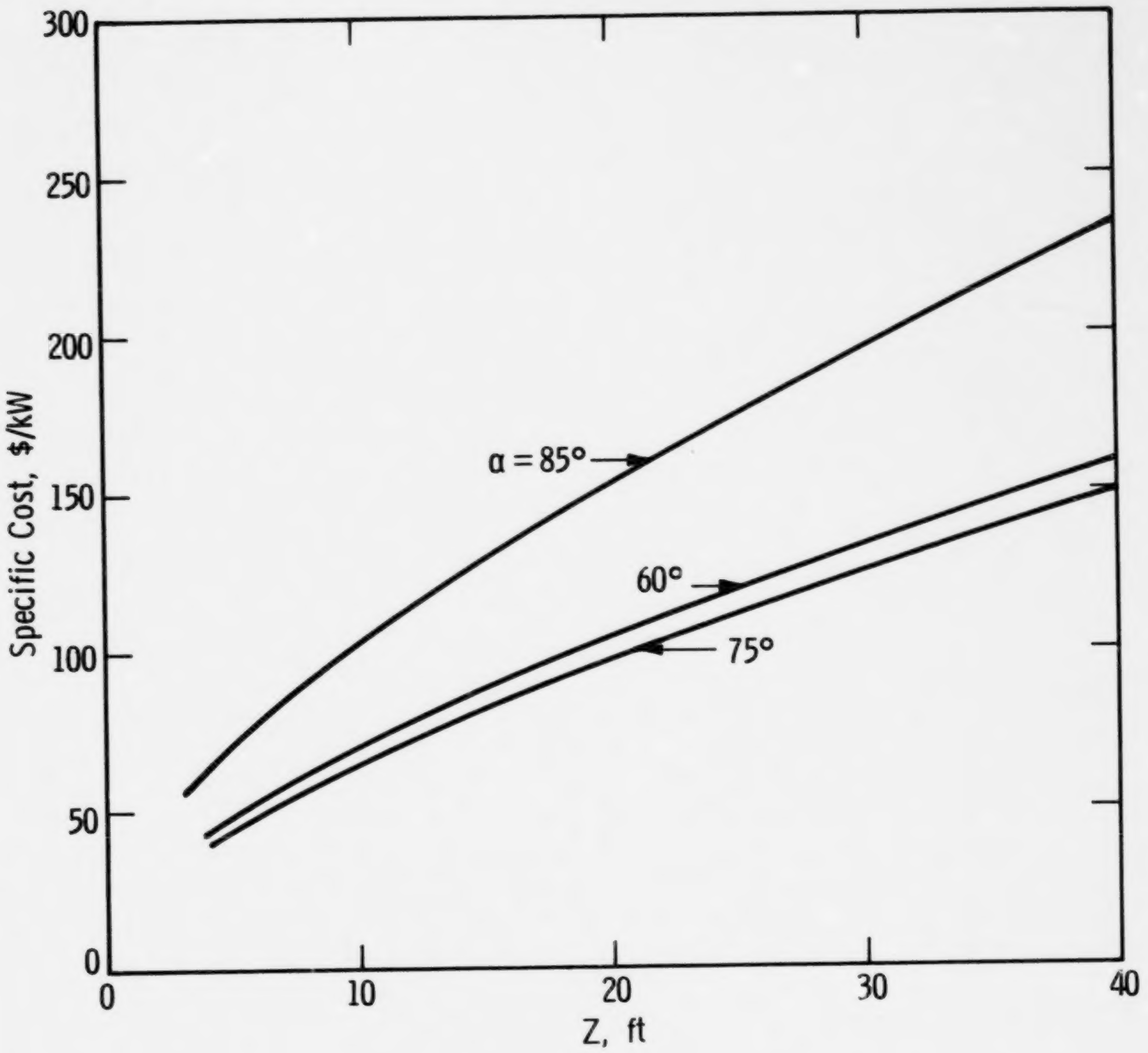

Fig. 3.20—Estimated purchase cost of vacuum chambers in centrifuge cascade made of CS glass and D.E.N., 439 resin

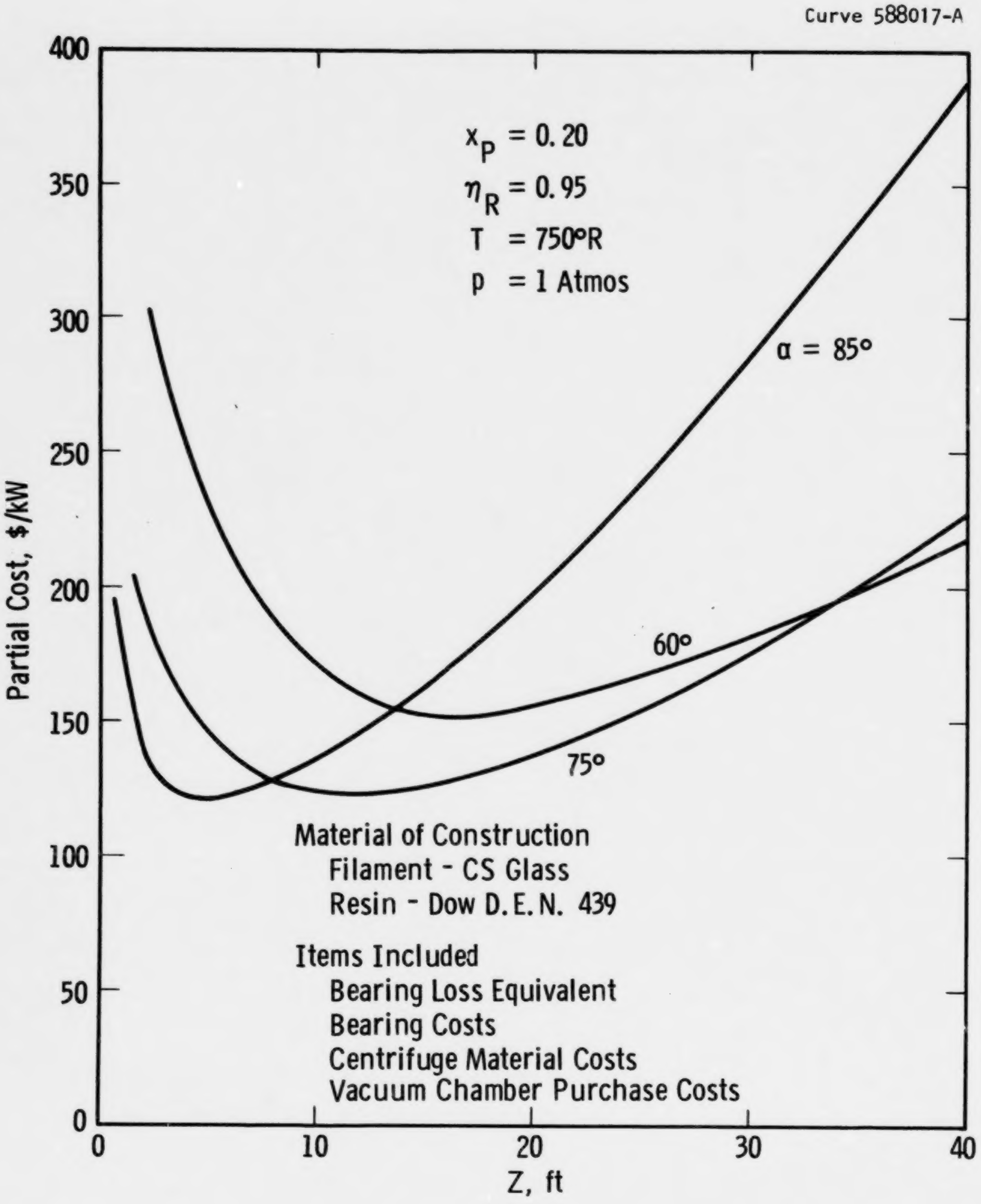

Fig. 3.21—Partial costs of centrifuge cascade system for 500 power plant

Curve 588011-A

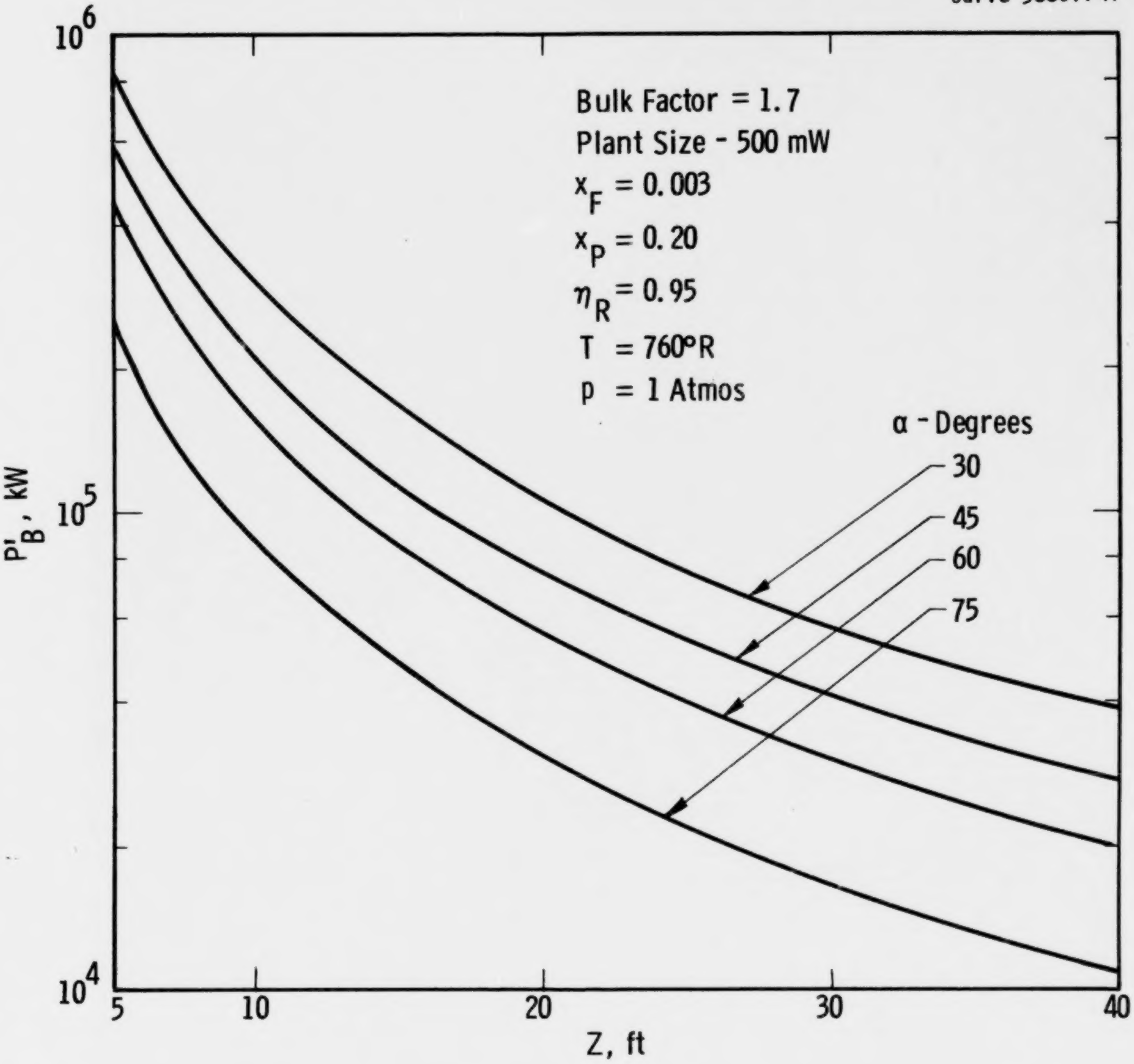

Fig. 3.22—Centrifuge bearing power requirement for cascade of centrifuges made of filament wound S glass and Dow D.E.N. 439 resin

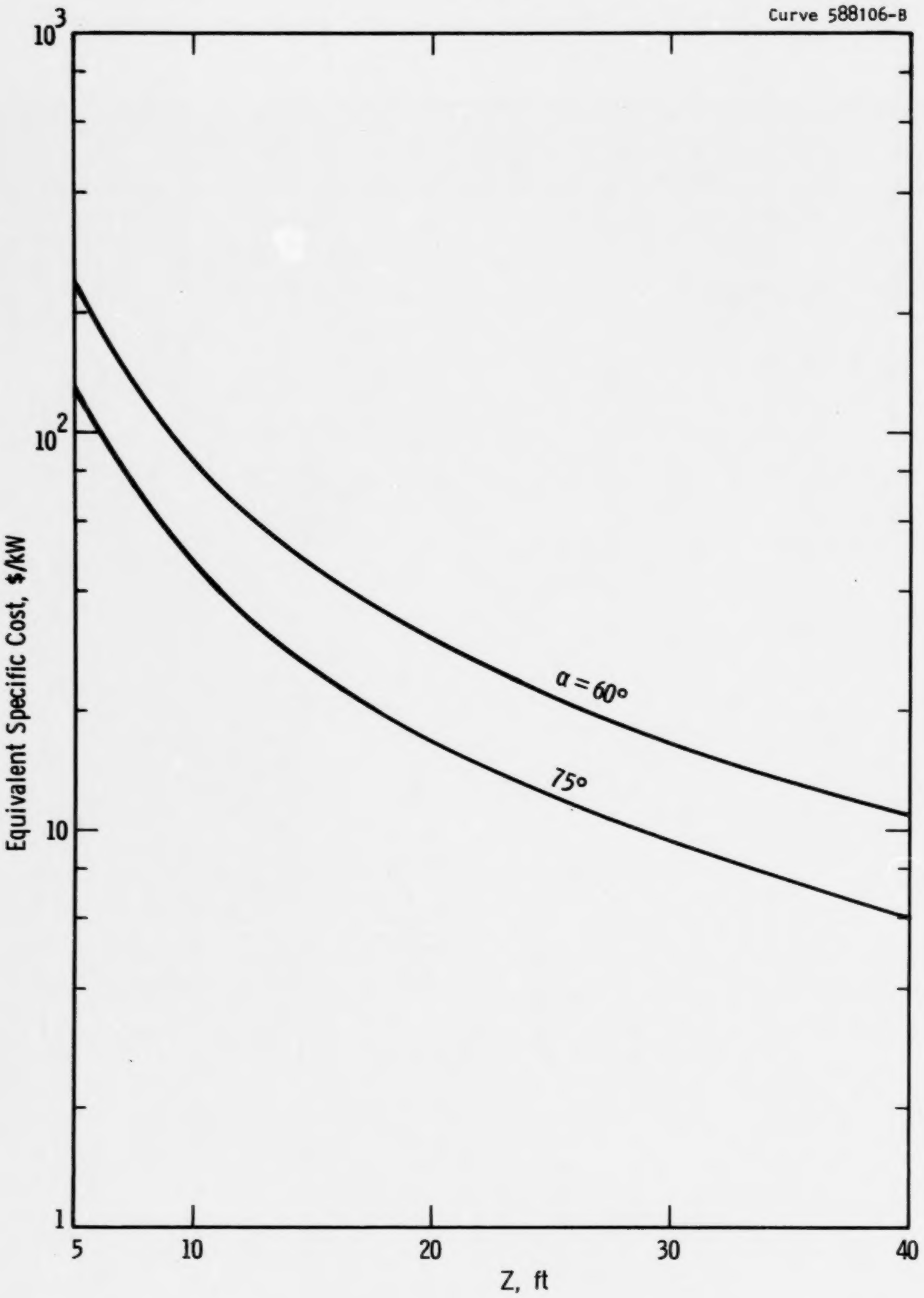

Fig. 3.23—Capital cost equivalent of bearing losses in cascade of centrifuge made of S glass and D.E.N. 439 resin

Curve 588009-A

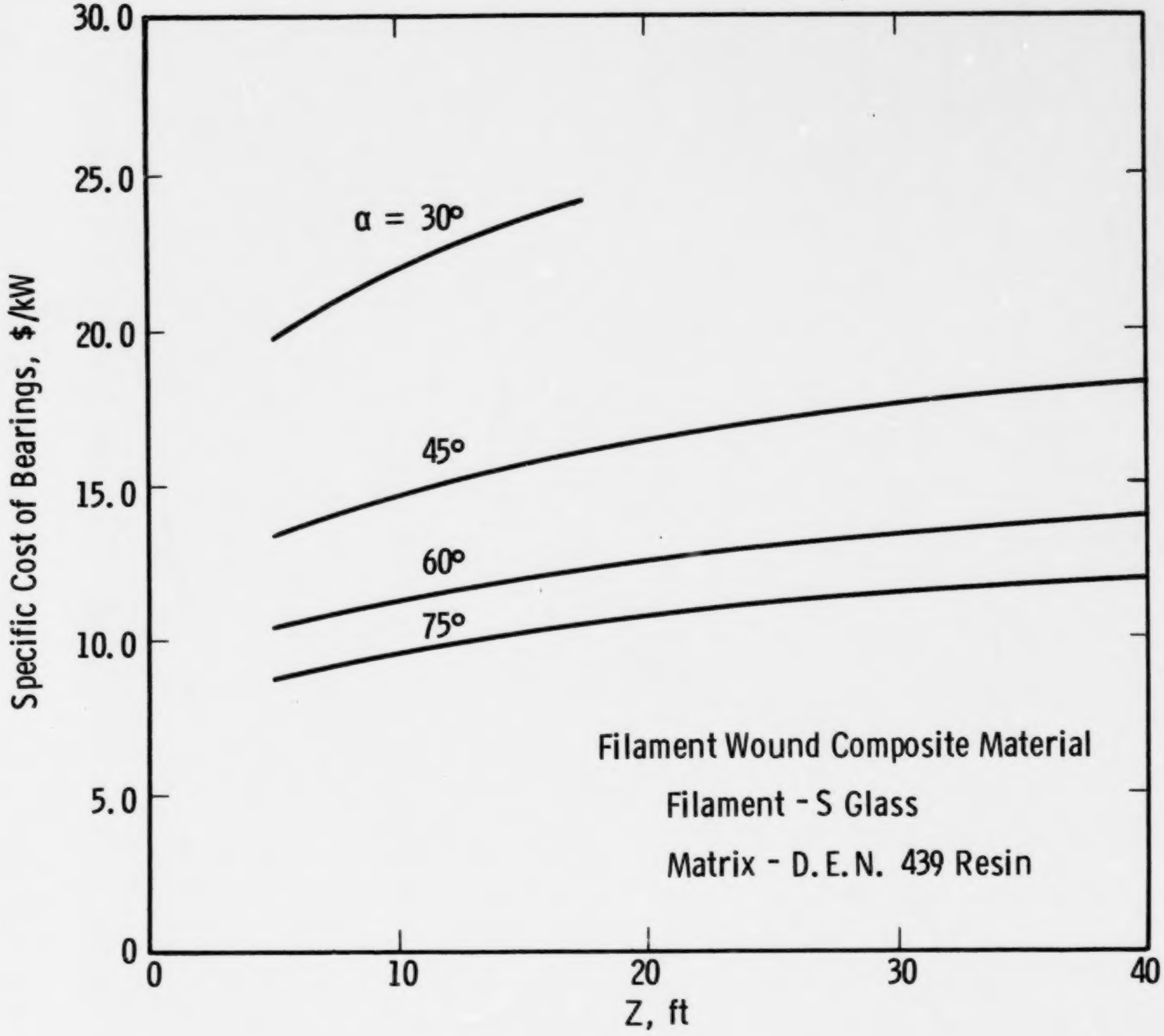

Fig. 3.24—Estimated cost of bearings for centrifuges in cascade for 500 mW power plant

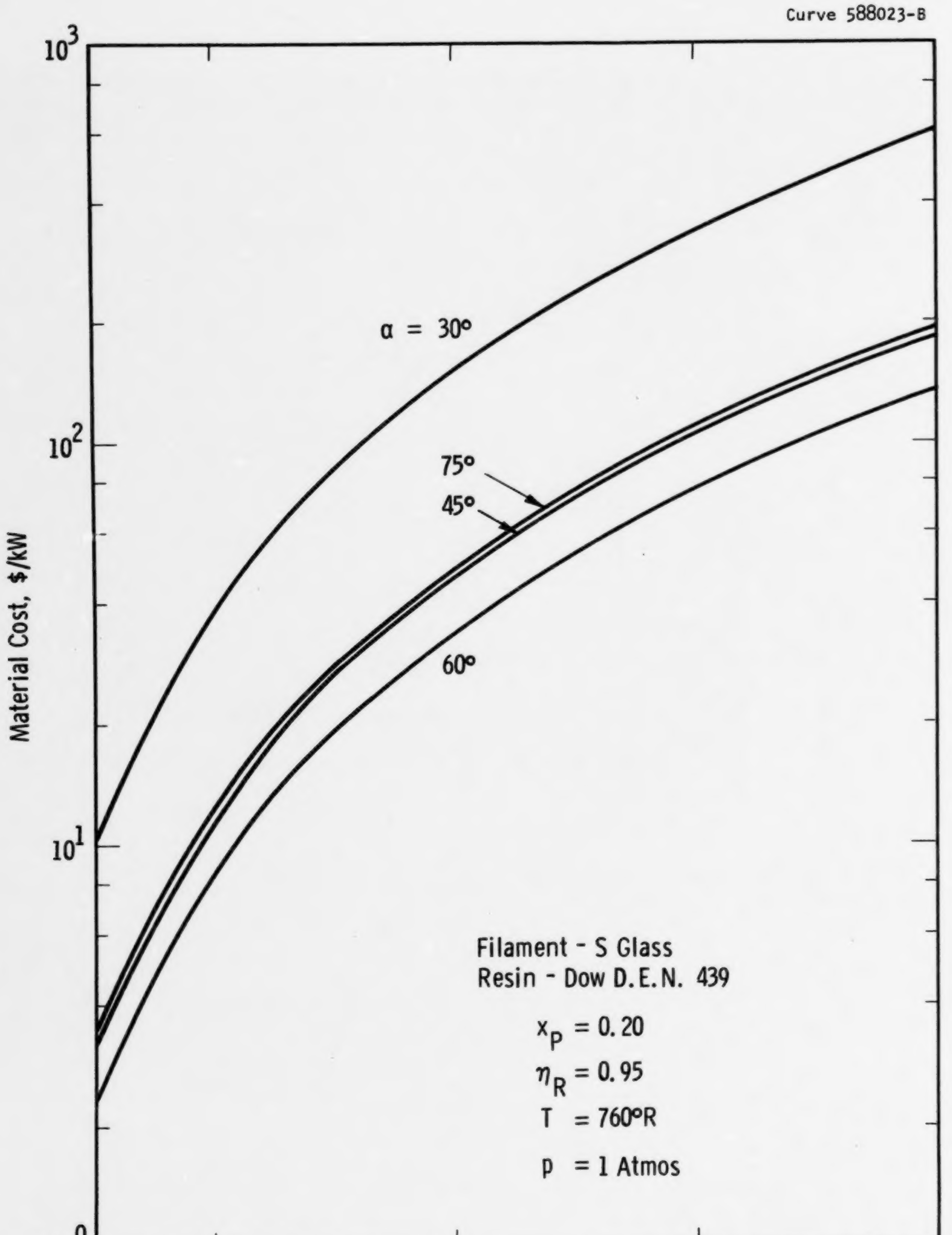

Fig. 3.25—Estimated cost of composite material required in centrifuge cascade for 500 mW power plant

Curve 588099-A

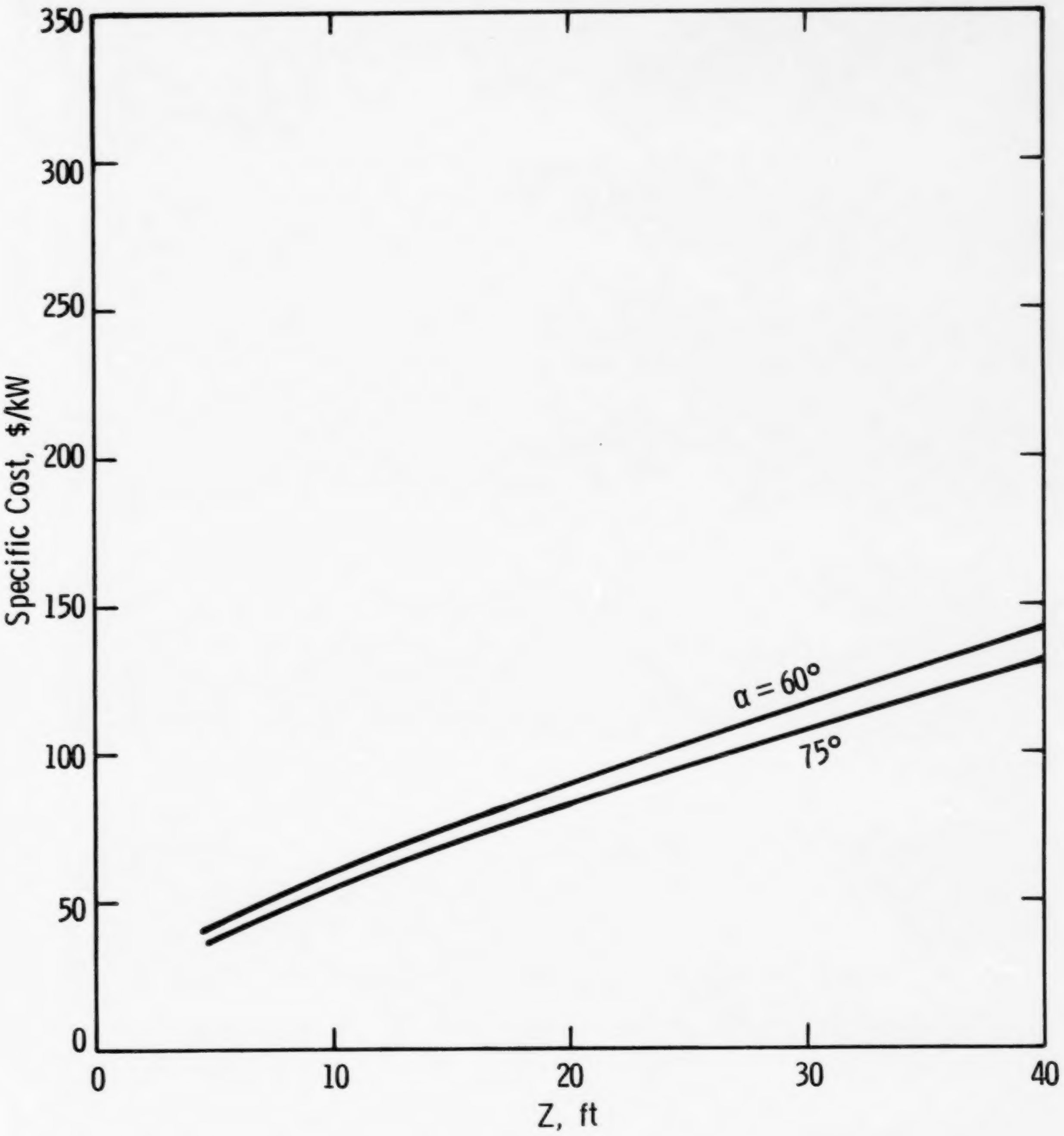

Fig. 3.26—Estimated figure purchase cost of vacuum chambers in centrifuge cascade made of S glass and D.E.N. 439 resin

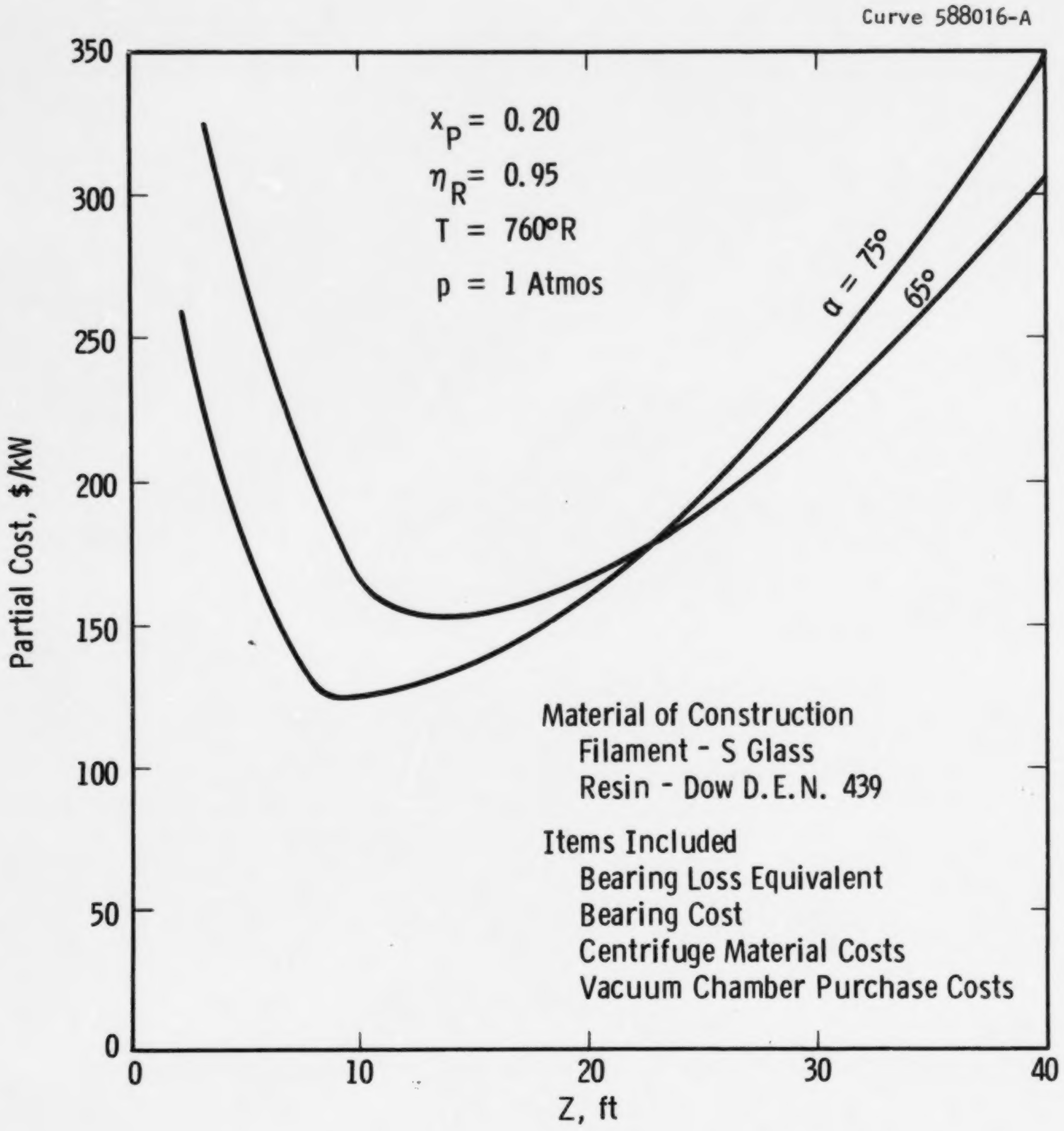

Fig. 3.27 —Partial costs of centrifuge cascade system for 500 mW power plant

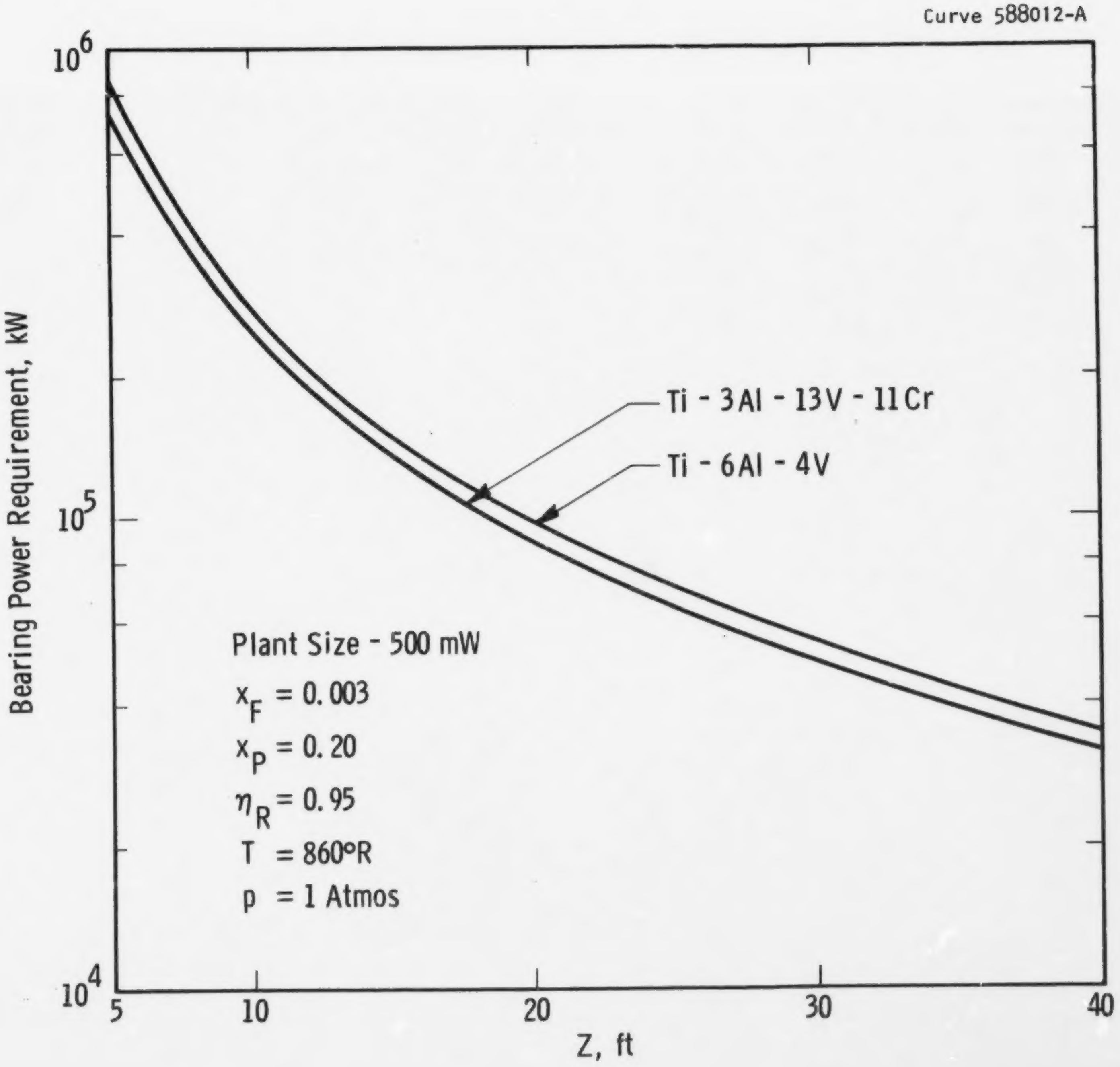

Fig. 3.28—Centrifuge bearing power requirement for cascade of centrifuges made of titanium

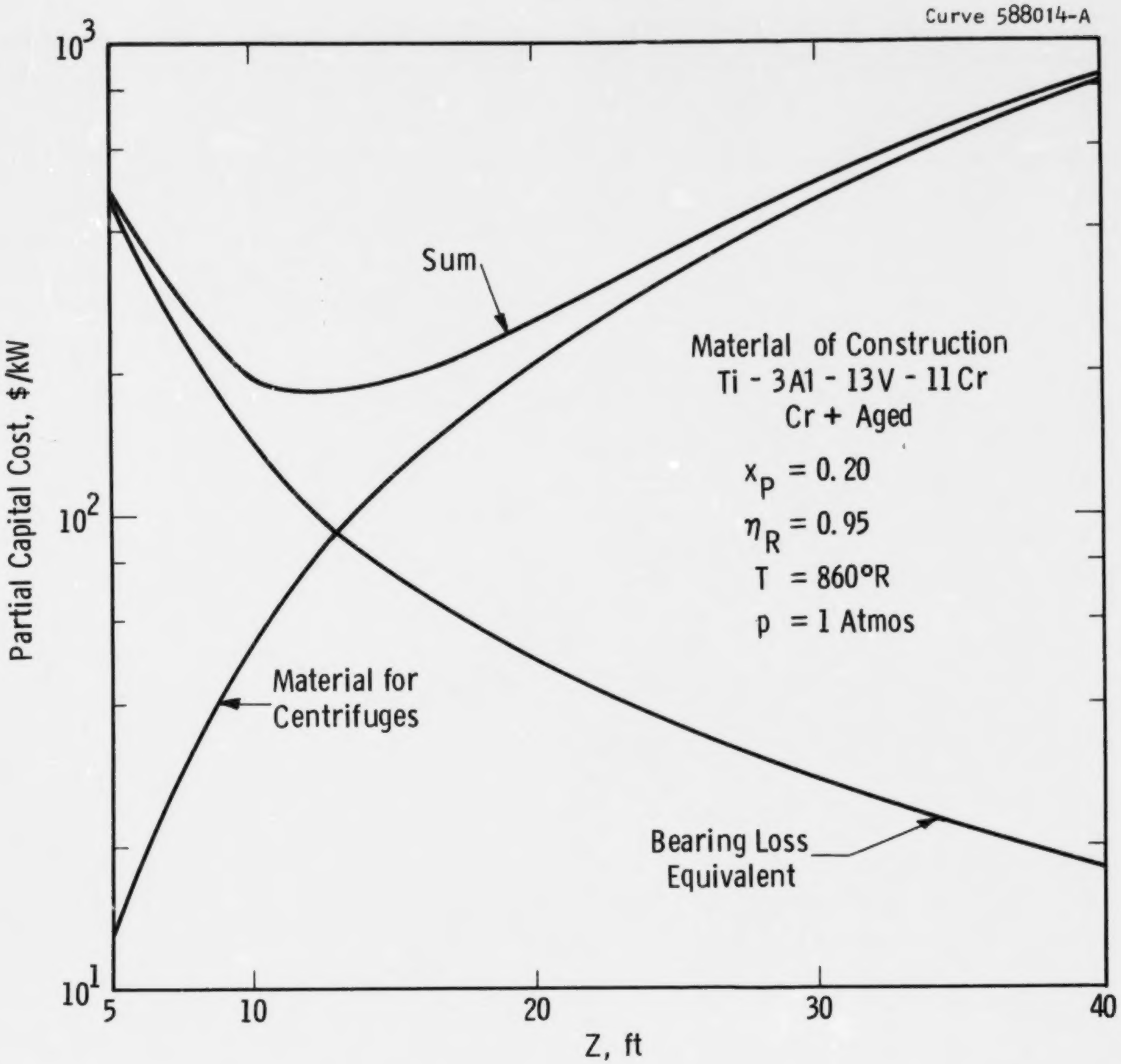

Fig. 3.29 —Partial cost of centrifuge cascade system for 500 mW power plant

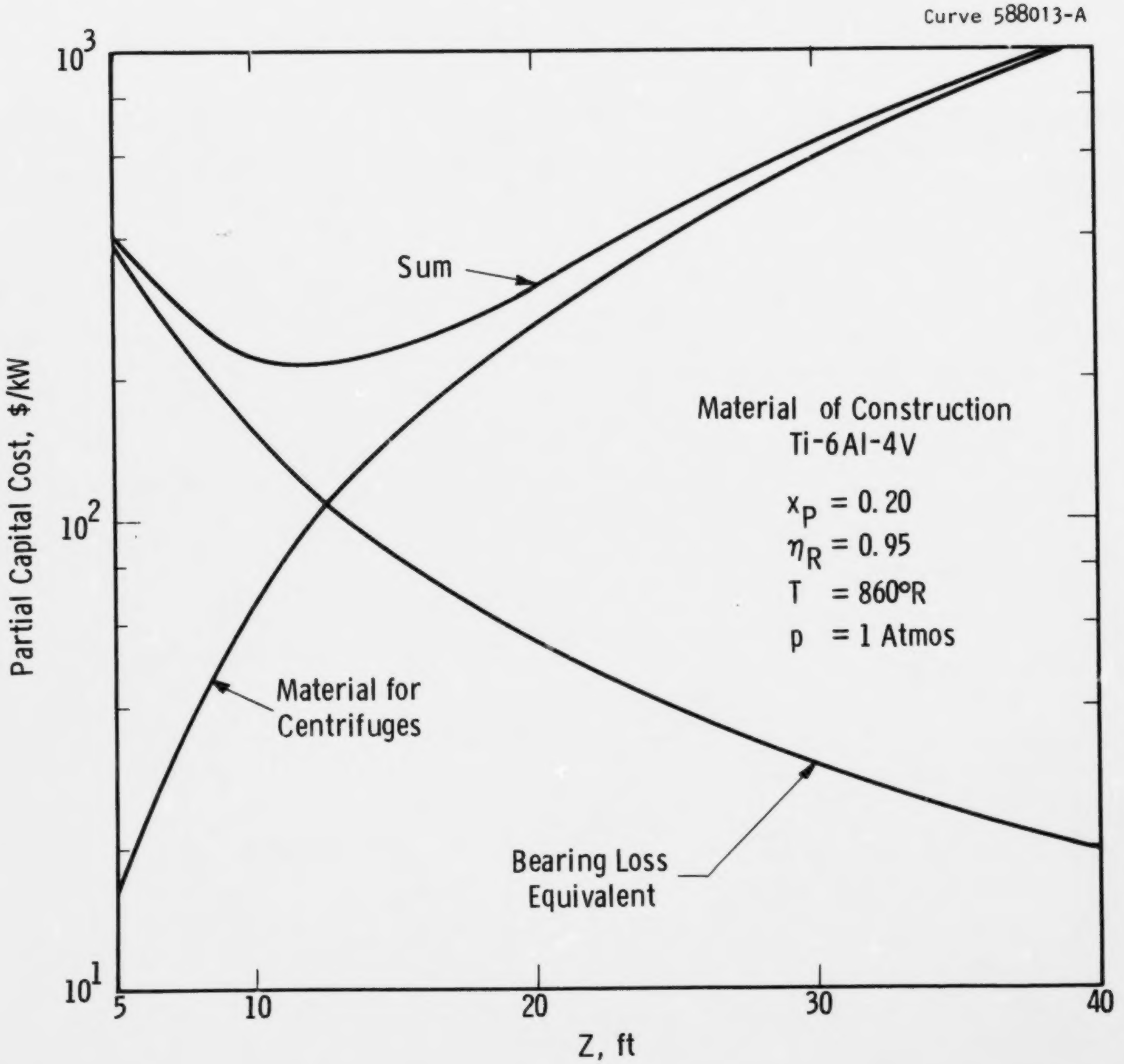

Fig. 3.30—Partial cost of centrifuge cascade system for 500 mW power plant

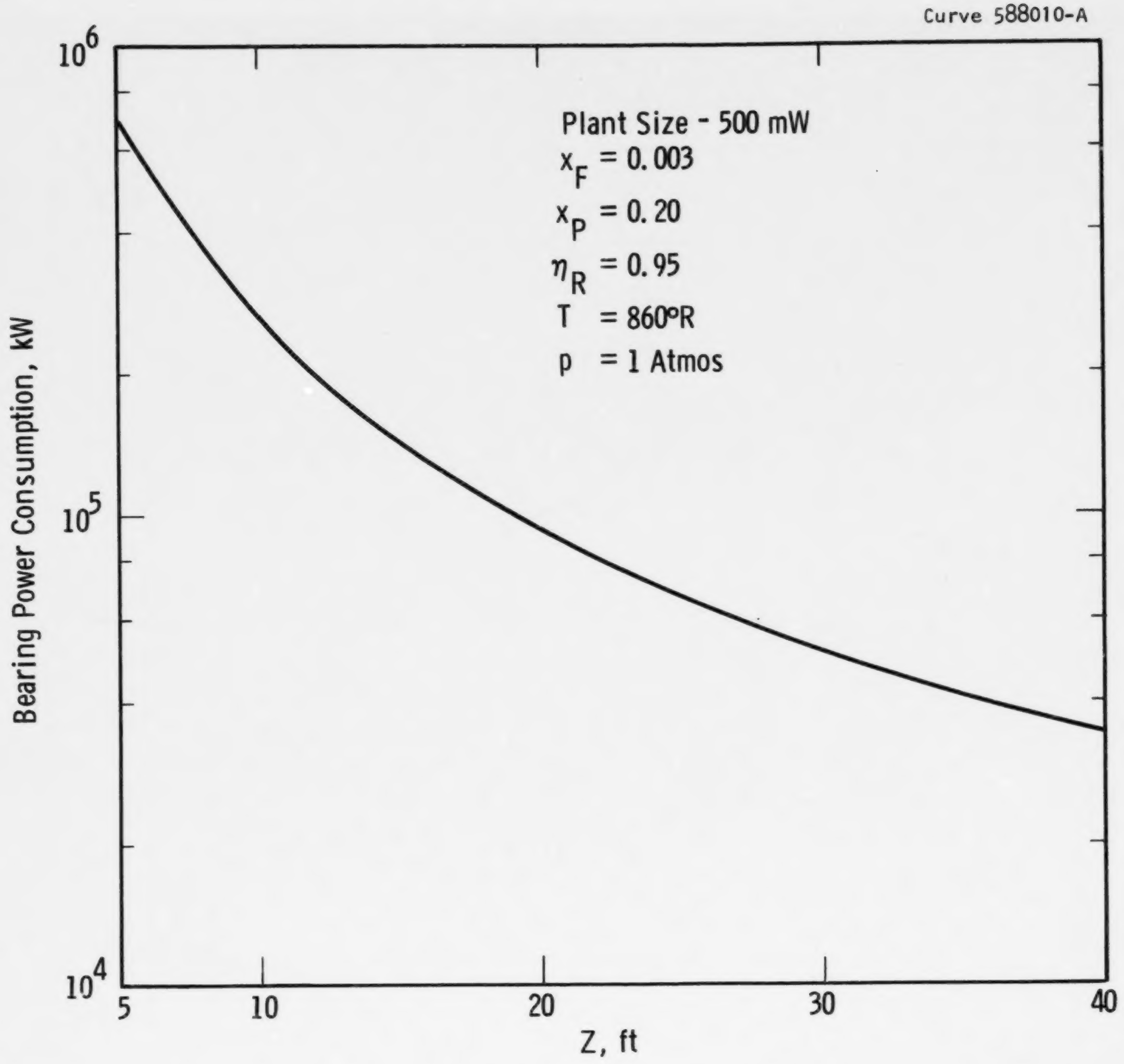

Fig. 3.31 —Centrifuge bearing power requirement for cascade of centrifuges made of 18% Ni maraging steel

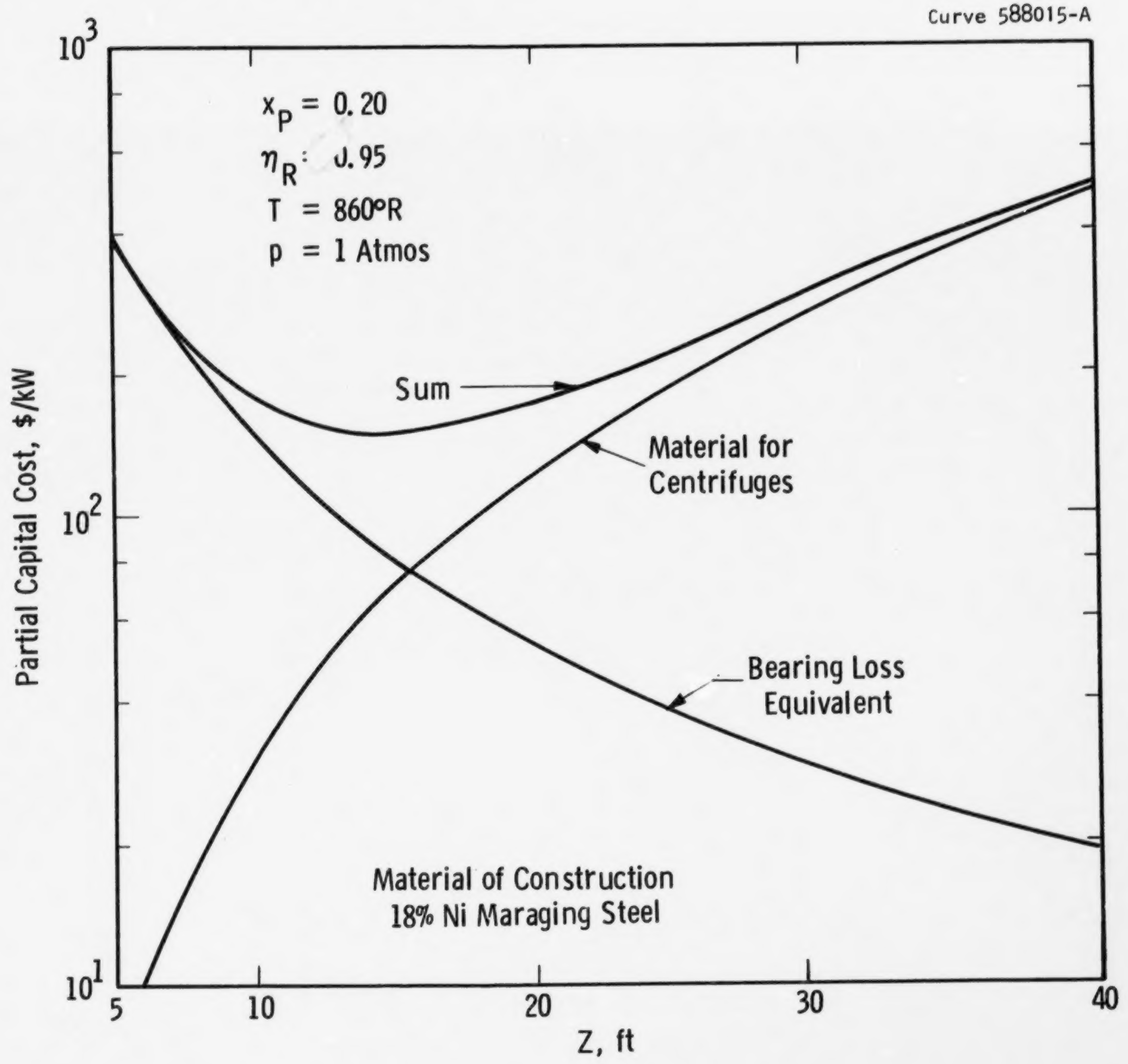

Fig. 3.32—Partial cost of centrifuge cascade system for 500 mW power plant

References

(1) F. A. Lindemann and F. W. Aston; Phil. Mag.[6] 37, 523, (1919).

(2) R. S. Mulliken; J. Am. Chem. Soc. 44, 1033, 1729, (1922); 45, 1592, (1923).

(3) W. D. Harkins; J. Frank. Inst. 194, 783, (1922).

(4) S. Chapman; Phil. Mag. [6] 38, 182, (1919); Phil. Trans. A217, 115, (1918).

(5) J. Joly and J. H. J. Pool; Phil. Mag. [6] 39, 372, (1920); 41, 818, (1921).

(6) J. W. Beams and F. B. Haynes; Phys. Rev. 50, 491, (1936).

(7) J. W. Beams and A. V. Masket; Phys. Rev. 51, 384, (1937).

(8) J. W. Beams; J. Appl. Phys. 8, 795, (1937); Phys. Rev. 55, 591, (1939).

(9) J. W. Beams; Revs. Mod. Phys. 10, 245, (1938).

(10) J. W. Beams and C. Skarstrom; Phys. Rev. 56, 266, (1939).

(11) K. Beyerle, W. E. Groth, E. Nann and K. H. Welge; Proc. 2nd. Int. Conf. Peaceful Uses Atomic Energy, 4, 439, (1958). Proc. Int. Symp. Iso. Sept., N. Holland Publ. Co., Amsterdam, (1956).

(12) J. Kistemaker, J. Los, and E. J.J. Veldhuyzen; Proc. 2nd. Int. Symp. Iso. Sep., N. Holland Publ. Co., Amsterdam, (1956).

(13) W. Bulang, W. Groth and E. Nann; Z. Physik Chem. 25, 283, (1960).

(14) G. Zippe; Report No. EP-4420-101-60U, (1960), Research Laboratories for the Engineering Sciences, University of Virginia, Charlottesville, Virginia.

(15) Cohen, Karl; "The Theory of Isotope Separation as Applied to the Large-Seale Production of U^{235}, McGraw-Hill, New York, 1951, p. 103.

(16) Kirk-Othmer; Encyclopedia of Chemical Technology - Second Edition Vol. 7, Interscience Publishers, New York, 1965, p. 156.

(17) Bulang, W.; et al "On the Separation Potential of Thermally Driven Countercurrent Gas Centrifuges," Report No. EP-4422-117-60U, Sept. 1960, Res. Lab. for the Eng. Sciences, University of Virginia.

(18) Kirk-Othmer; Encyclopedia of Chemical Technology - Second Edition, Vol. 7, Interscience Publishers, New York, 1965, p. 159.

(19) Kirk-Othmer; Encyclopedia of Chemical Technology - Second Edition, Vol. 7, Interscience Publishers, New York, 1965, p. 84.

(20) Ibid, p. 87.

(21) Martin, H., Z. Elektrochem; Vol. 54, pp. 120-129 (1950).

(22) Benedict and Pigford; "Nuclear Chemical Engineering," McGraw-Hill, New York, 1957, Appendix B.

(23) Personal Communications with Burnswick Corporation. Lincoln, Nebraska.

3.4 Separation of SO_2 from Flue Gases by Condensation

Separation of gases may be carried out by condensation of the high-boiling component or components. In current practice, primary purification of the mixture is usually necessary in order to remove impurities such as water vapor or CO_2 and several stages of condensation are used depending on the gas mixture. With mixtures at high pressure, the Joule-Thomson effect or expansion of the gases in a turbine are possible sources of refrigeration. These processes may be restricted by solid deposition if the higher boiling component is below its triple point. Solids removal in heat exchangers may be effected by using reversing or switching heat exchangers.

In analysing the SO_2 separation problem, the flue gas composition as specified in the RFP for this contract, is selected and listed below together with partial pressures (total pressure 1 atm) and corresponding saturation temperatures. Saturation properties of SO_2 and CO_2 are given in Appendix 6.8.

Component	% by Volume	Partial Pressure psia	Saturation Temperature °F
N_2	74.9	11.000	- 324
CO_2	14.7	2.160	- 147
H_2O	7.3	1.073	104
O_2	2.8	0.411	- 341
SO_2	0.3	0.044	- 140

It can be seen from the values of the saturation temperatures that SO_2 will start to condense at -140°F while CO_2 will precipitate out as a solid at -147°F. Thus any condenser for liquid SO_2 must be capable of removing the solid CO_2 as well. If specifications of 95% removal of SO_2 are adhered to, the partial pressure of SO_2 in the flue gas should be 0.0022 psia with the corresponding saturation temperature of -194°F. Assuming that the gases are cooled to -194°F, 99.5% of the CO_2 would separate out as a solid. With the large volumes of CO_2 present in the flue gases, solids removal from a condenser would indeed be a formidable task. Reversing heat exchangers, which are commonly used in gas purification plants, cannot be used in the SO_2 separation case because they would employ the process gases leaving the plant to re-evaporate the CO_2 and SO_2 deposits. The use of multiple heat exchanger units and switching techniques would also present the problem of separating the SO_2 and CO_2 that condensed out. Thus, it may be seen that the relatively large percentage of CO_2 in the flue gas has compounded the problems in using condensation techniques for SO_2 separation. In fact, the technical feasibility of using heat exchangers with large amounts of solids separation is highly questionable. It must be mentioned here that the use of scrubbing or sorption methods for removing H_2O and CO_2 prior to condensation of SO_2 have not been considered as these very methods may be used for SO_2 removal in the first place.

In order to more aptly illustrate the difficulties involved and to develop a feel for their magnitude, three flow diagrams will be considered using outside refrigeration, the Joule-Thomson effect and in Figures 3.33, 3.34 and 3.35 respectively. The temperature levels and cost estimates are merely illustrative and should not be considered exact. estimates are merely illustrative and should not be considered exact. It is assumed the flue gas leaves the precipitator or bag filter house at 300°F with a flow rate of 10^6 SCFM which corresponds approximately to a 500 MW plant. It should be stated here that in the following analysis, the effect of N_2 on the phase equilibria of the other components has not been considered.

I. Cryogenic Refrigeration

Figure 3.33 presents a flow diagram where the primary refrigerating effect is provided by an outside refrigerant, say N_2. Consider each unit individually.

High Temperature Recuperator

The primary purpose of this heat exchanger is for H_2SO_4 removal from the incoming flue gas and the reheating of the stack gases. The fraction of SO_3 in the flue gas is assumed to be 1.5% of the SO_2 fraction and gives an acid dew point of 221°F. Experimental investigations have indicated that the acid deposition rate reaches a maximum at surface temperatures of about 120°F below the acid dew point. The flue gas exit temperature is thus selected at 100°F.

Total heat transfer surface required based on an overall coefficient of 10 BTU/hr. $ft^2F = 4.3 \times 10^5\ ft^2$

High temperature recuperator costs (based on \$10 per ft^2) $= \$4.3 \times 10^6$

Compressor and Aftercoolers

The compressor provides for the pressure drop in the heat exchangers which is assumed to be 15 psia.

HP required = 50,000

Compressor costs (at \$200/HP installed) = $\$10 \times 10^6$

Surface area of aftercooler = $1.8 \times 10^5\ ft^2$

Cost of aftercooler at $\$10/ft^2 = \$1.8 \times 10^6$

Low Temperature Recuperator

This heat exchanger condenses water at the rate of 2700 lb_m/min with 100 lb_m/min of ice formation on the low temperature surfaces. Therefore multiple units in parallel must be provided to enable them to be switched for solids removal. The heat exchangers have been depicted in two stages.

Surface area required = $3.8 \times 10^5\ ft^2$

Cost of low temperature recuperators with 25% extra capacity for switching = $\$5.0 \times 10^6$

SO_2 Condenser

The condenser must be capable of handling the 487 lb_m/min of liquid SO_2 and in addition about 14,000 lb_m/min of solid CO_2. The technical feasibility of heat exchangers to handle such large amounts of solid formation is questionable. Even with multiple units in parallel the onstream time of each unit could not be more than 4 minutes, while the time required for each unit to get back on the line is estimated to be in excess of an hour. This makes the system impractical. With regard to the refrigerant, the cost of N_2 to effect the required cooling amounts to \$50,000 per hour and with a normal operation of 8000 hours per year, the yearly cost of N_2 alone would be \$400 x 10^6.

It seems evident that the cost of refrigerant and the problem of solid CO_2 removal from the heat exchangers would eliminate this system from further consideration.

II. The Joule-Thomson Effect

With a view to obviating the problem of solid CO_2 deposits in the heat exchangers, the possibility of freezing out the CO_2 in the stream together with the liquid SO_2 and collecting both with a conventional solids cyclone separator was considered. This method has been used for removing CO_2 from natural gas by a Joule-Thomson expansion. In this case the natural gas is already at an elevated pressure and methane has a large J-T cooling effect. A schematic of a possible system for the case of SO_2 removal is shown in Figure 3.34.

In order to produce refrigeration by a J-T expansion, the initial state of the fluid must be such that its isothermal enthalpy change on expansion is an increase. On examining a pressure-enthalpy diagram for N_2 and methane, it becomes clear that the isothermal enthalpy change for the same conditions is much larger in the case of methane than in the case of N_2, indicating a much smaller J-T cooling effect with N_2. In the case of the flue gases, the temperature after a J-T expansion is fixed because the requirement of 90% or 95% removal of SO_2 fixes the SO_2 partial pressures and the corresponding temperatures at -182°F and -194°F respectively. In order to avoid deposition of solid CO_2 in the heat exchangers, the temperature of the flue gas cannot be decreased below the triple point temperature of CO_2 which is -69.9°F. Therefore the temperature before the expansion valve is fixed at -65°F. With the temperature before expansion restricted thus, the flue gas pressure would have to be in excess of 250 atm. in order to give the required cooling and meet the specification of 95% SO_2 removal.

Figure 3.34 indicates that if the flue gas is compressed to 250 atm., the resulting temperature after the J-T expansion would be -170°F which would correspond to 80% removal of SO_2. The solids cyclone separator would have to be capable of collecting 1000 lb_m/min of solid CO_2 and 13 lb_m/min of liquid SO_2, with most of the CO_2 and SO_2 condensing out as liquid in the heat exchangers. Further discussion of the heat exchanger design costs is not warranted when faced with the prospect of compressing the flue gas to pressures over 250 atm. with resulting compressor costs alone in excess of $\$100 \times 10^6$. Therefore it is felt that this system does not merit further consideration.

III. The Expansion Turbine

A considerably larger cooling effect may be obtained with an isentropic expansion in a turbine than with an isenthalpic expansion, with some of the work of compression returned as useful work in the turbine. Thus the pressure to which the flue gases would have to be compressed, to obtain the desired temperature after expansion, would be much lower.

A flow diagram incorporating an expansion turbine is shown in Figure 3.35. As indicated, compression of the flue gases up to 20 atm. would be required to obtain the low temperature of -194°F and meet the specification of 95% SO_2 removal, assuming a turbine efficiency of 70%. However a difficulty arises in that solid CO_2 and liquid SO_2 would be precipitated out in the turbine. Erosion of the turbine blades could be a serious problem. It is also possible that build up of solid CO_2 on the blade surface could lead to mechanical failure and breakdown of the unit. The turbine blades would have to be specially designed to withstand the erosion from solid particles. Technical feasibility of such a turbine design should rightly be a separate study. However the capital costs involved in compressing the flue gas even to 20 atm. do not look encouraging and this method will likewise be eliminated.

In addition to the above three methods, scrubbing the flue gases with liquid N_2 was considered. Here again, in order to reduce the N_2 load, low temperature refrigeration would be needed prior to the scrubbing operation, and the process economics would not enable scrubbing to compete with current processes now in use.

In conclusion it may be said that there are two main difficulties with the use of condensation techniques for the removal of SO_2 from flue gases, namely, solids formation in heat exchangers and turbines, and the high cost of providing low temperature refrigeration. In view of the above, it may be stated that condensation techniques for the removal of SO_2 from flue gases do not show any promise.

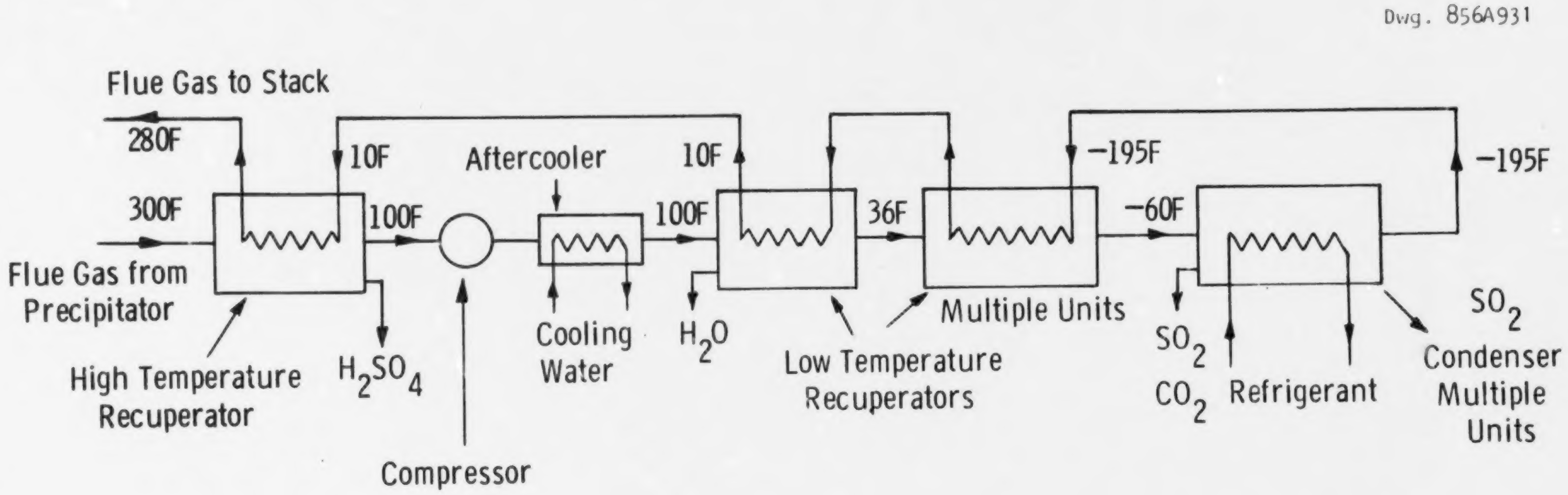
Dwg. 856A931
Flue Gas to Stack
280F
300F
Flue Gas from Precipitator
High Temperature Recuperator
10F
100F
H_2SO_4
Compressor
Aftercooler
Cooling Water
10F
100F
H_2O
36F
Low Temperature Recuperators
Multiple Units
−195F
−60F
SO_2
CO_2
Refrigerant
−195F
SO_2 Condenser Multiple Units

FIG. 3.33 - Flow Diagram For SO_2 Removal Using Cryogenic Refrigeration

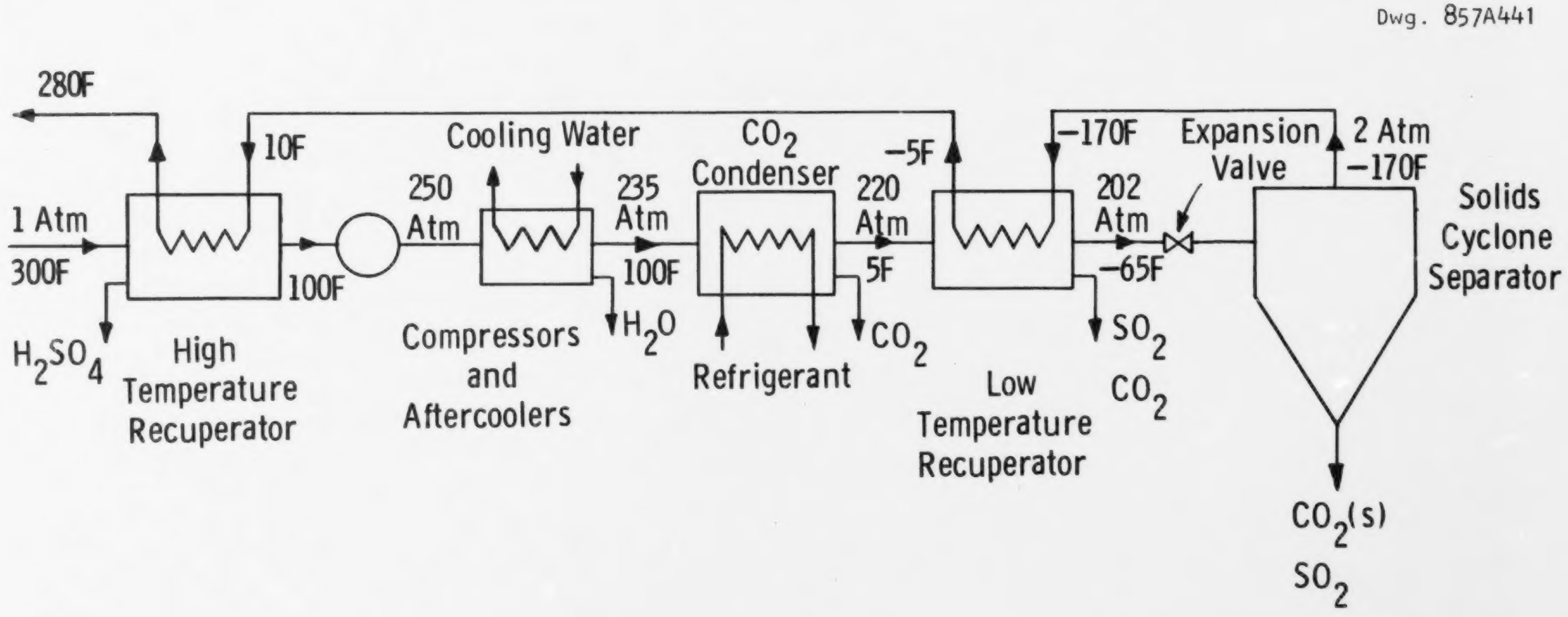
Dwg. 857A441
280F
10F
1 Atm
300F
H_2SO_4
100F
High Temperature Recuperator
250 Atm
Cooling Water
Compressors and Aftercoolers
235 Atm
100F
H_2O
CO_2 Condenser
Refrigerant
220 Atm
5F
CO_2
−5F
Low Temperature Recuperator
−170F
202 Atm
−65F
SO_2
CO_2
Expansion Valve
2 Atm
−170F
Solids Cyclone Separator
$CO_2(s)$
SO_2

FIG. 3-34 - Flow Diagram for SO_2 Removal Using Joule-Thompson Effect.

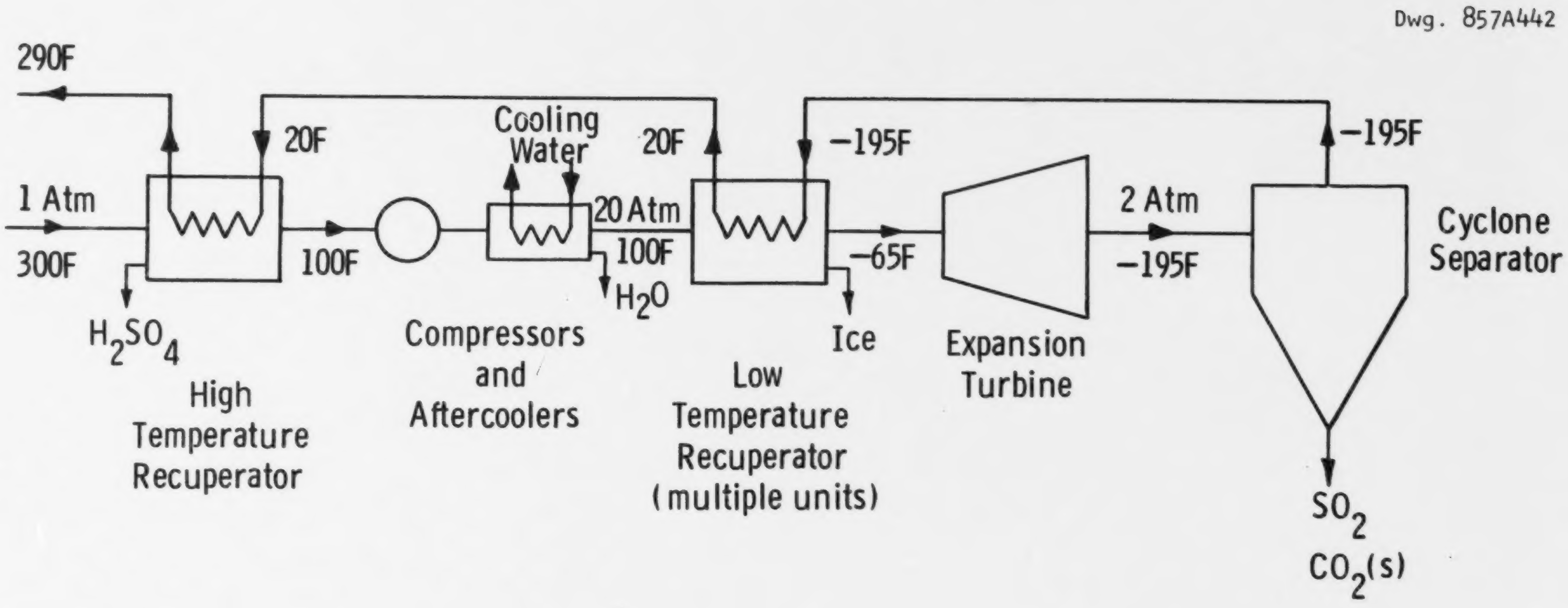
Dwg. 857A442
290F
1 Atm
300F
20F
H_2SO_4
High Temperature Recuperator
100F
Cooling Water
20 Atm
100F
H_2O
Compressors and Aftercoolers
20F
−195F
−65F
Ice
Low Temperature Recuperator (multiple units)
Expansion Turbine
2 Atm
−195F
−195F
Cyclone Separator
SO_2
$CO_2(s)$

FIG. 3-35 - Flow Diagram for SO_2 Removal Using Expansion Turbine

3.5 Feasibility Analysis of Mass Spectrometer for Removal of SO_2 From Flue Gases

In 1940 the mass spectrograph was used by Neir to separate the minute quantities of uranium isotopes used to experimentally establish thermal-neutron fission of uranium.(1) Later, Lawrence at the University of California developed a mass spectrometer of greatly increased capacity for use in separation of uranium isotopes, and a number of these were installed at the Oak Ridge isotope separation plant.(2) However, this plant was taken off uranium isotope separation when the gaseous diffusion plant proved to be less costly.

The method is widely used today in isolating small quantities of isotopes for research use.(2) It is well suited for this since the mass spectrometer can be used for the separation of all elements from hydrogen to uranium.

The mass spectrometers which have been used for isotope separation have the following features which make them unattractive for large scale separation of a mixture of gases.(3)

1. It is a batchwise process. The cycle involves start-up, production, and cool-down.
2. The collector which is made of some material which can hold the product in a non-volatile form must be removed after each run or series of runs and sent to a chemical laboratory for product recovery.

It is thought that mass spectrometers could be developed for continuous operation. However, the output of a single mass spectrometer unit is very limited. Maximum ion beam currents achievable are in the range of $1\text{-}10 \times 10^{-3}$ amperes or $10^{-6}\text{-}10^{7}$ ions/sec which is equivalent to micrograms of material per second. In the case of pollutants at low concentrations this would be reduced by several orders of magnitude.

Other disadvantages of the mass spectrometer are:(3)

1. The recovery of the separated component per pass is poor.
2. The operating pressure is in the order of 2×10^{-5} mm of mercury.

In view of the above data on the mass spectrometer, it is concluded that the use of this method for large scale separation of SO_2 from flue gas is not feasible.

References

1. Smyth, Henry D., "Atomic Energy for Military Purposes," Princeton Univ. Press, 1945.
2. Benedict and Pigford, "Nuclear Chemical Engineering," McGraw-Hill, New York, 1957.
3. Perry, J. H., "Chemical Engineers Handbook-4th Ed.," McGraw-Hill, New York, 1963.

3.6 Feasibility Study on Magnetic Separation of SO_2 from Flue Gases

SUMMARY

The effects of a magnetic field on the transport properties of gaseous mixtures are reviewed. Although a magnetic field is known to influence selectively the diffusivities of different molecular species, it is unlikely that such effects could be used in a practical system for separation of components of effluent gas mixtures for the following reasons:

1. At the pressures considered, extremely large magnetic fields (10^5 to 10^6 gauss) would be required to obtain slight separation effects.

2. At the flow rates involved, the gas mixture is turbulent, and the eddy diffusivity, which is at least three orders of magnitude larger than the molecular diffusivities, will cause mixing which will wipe out any selective effects based on the molecular diffusivity.

3. The selective effects themselves appear from experiment to be dependent on the composition of the gaseous mixture; this leads to difficulties in analyzing and predicting results.

DETAILS

For many years, it has been known that the transport properties of gas mixtures, i.e., diffusivity, viscosity, and thermal conductivity, which respectively pertain to the transport of mass, momentum and energy by means of molecular collisions, may depend on externally applied forces. For instance, because of the gradient of atmospheric pressure with height as a result of the gravitational field, the heavier molecular components of the atmosphere tend to sink, and the lighter to rise (actually, the natural turbulence of the atmosphere, i.e., eddy diffusion, greatly masks this effect). Similar effects of this so-called "pressure diffusion" occur in the gas centrifuge. It is also known that thermal gradients applied to a gas mixture can result in differential transport of masses of the molecular species involved. This is the so-called thermal diffusion phenomenon. Differential transport may also result from differences in molecular accelerations resulting from external forces such as magnetic or electric fields, although these effects are expected to be small.

The formalism of the kinetic theory of nonuniform gases makes use of the so-called molecular velocity distribution function, $f(\vec{r},\vec{v},t)$, to describe the state of the gas, i.e., to make the connection from the microscopic molecular velocities ($\vec{v}$) and positions ($\vec{r}$) to macroscopic properties such as pressure, flow, temperature, etc. The functions $f(\vec{r},\vec{v},t)$ depend on the velocities and positions of the molecules, and not on their structure or other internal characteristics; $f(\vec{r},\vec{v},t)$ is determined as a solution to the well-known Boltzmann equation, which can be solved by methods given by Chapman and Enskog.[1] On this basis we may obtain an expression for the diffusion of gases in a binary mixture:

$$\overline{\vec{V}}_1 - \overline{\vec{V}}_2 = -\frac{n^2}{n_1 n_2} D_{12} \left[\overrightarrow{\text{grad}} \left(\frac{n_1}{n}\right) + n_1 n_2 (m_2 - m_1)\, \overrightarrow{\text{grad}}\, (\ell n P) - \frac{\rho_1 \rho_2}{P\rho} (\vec{F}_1 - \vec{F}_2) \right] - \frac{n^2}{n_1 n_2} \frac{D_T}{T}\, \overrightarrow{\text{grad}}\, T(\vec{r}). \tag{3.58}$$

Here, $\overline{\vec{V}}_1$ and $\overline{\vec{V}}_2$ are the average velocities of the two components, n_1 and n_2 their number densities, m_1 and m_2 their molecular masses ($m_2 > m_1$), and ρ_1 and ρ_2 their mass densities ($n = n_1 + n_2$, $\rho = \rho_1 + \rho_2$). The pressure $P(\vec{r},t)$ and temperature $T(\vec{r},t)$ are, in general, functions of position and time. The external forces acting on individual molecules are $\vec{F}_1$ and $\vec{F}_2$, while the symbols D_{12} and D_T represent diffusion coefficients. Inspection of equation (3.58) thus allows us to identify the physical phenomena which affect the uniformity of a gas mixture. The first term on the right hand side represents diffusion, tending to reduce the inhomogeneity of the non-uniform gas; the second term indicates that for non-uniform pressures, the heavier molecules diffuse toward the higher pressure region (this is the pressure diffusion mentioned above). The third term represents effects of external forces acting on the molecules, and the fourth term describes the effect of a temperature gradient producing a non-uniform distribution in the gas (thermal diffusion). From the form of equation (1), we might then expect that for some configurations of temperature gradient and external field, the applied field could act to enhance the thermal diffusion separation effect.

A difference in the transport properties of a gas with and without an applied field was actually discovered by Semftleben in 1930,[2] when he reported that the viscosity and heat conductivity of 0_2 and NO decreased by about 1% in a magnetic field. Originally, it was thought that this effect involved only paramagnetic gases, i.e., those gases composed of molecules having a permanent magnetic dipole moment in the ground state, of which 0_2 and NO are the outstanding examples among atmospheric components. Recent work, however, has shown that this behavior is related simply to the nonsphericity of the molecules,[3,4,5] and thus any molecule in a state of non-zero angular momentum should exhibit the effect to some degree (this would include nonsphericity due to nuclear and rotational magnetic moments).

Since heat conductivity and viscosity are transport properties of the gas and are, as indicated above, affected by a magnetic field in some cases, we should expect that diffusion and thermal diffusion, being transport properties, should also be affected. It is known that thermal diffusion is considerably more sensitive than other transport properties to small changes in the intermolecular potential, thus we may reasonably expect 1% or larger changes in this transport property when a large enough magnetic field is applied.

An unsuccessful attempt to enhance thermal diffusion separation by application of a magnetic field to a binary gas mixture was made by A. Tip and his colleagues in 1966.[6] These workers found that a magnetic field of 3000 gauss changed the separation factor of Krypton in Oxygen by less than 0.5%, a surprisingly low figure in view of the preceding experimental and theoretical work. A more extensive theoretical analysis of their experiment uncovered the fact that in gas mixtures, effect of the field is strongly dependent on the composition of the gas; if there is a preponderance of nonspherical (in this case the paramagnetic gas 0_2 molecules), the effect vanishes.

Further theoretical work by Maksimov and his co-workers has yielded a more complete description of the effects of external fields on transport coefficients of polyatomic gases in general, including even the effects of an electric field on heat conduction and viscosity.[7,8] The common physical character of all of these phenomena is that the external field causes the molecular moments to precess about the field; the moments involved in the case of a paramagnetic gas are the magnetic dipole moments, but in the case of other gases, there is a small magnetic moment connected with the rotation of the nuclei which is not compensated for by the electron cloud. The precession about the field then leads to an effective change in the collision cross section of the molecules, since for colliding non-spherical molecules, the collision cross section depends not only on their relative velocity, but also on their orientation. The field thus acts only indirectly on the translational degrees of freedom of a neutral gas, through the precession mechanism. To obtain the more complete formal description of the effect of a field on the transport properties, the molecular distribution function $f(\vec{r},\vec{v},t)$ must be considered to be a function also of the angular momentum, $\vec{S}$, of the molecule:

$$f(\vec{r},\vec{v},t) \rightarrow f(\vec{r},\vec{v},\vec{S},t).$$

Treatments on this basis are described in references 4, 6 and 8.

In different gases, the effect depends on the factor

$$M = K\mu_{eff} \frac{H}{P}, \text{ where} \tag{3.59}$$

μ_{eff} is the effective magnetic moment of the molecule, K is a parameter depending on the particular gas, H is the applied field, and P the pressure.

For a single component gas, the change in transport coefficients is thus dependent on the ratio H/P; physically, this is the ratio of the molecular precession frequency ω_P in a field H to the collisional frequency ω_c. For higher values of H/P, the effect should saturate, since the averaging over orientations between collisions will then be complete.

For an estimate of the magnitude of this phenomenon we may refer to some measurements on the effect of a magnetic field on the thermal conductivity of Nitrogen.[9] In this experiment, for H/P values of 6000 Oersted/mmHg, the thermal conductivity of N_2 changed by about - 0.3%. For the paramagnetic gases O_2 and NO, H/P values of only about 6 Oersted/mmHg yield an effect of the same magnitude.[2] The difference, as expected, lies in the relative values of the molecular magnetic dipole moment. For the molecules of interest in this study, we list in Table 3.4 pertinent information on the molecular structure and the effective rotational g_J factors. From the latter, we may find the effective molecular rotational magnetic dipole moment as

$$\mu_{eff} = \mu_n g_J J, \tag{3.60}$$

where μ_n is the nuclear magneton, and J the quantum number of the molecular rotational state. In a gas, values of J are distributed statistically depending on the molecular symmetry, structure, and temperature. The distribution peaks at a value of J which is of the order of 5 to 10 at room temperature, but the most probable J value increases rapidly as the temperature increases.

Unfortunately, the factors K in Equation (2) have not been determined for any gases, except that $K(N_2) = K(O_2)$ (Ref. 10); the K's for all gases, however, should be of the same order of magnitude.

In estimating the feasibility of using these effects to achieve removal of SO_2 from stack gases, three fundamental problems must be considered. The first is that of the composition dependence of the effect. For the flue gas composition given, we may consider N_2 as the carrier gas (74.9% by volume), with CO_2 (14.7%) and H_2O (7.25%) the largest admixtures. If we consider simply the g_J factors listed in Table 3.4, it is apparent that the carrier gas, N_2, is more paramagnetic than any of the other components, with the exception of O_2 and NO. By far the largest effect would thus be a change in the diffusivities of O_2 and NO, and whatever separation effects could be developed would result predominantly in a separation of O_2 and NO from the initial mixture. From the remaining mixture of N_2, CO_2, H_2O, SO_2,

N_2O, etc., the experience of reference 6 indicates that it would be almost hopeless to expect any separation of SO_2, due to the fact that the more paramagnetic gas predominates.

A second problem is that of the magnetic field strengths required to achieve the maximum effect on the transport properties. For the paramagnetic gases, saturation of the effect will occur at H/P values of the order of 30 Oersted/mmHg; for gases at pressures near atmospheric, fields of the order of 10^4 Oersted would be required. This is well within the state of the art, but the costs of the large installations required would be high. For the nonparamagnetic gases, as we have seen, H/P ratios at least 100 times larger would be required; this means that magnetic fields of the order of 10^5-10^7 Oersted would be needed, and to obtain such fields is difficult and costly at the present time, even in the laboratory.

The third and perhaps primary problem is that of the competition between large scale mixing effects in the flowing gas and the selective diffusion which could be set up by a magnetic field. For the flow rates ($\sim$ 1500 cm/sec) and duct dimensions (600 cm) under consideration, the flow is turbulent (Reynolds Number $\sim 10^7$). In such cases, the diffusivities corresponding to large scale motion ("eddy diffusivity") are of the order of $10^3 \frac{cm^2}{sec}$, compared to molecular diffusivities (D_{12} or D_T in Equation (3.58) which are of the order of $1\frac{cm^2}{sec}$. This means that for the system considered, any magnetic field effects on transport properties will be diluted by at least 10^3:1 by the large scale mixing.

In view of the problems indicated above, we must conclude that pure magnetic field effects cannot be used in any practical system to achieve separation of the components in a typical mixture of neutral flue gases.

Table 3.4

MOLECULAR STRUCTURE AND ROTATIONAL g_J FACTORS FOR SOME EFFLUENT GASES

Molecule	Structure	Ground State	g_J (In Nuclear Magnetons)
N_2	Homonuclear Diatomic	$^1\Sigma g^+$	1.5
CO_2	Linear Symmetric	$^1\Sigma g^+$	-.055
H_2O	Bent	$^1A_1$	.586
SO_2	Bent	$^1A_1$	.084
N_2O	Linear, Non-symmetric	$^1\Sigma^+$	.086
NO_2	Bent	$^2A_1$	---
O_2	Homonuclear Diatomic	$^3\Sigma g^-$	1850 (Paramagnetic)
NO	Linear	$^2\Pi_{1/2}$	1850 (Paramagnetic)

References

1. See, for example, S. Chapman and T.G. Cowling, "The Mathematical Theory of Non-Uniform Gases", Cambridge U. Press, 1964.

2. a. H. Senftleben, Physik Zeitschr. 31, 961 (1930).
   b. H. Senftleben, Phys. Z. 33, 724 (1932).

3. Y. Kagan and L.A. Maksimov, Soviet Physics - JETP 14, 604 (1962).

4. H.F.P. Knapp and J.J.M. Beenakker, Physica 33, 643 (1967).

5. F.R. McCourt and R.F. Snider, J. Chem. Phys. 47, 4117 (1967).

6. A. Tip et.al., Physica 32, 1429 (1966).

7. Yu. V. Mikhailova and L.A. Maksimov, Soviet Physics - JETP 24, 265 (1967).

8. Yu. Kagan and L.A. Maksimov, Soviet Physics - JETP 24, 1272 (1967).

9. J.J.M. Beenakker et.al., Phys. Lett. 2, 5 (1962).

10. L.L. Gorelik and V.V. Sinitsyn, Soviet Physics - JETP 46, 272 (1964).

3.7. Study on Application of Electromagnetic Excitation Techniques for Removal of SO_2 from Flue Gases

As in the case of electrical excitation methods, the only concept for removal of SO_2 from flue gases by electromagnetic techniques which would appear to be of promise is that of bringing about the oxidation of SO_2 to SO_3, or conversion of SO_2 to some other product, with energy for the reaction being obtained by absorption of electromagnetic energy by the gas, i.e., a photochemical or photolysis process. The desired reaction product would then be condensed out of the gas stream, preferably in the form of sulfuric acid or sulfur.

We resolve the problem into two parts:

1. The determination of the feasibility of coupling electromagnetic energy into the mixture of gases in such a way as to bring about the desired reaction. For this we need information on the absorption spectra of the components of the mixture, and output wavelengths and intensities of spectral sources.

2. Determination of the chemical kinetics of the system under irradiation. Although a considerable amount of experimental work has been done on the photochemistry of pure SO_2 and SO_3, it appears as though additional experimental work will be needed to generate information on the photochemical kinetics of the specific flue gas mixture, which will no doubt be more complicated.

In the following, we give a more detailed discussion of these two problems, on the basis of currently available information.

1. Absorption Spectra of Flue Gas Components

Molecules making up the flue gas interact strongly with electromagnetic energy in two general regions of the spectrum, namely the ultraviolet (wavelengths of about 4000Å and shorter) and the infrared (1 micron and longer). The initiation of a true photochemical reaction generally requires that a molecule absorb a photon with energy corresponding closely to the dissociation energy of the molecule; the associated electronic transitions involve ultraviolet photons.

The absorption of an infrared photon excites molecular vibrations, but does not initiate a photochemical reaction as such. However, since the vibrational state of a molecule involves changes in the distances between its constituent atoms, and the potential energy of the system is dependent on these distances, we expect that the chemical kinetics should be affected to some extent by the direct absorption of infrared energy. Although usually after many collisions with other molecules this vibrational energy is transformed into translational energy of the molecules (i.e., heat), we will see later that the system, in equilibrium with the radiation field, has an effective "temperature" higher than the translational temperature, leading us to expect enhanced reaction rates.[1]

In terms of sources of radiation for the above mechanisms, typical flashlamps used for flash photolysis experiments convert about 10% of the input electrical energy into ultraviolet radiation in the 1500Å-4000Å region. Molecules absorb more selectively in the infrared region, however, and it is for this reason that we expect that conventional sources of infrared radiation such as tungsten lamps, arc lamps, etc., would not be very efficient for use in the infrared. The laser systems which operate in this region, namely the neodymium-doped crystalline lasers (output wavelength 1.06 microns, overall efficiency 1% to 5%), and CO_2-N_2-He gas lasers (output wavelength 10.6 microns, overall efficiency 10% to 20%), are intense, narrow band, reasonably efficient sources which might be valuable if their output wavelengths could be matched to infrared absorption bands of the proper flue gas constituents, mainly SO_2.

In Table 3.5 we list the infrared active bands of the flue gas components, and in addition the dissociation energies and corresponding wavelengths in the ultraviolet. In Table 3.6, we list the output characteristics of the spectral sources which should prove most efficient for this application.

We may conclude that there is not a very good match between the absorption region of SO_2 in the ultraviolet (∿ 2200Å) and the output wavelength of the efficient low pressure mercury arc (2537Å); any scheme based on this reaction would also yield NO as an undesirable side-product, since the O-NO dissociation energy of NO_2 is only 3.114 eV. (3980Å).

There also is no good match between the output of the 1.06μ solid state neodymium laser systems and the absorption spectra of the gas constituents; by means of harmonic generation techniques;[2] the laser wavelength may be converted in two steps to 2650Å, but the present state of the art will not allow power conversion efficiencies of more than a few percent for this process, and we could expect from such a system only a few watts at 2650Å, with an overall efficiency of less than 0.1%.

The long wavelength infrared region offers some hope, however. The sulfur oxides SO, SO_2, and SO_3 all have strong absorption bands in the 1100 cm^{-1} (9 micron) region. Although the CO_2 laser may be frequency tuned by selecting P- or R-branch transitions with a dispersive element in the laser cavity and by using different isotopic species of CO_2[3] the shortest operating wavelength possible at this time appears to be about 9.4μ (operation on R-branch transitions in $C^{12}O_2^{18}$); this does not correspond very closely with the absorption band in SO_2 at 8.69 microns. However, these bands will exhibit a large amount of pressure-broadening under the operating conditions of the system, and this will insure that the CO_2 laser can interact strongly with the SO_2 molecules. An estimate of the interaction strength may be obtained from some published measurements on infrared absorption of sulfur monoxide. Jones[4] presented evidence to show that the product obtained by streaming SO_2 through a high voltage discharge in the presence of sulfur vapor was actually S_2O_2. Absorption bands of this compound near 679 cm^{-1} and 1165 cm^{-1} are shown in reference 4, and we may see that at a partial pressure of .8 mm Hg (total pressure ∿ 30 mm Hg), the linewidth is about 50 cm^{-1} for the 1165 cm^{-1} band, and the peak absorption in a 100 cm path is 50%. Similar linewidths and absorption strengths should hold for SO_2; initial absorption measurements on SO_2 infrared spectra indicated a peak absorption of 80% for SO_2 at 4.6 mm Hg in a 45 cm long cell.[5] Similar results have been observed for SO_3.[6]

For the flue gas mixture considered in this study, namely:

Component	% By Volume
N_2	74.9
O_2	2.8
CO_2	14.7
SO_2	0.3
H_2O	7.25
NO_2	.005

Total Pressure: 760 mm Hg
Temperature: 325°F
(= 436°K)

we expect the linewidth of the SO_2 absorption band at 1151 cm^{-1} to be at least 200 cm^{-1}; this means that a CO_2 laser operating in the 9.4 micron region should interact strongly with the SO_2 component fo the flue gas, and that the optical depths for the 9.4 micron radiation under these conditions should be of the order of one meter. More accurate information must be obtained experimentally.

2. Chemical Kinetics and Vibrational Excitation

Assume that M is a molecule, in some well defined vibrational state, which can absorb another quantum of infrared radiation to become a vibrationally excited molecule M*. This excited molecule may undergo the following processes:

1. Radiative relaxation; re-emission of a photon of infrared energy, hν, by the spontaneous or induced emission process.

2. A unimolecular process of chemical change, e.g., isomerization or dissociation, into some product(s), P_1.

3. A bi-molecular process through interaction with another molecule, e.g., collisional deactivation or activation of vibrations by identical or foreign molecules, X.

4. A chemical reaction with some reactant species, R, to yield a product species P_2.

We may represent these processes by the diagram below.[6a]

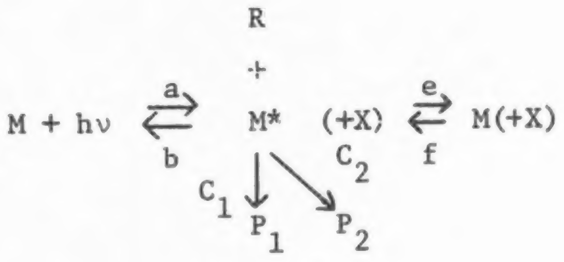

Fig. 3.36 - Chemical kinetics of vibrationally excited molecules.

In terms of rate constants $k_a, k_f, \ldots,$ for the various processes, the number density m* of vibrationally excited molecules will change as follows:

$$\frac{dm^*}{dt} = B\phi m - (A + B\phi)m^* \qquad (3.61)$$

Here, ϕ is the radiation field density and A and B are the Einstein coefficients for spontaneous and stimulated radiation ($k_a \equiv B\phi$, $k_b \equiv A + B\phi$).

$$\frac{dm^*}{dt} = -k_{c_1} m^* \tag{3.62}$$

$$\frac{dm^*}{dt} = -k_e m^* x + k_f mx \tag{3.63}$$

$$\frac{dm^*}{dt} = -k_{c_2} m^* r \tag{3.64}$$

We have assumed here that the reactant molecule R is of a type whose vibrational energy does not intervene in process (3.62) and also that the vibrationally interacting species X is of a type which does not intervene in the chemical process (3.64).

If we assume that the number density of M-type molecules is much lower than that of the R or X species, we may consider r and x to be more or less constant during the process, and we redefine

$$\begin{aligned} k_e' &\equiv k_e x \\ k_f' &= k_f x \\ k_d' &= k_d r \end{aligned} \tag{3.65}$$

Under conditions in which the system reaches a stationary state with the radiation field, the rate of change of m* due to all processes is zero:

$$\frac{dm^*}{dt} = 0 = B\phi m-(A+B\phi)m^*-k_c m^*-k_e' m^* + k_c' m-k_d' m^* \tag{3.66}$$

$$\frac{m_e^*}{m} = \frac{(B\phi + k_f')}{A + B\phi + k_c + k_d' + k_e'} \tag{3.67}$$

The rate at which product molecules are formed will be, in steady state,

$$\text{(a)} \qquad \frac{dp_1}{dt} = k_c m_e^* = mk_c \left[\frac{(B\phi + k_f')}{A+B\ +k_c+k_d'+k_e'}\right]$$

$$\text{(b)} \qquad \frac{dp_2}{dt} = k_d' \ m_e^* = mk_d' \left[\frac{B\phi + k_f'}{A+B\phi+k_c+k_d'+k_e}\right] \tag{3.68}$$

In the presence of very intense electromagnetic radiation, these rates will saturate at values

$$\frac{dp_1}{dt} \xrightarrow[\phi\to\infty]{} mk_c$$

$$\frac{dp_2}{dt} \xrightarrow[\phi\to\infty]{} mk'_d$$

We may make some estimates of the photon flux densities required to reach this saturation point as follows. The dominant process competing with the vibrational excition via the radiation field is the collisional relaxation process in the gas, described by the rate k_e'. This disperses vibrational energy of the excited SO_2 molecule (1151 cm^{-1}) into translational energy of the surrounding gases, but for SO_2, the transition takes place in a somewhat different manner than in most molecules, as seen in Figure (3.37). The rate determining process is the V-V transformation of a single quantum of vibrational energy in the symmetric stretching mode to two quanta (2×519 cm^{-1}) of the bending mode, which then is relaxed at a slower rate. The limiting rate is pressure dependent, and is given by $\frac{k_e}{P} = 1.8 \times 10^6$/sec-atmosphere for pure SO_2. The rate could be faster in the presence of additive molecules with nearby vibrational levels.

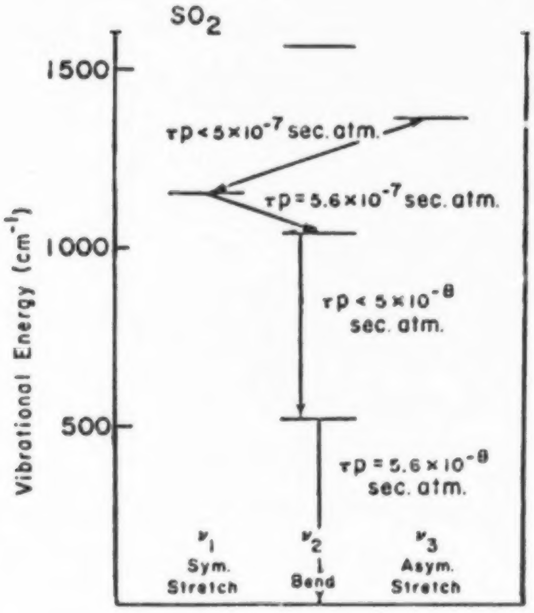
SO_2
1500
1000
500
Vibrational Energy (cm^{-1})
$\tau p < 5 \times 10^{-7}$ sec. atm.
$\tau p = 5.6 \times 10^{-7}$ sec. atm.
$\tau p < 5 \times 10^{-8}$ sec. atm.
$\tau p = 5.6 \times 10^{-8}$ sec. atm.
ν_1 Sym. Stretch
ν_2 Bend
ν_3 Asym. Stretch

Fig. 3.37 - Relaxation Path For SO_2 Vibrational Energy.

The rate k_f' cannot be larger than k_e'. The spontaneous emission rate for most vibrational transitions is of the order of 10^3/sec., and will be neglected here. Assuming we have a flux density $\Phi = c\phi$ in the laser beam of $\frac{1000 \text{ watts}}{cm^2}$ $(5 \times 10^{22} \frac{\text{photons}}{cm^2 \text{ sec}})$, and an effective absorption cross section in the SO_2 molecule of 5×10^{-17} cm^2, we find

$$B\phi = \sigma\Phi = 2.5 \times 10^6/\text{sec}$$

From Figure 3.37 we see that $k_e' \approx 1.8 \times 10^6$/sec. This implies, from Equation (3.68) with $(k_f', k_d', k_c') < k_e'$, that the steady state rates of product formation will be

$$\frac{dp_1}{dt} = .58\ mk_c$$

$$\frac{dp_2}{dt} = .58\ mk'_d$$

where k_c and k'_d are, respectively, unimolecular and bimolecular rates for the processes in which a vibrationally excited molecule M* forms products

$$M^* \xrightarrow{k_c} P_1$$

$$M^* + R \xrightarrow{k'_d} P_2$$

If M* is a vibrationally excited SO_2 molecule, we may consider for the second process the direct oxidation of SO_2:

$$2SO_2 + O_2 \xrightarrow{k_d} 2SO_3$$

The rate k_d is slow for the case of unexcited SO_2, since it involves either collisions of three molecules, or a bimolecular collision with a large activation energy. The rate constant may be estimated to be

$$k_d = pA_e^{-\frac{E_o}{RT}}$$

with P, the steric factor, $\cong 10^{-4}$; A, the frequency factor $\cong 10^{-13}$ $\frac{cm^3}{\text{molecule sec}}$; and the activation energy E_o probably of the order of 0 to 10 Kcal/mole.[8] Assuming the lower or higher values for the activation energy thus gives rate constants

$$k_d = 10^{-17}\ \frac{cm^3}{\text{molecule sec}} \text{ to } 10^{-23}\ \frac{cm^3}{\text{molecule sec}} \quad .$$

At the partial pressures of SO_2 and O_2 present in the flue gas, and at its temperature of 436°K, the number densities of SO_2 and O_2 are

$$SO_2 \ (\sim 2.3 \text{ Torr}), \ m = 5.1 \times 10^{16} \ \frac{\text{molecules}}{\text{cm}^3}$$

$$O_2 \ (\sim 21.3 \text{ Torr}), \ r = 4.7 \times 10^{17} \ \frac{\text{molecules}}{\text{cm}^3} \ ,$$

and the rate is expected to be in the range

$$10^{11}/\text{cm}^3\text{sec} < \frac{dp_2}{dt} < 1.4 \times 10^{17}/\text{cm}^3\text{sec}$$

Using a collisional calculation based on the rigid sphere approximation, Gibert[1] has shown theoretically that excitation of molecules to higher vibrational levels (i.e., to an effective temperature T" somewhere between the translational temperature T and the equilibrium temperature T' of the molecule interacting only with the radiation field) can result in a very large increase in the reaction rate. In fact, it is evident from our calculation of the steady state value of m* that the effective temperature T" is very high for the case considered:

$$\frac{m_e^*}{m} = .58 \equiv e^{-\frac{h\nu}{kT''}}$$

implies that T" is of the order of 10^3°K! Considering the results of reference (1), it would not be overoptimistic to consider k_d enhanced by 10^2 to 10^3 as a result of this effect, so in absence of competing reactions we might expect a rate of $SO_2 \rightarrow SO_3$ conversion of the order of 10^{19} to $10^{20}/\text{cm}^3\text{sec}$, if we supply energy to the system at a rate of $\sim \frac{5 \times 10^{32} \text{ photons}}{100 \text{ cm}^7 \text{ sec}} = 10 \text{ watts/cm}^3$. The "quantum efficiency" under these conditions is thus about 20%.

The unimolecular process of direct dissociation of SO_2 by thermal means should also be considered. In one of the first investigations on photolysis of SO_2 by ultraviolet irradiation, Wieland[9] found that at temperatures above 300°C, dissociation of SO_2 took place according to the following process:

$$SO_2 + 12.6 \frac{\text{Kcal}}{\text{mole}} = \frac{1}{6} S_2 + \frac{4}{6} SO_3,$$

the required energy becoming available as a result of thermalization of the incident ultraviolet energy. Again, the rate constant k_c for this reaction is unknown; we can, however, note that the required energy for the reaction is equivalent to that available from about 5 photons:

$$12.6 \frac{\text{Kcal}}{\text{mole}} = .55 \frac{\text{eV}}{\text{molecule}}$$

$$E_{\text{photon}} = h\nu = .12 \text{ eV}$$

The quantum efficiency of this process would thus be similar to that of the preceding one, namely about 20%.

The above calculations must be considered very tentative; the lack of information on rate constants of gas phase reactions of flue gas components is a major factor here, as well as a dearth of any experimental results concerning effects of vibrational excitation on chemical kinetics in the gas phase.

Brockmeier(10) investigated the use of microwave discharges for inducing chemical reactions. His results indicated that

$$SO_2 + O_2 \rightarrow SO_3$$

does not go in this case but that the thermolecular process

$$SO_2 + N_2 + O_2 \rightarrow SO_3 + NO_x$$

does go. It was found that 4.8 kwhr per pount of SO_3 is required for this conversion. This is equivalent to 1.0 kwhr/SCF of SO_2. Section 3.8 shows that the maximum allowable energy consumption for an SO_2 SO_3 conversion is 0.055 kwhr/SCF of SO_2.

Feasibility Study Conclusions

The high power continuous gaseous CO_2-N_2-He laser appears to be the only system which can efficiently deliver large enough amounts of power to flue gas mixtures to initiate SO_2 oxidation or dissociation, and this will take place via a thermal or "photothermal" reaction. On the basis of optimistic estimates for the SO_2 oxidation rate constant, and on the basis of known values for the thermal dissociation energy of SO_2, the quantum efficiency for the reaction is estimated to be about 20%. Competing reactions and back reaction rates were not considered.

Before the final conclusions can be made on the feasibility, experimental data must be obtained on gas phase reaction rate constants and on the laser photothermal catalysis of gas phase reactions.

Cost Analysis

1. Power Requirements

For a unit with a typical flue gas flow rate of 1.35×10^6 cubic feet/minute, we have a flow, at 325°F, of 1.04×10^{29} molecules/sec, of which .3%, or 3.1×10^{26}/sec, are SO_2 molecules. At a quantum efficiency of 20%, and photon energy of 1.87×10^{-20}J, this is a power requirement of 28 Megawatts for such a unit.

2. Cost of Operation

The current overall operating costs (including maintenance and gas supply) of 250 watt laser units are \$1.20/Laser Kilowatt Hour; since the laser efficiency is 20%, only a small portion of this cost is due to input power requirements. The hourly operating cost corresponding to the 28 Mw power requirement would be \$$33.6 \times 10^3$, which corresponds to about \$600/ton of 2% sulfur content coal, and is clearly uneconomical. It is unlikely that the laser costs will be reduced by more than a factor of ten in the near future.

3. Initial Costs

The initial costs for current CO_2 laser systems are about \$80/watt, which implies an initial cost of \$2.2 x 10^9 for the 28 Mw system considered above.

Although it is possible that feasibility can be demonstrated, cost considerations will rule out electromagnetic excitation techniques for SO_2 removal from flue gases.

Table 3.5

ABSORPTION REGIONS OF FLUE GAS COMPONENTS

Wavelength Region

Molecule	Infrared	Ultraviolet
	Wavelengths in cm^{-1} and Microns	Dissociation Energy (eV) and Corresponding Wavelength
N_2	None	7.373 eV (1681A)
O_2	None	5.080 eV (2440A)
CO_2	667.3(14.99μ), 1285.5(7.78μ), 1388.3(7.20μ), 2349.3(4.26μ)	O+CO, 5.453 eV (2273A)
SO_2	519(19.27μ), 606(16.5μ), 1151.2(8.69μ), 1361(7.48μ), 1871(5.34μ), 2305(4.34μ), 2409(4.0μ)	O+SO, 5.61 eV (2200A) O_2+S, 5.86 eV (2120A)
H_2O	1595(6.27μ), 3151.4(3.17μ), 3651.7(2.74μ), 3755.8(2.66μ)	H+OH, 5.113 eV (2424A)
NO_2	648(15.43μ), 1000(10μ), 1320(7.58μ), 1373(7.28μ), 1621(6.17μ), 2220(4.5μ)	O+NO, 3.114 eV (3980A) N+O_2, 4.505 eV (2750A)
SO_3	530(18.87μ), 543(15.31μ), 1068(9.36μ), 1332(7.51μ)	O+SO_2, 3.541 eV(3500A)
SO	1124(8.9μ)	4.001 eV (3098A)
NO	1875.9(5.33μ)	5.29 eV (2343A)
CO	2143.2(4.67μ)	11.108 eV (1117A)

Table 3.6

SOME CHARACTERISTICS OF SPECTRAL SOURCES

Source	Output Wavelength	Linewidth (CPS)	Tunability	Output (Watts) of Typical Unit	Overall Efficiency	Spectral Radiance $\left(\frac{\text{Watts}}{\text{cm}^2\ \text{ster. CPS}}\right)$
Low Pressure Mercury Arc Lamp	2537A	10"	None	20	50%	3×10^{-15}
Continuous Nd-YAG Laser	1.06	10^4	None	100	1% - 5%	2×10^5
CO_2-N_2-He Gas Laser	10.6	10	$C^{12}O_2 16$ 10.2μ→10.9μ $C^{12}O_2 18$ 9.4μ→10.6μ	1000	5% - 20%	10^8

References

1. R. Gibert, "Conditions on the Possibility of Isotopic Enrichment by a Photochemical Reaction", Journal de Chimie Physique 60, 205 (1963). (In French).

2. See, for example, N. Bloembergen, "Nonlinear Optics", W.A. Benjamin, N.Y., 1965.

3. I. Wieder and G.B. McCurdy, Phys. Rev. Lett. 16, 565 (1966).

4. A. Vallance Jones, "Infra-red and Ultraviolet Spectra of Sulfur Monoxide", J. Chem. Phys. 18, 1263 (1950).

5. C.R. Bailey et.al., Proc. Roy. Soc. (London) 130, 142 (1930).

6. H. Gerding and J. LeComte, "The Infrared Absorption Spectrum of Gaseous and Liquid Sulfur Trioxide", Physica VI, 737 (1939). In German.

6a. See, for example, B. Stevens, "Collisional Activation in Gases", Pergamon Press, N.Y., 1967. Ch. 4.

7. C.B. Moore, "Laser Excited Vibrational Fluorescence and Its Application to Vibration → Vibration Energy Transfer in Gases", Ch. 3 of "Fluorescence, G. Guilbault, ed., Dekker, N.Y., 1967.

8. A.A. Frost and R.G. Pearson, "Kinetics and Mechanism", 2nd Ed., Wiley, N.Y. 1961.

9. K. Wieland, "Thermo-Optical Dissociation of Sulfur Dioxide", Trans. Far. Soc. 30, 260 (1934).

10. Brockmeier, Norman F., "Chemical Reactions Induced in a Microwave Discharge," Ph.D. Thesis, Department of Chem. Engrg., MIT, August, 1966.

3.8. Feasibility Analysis of Applicability of Electrical Excitation Methods to the Separation of SO_2 from Flue Gases

The only concept which appears to be feasible for the utilization of electrical excitation in the separation of SO_2 from flue gases is the oxidation of SO_2 to SO_3 which is then condensed out of the gas stream in the form of sulfuric acid. Two methods have been studied and reported in the literature. General Electric(1) has done an evaluation of corona discharge catalysis of sulfur dioxide. This study is an engineering feasibility study and indicates the basic reactions involved. It does not find the method promising, but offers a direction for future study. W. C. Holmes Co. Ltd. has patented what would be classified as a flow discharge conversion chamber.(2,3) This method looks reasonable in power cost to oxidize SO_2 when the concentration is very high, 5% at least; but not useful for flue gas.

There is no literature available on the specific reactions which were involved in the above processes. Other reactions may be important, but it seems most reasonable to assume that the associative detachment reaction is the most important one in these methods. General information on electrical excitation reactions can be found in a number of books,(4-8) but they contain no specific references to SO_2. More specific results on closely related associative detachment processes are discussed by Moruzzi and Phelps(9-10) of these laboratories.

In using electrical excitation for $SO_2 \rightarrow SO_3$ conversion there are 3 possible reactions chains to consider

$$O^2 + e \rightarrow O + O^- \; ; \; O^- + SO_2 \rightarrow SO_3 + e$$

$$O^2 + e \rightarrow O + O + e; \; O + SO_2 \rightarrow SO_3$$

$$SO_2 + e \rightarrow SO + O^- \; ; \; SO + O_2 \rightarrow SO_3$$

At present there is no published data on the reaction rate for the reaction.

$$O^- + SO_2 \rightarrow SO_3 + e \qquad (3.69)$$

However we have some indication that it may be as high as 6.3×10^{-10} cm^3/sec which is close to the kinetic rate. The major competing reaction would probably be

$$O^- + CO_2 + CO_2 \rightarrow CO_3^- + CO_2 \qquad (3.70)$$

which has a reaction rate of 9×10^{-29} cm^6/sec and CO_3^- is stable. The minimum energy required to produce O^- is 5 ev.(11) The energy of formation of the free radical O is 2.7 ev.(12) These are theoretical values for the $SO_2 \rightarrow SO_3$ conversion process since the efficiency of producing O^- or O and the effect of competing reactions are not included, and the reaction would probably have to operate at a pressure of a few Torr for optimum production of O^-. To achieve continuous reactions through electrical excitation, power must be continuously fed to the reaction cell, since the exothermic heat is not recovered.

It is clear that reactions such as $O^- + SO_2 \rightarrow SO_3 + e$ could be used to convert SO_2 into SO_3 in a flue-gas purification system. However, to be economically competitive the total operating cost of the electrical excitation equipment must be less than that of vanadium catalysts such as are used in the Penelec(13) catalytic oxidation system.

Katell(14,15) has supplied estimated capital costs for the Penelec system attached to an 800 MW plant burning 3% S coal with 20% excess air. The annual operating cost for the catalytic converter portion of the Penelec system is

Make-up Catalyst	$139,900
Operating Labor	16,400
Maintenance	33,700
Capital Charges	157,200
Total	$347,200

The full load flow rate of SO_2 is about 3.0×10^3 SCFM. Assuming an 80% load factor for the plant and 100% removal gives a specific cost for SO_2 removal of 0.28 mills/SCF.

For the electrical excitation conversion method, the specific cost must not exceed the above value for the vanadium catalyst. The maximum allowable energy consumption can be obtained by assuming that the proposed system has no capital cost and that all of the operating costs are zero except the power costs. Therefore, the maximum allowable specific power cost for the electrical excitation method is 0.28 mills/SCF. Assuming that electrical power is worth 5 mills/kw hr at the plant site, this is equivalent to a specific energy consumption of 0.055 kw hr/SCF or about 1.6 ev per molecule oxidized.

It has been shown that the maximum allowable specific power consumption for electrical excitation conversion of SO_2 to SO_3 is about 60 percent of the minimum theoretical power requirement. Therefore, although the conversion of SO_2 to SO_3 by electrical excitation has been demonstrated to be technically feasible, it is clearly not economically feasible.

It has been pointed out that for endothermic reactions or in cases where no catalyst is available electrical excitation methods may prove to be worth considering; but, it is unlikely for electron activation methods to have industrial potential for exothermic reactions where a suitable catalyst is commercially available.(16) A basic reason for the low effective energy cost per reaction with thermal catalysts is that once a thermal catalyst achieves its working temperature the exothermicity of the oxidation maintains this temperature without a supply of external heat.(16)

References

1. W. R. Browne, E. E. Stone, "Sulfur Dioxide Conversion Under Corona Discharge Catalysis," General Electric Report of March 5, 1965 on Contract (PH 86-65-2), U. S. Dept. of Health, Education and Welfare.
2. A. J. Moyes, C. R. Smith, "Comparative Results for Thermal and Electronic Activation of Mixtures of SO_2 and O_2," Chem. Engr. (London) #190 (CE 163-166), 1965.
3. W. T. Cosby, C. R. Smith (H. C. Holmes Co. Ltd.), British Patent 1,009,331 (Cl. C01b), November 10, 1965.
4. Z. G. Szabo, "Advances in the Kinetics of Homogeneous Gas Reactions," Methuen & Co. Ltd., (London, 1964).
5. K. J. Laidler, "The Chemical Kinetics of Excited States," pp. 57-65, The Clarendon Press, (Oxford, 1955).
6. J. F. Pailson, "Some Negative Reactions in Simple Gases," pp. 28-43, Ion Molecule Reactions in the Gas Phase Symposium at 152nd Meeting of American Physical Society, Sept. 12-13, 1966 (New York).
7. F. H. Field and J. L. Franklin, "Electron Impact Phenomena, pp. 145-152, Academic Press (New York, 1957).
8. H. S. W. Massey, E. H. S. Burhop, "Electron and Ionic Impact Phenomena," pp. 519-530, The Clarendon Press (Oxford, 1952).
9. J. L. Moruzzi, J. W. Ekin, Jr., and A. V. Phelps, "Electronic Production by Associative Detachment of O^- Ions with NO, CO, and H_2," J. Chem. Phys., 48, 7, (April 1968), 3070-3076.
10. J. L. Moruzzi, and A. V. Phelps, "Survey of Negative-Ion-Molecule Reactions in O_2, CO_2, H_2O, CO, and Mixtures of These Gases at High Pressures."
11. Gould, R. et al., "Ion-Molecule Reactions on the Gas Phase," American Chemical Society Publications, p. 34, 1966.
12. Field, F. and Franklin, J., "Electron Impact Phenomena and the Properties of Gaseous Ions," Academic Press Inc., p. 129, 1957.
13. R. F. Bovier, "Sulfur Smoke Removal System," Proceedings of the American Power Conference, 1964, Vol. XXVI, 138-144.

14. Katell, S., "An Evaluation of Dry Processes for the Removal of Sulfur Dioxide for Power Plant Flue Gases," Symposium on Economics of Air Pollution Control, May 15-18, 1966, Am. Inst. of Chem. Engrs.

15. Personal communications with S. Katell.

16. A. J. Moyes and C. R. Smith, "Comparative Results for the Thermal and Electronic Activation of Mixtures of Sulfurdioxide and Oxygen," The Chem. Engr., July 1965, 163-166.

3.9 Separation of SO_2 from Flue Gases by Nuclear Radiation Excitation

As mentioned in the original proposal, the removal of SO_2 from flue gases by means of nuclear radiation excitation is not a fruitful approach. We have made a further study and confirmed our earlier conviction.

Nuclear radiation is known to convert one chemical species into another. Radiations, such as α-, β-, γ-rays, can cause ionization and excitation in the medium and thus induce chemical changes. A classical example is the decomposition of water into hydrogen and oxygen in a solution of radium salt. This was observed by Curie, Soddy et al, at the turn of the century.

A conceivable way that nuclear radiation might help in the treatment of flue gases is the possibility that SO_2 may be converted into SO_3 in the presence of radiation. This would facilitate the removal of sulfur because it is much easier to remove SO_3 than SO_2.

A search of the literature revealed that very little work has been carried out on the irradiation of SO_2. Rothschild[1] irradiated pure liquid SO_2 by Co-60 γ-rays at -17°C and found the following reaction occurs:

$$3\ SO_2 \rightarrow 2\ SO_3 + S$$

The G-value for the reaction is 1.31. G-value in radiation chemistry is generally regarded as the number of molecules changed or transformed for each 100 eV of radiation energy absorbed. Bennett and his co-workers at Oak Ridge National Laboratory[2,3] also studied the irradiated SO_2 in order to learn if SO_2 can be used as a cooling gas in a breeder reactor (this is an indication that SO_2 is relatively stable against radiation action) and noted that SO_2 probably decomposes into sulfur and O_2. But they were not able to determine quantitatively any difference between the original and irradiated gases although some qualitative changes were noted initially.

Since there is no direct irradiation of SO_2 in flue gases, we assume a G-value of 10 for the transformation of SO_2 into either SO_3 or S. This is a very optimistic value. Based on experience with radiation chemistry, a G-value of 10 is an unusually high value. Nevertheless, the following calculation will indicate that the radiation power is prohibitively high to be useful for the purpose.

Since high energy electrons are more efficiently absorbed in a gas, an accelerator is a more economical and convenient source for electrons than radioactive β-sources.* We assume the energy of the electrons from an accelerator to be 1.6 MeV because the penetration length of this energy is about 20 ft. in flue gases at room temperature. The penetration length is longer at 325°F by a factor proportional to the gas density ratio.

We use the flue gas composition given elsewhere and a typical flow rate of 5.5×10^7 cu. ft./hr at STP for a typical flue of a plant.

The radiation power required is calculated as follows:

$$\begin{aligned}\text{Flow rate (at STP)} &= 5.5 \times 10^7 \text{ cu. ft./hr} \\ &= \frac{5.5 \times 10^7 \times 28.3}{22.4} \\ &= 6.95 \times 10^7 \text{ moles/hr} \\ &= 4.17 \times 10^{31} \text{ molecules/hr} \\ &= 1.16 \times 10^{28} \text{ molecules/sec}\end{aligned}$$

For a G-value of 10, each SO_2 molecule should receive 10 eV. The flue gas contains 0.3% by mole of SO_2. The radiation power required for SO_2 only is:

$$\frac{1.16 \times 10^{28} \times 0.003 \times 10}{6.24 \times 10^{18}} = 5.57 \times 10^7 \text{ watts}$$

In order to put radiation energy into SO_2, all the flue gases have to be irradiated. The absorption of radiation is proportional to the weight of the gases. Since the flue gases contain about 0.64% of SO_2 by weight, the total radiation power required becomes:

---

[*] A 1-kw one MeV electron beam is equivalent to 1.69×10^5 curies of β-emitters with an average energy of one MeV.

$$\frac{5.57 \times 10^7}{0.0064} = 8.7 \times 10^9 \text{ watts}$$

$$= 8.7 \times 10^6 \text{ kW}$$

This is equivalent to 1.47×10^{12} curies of a β-ray emitter with an average energy of 1 MeV! For 1.6 MeV electrons, the accelerator or accelerators should deliver a current of 5.44×10^3 amps. The power level and current value are prohibitively large.

The current cost of electron accelerators is \$5,000 to \$50,000 per kW. The operation cost is \$5 to \$50 per kWH. If one uses lower figures for a 500 MW plant, the initial cost of the accelerators will be $\$4.35 \times 10^{10}$ and the operation cost will be $\$4.35 \times 10^7$ per hour. It is obvious the cost of supplying radiation power is also prohibitive.

The only possibility that the cost can be reduced is that the G-value of the reaction can be increased a million fold or more. This is definitely inconsistent with present knowledge and experience in radiation chemistry.

We therefore conclude that radiation treatment of the flue gases should be ruled out.

References

1. G. Rothschild, Gamma-ray Decomposition of Pure Liquid Sulfur Dioxide, J. Am. Chem. Soc., 86, (7), 1307 (1964).
2. R. L. Bennett and G. W. Keilholtz, Thermal Radiation and Chemical Stability of Sulfur Dioxide, Oak Ridge National Laboratory, ORNL-TM-747.
3. P. S. Rudolph and R. L. Bennett, Alpha-Particle Irradiation of Gaseous Sulfur Dioxide, Chemistry Division Annual Progress Report For Period Ending May 1965, Oak Ridge National Laboratory, ORNL-3832, p. 50.

Hilsch Vortex Tube

The vortex tube as a cooling device was first proposed by M. G. Ranque(1) and later experimented on and described by R. Hilsch(2). A model of the vortex tube is shown in Figure 3.38. A stream of compressed air (or other gas) is delivered to a vortex chamber on one side of which is an orifice or nozzle discharging part of the air into the atmosphere (or region to be cooled), and on the other side of which is a length of pipe leading to a valve through which the balance of the air is discharged.

The literature concerning the use of the vortex tube for the separation of gases of different molecular weight is limited. Mürtz and Nöller(3) have reported the results of their experimentation indicating the effect of some of the process variables. They have applied for a patent on a vortex tube separator(4). Bornkessel and Pilot(5) have also reported on the use of a vortex tube for isotope separation.

In the vortex tube separation process, just as in the refrigeration application, the gas mixture to be separated is injected tangentially into a cylindrical chamber to create the high intensity vortex(6). At a pressure level of about 5 mm Hg the flow in the high velocity vortex is laminar; and, due to the centrifugal field set up, the higher molecular species are concentrated near the periphery and the lower molecular species in the essentially stagnant core region. A concentric skimmer at the end of the tube separates the two streams.

Mürtz and Nöller(3) have developed the following expression for the equilibrium separation factor of the vortex tube,

$$\alpha = (p_P/p_c)^{(M_B-M_A)/\bar{M}} \qquad (3.71)$$

where p_P is the pressure at the periphery and p_c is the pressure at the core. A number of other characteristics of the vortex tube separation system were revealed in their experiments(6). At a constant jet nozzle inlet pressure, the flow through the vortex is approximately inversely proportional to the mean molecular weight of the gas mixture. The ratio of the peripheral pressure to the pressure at the central core is also a function of the mean molecular weight. Figure 3.39 shows their data for molecular weights up to 100.

The mean molecular weight of the flue gas composition specified for this study is 29.83. Figure 3.39 gives a value of 4.3 for p_P/p_c for this mean molecular weight. Inserting this number and the molecular weights of sulfur (64) and of the flue gas without the sulfur (29.74) into equation (3.71) gives a value of 5.36 for the equilibrium separation factor. While in the gas centrifuge the separation factor with flow is significantly greater than the equilibrium value, especially with countercurrent flow, there is nothing to indicate that this would be so in the vortex separator. Therefore, it is assumed that the equilibrium separation factor is valid for use in evaluating the vortex separator.

Assuming a cut of 0.5 in an ideal countercurrent cascade, a separation factor of 5.36 gives the following for $X_p = 0.2$ and $X_w = 0.0003$.

Total number of stages - 7
Number of stages in the stripping section - 2

Way$^{(7)}$ has developed the following expression for the overall pressure ratio of a Hilsch tube using the model shown in Figure 3.38.

$$\frac{p_e}{p_o} = \left\{ \frac{1 - q^2}{1 + q_3^2} \times e^{-2/7\, N_2} \right\}^{\frac{k}{k-1}} \tag{3.72}$$

where

$$q^2 = 1 - \left(\frac{p_{2a}}{p_o}\right)^{\frac{k-1}{k}} \tag{3.73}$$

$$q_3^2 = \left(\frac{p_{2m}}{p_{3m}}\right)^{\frac{k-1}{k}} - 1 \tag{3.74}$$

and

$$N_2 = \frac{u_{ta}^{\ 2}}{2\ R\ T_2} \tag{3.75}$$

Assuming that u_{ta} is equal to the velocity out of the nozzle and that the pressure at the nozzle outlet is equal to the pressure at the periphery gives

$$u_{ta} = \left\{ 2g\ (\frac{k}{k-1})\ R\ T_o \left[1 - (\frac{p_{2a}}{p_o})^{\frac{k-1}{k}} \right] \right\}^{1/2} \tag{3.76}$$

Combining equations (3.72), (3.73), and (3.74) gives:

$$\frac{p_e}{p_o} = \frac{(p_{2a}/p_o)}{(p_{2m}/p_{3m})} \left[e^{-\frac{2}{7} N_2} \right]^{\frac{k}{k-1}} \tag{3.77}$$

and

$$\frac{p_e}{p_{2a}} = (\frac{p_{3m}}{p_{2m}}) \left[e^{-\frac{2}{7} N_2} \right]^{\frac{k}{k-1}} \tag{3.78}$$

If the axial velocity at station 3 is assumed to be 500 ft/sec and b/a = 0.5, then

$$\frac{p_{3m}}{p_{2m}} = 0.884 \tag{3.79}$$

and for k = 1.4

$$q_3^2 = (1.13)^{0.286} - 1 = 0.0356 \tag{3.80}$$

From Figure 3.39 and equation (3.79)

$$\frac{p_{2a}}{p_{3m}} = 4.3 \times 1.13 = 4.86 \qquad (3.81)$$

If p_{3m} is the same as p_e

$$\frac{p_{2a}}{p_e} = 4.86 \qquad (3.82)$$

Combining equations (3.78), (3.79), and (3.82) gives

$$e^{-\frac{2}{7} N_2} = \left(\frac{1}{4.86 \times 0.884} \right)^{\frac{k-1}{k}} \qquad (3.83)$$

For k = 1.4

$$e^{-\frac{2}{7} N_2} = (0.2325)^{0.286} = 0.658 \qquad (3.84)$$

and

$$\begin{aligned} N_2 &= - \frac{7}{2} \ln 0.658 \\ &= - \frac{7}{2} \times - 0.419 = 1.465 \qquad (3.85) \end{aligned}$$

By combining equations (3.75) and (3.76) and substituting (3.85) one obtains

$$\frac{p_{2a}}{p_o} = \left[1 - 0.013 \left(\frac{T_2}{T_o} \right) \right]^{3.5} \qquad (3.86)$$

For $\theta = 0.5$, $k = 1.4$, and $b/a = 0.5$ the ratio of $\Delta T/T_o$ was developed by Way$^{(7)}$ to be:

$$\frac{\Delta T}{T_o} = 1 - \beta^2 \left[(1 + q_3^2) \frac{0.875}{N_3} + \frac{\phi(N_3)}{4} \right] \quad (3.87)$$

where

$$\beta = \frac{u_{ta}}{\sqrt{2C_p T_o}} \quad (3.88)$$

$$N_3 = \frac{u_{tb}^2}{2 R T_3} \quad (3.89)$$

and

$$\phi(N) = \frac{e^N (N-1) + 1}{N (e^N - 1)} \quad (3.90)$$

Figure 3.40 is a plot of $\Delta T/T_o$ for $q_3^2 = 0.0356$ as a function of q^2 where q^2 is equal to $1 - (p_{2a}/p_o)^{(k-1)/k}$. By iteration

$$\frac{p_{2a}}{p_o} = 0.95 \quad (3.91)$$

Combining equations (3.82) and (3.91) gives

$$\frac{p_o}{p_e} = 5.1$$

The vortex separator described in reference 3 is shown in Figure 3.41. The pressure loss in this device would be comparable to that in the device shown in Figure 3.38 with a diffuser added to the end of the smaller tube. With a diffuser efficiency of 100% the corresponding value of p_o/p_e would be 4.5. With no allowance for pressure loss in the connecting lines, the power requirements for a cascade to handle the flue gas for a 600 MW plant would be about 565 MW. This value is high compared to that for the diffusion cascade because the total interstage flow would have to be compressed rather than just the tails flow.

The estimated power consumption for a cascade of vortex separators is nearly as large as the plant output so this method is clearly uneconomic. In addition the system volume would be huge because of the need for operating at about 5 mm Hg pressure.

Dwg. 859A256

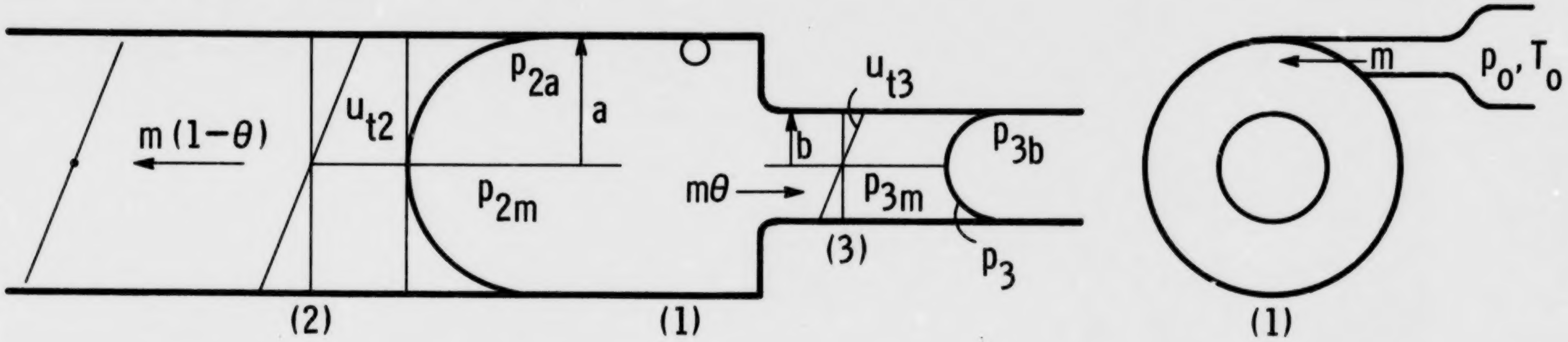
p_{2a}
a
u_{t2}
$m(1-\theta)$
p_{2m}
(2)
(1)
u_{t3}
b
$m\theta$
p_{3b}
p_{3m}
(3)
p_3
m
p_0, T_0
(1)

Fig. 3.38—Vortex tube model

Curve 589570-A

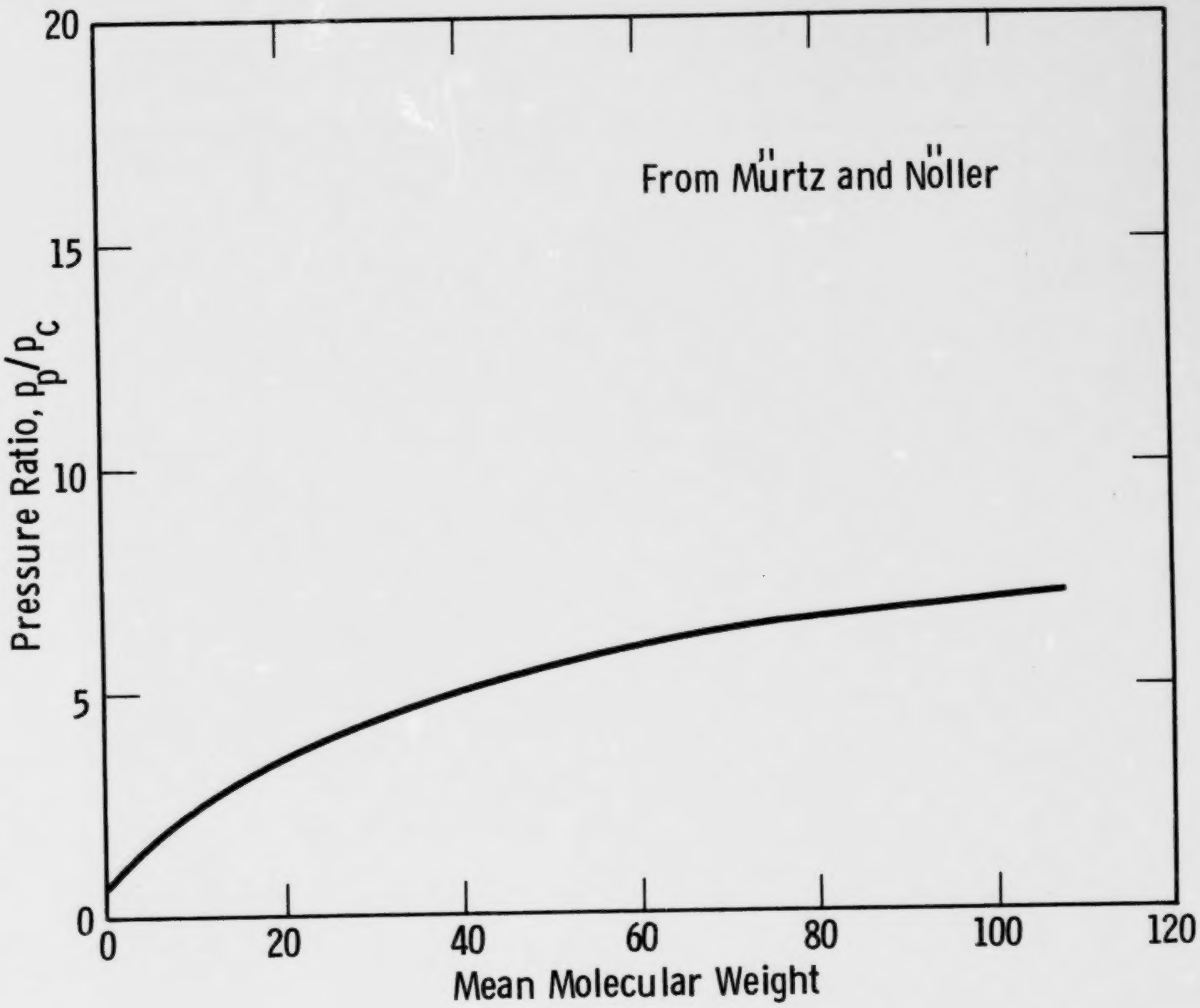

Fig. 3.39—Ratio of peripheral to core pressures in a vortex tube as a function of mean molecular weight

Curve 589571-A

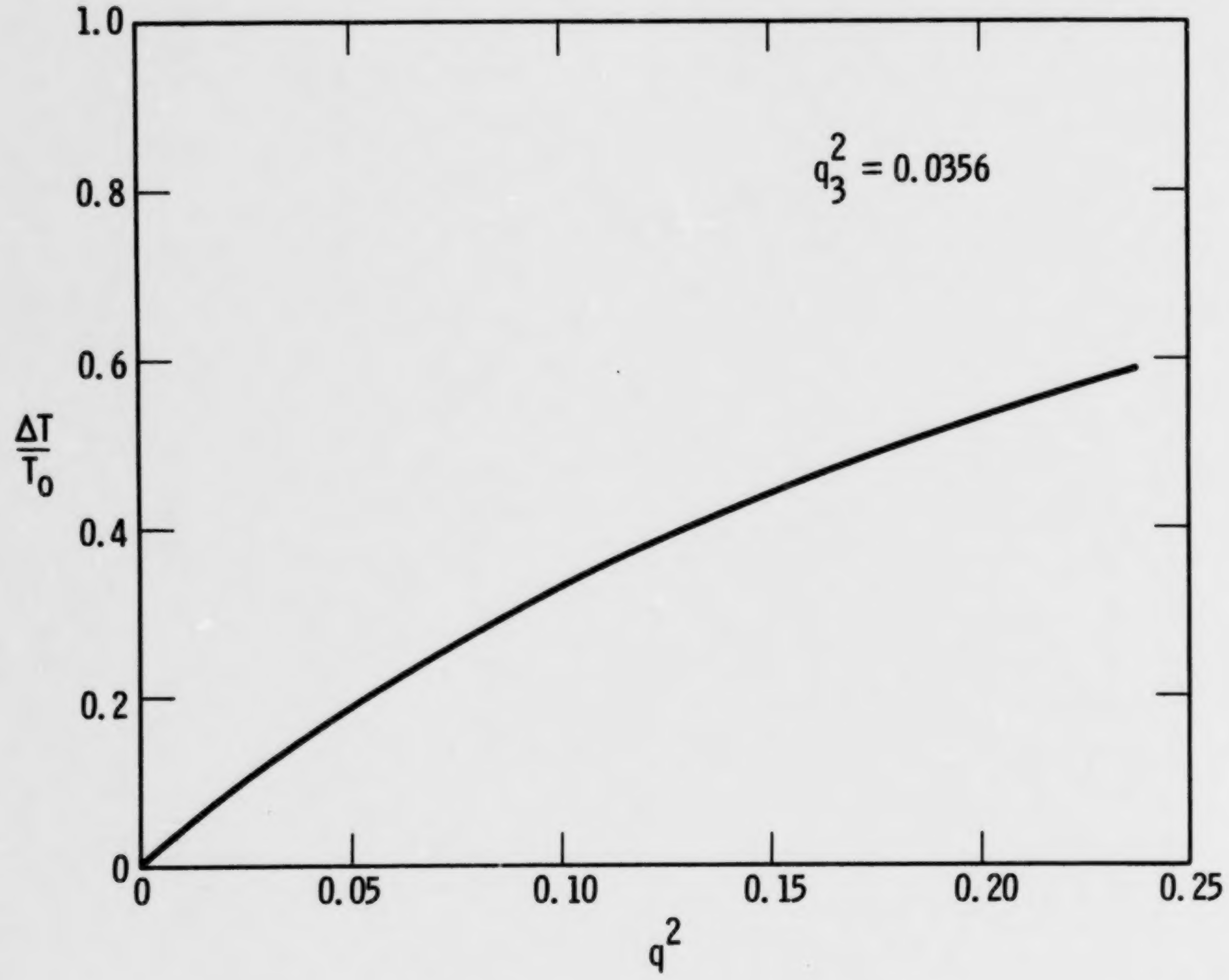

Fig. 3.40—Ratio of temperature change in vortex tube to inlet gas temperature

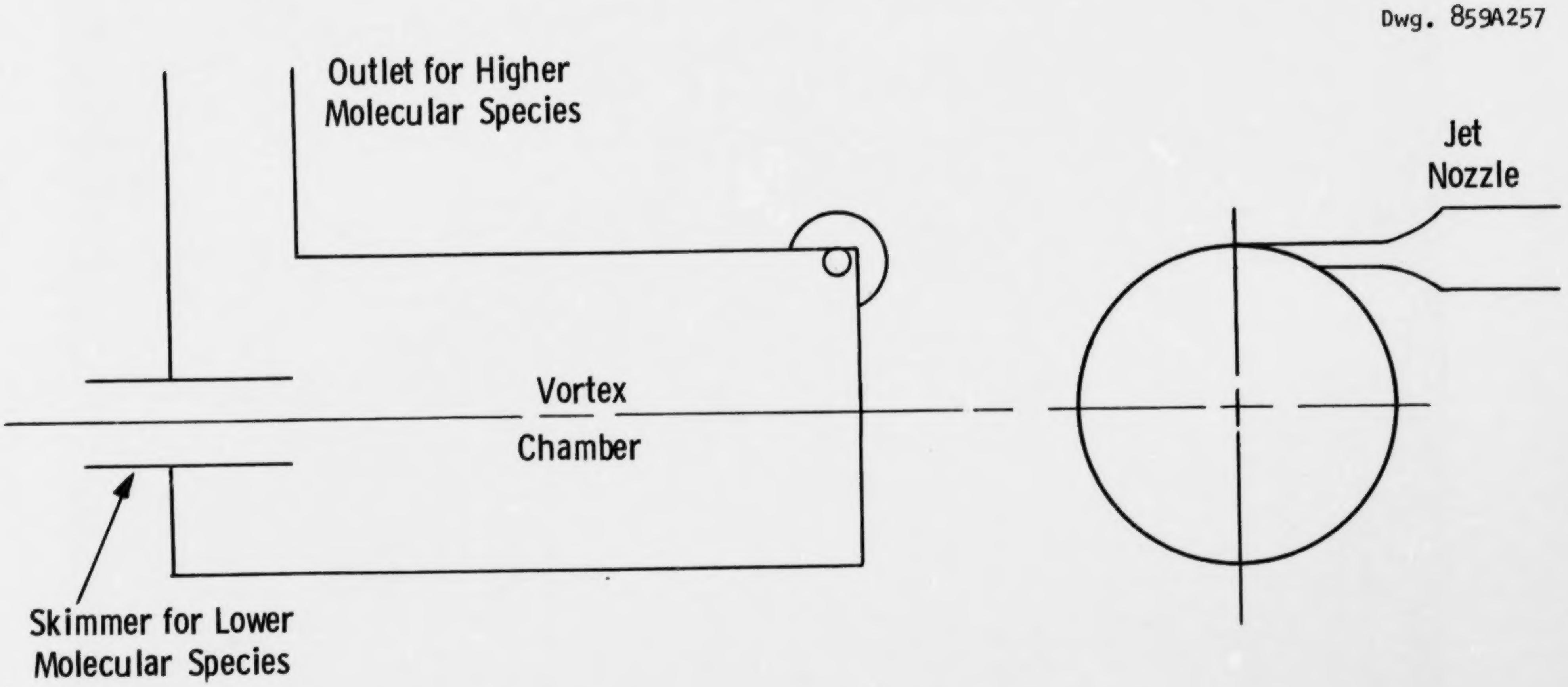
Dwg. 859A257
Outlet for Higher Molecular Species
Jet Nozzle
Vortex Chamber
Skimmer for Lower Molecular Species

Fig. 3.41—Vortex tube model for separation

List of Symbols

a	radius of larger tube
b	radius of smaller tube
k	ratio of specific heats
M_A	molecular weight of lower species
M_B	molecular weight of higher species
$\bar{M}$	mean molecular weight of gas mixture
p_{2a}	peripheral pressure in larger tube
p_c	core pressure
p_e	exit pressure from vortex open end
p_{2m}	core pressure of larger tube
p_{3m}	core pressure of smaller tube
p_o	nozzle inlet pressure
p_p	peripheral pressure
R	gas constant
T_o	nozzle inlet temperature
T_2	temperature in larger tube
T_3	temperature in smaller tube
u_{ta}	peripheral tangential velocity in larger tube
u_{tb}	peripheral tangential velocity in smaller tube
X_p	mole fraction of SO_2 in product
X_w	mole fraction of SO_2 in waste
α	separation factor
ΔT	temperature depression in vortex tube (when $\theta = 0.5$, this is also the temperature elevation)
θ	cut of separation device

References

1. Ranque, G., "Method and Apparatus for Obtaining from a Fluid under Pressure Two Currents of Fluids at Different Temperature," U.S. Patent 1,952,281.
2. Hilsch, R., "Use of the Expansion of Gases in a Centrifugal Field as Cooling Process," The Review of Scientific Instruments, Vol. 18, No. 2, February 1947.
3. Mürtz, H. J., and Nöller, H. G., Z. Naturforsch, 16a, 569-577 (1961).
4. German Patent 1,154,793 (September 26, 1963), H. G. Nöller.
5. Bornkessel, K., and Pilot, J., Z. Physik. Chem. 221, 177-184 (1962).
6. Kirk and Othmer, "Encylopedia of Chemical Technology - 2nd Edition," Vol. 7, pp. 165-7.
7. Way, S., "Theoretical Performance of Hilsch-Ranque Tube," Westinghouse Research Report 60-8-05-24-R13, March 2, 1955.

4. CONCLUSIONS

Based on the analyses of the various physical methods of separating SO_2 from flue gas, the following conclusions may be drawn:

1. Gaseous Diffusion
   a. The separation of SO_2 from flue gas by gaseous diffusion or effusion is technically feasible with the use of a separation cascade made up of several stages.
   b. Estimates of the capital cost alone of the order of #650/kW make this process uneconomic.
2. Membrane Separation
   a. The use of permselective membranes, such as silicone rubber, for SO_2 separation was found to technically feasible.
   b. Capital cost estimates of about $130/kW are still excessive.
3. Centrifugation
   a. The use of a cascade of centrifuges in SO_2 separation from flue gas is technically feasible. The materials having the highest potential for this application are titanium, maraging steel and filament wound glass-resin composites.
   b. Cost estimates of the components of a centrifuge cascade system indicate that the process is not economically feasible.
4. Condensation
   a. The technical feasibility of condensing SO_2 by using surface heat exchangers and providing cryogenic refrigeration is questionable because of the fouling of heat exchanger surfaces by deposition of solid CO_2. The use of an expansion turbine to provide the refrigeration is likewise questionable because of solid CO_2 fouling. However the use of the Joule-Thompson effect is technically feasible.

   b. The Joule-Thompson process requires the flue gas to be compressed to about 250 atmospheres, which makes the capital costs of compressors prohibitive. Cost of refrigerants, such as liquid N_2 is estimated at $50,000 per hour. With the addition of heat exchanger costs, the condensation technique is found to be uneconomic.

5. Mass Spectrometry
   a. There is no question about the technical feasibility.
   b. Because the capacity of a mass spectrometer is very low and the operation pressure of the order of 2×10^{-5} Torr, this process is not economically feasible.
6. Magnetic Field Effects
   a. A magnetic field is known to affect selectively the molecular diffusivities of different molecular species.
   b. At the pressures considered extremely large magnetic fields are required to obtain a slight effect. Therefore, the use of magnetic fields for in direct separation processes is not considered commercial.
7. Electromagnetic Excitation
   a. The conversion of SO_2 to SO_3 might be technically feasible with the use of a high power continuous gaseous CO_2-N_2-He laser.
   b. Operating costs, estimated to be about $600/ton of coal, make it uneconomical.
8. Electrical Excitation
   a. The conversion of SO_2 to SO_3 by electrical excitation is technically feasible.
   b. Based on 5 mill/kW hr, the minimum cost of the conversion of SO_2 to SO_3 by electrical excitation is more than 1.6 times the cost of catalytic oxidation techniques. Therefore the process is not economically feasible.
9. Nuclear Radiation Excitation
   a. Conversion of SO_2 to SO_3 by nuclear radiation excitation is technically feasible.

b. The cost of operating a nuclear radiation source is estimated to be about $40 million per hour, which makes this process uneconomical.

10. Vortex Tube
    a. Separation of SO_2 from flue gas is technically feasible.
    b. Because of low operating pressure level and high power requirements, this device is not economically feasible.

5. RECOMMENDATIONS

In view of the negative results obtained in the feasibility study of the use of physical methods for the separation of SO_2 from flue gas in Phase I of this contract, it is recommended that no further work be done in this area until such time as new concepts are developed which were not available at the time of this study.

6. APPENDICES

6.1. Bibliographies

Cascade Theory and Design
Gaseous Diffusion
Membrane Separation
Centrifugation
Condensation
(Mass Spectroscopic) Separation
Magnetic Field
Electromagnetic Excitation
Filament Wound Glass Resin Composite Materials
Vortex Tube

Cascade Theory and Design

1. Benedict and Pigford, "Nuclear Chemical Engineering," McGraw-Hill, New York, 1957, Chapter 10, pp. 378-405.
2. Kirk-Othmer, "Encyclopedia of Chemical Technology," 2nd Edition, Vol. 7, pp. 94-109.
3. Cohen, K., "Theory of Isotope Separation," McGraw-Hill Book Co., New York, 1951, Chapters 1-4 inclusive.
4. Garrett, G. A., and Shacter, J., "Evaluation of Isotope Separation Processes," Proc. International Symposium on Isotope Separation, Amsterdam, 1957.
5. Kronberger, H. K., and Geoghegan, G. R. H., "Some Aspects of the Design Theory for Diffusion Plant Stages," Proc. of the Int. Symp. on Isotope Separation, Amsterdam, 1957.
6. Geoghegan, G. R. H., "The Theory of Series and Parallel Diffusion Plant Stage Connections," Proc. of the Int. Symp. on Iso. Sep., Amsterdam, 1957.
7. Levin, S. H., and von Halle, E., "Applicability of a Separation Process for Large-Scale Isotope Production," Proc. 2nd U.N. Conf. on the Peaceful Uses of Atomic Energy, Geneva, 1958, V. 4, pp. 366-70.
8. Oliveri, E., "Squaring Criteria for Diffusion Cascade," Energia Nucleare, V. 8, N. 7, July 1961, pp. 453-9.
9. De La Garza, A., "Generalization of Matched Abundance-Ratio Cascade for Multi-Component Isotope Separation," Chem. Eng. Science, V. 18, N. 2, February 1963, pp. 73-82.
10. Apelblat, A., and Pery, G., "Total Flow Rates in Isotope Separation System," Indus. and Eng. Chem. Fundamentals, V. 3, N. 1, February 1964, pp. 83-5.
11. De La Garza, A., et al, "Generalized Cascade for Multi-Component Isotope Separation," Chem. Eng. Progr. Sym. Series, V. 61, N. 55, 1965, pp. 27-33.
12. Troetsch, E., and Dickel, G., "Calculation of Squared-Off Cascades for Isotope Separation by Diffusion," Kerntechnik, V. 8, N. 1, Jan. 1966, pp. 18-22.

Gaseous Diffusion

1. Benedict, M. and Pigford, T. H., "Nuclear Chemical Engineering," McGraw-Hill Book Co., New York, 1957, pp. 472-510.
2. Kirk-Othmer, "Encyclopedia of Chemical Technology," 2nd Edition, Vol. 7, pp. 109-149.
3. Wiegandt, H. F., "Mechanical Energy Improves Diffusional Separations," Chemical Engineering, V. 64, N. 8, August 1957, pp. 273-9.
4. Whatley, M. E., "Summary of Separation Operations," Oak Ridge National Laboratory, Publ. ORNL, 2477, April 11, 1958.
5. Watson, W. W., "The Performance of Thermal Diffusion Columns," Proc. of the International Symposium on Isotope Separation, Amsterdam, 1957.
6. Grove, G. R., Foster, K. W., and Vallee, R. E., "Parameters of Thermal Diffusion Columns," Proc. of the Int. Symp. on Isotope Separation, Amsterdam, 1957.
7. Massignon, D., "Sur La Theorie de la Separation des Constituants d'un Melange Gazeux Isotopique par Diffusion a Travers une Barriere Poreuse," Proc. Int. Sym. on Iso. Separation, Amsterdam, 1957.
8. Caldirole, P. and Rossi, G., "Isotopic Effects in Adsorption and Surface Migration," Proc. Int. Symp. on Iso. Separation, Amsterdam, 1957.
9. Heymann, D. and Kistemaker, J., "Separation of Some Isotopes by Convection Diffusion," Proc. Int. Symp. on Iso. Separation, Amsterdam, 1957.
10. Becker, E. W., "Das Trenndüsenverfahren," Proc. Int. Symp. on Iso. Separation, Amsterdam, 1957.
11. Nardelli, G. and Repanai, A., "Physical Principles of 'Trennduese' Method," Energia Nucleare, V. 4, N. 4, August 1957, pp. 293-300, V. 5, N. 4, April 1958, pp. 247-60.
12. Perona, G., "Experimental Investigation of Efficiency Variations versus Pressure in Isotope Separation by Gaseous Diffusion Method," Energia Nucleare, V. 5, N. 5, May 1958, pp. 327-31.
13. Liu, V. C., "Note on Diffusive Separation of Gas Mixtures in Flow Fields," Applied Physics J., V. 29, N. 8, August 1958, pp. 1188.

14. Gambill, D. W. R., "Predict Diffusion Coefficients," Chemical Engineering, V. 65, N. 11, June 2, 1958, pp. 125; V. 65, N. 13, June 30, pp. 113-16.

15. Berman, A. S. and Lund, L. M., "Deviations in Classical Kinetic Theory in the Low Pressure Transport of Gases through Porous Media," Proc. of the 2nd U.N. Conference on the Peaceful Uses of Atomic Energy, Geneva, 1958, V. 4, pp. 359-65.

16. Roubeix, G., Dore, R., and Coche, Y., "Application of Conventional Techniques to the Construction of a Pilot Plant for the Isotopic Separation of Uranium by Gaseous Diffusion," Proc. 2nd U.N. Conf. on the Peaceful Uses of Atomic Energy, Geneva, 1958, V. 4, pp. 375-9.

17. Charpin, J., Plurien, P., and Mommejac, S., "Application of General Methods of Study of Porous Bodies to the Determination of the Characteristics of Barriers," Proc. 2nd U.N. Conf. on the Peaceful Uses of Atomic Energy, Geneva, 1958, V. 4, pp. 380-7.

18. Massignon, D., "Characteristics of Barriers that can be Used for Isotope Separation by Gaseous Diffusion," Proc. 2nd U.N. Conf. on Peaceful Uses of Atomic Energy, Geneva, 1958, V. 4, pp. 388-94.

19. Martensson, M., et al, "Some Types of Membranes for Isotope Separation by Gaseous Diffusion," Proc. 2nd U.N. Conf. on Peaceful Uses of Atomic Energy, Geneva, 1958, V. 4, pp. 395-404.

20. Bilous, O., and Counas, G., "Determination of the Separation Factor of the Uranium Isotopes Produced by Gaseous Diffusion," Proc. 2nd U.N. Conf. on Peaceful Uses of Atomic Energy, Geneva, 1958, V. 4, pp. 405-11.

21. Albert, H., "Design of a Gaseous Diffusion Uranium Hexafluoride Isotopic Concentration Experimental Line," Proc. 2nd U.N. Conf. on Peaceful Uses of Atomic Energy, Geneva, 1958, V. 4, pp. 412-7.

22. Frejacques, C., et al, "Principal Results Obtained in France in Studies of the Separation of the Uranium Isotopes by Gaseous Diffusion," Proc. 2nd U.N. Conf. on Peaceful Uses of Atomic Energy, Geneva, 1958, V. 4, pp. 418-21.

23. Bilous, O., "Study of the Economics of a Plant for the Separation of Uranium Isotopes by Gaseous Diffusion," Proc. 2nd U.N. Conf. on Peaceful Uses of Atomic Energy, Geneva, 1958, V. 4, pp. 422-7.

24. Becker, E. W., et al, "Separation of the Uranium Isotopes by the Nozzle Process," Proc. 2nd U.N. Conf. on Peaceful Uses of Atomic Energy, Geneva, 1958, V. 4, pp. 455-7.

25. Gverdtsiteli, L. G., et al, "Isotope Separation by Diffusion in a Current of Steam," Proc. 2nd U.N. Conf. on Peaceful Uses of Atomic Energy, Geneva, 1958, V. 4, pp. 608-18.

26. Barrer, R. M., "New Selective Sorbents: Porous Crystals as Molecular Filters," Brit. Chem. Eng., V. 4, N. 5, May 1959, pp. 267-79.

27. Hurley, F. I., "Isotope Separation," Engineering, V. 187, N. 4849, February 1959, pp. 202.

28. Liu, V. C., "On Separation of Gas Mixtures by Suction of Thermal Diffusion Boundary Layer," Quarterly Journal of Mechanics and Applied Mathematics, V. 12, pt. 1, February 1959, pp. 1-13.

29. Reeds, J. N., and Kammermeyer, K., "Adsorption of Mixed Vapors," Industrial and Engineering Chemistry, V. 51, N. 5, May 1959, pp. 707.

30. Gose, E. E., "On Separation of Gas Mixtures in Jet," AIChE J., V. 6, N. 1, March 1960, pp. 168.

31. Currie, J. A., "Gaseous Diffusion in Porous Media," Brit. J. Applied Physics, V. 11, N. 8, August 1960, pp. 314-24.

32. Dore, R., "Problems Encountered in the Technique of Gaseous Diffusion; Uranium Separation through Porous Barriers," LeVide, V. 14, N. 82, July-August 1959, pp. 183-96.

33. Oliveri, E., "Separation Efficiency in Processes of Isotope Enrichment by Diffusion," Energia Nucleare, V. 8, N. 7, July 1961, pp. 474.

34. Haselden, G. G., "Thermodynamics of Separation," Ingenieur, V. 74, N. 8, February 23, 1962, pp. Ch. 9-16.

35. Gilliland, G. R., et al, "Flow of Gases through Porous Solids under the Influence of Temperature Gradients," AIChE J., V. 8, N. 4, September 1962, pp. 530-6.

36. Scott, D. S., and Dullien, F. A., "Diffusion of Ideal Gases in Capillaries and Porous Solids," AIChE J., V. 8, N. 1, March 1962, pp. 113-7.

37. Boettger, O., and Pingel, H., "Isotope Separation by Molecular Pump," Vakuum Technik, V. 12, N. 2, March 1963, pp. 33-7.

38. Pecqueur, M., "Separation of Uranium Isotopes," Annales des Mines, November 1963, pp. 658-76.

39. Carter, J. W., "Advances in Adsorption Processes," Brit. Chem. Eng., V. 9, N. 4, April 1964, pp. 232-8.

40. Frejacques, C., and Galley, R., "Information Derived from French Studies and Achievements in the Field of Uranium Isotope Separation," Proc. 3rd U.N. Conf. on the Peaceful Uses of Atomic Energy, Geneva, 1964, V. 12, pp. 329-33.

41. Fiocchi, R., "Separation Efficiency in the Diffusion of Non-Isotopic Gaseous Mixtures," Energia Nucleare, V. 12, N. 7, July 1965, pp. 372-7.

42. Friedlander, H. Z., and Rickles, R. N., "Membrane Separation Processes," Chem. Eng., V. 73, N. 9, April 25, 1966, pp. 163-8.

43. Burnett, R. W., and Turnbull, W., "Industrial Applications of Molecular Sieves," Brit. Chem. Eng., V. 11, N. 4, April 1966, pp. 261.

44. Barrer, R. M., "Surface Flow and Mixture Separation in Micro-Porous Media," AIChE Inst. Chem. Engrs. 1, Joint Conf. on Advances in Separation Techniques, Paper 1-11, London, June 1965, pp. 93-103.

45. Ellis, S. R. M., "Selection of Methods of Separation," J. of Applied Chemistry, V. 16, N. 6, June 1966, pp. 184-6.

46. Saxena, V. K., and Saxena, S. C., "Isotope Separation by Thermal Diffusion Columns," Indian Journal of Technology, V. 4, N. 8, August 1966, pp. 227-30.

47. Carter, J. W., "Adsorption Processes," Chem. and Process Eng., V. 47, N. 8, 9, August 1966, pp. 37, Sept. 1966, pp. 70.

48. Stern, S. A., "Industrial Applications of Membrane Processes - Separation of Gas Mixtures," Southern Research Institute, Proc. Sym. on Membrane Processes for Industry, May 1966, pp. 196-217.

49. Henry, J. P., et al, "Diffusion of Gases in Porous Solids over 1300/1 Pressure Range," Chem. Eng. Science, V. 22, N. 1, January 1967, pp. 11-20.

50. Schuette, R., and Seidel, D., "Jet Separation of Uranium Isotopes in Closed Circulation System," Chemie-Ingenieur-Technik, V. 39, N. 2, January 24, 1967, pp. 80-4.

51. Saxena, V. K., and Saxena, S. C., "Determination of Optimum Operating Conditions in Thermal Diffusion Column," Indian Journal of Technology, V. 4, N. 12, Dec. 1966, pp. 347-53.

52. Whitaker, S., "Diffusion and Dispersion in Porous Media," AIChE J., V. 13, N. 3, May 1967, pp. 420-7.

53. Anderson, J. B., "Separation of Gas Mixtures in Free Jets," AIChE J., V. 13, N. 6, Nov. 1967, pp. 1188-92.

54. Spiegler, K. S., "Diffusion of Gases across Porous Media," Indus. and Eng. Chem. Fundamentals, V. 5, N. 4, Nov. 1966, pp. 529-32.

55. Rutherford, W., "Isotope Separation Process Relies on Tight Control of Leakages," Chem. Eng., V. 74, July 17, 1967, pp. 176-8.

56. Lagrange, P., and Bilous, O., "Re-enrichment of Depleted Uranium by Passage through a Gaseous Diffusion Installation," Proc. 2nd U.N. Conf. on the Peaceful Uses of Atomic Energy, Geneva, 1958, V. 13, pp. 607-13.

57. Danatos, S., "Unusual Separations," Chem. Eng., V. 71, December 7, 1964, pp. 155-168.

58. Rozen, A. M., and Mikhailichenko, A. J., "Dependence of Separation Factor during Isotopic Exchange on Properties of Molecules," Atomnaya Energiya, V. 18, N. 2, Feb. 1965, pp. 147-56. English translation in Soviet Atomic Energy, V. 18, N. 2, Feb. 1965, pp. 180-90.

59. Frejacques, C., "Isotope Separation," Energia Nucleare, V. 6, N. 8, Dec. 1964, pp. 531-2.

60. Andrew, S. P. S., "Simple Method of Measuring Gaseous Diffusion Coefficients," Chem. Eng. Science, V. 4, N. 6, Dec. 1955, pp. 269-72.

Membrane Separation

1. Michaels A. S. and Bixler H. J., J. Polymer Science 50, 393 (1961).
2. Michaels A. et al, J. Applied Physics 34, 1, (1963).
3. Michaels A. S., Bixler H. J., and Fein, H. L., J. Appl. Phys., 35, 3165 (1964).
4. Barrer, R. M., J. Phys. Chem., 61, 178 (1957).
5. Meares, P., Trans. Faraday Soc., 53, 10 (1959); 54, 40 (1958).
6. Brandt, W. W., J. Phys. Chem., 63, 1080 (1959).
7. Michaels, A. S., Vieth, W. R., and Barrie, J. A., J. Appl. Phys., 34, 13 (1963).
8. Michaels A. S., and Bixler, H. J., J. Polymer Sci., 50, 413 (1961).
9. Lasoski, S. W., Jr., and Cobbs, W. H., Jr., J. Polymer Sci., 36, 21 (1959).
10. Michaels, A. S., Baddour, R. F., Bixler, H. J., and Choo, C. Y., Ind. Eng. Chem. Process Design Develop., 1, 14 (1962).
11. Baddour, R. F., Michaels, A. S., Bixler, H. J., deFilippi, R. P., and Barrie, J. A., J. Appl. Polymer Sci., 8, 897 (1964).
12. Li, N. N., Long, R. B., and Henley, E. J., Ind. Eng. Chem., 57, 18-29 (1965).
13. Rickles, R. N., Ind. Eng. Chem., 58, 18-35 (1966).
14. Weller, S., and Steiner, W. A., J. Appl. Phys., 21, No. 4, 279 (1950).
15. Weller, S., and Steiner, W. A., Chem. Eng. Progr., 46, No. 11, 585 (1950).
16. Breuer, M. E., Ph.D. Thesis, Univ. of Iowa (1966); Separation Science, 2, No. 3, 319 (1967).
17. Barrer, R. M., Proc. Brit. Ceram. Soc., 5, 21 (Dec. 1965); A.I.Ch.E.-Inst. Chem. Engrs. (London) Symp. Ser., 1, 112 (1965).
18. Aylmore, L. A. G., and Barrer, R. M., Proc. Roy. Soc. (London) Ser. A, 290, No. 1423, 477 (1966).
19. Kammermeyer, K., and Rutz, L. D., Chem. Eng. Progr. Symp. Ser., 55, No. 24, 163 (1959).

20. Paper presented at NATO Advanced Study Institute on Synthetic Polymer Membrane Systems, Ravello, Italy (Sept. 1966).
21. Tock, R. W., M.S. Thesis, Univ. of Iowa (1964).
22. Sobolev, I., Meyer, J. A., Stannett, V., and Szwarc, M., Ind. Eng. Chem., 49, No. 3, 441 (1957).
23. Robb, W. L., General Electric Co., Report No. 65-C-031 (Oct. 1966).
24. Barrer, R. M., and Chio, H. T., J. Polymer Sci. C, 10, 11 (1965).
25. Lebovitz, A., Mod. Plastics, 43, No. 7, 139, 144, 194 (1966).
26. Stern, S. A., "Industrial Applications of Membrane Processes: The Separation of Gas Mixtures," presented at Proc. Symp. Membrane Processes Ind., 1966, 196.
27. Rogers, C. E., "Permeability and Chemical Resistance," in Engineering Design for Plastics, Reinhold, New York, 1964.
28. Ash, R., Barrer, R. M., and Pope, C. G., Proc. Roy. Soc. (London), Ser. A, 271, 1, 19 (1963).
29. Li, N. N., and Henley, E. J., A.I.Ch.E. J., 10, No. 5, 666 (1964).
30. Li, N. N., Long, R. B., and Henley, E. J., "Membrane Separation Processes," in Ind. Eng. Chem., 57, No. 3, 18 (1965).
31. Major, C. J., and Tock, R. W., Atmosphere in Space Cabins and Closed Environments, Appleton-Century Crofts, New York (1966), pp. 120-144.
32. Kammermeyer, K., Ind. Eng. Chem., 49, No. 10, 1685 (1957); U.S. Pat. 2,966,235 (Dec. 27, 1960).
33. Robb, W. L, Chem. En., 71, No. 24, 94 (1964); General Electric Co., Res. Lab. Bull., Winter 1964-65, pp. 7-8.
34. Perry, E. S., "Progress in Separation and Purification", Volume 1, John Wiley & Sons, New York, 1968.

Centrifugation

1. Kirk and Othmer, "Encyclopedia of Chemical Technology, Second Edition," Interscience Publishers, New York, 1965, Vol. 4, pp. 755-8 and Vol. 7, pp. 148-165.
2. Beams, J. W., Rev. Mod. Phys. 10, 245 (1938).
3. Beams, Snoddy, and Kuhlthan, "Tests of the Theory of Isotope Separation by Centrifuging," Proc. 2nd U. N. Conf. Peaceful Uses of Atomic Energy, Geneva, 1958, Vol. 4, pp. 428-34.
4. Benedict, M. and Pigford, T. H., Nuclear Chemical Engineering, McGraw-Hill Book Co., New York, 1957.
5. Groth, Beyerle, Nann, and Welge, "Enrichment of the Uranium Isotopes by the Gascentrifuge Method," Proc. 2nd U. N. Conf. on Peaceful Uses of Atomic Energy,Geneva,1958, Vol. 4, pp. 439-46.
6. Cohen, K., Theory of Isotope Separation, McGraw-Hill Book Co., New York, 1951.
7. Kistemaker, Los, and Veldhuyzen, "The Enrichment of Uranium Isotopes with Ultracentrifuges," Proc. 2nd U. N. Conf. on Peaceful Uses of Atomic Energy, Geneva, 1958, Vol. 4, pp. 435-38.
8. Lindemann, F. A. and Aston, F. M., Phil. Mag. 37, 530 (1919).
9. Milliken, R. S., J. Chem. Soc. 44, 1033 (1922).
10. Los and Kistemaker, "On the Influence of Temperature Distributions Inside a Gas-Centrifuge," Proc. Symposium on Isotope Separation, Amsterdam, 1957, pp. 695-700.
11. Hamel, P., "Analyzing Gas Centrifuge for Fuel Fabrication," Canadian Nuclear Technology, Spring 1962, pp. 48-53.
12. Zippe, G., "The Development of Short Bowl Centrifuges," Report No. EP-4420-101-60U, July 1960, submitted to U. S. Atomic Energy Comm. by Research Laboratories for the Engineering Sciences, University of Virginia.
13. Beams, J. W., "Notes on the History of Isotope Separation by Centrifuging," University of Virginia.
14. Hertz, H. G. and Nann, E., "On the Dependence of the Separation Effort on the Countercurrent Circulation in the Gas Centrifuge,"

Z. Naturforschg, 10a, 170-171, Jan. 1955. English translation in Report No. EP-4422-133-61U, Feb. 1961, Res. Lab. for Eng. Sci., University of Virginia.

15. Bulang, W., Groth, W., Jordan, L., Kolbe, W., Nann, E., and Welge, K. H., "On the Separation Potential of Thermally Driven Countercurrent Gas Centrifuges," Zeitschrift für Physikalische Chemie Neue Folge, Bo.24,5.249-264 (1960). English translation in Report No. EP-4422-117-60U, Sept. 1960, Res. Lab. for the Eng. Sci., Univ. of Virginia.

16. Mottley, J. D., "Minutes of Westinghouse Presentation to the Atomic Energy Comm. on Application of New Technologies to Uranium Enrichment, Nov. 1966," Report WCAP-7005, Westinghouse Atomic Power Division.

17. Ouwerkerk and Los, "The Separative Power of Short Countercurrent Centrifuges," Proc. of 3rd U.N. Conf. on Peaceful Uses of Atomic Energy-Geneva-1964, Vol. 12, pp. 367-71.

18. Jordan, Kolbe, and Barges da Silva, "Separation of Stable Isotopes by the Gas Centrifuge Method: Influence of the Axial Pressure on the Separation of Argon Isotopes," Proc. 3rd U.N. Conf. on Peaceful Uses of Atomic Energy-Geneva-1964, Vol. 12, pp. 358-64.

19. Takashima, Kanagawa, and Oyama, "Isotope Separation by Concurrent Gas Centrifuge," Proc. 3rd U.N. Conf. on Peaceful Uses of Atomic Energy-Geneva-1964, Vol. 12, pp. 352-5.

20. Boettgen, O., "Isotope Separation by Gas Centrifuges," Kerntechnik 6:571-6 (Dec. 1964). (In German)

21. AEC-TR-5986, Isotope Separation and Enrichment from Chem. Ing. Tech. 34:580 (1962). Translated by K. Bier et al.

22. AEC-TR-4983, Gas Centrifugal Separation by Akina Kanagawa from Gen. Hatsuden 4:Nos. 3-4, 49-61 (1960). Translated by ORNL.

23. CEA-TR-X-397, Industrial Methods for Enrichment of U235, by Istvan Kies from Energia Atomtech, Vol. 11:466-73 (1958). Translated into French.

24. Strnad, J., "Separation in Centrifuge-Model," Applied Science Research, Sec. A, V. 10, N. 5, 1961, pp. 307-10.

25. Ambler, C. M., "Centrifugation Equipment," Indus. and Eng. Chem., V. 53, N. 6, June 1961, pp. 430-33.

Condensation

1. Ruhemann, M., "The Separation of Gases," Oxford University Press, 1949.
2. Kohl, A. L., and Riesenfeld, F. C., "Gas Purification," McGraw-Hill Book Co., Inc., 1960.
3. Kirk-Othmer, "Encyclopedia of Chemical Technology," 2nd Edition, V. 6, pp. 471-481.
4. Arregger, J. E., "Production and Purification of Argon," Chem. and Process Eng., V. 47, N. 10, Oct. 1964, pp. 549.
5. Bewilogua, L., "Continuously Working Plant for the Separation of Neon-Helium Mixtures," Cryogenics, V. 2, N. 5, Sept. 1962, pp. 290-1.
6. Estrin, J., et al, "The Condensation of Mixed Vapors," AIChE J., V. 11, N. 5, Sept. 1965, pp. 800-3.
7. Downer, W., "Ammonia Absorption Refrigeration Selected for Gasoline Plant," Petroleum Engineer, V. 29, N. 7, July 1957, pp. C25, 28-30.
8. Updegraff, N. C., "Gas Prepurification for Low Temperature Processing," Chem. Eng. Progress, V. 5, N. 6, June 1957, pp. 268.
9. Mogain, W. A., "Reciprocating Expansion Engine used for Generating Very Cold Temperatures," Iron and Steel Engr., V. 35, N. 6, June 1958, pp. 130.
10. Perry, E. J., "Low Temperature Refrigerating Plant for Atomic Diffusion Process," Journal of Refrigeration, V. 1, N. 1, Nov.-Dec. 1957, pp. 15-8.
11. "Joint Symposium on Recent Developments in Industrial Low Temperature Gas Separation," Instn. Chem. Engrs. - Trans. V. 36, N. 3, June 1958, pp. 123-223.
12. Bras, G. H. P., "Design of Cooler-Condensers," Indus. Chemist, V. 33, N. 394, Dec. 1957, pp. 604-12.
13. Young, A. R., "Liquid Methane - Cheaper Means of Peak Shaving," Oil and Gas J., V. 57, N. 13, March 23, 1959, pp. 75.
14. Clark, W. E., and Kurata, F., "Freezing CO_2 from Natural Gas," Petroleum Refiner, V. 38, N. 6, June 1959, p. 249.
15. Madejski, J., "Design of Cooler Condensers," Brit. Chem. Engr., V. 4, N. 3, March 1959, pp. 148-53.

16. Francis, A. W., and Lowd, J. D., "How to Increase Liquid Recovery from Your Gas Condensate Wells," Oil and Gas J., V. 57, N. 51, December 14, 1959, p. 68.
17. Lafay, F., "New Machine for the Industrial Liquefaction of Gases," Genie Civil, V. 139, N. 9, May 1, 1962, pp. 206-11.
18. "Growing Importance of Cryogenic Engineering - Separation of Gases at Stoke-on-Trent," Modern Refrigeration, V. 66, N. 789, Dec. 1963, pp. 1124-7.
19. Mulvihill, J. W., et al, "Cost Estimates of Processes for Separating Mixtures of Methane and H_2," U.S. Bureau of Mines, Report of Investigations 6530, 1964, 43 p.
20. Mizushina, T., et al, "Simplified Calculations for Cooler Condensers for Gas-Multicomponent Vapor Mixtures," Int. J. of Heat and Mass Transfer, V. 7, N. 1, Jan. 1964, pp. 95-100.
21. Mercer, S., "Chemical Engineering Below 70°K," Chem. and Process Eng., V. 45, N. 10, Oct. 1964, p. 555.
22. Schuftan, P. M., "Recent Advances in Air Separation," Chem. and Process Eng., V. 45, N. 10, Oct. 1964, pp. 545-8.
23. Ross, K., "Condensation of H_2SO_4 from Flue Gas on Cooled Cylinder," Inst. of Fuel J., V. 38, N. 293, June 1965, pp. 273-7.
24. Mellen, A. W., "Cryogenics and Gas Processing Industry," Natural Gas Processors Assn., 44th Annual Convention Proc., March 24-26, 1965, pp. 12-17.
25. Ruhemann, M., and Charlesworth, P. L., "Thermodynamic Efficiency of Gas Separation Plants," Brit. Chem. Eng., V. 11, N. 8, Aug. 1966, pp. 839-42.
26. Schuftan, P. M., "Extraction of Helium, Neon, and Hydrogen," Chem. and Process Eng., V. 48, N. 4, April 1967, p. 59, 66.
27. Salama, C., and Eyre, D. V., "Multiple Refrigerants in Natural Gas Liquefaction," Chem. Eng. Progress, V. 63, N. 6, June 1967, pp. 62-7.
28. Bras, G. H., "Design of Cooler Condensers for Vapor Gas Mixtures - I and II," Chem. Eng., April 1953, pp. 223-6, May 1953, pp. 238-40.

(Mass Spectroscopic) Separation

1. Smyth, Henry D., "Atomic Energy for Military Purposes," Princeton Univ. Press, 1945.
2. Smith, M. L., "Operational Experience with Hermes; The Harwell Active Electromagnetic Separation," Proc. of Int. Symposium on on Isotope Separation, Amsterdam, 1951, North Holland Publishing Co., Amsterdam, 1958, pp. 581-96.
3. Livingston, R. S., and Martin, J. A., "Electromagnetic Separation of the Isotopes of the Heavy Elements," ibid. pp. 597-609.
4. Livingston, R. S. and Martin, J.A., "Special Isotope Separation for Identification or Purification of Radioactive Species," ibid, pp. 510-14.
5. Love, L. O. et al, "Present Status of Electromagnetic Separation of Stable Isotopes at the Oak Ridge National Laboratory," ibid, pp. 615-21.
6. Morozov, P. M., "An Ion Source of Stable Isotope Separation," 2nd U.S. Int. Conference on Peaceful Uses of Atomic Energy, *Geneva 1958, Vol. 4, pp. 447-49.
7. Neglin and Morozor, "Influence of Electric Fields in Ion Beams on Electromagnetic Separation of Stable Isotopes," ibid, pp 450-54.
8. Alexjeev, B. A. et al, "Isotope Separation of Rare-Earth Elements by the Electromagnetic Method, ibid, pp. 465-70.
9. Zolotarev, V. S. et al, "Isotope Separation by Electromagnetic Separators in the Soviet Union, ibid, pp. 471-79.
10. Zuk, W., et al, "Electromagnetic Isotope Separator at Lublin, "Nuclear Instrument and Methods, Vol 37, pp. 249-38 (Nov. 1965).
11. "Electromagnetic Isotope Separators and their Applications," Proceedings of the International Conference, Aarhus, Denmark, 1965, Nuclear Instruments and Methods, Volt 38, pp. 1-325 (1965).

Magnetic Field

1. H. Senftleben and O. Riechemier, "On Reaction Kinetics in the Formation of Hydrogen Molecules From Atoms," Physik. Zeits. 31, 961 (1930) (In German).
2. H. Englehardt and H. Sack, "Influence on the Inner Friction of O_2 by Means of a Magnetic Field," Physik. Zeits. 33, 724 (1932).
3. F. Zernike and C. vanLier, "Theory of the Senftleben Effect," Physica VI, 961 (1939).
4. C. J. Gorter, "On the Interpretation of the Senftleben Effect," Naturiss. 26, 140 (1938).
5. J. O. Hirschfelder et.al., "Molecular Theory of Gases and Liquids," Wiley & Sons, N. Y., 1954.
6. C. S. Wang Chang and G. E. Uhlenbeck, "Transport Phenomena in Polyatomic Gases," U. of Michigan Report CM-681 (1951).
7. C. E. Curtiss, "Kinetic Theory of Nonspherical Molecules," J. Chem. Phys. 24, 225 (1956).
8. L. Monchick et.al., "Formal Kinetic Theory of Transport Phenomena in Polyatomic Gas Mixtures," J. Chem. Phys. 39, 654 (1963).
9. J. J. M. Beenakker et.al., "The Influence of a Magnetic Field on the Transport Properties of Diatomic Molecules in the Gaseous State," Phys. Lett. 2, 5 (1962).
10. J. S. Dahler and N. F. Sather, "Kinetic Theory of Loaded Spheres I." J. Chem. Phys. 38, 2363 (1962).
11. L. L. Gorelik and V. V. Simtsyn, "Influence of a Magnetic Field on the Thermal Conductivity of Gases with Nonspherical Molecules," Soviet Physics, JETP 19, 272 (1964).
12. L. L. Gorelik, "Oxygen Gas Analyzers Using the Variation of Thermal Conductivity of Oxygen in a Magnetic Field," Soviet Physics Technical Physics 8, 1084 (1964).
13. L. L. Gorelik et.al., "Influence of a Magnetic Field on the Thermal Conductivity of Gases with Nonspherical Molecules," Soviet Physics JETP 21, 503 (1965).

14. S. I. Sandler and J. S. Dahler, "Kinetic Theory of Loaded Spheres II," J. Chem. Phys. 43, 1750 (1965).

15. D. W. Condiff et.al., "Transport Properties of Polyatomic Fluids, a Dilute Gas of Perfectly Rough Spheres," J. Chem. Phys. 42, 3445 (1965).

16. J. Korving et.al., "The Influence of a Magnetic Field on the Viscosity of CH_4 and CF_4 (Rough Spherical Molecules)," Phys. Lett. 17, 33 (1965).

17. J. Korving et.al., "The Influence of a Magnetic Field on the Transport Properties of Polyatomic Gases: Cr Comparison of Theory with Experiment," Phys. Lett. 24A, 755 (1967).

18. J. Korving, "The Influence of a Magnetic Field on the Transport Properties of Gases of Polyatomic Molecules," dissertation, Der Rijksuniversiteit te Leiden, Leiden, The Netherlands, 1967.

19. J. Korving et.al., "Transverse Momentum Transport in Viscous Flow of Diatomic Gases in a Magnetic Field," Physics Lett. 21, 5 (1966).

20. S. M. Hess and L. Waldmann, "Kinetic Theory for a Dilute Gas of Particles with Spin," Z. f. Naturforsch., 21a, 1529 (1966).

21. H. F. P. Knaap and J. J. M. Beenakker, "Heat Conductivity and Viscosity of a Gas of Nonspherical Molecules in a Magnetic Field," Physica 33, 643 (1967).

22. R. F. Snider and K. S. Lewchuk, "Irreversible Thermodynamics of a Fluid System with Spin," J. Chem. Phys. 46, 3163 (1967).

23. F. R. McCourt and R. F. Snider, "Thermal Conductivity of a Gas of Rotating Diamagnetic Molecules in an Applied Magnetic Field," J. Chem. Phys. 46, 2387 (1967).

24. F. R. McCourt and R. F. Snider, "Senftleben-Beenakker Effect for the Viscosity of a Dilute Gas of Diamagnetic Diatomic Molecules," J. Chem. Phys. 47, 4117 (1967).

25. Yu Kagan and L. Maksimov, "Transport Phenomena in a Paramagnetic Gas," Soviet Physics JETP 14, 604 (1962).

26. A. Tip, "Formal Classical Kinetic Theory of Mixtures of Dilute Gases Consisting of Diatomic Molecules in the Presence of an External Magnetic Field," FOM-Institut vour Atoom-en Molecuulfysica, Amsterdam, The Netherlands, (1966) (Unpublished).

27. A. Tip et.al., "Thermal Diffusion and the Senftleben Effect," Physica 32, 1429 (1966).

28. F. R. W. McCourt, "Transport Properties of Gases with Rotational States," dissertation, University of British Columbia, Vancouver, Canada, (1966).

Electromagnetic Excitation

1. C. B. Moore, "Laser Excited Vibrational Fluorescence and Its Application to Vibration-Vibration Energy Transfer in Gases," Ch. III of "Fluorescence," ed. G. Guilbault, M. Dekker, Inc., New York (1967).
2. V. Ya. Shlyapintokh, "Chemiluminescence in Low-Temperature Gas Phase Oxidation Reactions," Ch. X of "Chemiluminescence Techniques in Chemical Reactions," Consultants Bureau, New York (1968).
3. P. G. Ashmore et al., editors, "Photochemistry and Reaction Kinetics, Cambridge University Press, 1967.
4. B. Stevens, "Collisional Activation in Gases," Pergamon Press, Oxford, 1967.
5. N. B. Slater, "Theory of Unimolecular Reactions," Cornell University Press, Ithaca, New York, 1959.
6. C. S. Nalman, et al., Quarterly Report, May 1965, (Studies of the Effect of Laser Radiation on Chemical Activation and Vapor Fog Nucleation), AD 468165.
7. J. T. Yardley and C. B. Moore, "Laser Excited Vibrational Fluorescence and Energy Transfer in Methane," J. Chem. Phys. 45, 1006 (1966).
8. G. Porter and J. I. Steinfeld, "Giant Pulse Laser Flash Photolysis of Phthalocyanine Vapor," J. Chem. Phys. 45, 3456 (1966).
9. W. B. Tiffany, et al., "Selective Laser Photocatalysis of Bromine Reactions," Science 157, 40 (1967).
10. L. M. Epstein and K. H. Sun, "Chemical Reactions Induced in Gases by Means of a Laser," Nature 211, 1173 (1966).
11. E. W. Sucov, et al., "Plasma Production by a High Power Q-Switched Laser," Phys. of Fluids 10, 2035 (1967).
12. R. G. Tomlinson, et al., Report, 1 December 1965 (Comparison of Available Data on Laser-Induced Gas Breakdown) AD 478078.
13. C. Hsiung and A. A. Gordus, "Momentum Transfer to an Atom in a Molecule: Internal Excitation and Bond Dissociation," J. Chem. Phys. 36, 947 (1962).

14. D. J. Wilson, "Photochemical Reactions in the Gas Phase and Slater's 'New Approach to Rate Theory'," J. Chem. Phys. 38, 1098 (1963).
15. K. B. Eisenthal, et al., "Laser-Induced Luminescence and Dissociation in Biphenyl," J. Chem. Phys. 44, 4492 (1966).
16. W. B. Valance and E. W. Schlag, "Theoretical Rate Constant for Thermal Unimolecular Reactions in a Multilevel System," J. Chem. Phys. 45, 216 (1966).
17. E. Thiele, "Quantum Theory for the Unimolecular Rate Constant."
18. A. E. Douglas, "Anomalously Long Radiative Lifetimes of Molecular Excited States," J. Chem. Phys. 45, 1007 (1966).
19. R. N. Porter, "Theoretical Studies of Hot-Atom Reactions: I. General Formulation," J. Chem. Phys. 45, 2284 (1966).
20. R. T. Ross, "Some Thermodynamics of Photochemical Systems," J. Chem. Phys. 46, 4590 (1967).
21. B. J. Berne, et al., "Vibrational Relaxation of Diatomic Molecules in Gases and Liquids," J. Chem. Phys. 47, 1600 (1967).
22. L. Blum, "Theory of Unidimensional Molecular Collisions," J. Physical Chemistry 70, 2758 (1966).
23. A. M. Fainzil'ber and N. A. Fridlender, "Optical Conditions for Chemical Reactions in Gas Streams," British Chemical Engr. 12, 1100 (1967).
24. C. A. Eckert, "Molecular Thermodynamics of Chemical Reactions," Industrial and Engineering Chemistry 59, 20 (1967).
25. R. M. Noyes, "Reactions of Diatomic Molecules: I. A Method for Predicting Mechanisms," Jour. A.C.S. 88, 4311 (1966).
26. R. M. Noyes, "Reactions of Diatomic Molecules: II. Predictions and Comparison with Experiment," Jour. A.C.S. 88, 4318 (1966).
27. P. R. Walton and R. M. Noyes, "Reactions of Diatomic Molecules: III. Kinetics of Formation of Iodine Bromide."
28. E. D. Bugrim, et al., "On the Vibrational Relaxation of Diatomic Molecules in an Excited Electronic State," Optics and Spectroscopy 21, 13 (1966).

29. T. A. Garibyan, et al., "Study of the Mechanism of the Gas-Phase Photochemical Oxidation of Hydrocarbons by Means of Electron Paramagnetic Resonance," Doklady Physical Chemistry 176, 735 (1967).
30. G. A. Askar'yan, "Excitation and Dissociation of Molecules in an Intense Light Field," Soviet Physics, JETP 19, 273 (1964).
31. F. V. Bunkin, et al., "Dissociation of Molecules in a Strong Radiation Field," Soviet Physics, JETP 20, 145 (1965).
32. A. V. Phelps, "Theory of Growth of Ionization During Laser Breakdown," in Physics of Quantum Electronics, ed. P. L. Kelley, et al., McGraw-Hill, New York, 1966 (p. 538).
33. A. F. Haught, et al., "Electrical Breakdown of Gases by Optical Frequency Radiation," Ibid., p. 509.
34. R. W. Minck and W. G. Rado, "Investigation of Optical Frequency Breakdown Phenomena," Ibid., p. 527.
35. J. D. Feichtner, "Application of Lasers to Uranium Iostope Separation," Westinghouse Research Report 66-1C1-LNLIN-M2 (1966).
36. G. Porter, "Initiation of Hydrogen Chlorine Reaction by Red Laser Light," Nature 215, 502 (1967).
37. A. E. Cassano, et al., "Photochemical Reaction Engineering," Industrial and Engineering Chemistry, 59, No. 1, p. 18 (1967). Note - This paper also contains an extensive list of references (54 papers, 18 books) on photochemistry and reaction kinetics.
38. C. A. Eckert, "Molecular Thermodynamics of Chemical Reactions," Industrial and Engineering Chemistry 59, No. 9, p. 21 (1967).
39. H. Gerding and J. Lecomte, "The Infrared Absorption Spectrum of Gaseous and Liquid Sulfur Trioxide Physica VI, 737 (1939). (In German).
40. R. Gibert, "Conditions on the Possiblity of Isotope Enrichment by a Photochemical Reaction," J. Chim. Phys. 60, 205 (1963).
41. E. E. Nikitin, "Theory of Thermally Induced Gas-Phase Chemical Reactions," Indiana University Press, Bloomington, Indiana, 1966.
42. J. Rozenberg, "Photochemical Separation of Isotopes," Isotopes and Radiation Technology 3, No. 3, p. 200 (1966).

43. W. G. Valance, et al., "Theory of the Dissociation Kinetics of Diatomic Molecules," J. Chem. Phys. 47, 3284 (1967).

44. O. L. Chapman, "Organic Photochemistry," V. 1, M. Dekker, New York (1967).

45. W. G. Herkstroeter and G. S. Hammond, "Mechanisms of Photochemical Reactions in Solution. XXXIX. Study of Energy Transfer by Kinetic Spectrophotometry," Jour. A.C.S. 88, 4769 (1966).

46. D. R. Crosley, "Use of Optical Pumping to Detect Free Radicals During a Gas-Phase Photolysis," J. Chem. Phys. 47, 1366 (1967).

47. D. A. Buddenhagen, et al., "Observations of Ruby-Laser Beam Intensity Patterns with Dye-Sensitized Photopolymers," Proc. N.A.S. 48, 303 (1962).

48. Y. Pao and P. Rentzepis, "Laser-Induced Production of Free Radicals in Organic Compounds," Appl. Phys. Lett. 6, 93 (1965).

49. J. R. Novak and M. W. Windsor, "Laser Photolysis and Spectroscopy in the Nanosecond Time Range: Excited Singlet State Absorption in Coronene," J. Chem. Phys. 47, 3075 (1967).

50. A. M. Ronn, "Laser-Induced Fluorescence," J. Chem. Phys. 48, 511 (1968).

51. W. B. Tiffany, "Selective Photochemistry of Bromine Using a Ruby Laser," J. Chem. Phys. 48, 3019 (1968).

52. H. Brunet, "Vibrational Excitation of Molecules with CO_2 Laser Radiation," Paper 76-3, International Quantum Electronics Conference, Miami, 1968.

53. N. V. Karlov and A. M. Prokhorov, "Pulse CO_2 Lasers with Double Modulation and Bleachable Filters," Paper 76-7, International Quantum Electronics Conference, Miami, 1968.

54. N. V. Karlov, et al., "Q-Switching of a CO_2 Laser with a Saturating Filter Based on Boron Trichloride," Soviet Physics, JETP Letters 7, 174 (1968)(Original Russian Volume No. and Page).

55. L. E. S. Mathias, et al., "Laser Oscillations at Submillimeter Wavelengths From Pulsed Gas Discharges in Compounds of Hydrogen, Carbon, and Nitrogen," (1965).

56. P. Barchewitz, et al., "Continuous Laser Emission by Direct High Frequency Excitation of CO_2 and N_2O with Vibrational Transitions 00°1-10°0 and 00°1-02°0," Comptes Rendus 260, 5491 (1965).

57. J. S. Polanyi, "Proposal for an Infrared Maser Dependent on Vibrational Excitation," J. Chem. Phys. 34, 347 (1961).

58. P. D. Coleman, Final Report, 31 December 1965 (Molecular Gas Lasers) AD 632306.

59. L. N. Large and H. Hill, "A Compact Pulsed Gas Laser for the Far Improved," App. Optics 4, 625 (1965).

60. E. H. Weinberg, ONR Letter, December 1965 (Lasers in the United Kingdom) AD 476670.

61. C. K. N. Patel, et al., "CW High-Power CO_2-N_2-He Laser," App. Phys. Lett. 7, 290 (1965).

62. L. E. S. Mathias and A. Archer, "Stimulated Emission in the Far Infrared from Water Vapor and Denterium Oxide Discharges," Phys. Lett. 13, 35 (1964).

63. G. Moeller and J. Dane Rigden, "Observation of Laser Action in the R-Branch of CO_2 and N_2O Vibrational Spectra," App. Phys. Lett. 8, 69 (1966).

64. W. J. Witteman, "Inversion Mechanisms, Population Densities, and Coupling-Out of a High Power Molecular Laser," Philips Res. Reports 21, 73 (1966).

65. M. A. Kovacs, et al., "Q-Switching of Molecular Laser Transitions," App. Phys. Lett. 8, 62 (1966).

66. G. W. Flynn, et al., "Vibrational and Rotational Studies Using Q-Switching of Molecular Gas Lasers," App. Phys. Lett. 8, 63 (1966).

67. W. J. Witteman and G. V. d. Goot, "High Power Infrared Laser with Adjustable Coupling-Out," J. App. Phys. 37, 2919 (1966).

68. I. Wieder and G. B. McCurdy, "Isotope Shifts and the Role of Fermi Resonance in the CO_2 Infrared Maser," Phys. Rev. Lett. 16, 565 (1966).

69. B. Hartmann and B. Kleman, "Laser Lines from CO_2 in the 11-18 Micron Region," Can. J. Phys. 44, 1609 (July 1966).

70. O. R. Wood and S. E. Schwarz, "Passive Q-Switching of a CO_2 Laser," App. Phys. Lett. 11, 88 (1967).

71. R. Farreng, et al., "Molecular Spectroscopy with a Laser Source Study of the CO_2 Bond at 1064 cm^{-1}." Comptes Rendus B263, 241 (1966).

72. C. Rossetti, et al., "Molecular Optics: Molecular Spectroscopy with a Laser Source; Transition Moment of Rotation-Vibration for the 00°1-10°0 Transition of CO_2," Comptes Rendus 262, 1684 (1966).

73. G. B. Jacobs and H. C. Bowers, "Extension of CO_2 Laser Wavelength Range with Isotopes," J. App. Phys. 38, 2692 (1967).

74. J. Y. Coester and Ph. Vautier, "Development of a High Gain Amplifier without Circulating Gas, Operating Between 9 and 11 Microns," Infrared Physics 7, 173 (1967). (In French).

75. R. T. Ross, "Thermodynamics Limitations on the Conversion of Radiant Energy Into Work," J. Chem. Phys. 45, 1 (1966).

76. Brockmeier, Norman F., "Chemical Reactions Induced in a Microwave Discharge," Ph.D., Thesis Dept. of Chem. Engineering, MIT, August, 1966).

Bibliography on Filament Wound Glass Resin Composite Materials

1. Riley, Malcolm W., "What You Can Expect from Filament Wound Parts," Materials in Design Engineering, August, 1960, pp. 128-39.
2. Lub, J. H., and Jaffe, E. H., "How to Evaluate Materials for Filament Winding," Materials in Design Engineering, August, 1960, pp. 140-3.
3. Miller, S. A., and Carter, J. S., "How Process Variables Affect Filament Wound Plastics," Materials in Design Engineering, August, 1960, pp. 144-6.
4. Proceedings of Filament Winding Conference, SAMPE, San Gabriel Valley Chapter, March 28-30, 1961, Pasadena, California.
5. PLASTIC Report 10, "A Survey of Filament Winding: Materials, Design Criteria, Military Applications," Plastics Technical Evaluation Center, Picatinny Arsenal, Dover, New Jersey, May, 1962.
6. "Reinforcements: New Glasses, Fibers Developed," Materials Engineering, Feb., 1968, pp. 40-1.
7. Rosato, D. X., and Grove, C. S., "Filament Winding - Its Development, Manufacture, Applications, and Design," Interscience Publishers, New York, 1964.
8. Broutman and Kroch, "Modern Composite Materials," Addison-Wesley Publishing Co., 1962.
9. deDani, A., "Glass Fibre Reinforced Plastics", Interscience Publishers, Inc., New York, 1960, pp. 226-246.
10. Faupel, J. H., "Engineering Design", John Wiley, New York, 1964, pp. 312-317.
11. Dietz, A. G. H., "Composite Materials," Edgar Marburg Lecture presented at 68th ASTM Annual Meeting, June 16, 1965, West Lafayette, Indiana, ASTM, Philadelphia, Pennsylvania, 1965.
12. Shaffer, B. W., "Material Properties of Reinforced Plastics," SPE Transactions, Oct. 1964, pp.267-276.

Bibliography on Hilsch Vortex Tube

1. Hilsch, R., "Use of the Expansion of Gases in a Centrifugal Field as Cooling Process," The Review of Scientific Instruments, Vol. 18, No. 2, February 1947.
2. Ranque, G., "Method and Apparatus for Obtaining from a Fluid under Pressure Two Currents of Fluids at Different Temperature," U.S. Patent 1,952,281.
3. "The Maxwellian Demon," Industrial and Engineering Chemical Reports on the Chemical World Today, Technology, p. 5, May 1946.
4. "Low Temperature Research," Industrial and Engineering Chemistry, p. 5-14, December 1946.
5. "Miscellaneous Developments in German Science and Industry," p. 29, Report No. 68, Joint Int. Objectives Agency, Washington, D.C.
6. Johnson, A. F., "Quantitative Study of the Hilsch Heat Separator," Canadian Journal of Research, F, 25:299, September 1947.
7. Roebuck, J. R., "A Novel Form of Refrigerator," Journal of Applied Physics, Vol. 16, No. 5, p. 285-295, May 1945.
8. Knoernschild and Morgensen, "Application of the Hilsch Tube to Aircraft and Missiles," Serial No. MCREXE-664-510A, Air Materiel Command, Wright-Patterson Field, Dayton, Ohio.
9. "Friction Laws and Energy Transfer in Circular Flow - Part II, Energy Transfer in Circular Flow and Possible Applications (Explanation of the Hilsch or Ranque Effect)," Technical Report No. F-TR-2198-ND-GS-AAF-Wright Field No. 78, by Knoernschild and Kassuer.
10. Webster, D. S., "An Analysis of the Hilsch Vortex Tube," Refrigeration Engineering, Vol. 58, pp. 165-169, February 1950.
11. Burkhardt, G., Zeitschrift f. Naturforschung Sa, p. 46-51, 1947.
12. Higgins, D.G.H., "Convective Heat Transfer in Vortex Chamber," National Gas Turbine Establishment Rep. R127 (Title Announcement Bulletin Number AE6-627)
13. Van Gelder, H., "Efficiency Calculations of a Hilsch Tube Used in a Power Plant Steam Cycle," Memorandum No. 9091-6-6782-1, October 22, 1958.

14. Hendal, W. P., "Vortex Tube with Divergent Hot End," U.S. Patent 2,893,215, July 7, 1959.

15. Way, S., "Theoretical Performance of Hilsch-Ranque Tube," Westinghouse Research Report 60-8-05-24-R13, March 2, 1955.

16. "Application of Hilsch Tube to Aircraft Missiles," Central Air Documents Office - Wright Patterson Air Force Base A.T.I. 33095.

17. Baker, P. S. and Rathkamp, W. R., "Investigations on the Ranque-Hilsch (Vortex) Tube," Oak Ridge National Laboratory ORNL-1659.

18. Atkinson, R. G., "Recovery of Natural Gas Condensate," U.S. Patent 2,683,972, July 20, 1954.

19. Lay, J. E., "An Experimental and Analytical Study of Vortex-Flow Temperature Separation by Superposition of Spiral and Axial Flow," ASME Paper 58-WA-90.

20. Blatt, Thomas A., and Trusch, Raymond B., "An Experimental Investigation of an Improved Vortex Cooling Device," ASME Paper 62-WA-200.

21. Mürtz, H. J., and Nöller, H. G., Z. Naturforsch, 16a, 569-577 (1961).

22. Bornkessel, K., and Pilot, J., Z. Physik. Chem. 221, 177-184 (1962).

23. Foa, J. V., "Energy Separator," TR AE 6401, Dept. of Aero Eng. and Astronautics, Rensselaer Polytechnic Institute, Troy, New York, January 1964.

24. Kirk and Othmer, "Encyclopedia of Chemical Technology - 2nd Edition," Vol. 7, pp. 165-7.

25. Fletcher, E. C., Gyarmathy, G., and Hasinger, S. H., "Separation of Submicron Condensate Particles in a Vortex Chamber," Technical Report ARL-66-0218, Aerospace Research Laboratories, Wright-Patterson Air Force Base, June 1966.

26. Poplawski, R., and Pinchak, A. C., "Aerodynamic Performance of Reversed Flow Vortex Chambers," Technical Report ARL-65-219, Aerospace Research Laboratories, Wright Patterson Air Force Base, October 1965.

27. Pinchak, A. C., and Poplawski, R., "On the Attainment of Extremely High Rotational Velocities in a Confined Vortex Flow," Paper presented at the AIAA 2nd Annual Meeting, San Francisco, July 26-29, 1965.

28. Applegate, M., "Vortex Tube Applications," Proceedings of the Conference on Cooling of Airborne Electronic Equipment, 1952, Ohio State University, Engineering Bulletin No. 148, July 1952, pp. 207-209.

29. Eckert, E.R.G., and Hartnett, J. P., "Experimental Study of the Velocity and Temperature Distribution in a High Velocity Vortex Tube Flow," Heat Transfer and Fluid Mechanics Institute, Stanford University, California, June 1956.

30. Elsler, K., and Hoch, M., "The Behavior of Various Gases and the Separation of Mixtures of Gases in a Vortex Tube," (translation by G. Coldewood from Zeitschrift für Naturforschung, vol. 6a, No. 1, 1951, pp. 25-31), R. A. E. Library Translation No. 400, February 1952.

31. Scheper, Jr., G. W., "The Vortex Tube - Internal Flow Data and Heat Transfer Theory," Refrigerating Engineering, Vol. 59, 1951, pp. 985-989.

32. Westley, R., "A Bibliography and Survey of the Vortex Tube," The College of Aeronautics, Cranfield, England, 1954.

6.2. Theory of Cascade Design Modified for SO_2 Removal Application

The material presented herein was adapted to the SO_2 application mainly from Benedict and Pigford$^{(1)}$. Material from other sources is referenced in the text.

Stage Considerations

Material balance of single stage

$$L = L' + L'' \tag{6.1}$$

Abundance ratio of a stream

$$R = \frac{x}{1-x} \tag{6.2}$$

Stage feed

Flow rate - L

Composition - $x = \frac{L_{SO_2}}{L}$,

$R = \frac{x}{1-x}$

Heads fraction - enriched in desired component

Flow rate - L'

Composition - $x' = \frac{L'_{SO_2}}{L'}$,

$R' = \frac{x'}{1-x'}$

Tails fraction - depleted in desired component

Flow rate - L"

Composition - $x'' = \frac{L''_{SO_2}}{L''}$,

$R'' = \frac{x''}{1-x''}$

By definition

$$x'' < x < x' \tag{6.3}$$

Cut (ratio of heads fraction to feed stream)

$$\theta = \frac{L'}{L} \tag{6.4}$$

Material balance on component being concentrated

$$Lx = L'x' + L''x'' \tag{6.5}$$

Solving for x gives

$$x = \left(\frac{L'}{L}\right) x' + \left(\frac{L-L'}{L}\right) x'' \tag{6.6}$$

Substituting (6.4) gives

$$x = \theta x' + (1-\theta) x'' \tag{6.7}$$

Solving for θ gives

$$\theta = \frac{x-x''}{x'-x''} \tag{6.8}$$

Stage separation factor

The degree of separation achieved by a single stage is the separation factor

$$\alpha = \frac{R'}{R''} = \frac{x'/(1-x')}{x''/(1-x'')} = \frac{x'(1-x'')}{x''(1-x')} \tag{6.9}$$

The separation factor α tends to be independent of composition whereas x'/x'' varies strongly with composition.

Heads separation factor

$$\beta = \frac{R'}{R} = \frac{x'(1-x)}{x(1-x')} \tag{6.10}$$

$$1 < \beta < \alpha$$

Relationships for x', x, and x"

$$x' = \frac{\beta x}{\beta x+1-x} = \frac{\alpha x''}{\alpha x''+1-x''} \qquad (6.11)$$

$$x = \frac{\alpha x''}{\alpha x''+ (1-x'')} = \frac{x'}{x'+\beta(1-x')} \qquad (6.12)$$

$$x'' = \frac{x'}{x'+\alpha(1-x')} = \frac{\beta x}{\beta x+\alpha(1-x)} \qquad (6.13)$$

Relationship among β, α, and θ.

$$\beta-1 = \frac{(\alpha-1)(1-\theta)}{1+\theta(\alpha-1)(1-x')} \qquad (6.14)$$

Cascade Considerations

Types of cascades

Simple - Feed for one stage is heads fraction from lower stage. The partially depleted tails fractions leaving each stage are not reprocessed, but are dumped. This type of cascade is not applicable to SO_2 separation, since the reduction of SO_2 concentration in the tails would be small.

Countercurrent recycle - The feed for one stage is the heads from the next higher stage. A countercurrent cascade has an enriching section and a stripping section. It separates F moles of feed of composition x_F into P moles of enriched product* of composition x_P and W moles of depleted waste* of composition x_W. These six quantities are called the external variables of the cascade. The internal flow rates and compositions are called the internal variables of the cascade. The enriching section is required to attain the desired product composition and the stripping section is required to attain the desired waste composition.

---

* In the separation of SO_2 from flue gas the enriched stream could logically be called the waste and the depleted stream the product. However, convention will be followed in this application.

The stages of the cascade are numbered consecutively from 1 at the waste end to n at the product end.

General cascade equations

Material balance of external equations

$$F = P + W \tag{6.15}$$

and

$$Fx_F = Px_P + Wx_W \tag{6.16}$$

Since there are two equations and six variables, four of the external variables can be specified independently.

In the application to the removal of SO_2 from flue gas, the quantities which are specified are feed rate, and product, feed, and waste compositions. The other two variables are given by:

$$P = \frac{F(x_F - x_W)}{(x_P - x_W)} \tag{6.17}$$

$$W = \frac{F(x_P - x_F)}{(x_P - x_W)} \tag{6.18}$$

Material balance for internal variables

Enriching section

$$L'_i = L''_{i+1} + P \tag{6.19}$$

and

$$L'_i x'_i = L''_{i+1} x''_{i+1} + Px_P \tag{6.20}$$

Stripping section

$$L'_j = L''_{j+1} - W \tag{6.21}$$

and

$$L'_j x'_j = L''_{j+1} x''_{j+1} - Wx_W \tag{6.22}$$

Combining (6.19) and (6.20) gives

$$x''_{i+1} - x'_i = \frac{x'_i - x_P}{L''_{i+1}/P} \tag{6.23}$$

As reflux ratio $(L''_{i+1}/P) \to \infty$, x''_{i+1} and x_i becomes equal.

Minimum number of stages

The number of stages required to separate the feed into an enriched stream and a depleted stream of specified composition is a minimum with total reflux, i.e., when $L''_{i+1}/P \to \infty$.

Under these conditions

$$x''_{i+1} = x'_i \tag{6.24}$$

and $$R''_{i+1} = R'_i \tag{6.25}$$

From (6.9), the enriched fractions abundance ratios for adjacent stages at total reflux are related by

$$\alpha = \frac{R'_{i+1}}{R''_{i+1}} = \frac{R'_{i+1}}{R'_i} \tag{6.26}$$

Applying this to stage 1 gives:

$$R'_2 = \alpha R'_1 \tag{6.27}$$

For stage 2 it is

$$R'_3 = \alpha R'_2 = \alpha^2 R'_1 \tag{6.28}$$

For the entire cascade this becomes

$$R'_n = \alpha^{n-1} R'_1 \tag{6.29}$$

But

$$R'_n = \frac{x_P}{1-x_P} \tag{6.30}$$

and

$$R'_1 = \alpha R''_1 = \alpha \left(\frac{x_w}{1-x_w}\right) \tag{6.31}$$

Therefore

$$\left(\frac{x_P}{1-x_P}\right) = \alpha^n \left(\frac{x_w}{1-x_w}\right) \tag{6.32}$$

and

$$n_{min} = \frac{\ln \dfrac{x_P(1-x_w)}{x_w(1-x_P)}}{\ln \alpha} = \frac{\ln \dfrac{R_P}{R_w}}{\ln \alpha} \tag{6.33}$$

The abundance ratio term in (6.33) is called the over-all separation of the cascade (w)

$$w = \frac{x_P(1-x_w)}{x_w(1-x_P)} \tag{6.34}$$

The minimum number of stages increases as the over-all separation increases and as the separation factor approaches unity.

Minimum Reflux Ratio

The difference in composition between corresponding streams in adjacent stages is a maximum when the number of stages is a minimum or the reflux is total. Conversely, the difference in composition approaches zero at minimum reflux. Therefore, the condition for minimum reflux is:

$$x'_{i+1} = x'_i \tag{6.35}$$

From (6.9)

$$x''_{i+1} - x'_{i+1} = \frac{-(\alpha-1)\ x'_{i+1}(1-x'_{i+1})}{x'_{i+1} + \alpha(1-x'_{i+1})} \tag{6.36}$$

which, at minimum reflux, becomes

$$x''_{i+1} - x'_i = \frac{-(\alpha-1)\ x_i(1-x'_i)}{x'_i + \alpha(1-x'_i)} \tag{6.37}$$

Equating this with (6.23) gives

$$\left(\frac{L''_{i+1}}{P}\right)_{\min} = \frac{(x_P-x'_i)[x'_i + \alpha(1-x'_i)]}{(\alpha-1)\ x'_i(1-x'_i)} \tag{6.38}$$

This can be expressed in terms of x''_{i+1} as

$$\left(\frac{L''_{i+1}}{P}\right)_{\min} = \frac{x_P(\alpha x''_{i+1} + 1-x''_{i+1}) - \alpha x''_{i+1}}{(\alpha-1)\ x''_{i+1}(1-x''_{i+1})} \tag{6.39}$$

When $x'_i << 1$,

$$\left(\frac{L''_{i+1}}{P}\right)_{\min} \approx \frac{x_P-x'_i}{x'_i}\ \frac{\alpha}{\alpha-1} \tag{6.40}$$

When $\alpha-1 << 1$,

$$\left(\frac{L''_{i+1}}{P}\right)_{\min} \approx \frac{x_P-x'_i}{(\alpha-1)\ x'_i(1-x'_i)} \tag{6.41}$$

These equations all show that the minimum reflux ratio increases as the composition departs from the product composition, and that the reflux becomes very large as α approaches unity.

Practical Reflux Ratio

In any practical plant the reflux ratio at any stage must fall between the minimum value, where the number of stages is infinite, and the infinite value needed for the minimum number of stages. In many industrial separation plants, it is customary to select a reflux ratio somewhat greater than the minimum value at the feed point and to use the same value for every stage of the cascade. In some cases the savings in equipment cost are sufficient to justify the use of a tapered cascade wherein the reflux ratio is reduced at intervals between the feed point and the product end of the cascade.

The Ideal Cascade

One type of tapered cascade which has minimum total interstage flow and gives minimum plant cost is the ideal cascade. An ideal cascade is one in which:

(1) The heads separation factor (β) is constant for all stages.

(2) The heads stream and tails stream concentrations fed to each stage have the same concentration, i.e.,

$$x''_{i+1} = x'_{i-1} = x_i \text{ for } i = 2,3, \cdots, n-1 \qquad (6.42)$$

The theory of ideal cascades was developed by Dirac and Peierls in England and Cohen and Kaplan in the U.S. and is described in detail in Reference 2.

Equation (6.42) can be expressed in terms of abundance ratios as

$$R''_{i+1} = R'_{i-1} = R_i \qquad (6,43)$$

By definition

$$R'_i = \beta R_i \qquad (6.44)$$

Combining (6.43) and (6.44) for the ideal cascade gives:

$$R'_i = \beta R''_{i+1} \qquad (6.45)$$

Similarly

$$R'_{i+1} = \beta R_{i+1} = \beta R'_i \tag{6.46}$$

Substituting (6.45) in (6.46) gives

$$R'_{i+1} = \beta^2 R''_{i+1} \tag{6.47}$$

By definition

$$R'_{i+1} = \alpha R''_{i+1} \tag{6.48}$$

Therefore

$$\beta = \sqrt{\alpha} \tag{6.49}$$

which is the key characteristic of the ideal cascade.

When $\beta-1$ and $\alpha-1$ are small compared to unity

$$\beta-1 \approx \frac{\alpha-1}{2} \tag{6.50}$$

Using a procedure similar to that used in deriving equation (6.33) for the minimum number of stages with total reflux, the total number of stages in an ideal cascade can be shown to be equal to

$$n = \frac{\ln \dfrac{x_P(1-x_W)}{(1-x_P)\ x_W}}{\ln \beta} - 1 = 2\ \frac{\ln \dfrac{x_P(1-x_W)}{(1-x_P)\ x_W}}{\ln \alpha} - 1 \tag{6.51}$$

Therefore, the number of stages required for a given separation with an ideal cascade is twice the number needed with total reflux minus 1.

The number of stages in the stripping section is:

$$n_W = \frac{\ln \dfrac{x_F(1-x_W)}{(1-x_F)\ x_W}}{\ln \beta} - 1 \tag{6.52}$$

and for the enriching section

$$n_P = \frac{\ln \dfrac{x_P(1-x_F)}{(1-x_P)\ x_F}}{\ln \beta} \tag{6.53}$$

The relationships between composition and stage number for the ideal cascade are:

$$R'_n = \beta^{n-i}\ R'_i \tag{6.54}$$

$$x'_i = x_{i+1} = x''_{i+2} = \frac{\beta^i x_P}{\beta^i x_P + \beta^n (1-x_P)} \tag{6.55}$$

$$x''_j = x_{j-1} = x'_{j-2} = \frac{\beta^{j-1}\ x_w}{\beta^{j-1}\ x_w + (1-x_w)} \tag{6.56}$$

Reflux Ratio for Ideal Cascade

The reflux ratio necessary to satisfy the conditions for an ideal cascade as given in (6.43) may be computed as follows:

From (6.23)

$$\frac{L''_{i+1}}{P} = \frac{x_P - x'_i}{x'_i - x''_{i+1}} \tag{6.57}$$

For an ideal cascade, $x'_i = x_{i+1}$ and $\alpha=\beta^2$. Substituting in (6.12) and combining with (6.57) gives:

$$\frac{L''_{i+1}}{P} = \frac{x_P(\beta x''_{i+1} + 1 - x''_{i+1}) - \beta x''_{i+1}}{(\beta-1)\ x''_{i+1}\ (1-x''_{i+1})} \tag{6.58}$$

$$= \frac{1}{\beta-1} \left[\frac{x_P}{x''_{i+1}} - \frac{\beta(1-x_P)}{1-x''_{i+1}} \right] \tag{6.59}$$

The corresponding equation for the stripping section is:

$$\frac{L'_j}{W} = \frac{1}{\beta-1}\left(\frac{1-x_w}{1-x'_j} - \frac{\beta x_w}{x'_j}\right) \tag{6.60}$$

Combining equations (6.55) and (6.59) gives the reflux ratio in the enriching section as a function of stage number.

$$\frac{L''_{i+1}}{P} = \frac{1}{\beta-1}\left[x_P(1-\beta^{i-n}) + (1-x_P)\beta(\beta^{n-i}-1)\right] \tag{6.61}$$

Combining this with (6.19) gives an expression for the stage heads flow in the enriching section. Similarly, an expression for the stripping section can be obtained from (6.56) and (6.60).

$$\frac{L'_j}{W} = \frac{1}{\beta-1}\left[x_w\beta(\beta^j-1) + (1-x_w)(1-\beta^{-j})\right] \tag{6.62}$$

which can be used to calculate the stage heads flow in the stripping section.

Shape of an Ideal Cascade

Figure 6.1 shows the shape of an ideal cascade for separation of natural uranium ($x_F = 0.0072$) into enriched uranium with $x_P = 0.80$ and depleted uranium waste with $x_w = 0.004$, by gaseous diffusion with $\alpha = 1.0043$. The height of the plot is proportional to the number of stages and the width is proportional to the heads flow rate for each stage. The large interstage flow rate at the feed point and its rapid decrease above and below the feed point are characteristic of the ideal cascade.

Total Flow Rates

The total interstage flow rate of heads or tails is a measure of the size of a separation plant. In a gaseous diffusion plant, the total amount of power required to pump the gas between stages is proportional to the total heads flow rate.

Dwg. 856A932

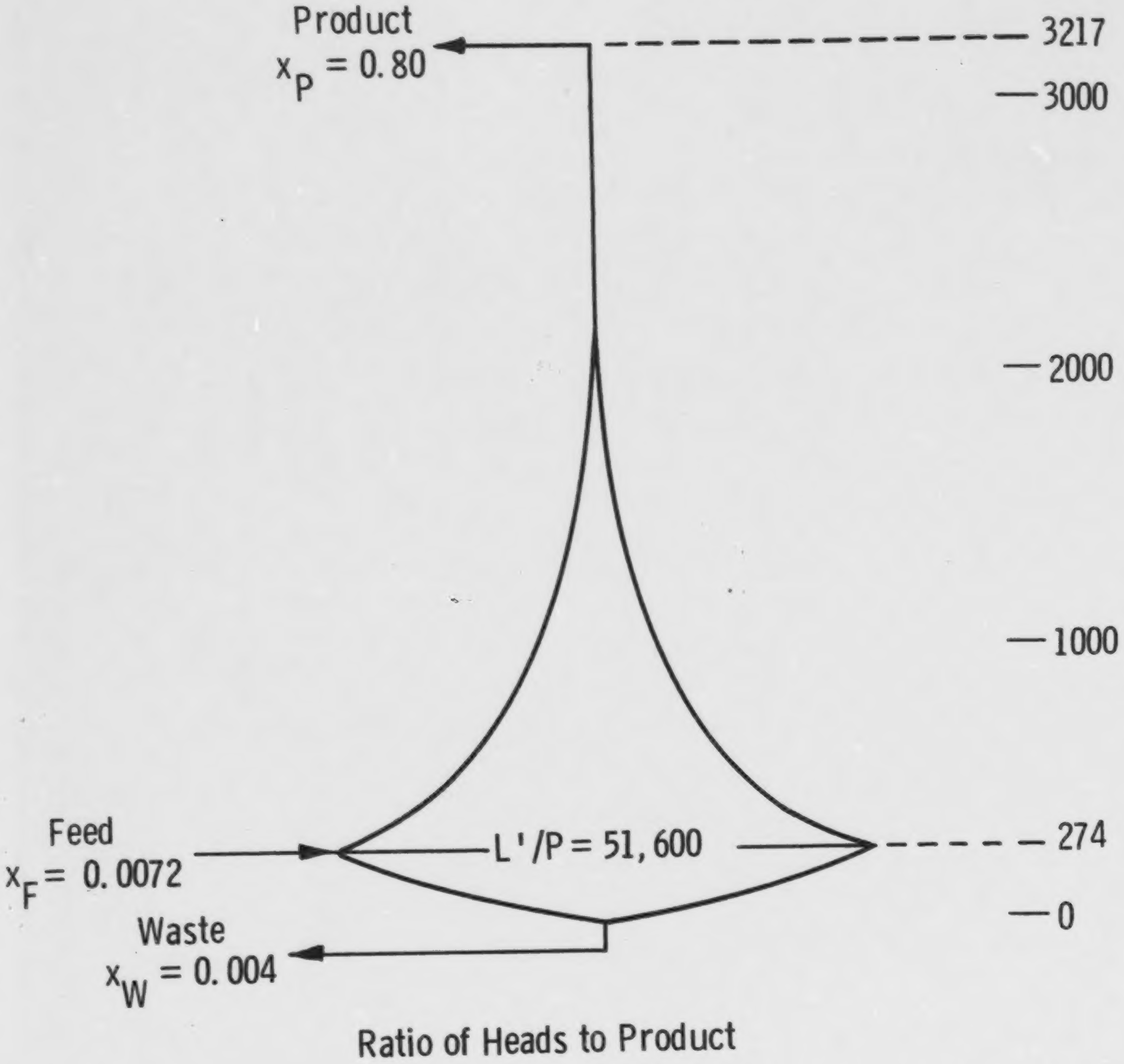
Product
$x_P = 0.80$
3217
3000
2000
1000
Feed
$x_F = 0.0072$
L'/P = 51,600
274
0
Waste
$x_W = 0.004$
Ratio of Heads to Product

FIG. 6-1 - Heads Flow Rate vs Stage Number In Ideal Cascade
$\beta = 1.00215$

Expressions for the total flow rate of heads and tails in either enriching or stripping sections may be obtained by summing Equations (6.61) and (6.62). The total heads flow rate in the stripping section is

$$J'_w = \sum_{j=1}^{n_w} L'_j = \frac{W}{\beta-1}\left[x_w\beta \sum_{j=1}^{n_w} (\beta^j-1) + (1-x_w) \sum_{j=1}^{n_w} (1-\beta^{-j})\right] \qquad (6.63)$$

Since

$$\sum_{j=1}^{n_w} \beta^j = \beta\,\frac{\beta^{n_w}-1}{\beta-1} \quad \& \quad \sum_{j=1}^{n_w} \beta^{-j} = \frac{1-\beta^{-n_w}}{\beta-1} \qquad (6.64)$$

this becomes

$$J'_w = \frac{W}{\beta-1}\left[Bx_w\left(\beta\,\frac{\beta^{n_w}-1}{\beta-1} - n_w\right) + (1-x_w)\left(n_w - \frac{1-\beta^{-n_w}}{\beta-1}\right)\right] \qquad (6.65)$$

Combining this with (6.52) gives:

$$J'_w = \frac{W}{\beta-1}\left\{[1-x_w(\beta+1)]\,\frac{\ln\dfrac{x_F(1-x_w)}{x_w(1-x_F)}}{\ln\beta} - \frac{\beta(x_F-x_w)(1-2\,x_F)}{(\beta-1)\;x_F(1-x_F)}\right\} \qquad (6.66)$$

Using similar procedures, the total tails flow rate in the stripping section can be shown to be

$$J''_w = \sum_{j=1}^{n_w} L''_j = \frac{W}{\beta-1}\left\{[\beta-x_w(\beta+1)]\,\frac{\ln\dfrac{x_F(1-x_w)}{x_w(1-x_F)}}{\ln\beta} - \frac{(x_F-x_w)[\beta^2-(\beta^2+1)\;x_F]}{x_F(1-x_F)(\beta-1)}\right\} \qquad (6.67)$$

the total tails flow rate in the enriching section can be shown to be:

$$J_P'' = \sum_{i=n_W}^{n-1} L_{i+1}'' = \frac{P}{\beta-1}\left\{ \frac{[x_P(\beta+1)-\beta]\ \ln \dfrac{x_P(1-x_F)}{x_F(1-x_P)}}{\ln \beta} + \frac{(x_P-x_F)[\beta^2-(\beta^2+1)\ x_F]}{x_F(1-x_F)\ \beta-1} \right\} \qquad (6.68)$$

and the total heads flow rate in the enriching section can be shown to be:

$$J_P' = \sum_{i=n_W}^{n-1} L_{i+1}' = \frac{P}{\beta-1}\left\{ \frac{[x_P(\beta+1)-1]\ \ln \dfrac{x_P(1-x_F)}{x_F(1-x_P)}}{\ln \beta} + \beta\ \frac{(x_P-x_F)(1-2\ x_F)}{x_F(1-x_F)(\beta-1)} \right\} \qquad (6.69)$$

The total flow in the entire cascade is obtained by adding (6.66), (6.67), (6.68), and (6.69). This gives

$$J = \frac{\beta+1}{(\beta-1)\ \ln \beta}\left[W(1-2\ x_W)\ \ln \frac{x_F(1-x_W)}{x_W(1-x_F)} + P(2x_P-1)\ \ln \frac{x_P(1-x_F)}{x_F(1-x_P)} \right] \qquad (6.70)$$

This can be rearranged by use of material balance relations to give

$$J = \frac{\beta+1}{(\beta-1)\ \ln \beta}\left[W(2x_W-1)\ \ln \frac{x_W}{1-x_W} + P(2x_P-1)\ \ln \frac{x_P}{1-x_P} - F(2x_F-1)\ \ln \frac{x_F}{1-x_F} \right] \qquad (6.71)$$

This can be simplified to

$$J = \frac{\beta+1}{(\beta-1)\ \ln\ \beta}\left[W\phi(x_W) + P\phi(x_P) - F\phi(x_F)\right] \qquad (6.72)$$

where

$$\phi(x) = (2x-1)\ \ln\ \frac{x}{1-x} \qquad (6.73)$$

is called the separation potential.

This expression shows that the total flow rate of the cascade is a function of the product of two factors. The first factor is a function only of the heads separation factor, β. The second factor contains three terms. The first term is a function of the waste flow rate and composition, the second term is a function of the product flow rate and composition, and the third is a function of the feed flow rate and composition.

The $\beta+1/(\beta-1)\ \ln\ \beta$ factor reflects the difficulty of the separation from the standpoint of the separative device. It is large when β is near unity and decreases as β increases. The second factor is a measure of the magnitude of the separation job; it is proportional throughout and varies directly with the differences between the product and waste compositions and the feed composition. This factor is often called the separative duty of the cascade.

Cohen$^{(2)}$ has shown that, if the flow in a cascade at no point differs from that in a corresponding ideal cascade by more than 20 percent, the integrated flow rate for the cascade will not differ from the ideal integral by more than 4%.

Close-Separation Cascade

As previously stated, in an ideal cascade with $\alpha-1<<1$; the relationship between α and β can be approximated by equation (6.50). Using this expression the tails flow rate in both enriching and stripping sections of an ideal cascade can be approximated by

$$L'' = \frac{P(x_P-x)}{(\beta-1)x(1-x)} \qquad (6.74)$$

or

$$L'' = \frac{2P(x_P-x)}{(\alpha-1)x(1-x)} \tag{6.75}$$

The difference in composition between stage heads and tails as obtained from (6.13)

$$x_i'-x_i'' = \frac{(\alpha-1)x_i(1-x_i)}{x_i' + \alpha(1-x_i')} \tag{6.76}$$

may be approximated by

$$x_i'-x_i'' = (\alpha-1)\ x_i'(1-x_i') \tag{6.77}$$

when $\alpha-1 \ll 1$.

Combining this with the material balance equation (6.23), gives a relation for the change in heads composition in the enricher section

$$x_i'-x_{i-1}' = (\alpha-1)\ x_i'(1-x_i') - \frac{P}{L_i''}\ (x_P-x_{i-1}') \tag{6.78}$$

Since x_i', x_i, and x_{i-1}' are nearly equal, this difference equation can be approximated by the differential equation

$$\frac{dx}{di} = (\alpha-1)x(1-x) - \frac{P}{L''}\ (x_P-x) \tag{6.79}$$

The corresponding equation for the stripper section is

$$\frac{dx}{di} = (\alpha-1)x(1-x) - \frac{W}{L''}\ (x_W-x) \tag{6.80}$$

The total tails flow in the enriching section is

$$J_P'' = \int_{n_W+1}^{n} L''di = \int_{x_F}^{x_P} L''\ \frac{di}{dx}\ dx$$

J_P'' will be a minimum when

$$L'' \frac{di}{dx} = \frac{1}{\dfrac{(\alpha-1)x(1-x)}{L''} - \dfrac{P}{(L'')^2}(x_P-x)} \qquad (6.81)$$

is a minimum at all values of x. This will obtain when L" is such that the derivative of the denominator is zero.

$$\frac{(\alpha-1)x(1-x)}{(L'')^2} + \frac{2P}{(L'')^3}(x_P-x) = 0 \qquad (6.82)$$

Thus

$$L''_{opt} = \frac{2P(x_P-x)}{(\alpha-1)x(1-x)} \qquad (6.83)$$

which is identical with (6.75). This is twice the minimum tails flow rate at which dx/di = 0.

In an ideal cascade with close-separation, the heads and tails fed to each stage have the same composition and the cut θ is 1/2. For $\alpha-1 << 1$

$$\beta=1 = (\alpha-1)(1-\theta)$$

At the optimum flow rate, the change in composition per stage, from (6.79), is

$$\frac{dx}{di} = \frac{\alpha-1}{2}x(1-x) \qquad (6.84)$$

which is one-half the value for total reflux, i.e., $\frac{P}{L''} = 0$.

The total number of stages in the enriching section is

$$n_P = \int_{x_F}^{x_P} \frac{di}{dx}dx = \frac{2}{\alpha-1}\int_{x_F}^{x_P} \frac{dx}{x(1-x)} = \frac{2}{\alpha-1}\ln\frac{x_P(1-x_F)}{x_F(1-x_P)} \qquad (6.85)$$

and

$$n_W = \frac{2}{(\alpha-1)} \ln \frac{x_F(1-x_W)}{x_W(1-x_F)} \tag{6.86}$$

These equations are approximately equal to Equations (6.52) and (6.53).

The total downflow rate in the enriching section at the optimum level is

$$J''_P = \int_{x_F}^{x_P} L''_{opt} \frac{di}{dx} dx \tag{6.87}$$

Substituting L''_{opt} from (6.83) and $\frac{di}{dx}$ from (6.84) into this gives

$$J''_P = \frac{4P}{(\alpha-1)^2} \int_{x_F}^{x_P} \frac{x_P - x}{x^2(1-x)^2} dx$$

$$= \frac{4P}{(\alpha-1)^2} \left[(2x_P-1) \ln \frac{x_P(1-x_F)}{x_F(1-x_P)} + \frac{(x_P-x_F)(1-2x_F)}{x_F(1-x_F)} \right] \tag{6.88}$$

The total heads flow reduces to the same expression.

Therefore, the total flow rate in both enriching and stripping sections is

$$J = \frac{8}{(\alpha-1)^2} \left[W(2x_W-1) \ln \frac{x_W}{1-x_W} + P(2x_P-1) \ln \frac{x_P}{1-x_P} \right.$$

$$\left. - F(2x_F-1) \ln \frac{x_F}{1-x_F} \right] \tag{6.89}$$

Square Cascades

It is impractical to construct cascades in which the cascade width varies continuously from stage to stage. Economic considerations limit the number of changes in the cascade width. This requires that the ideal cascade taper be approximated by a series of step changes or square sections where a section is made up of a series of steps of constant width L'.

Differential Equations (6.79) and (6.80) may be integrated directly, for constant L", to obtain a formula for the length of section required to span a concentration range. A simplified version of this equation is

$$n(x_B, x_T) = \frac{1}{(\alpha-1)(x_0-x_1)} \ln \frac{(x_T-x_0)(x_1-x_B)}{(x_B-x_0)(x_1-x_T)} \qquad (6.90)$$

where

x_B - concentrations at bottom of section

x_T - concentration at top of section

x_1 and x_0 - roots of the quadratic in x given by the right hand sides of Equations (6.79) and (6.80) where x_1 is the larger root

The greatest demand for width in a cascade is at the feed point; i.e. $L_{(min)}$, where dx/di is zero, is a maximum at the feed point. In an enricher section $L_{(min)}$ is a maximum at the bottom, and in a stripper section $L_{(min)}$ is a maximum at the top. These are the points in the sections which are the most critical. If the L for a section is too close to the critical $L_{(min)}$, then stages are wasted. On the other hand the use of a relatively large L value for a stage will waste stage size.

Separative Duty

As previously mentioned, the second factor of (6.71) is known as the separative duty (D). For a plant with a single feed, product, and waste stream

$$D = W(2x_w-1) \ln \frac{x_w}{1-x_w} + P(2x_P-1) \ln \frac{x_P}{1-x_P} - F(2x_F-1) \ln \frac{x_F}{1-x_F} \qquad (6.91)$$

In general for a plant with any number of external streams of composition x_i and flow rate N_i (positive for a product, negative for a feed), the total internal flow, J, is

$$J = \frac{8}{(\alpha-1)^2} D \tag{6.92}$$

where

$$D = \sum_i N_i \phi_i \tag{6.93}$$

and

$$\phi_i = (2x_i-1) \ln \frac{x_i}{1-x_i} \tag{6.94}$$

The function ϕ, the separation potential, is a function of composition only. A plot of ϕ vs. x is shown in Figure 6.2. ϕ is symmetrical about $x = 0.5$ where it is zero and increases to infinity at $x = 0$ and 1.0. This reflects the fact that a plant of infinite size is required to separate a pure component.

The importance of the separative duty is that it is an indication of the magnitude of the gas separation job. Many of the elements of a plant which determine its cost are proportional to the separative duty. For example, in a gaseous-diffusion plant consisting of an ideal cascade of stages operated at the same conditions, the total flow rate, the total pump capacity, the total power requirements, and the total membrane area are all proportional to the separative duty.

Separative Work

Another useful quantity in cascade design is the separation work

$$E = M_W\phi_W + M_P\phi_P - M_F\phi_F \tag{6.95}$$

This represents the quantity of work performed by a cascade in making M_P moles of product and M_W moles of waste from M_F moles of feed.

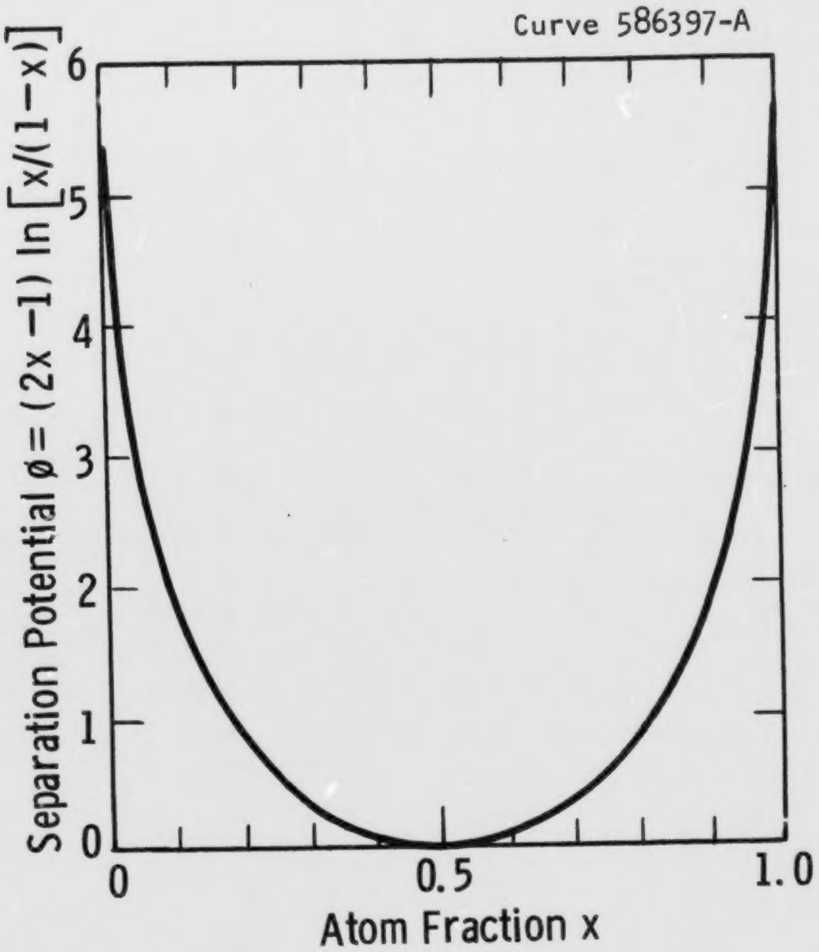

FIG. 6-2 - Separation Potential

In the SO_2 removal application the specific work per unit of feed is of interest, i.e.,

$$\frac{E}{M_F} = \frac{M_W}{M_F} \phi_W + \frac{M_P}{M_F} \phi_P - \phi_F \qquad (6.96)$$

Applications of Separation Potential in Cascade Problems

If the rate of separation by an ideal cascade is known at one set of feed and product conditions, the best possible performance of the cascade at another set of conditions can be calculated by assuming the separative duty to be a constant characteristic of the cascade. This will be true if, under the new set of conditions, the separating units are rearranged in series and parallel so that no mixing of streams of different compositions occurs.

Problems which may be solved by the application of the constant separative duty principle are:

(1) The effect of change in product rate on product purity.
(2) The effect of change in feed rate on product rate at constant product purity.
(3) The effect of change in feed composition on product rate.

Optimum Product Concentration in SO_2 Application

In the application of gas separation to the removal of SO_2 from flue gas, the quantity and concentration of feed are fixed and the concentration of the waste, i.e. cleaned flue gas, is specified to be a percentage of the feed concentration. Therefore, optimization of the concentration of SO_2 in the enriched stream must be made relative to the cost per unit of feed

Total flow and SO_2 mass balances give

$$\frac{M_W}{M_F} = \frac{(x_P - x_F)}{(x_P - x_W)} \qquad (6.97)$$

and

$$\frac{M_P}{M_F} = \frac{(x_F-x_w)}{(x_P-x_w)} \tag{6.98}$$

These combined with (6.96) give

$$\frac{E}{M_F} = \frac{(x_F-x_P)}{(x_w-x_P)} \cdot \phi_w + \frac{(x_F-x_w)}{(x_P-x_w)} \phi_P - \phi_F \tag{6.99}$$

This can be rearranged to give

$$\frac{E}{M_F} = \phi_w - \phi_F + (x_F-x_w) \frac{(\phi_P-\phi_w)}{(x_P-x_w)} \tag{6.100}$$

In the typical gas separation plant the initial cost of the plant is proportional to the separative duty of the process and the annual operating cost is proportional to the amount of separative work done per year. Therefore, the annual costs of capital invested and operation are equal to EC_E, where E is the amount of separative work performed per year and C_E is the unit cost of separative work.

It is assumed that the SO_2 which is removed from the flue gas by a physical gas separation process will ultimately be sold as a by-product either as relatively pure SO_2 or as H_2SO_4. It is further assumed that it will be uneconomic to concentrate the SO_2 to marketable quality in the gas separation process alone, and that one of the state-of-the-art methods of manufacturing H_2SO_4 from products of combustion of sulfur and air would be employed to produce a marketable by-product. Therefore, a by-product credit should be subtracted from the gross annual plant costs to obtain the net annual plant costs.

An expression for this by-product credit is $M_P x_P C_{SO_2}$ where $M_P x_P$ is the annual production of SO_2 in moles and C_{SO_2} is the difference between the market value of the by-product and the cost of producing it from the enriched stream of the physical gas separation process. C_{SO_2} is a function of x_P, and values of C_{SO_2} are readily obtainable for two values of x_P. For $x_P = 1.0$, C_{SO_2} would be the market value of commercial grade SO_2. For $x_P = 0.2$ which is a typical value for sulfuric acid plants where sulfur and air are burned$^{(4)}$, C_{SO_2} would be the equivalent of the profit on the manufacture of sulfuric acid.

The total annual charge is thereby

$$C = EC_E - M_p x_P \, C_{SO_2} \, (x_P) \tag{6.101}$$

If M_F moles of flue gas are processed per year, the cost per unit of feed is

$$C_F = \frac{C}{M_F} = \frac{E}{M_F} \; C_E - \frac{M_P}{M_F} \cdot x_P \, C_{SO_2} \, (x_P) \tag{6.102}$$

Substituting M_P/M_F and E/M_F from (6.98) and (6.100) gives

$$\begin{aligned} C_F = \; & \phi_w - \phi_F + (x_F - x_w) \frac{(\phi_P - \phi_w)}{(x_P - x_w)} \\ & - \frac{(x_F - x_w)}{(x_P - x_w)} \cdot x_P \cdot C_{SO_2} \, (x_P) \end{aligned} \tag{6.103}$$

Since C_{SO_2} (x_P) is known for two values of x_P, a linear approximation can be obtained, i.e.

$$C_{SO_2} = a + mx_P \tag{6.104}$$

Equation (6.103) then becomes

$$\begin{aligned} C_F = \; & \phi_w - \phi_F + (x_F - x_w) \frac{(\phi_P - \phi_w)}{(x_P - x_w)} \quad C_E \\ & - (x_F - x_w) \frac{(ax_P + mx_P^2)}{(x_P - x_w)} \end{aligned} \tag{6.105}$$

The optimum product composition is that at which

$$\frac{dC_F}{dx_P} = 0 \tag{6.106}$$

Differentiating (6.105) and setting it equal to zero gives

$$\left[(x_P-x_W)\frac{d\phi}{dx_P}-(\phi_P-\phi_W)\right]C_E-\left[(x_P-x_W)(a+2mx_P)-(ax_P+mx_P^2)\right]=0 \qquad (6.107)$$

This can be solved for optimum x_P by iteration using equations (6.73) and

$$\frac{d\phi}{dx}=\frac{(2x-1)}{(x-x^2)}+2\ln\frac{x}{1-x} \qquad (6.108)$$

It should be noted that x_F does not appear in this expression for optimum x_P. Therefore, there is no constraint on x_P except $x_P \geq x_F$.

Hold-up in a Cascade

The quantity of material held-up in a cascade is important because it affects the transient characteristics of the cascade and constitutes an investment of working capital if the material being processed is of significant value. In the case of flue gas, the value of the by-product material is relatively low so this is not a consideration.

The total amount of material in process in a section of a cascade is called the hold-up of that section. In most cascades the amount of hold-up in a stage is proportional to the flow in the stage. The hold-up per unit flow, denoted by h, is also the average process time per stage, expressed in seconds.

For transient considerations a more useful quantity is the net desired material hold-up (N.D.M.H.). The N.D.M.H. is the amount of the desired component in a cascade which attained equilibrium over and above that which would be contained in a like quantity of material at the feed concentration. It is represented by the following equation(2)

$$\text{N.D.M.H.}=\int_{x_F}^{x_P} h\,L_i(x_i-x_F)\,di \qquad (6.109)$$

The flow entering a stage is$^{(2)}$

$$L_i = \frac{(\alpha+1)\ P(x_p - x_i)}{(\alpha-1)\ x_i(1-x_i)} \tag{6.110}$$

Combining (6.109) and (6.110) gives

$$\text{N.D.M.H.} = \int_{x_F}^{x_p} h\, \frac{(\alpha+1)\ P(x_p - x_i)}{(\alpha-1)\ x_i(1-x_i)}\, (x_i - x_F)\, \frac{di}{dx}\, dx \tag{6.111}$$

Substituting (6.84) into (6.111) and integrating gives the following expressions for the close separation case.$^{(2)}$

$$\text{N.D.M.H.} \cong \frac{2hP}{(\alpha-1)^2}\ (x_p - 2x_p x_F + x_F)\ \ln \frac{R_p}{R_F} - 2(x_p - x_F) \tag{6.112}$$

Equilibrium Time for a Cascade

The equilibrium time for a cascade is the time after start-up before the plant can produce material of the desired concentration at the top. Equilibrium time is equal to the N.D.M.H. divided by the average transport of the desired material over the initial period of operation This average transport may be taken to be the net transport of the enriching section for steady state, i.e. $P(x_p - x_F)$. Dividing this into (6.112) gives the following expression for equilibrium time

$$t_{eq.} = \frac{2h}{(\alpha-1)^2}\ \frac{[(x_p - 2x_p x_F + x_F)\ \ln \frac{R_p}{R_o} - 2(x_p - x_F)]}{(x_p - x_F)} \tag{6.113}$$

The N.D.M.H. and the equilibrium time are minimum for ideal cascades. The formula for equilibrium time is the form

$$t_{eq.} = \frac{\text{N.D.M.H.}}{\text{average net transport}}$$

may also be applied to other than ideal cascades. However, the average net transport will not in general be $P(x_p - x_F)$.

List of Symbols

D	separative duty - moles/sec
E	separative work
F	feed flow - moles/sec
J	summation of flow in stripping section moles/sec
L	stage molar flow - moles/sec
M	number of moles
n	number of stages in a cascade
P	product flow - moles/sec
R	abundance ratio
t	time - sec
W	waste flow - moles/sec
w	overall separation of a cascade
x	mole fraction of component being separated
α	stage separation factor
β	heads separation factor
θ	stage cut (ratio of heads fraction to feed stream)

Subscripts

eq	equilibrium
i	stage number in enriching section counted from waste end
j	stage number in stripping section counted from waste end

Superscripts

'	indicates heads from stage
"	indicates tails from stage

References

(1) Benedict and Pigford, "Nuclear Chemical Engineering," McGraw-Hill, New York, 1957.

(2) Cohen, Karl, "The Theory of Isotope Separation as Applied to the Large-Scale Production of U^{235}," McGraw-Hill, New York, 1951.

(3) Garrett and Shacter, "Evaluation of Isotope Separation Processes," Proceedings of the Symposium of Isotope Separation, Amsterdam, 1957, p. 17.

(4) Kirk and Othmer, "Encyclopedia of Chemical Technology, 1st Ed.

6.3. Mechanical Design of High Speed Centrifuges

The wall of the centrifuge cylinder is subjected to two loads which cause hoop stress in the wall. First, the load due to the centrifugal force on the wall itself; and, second, the load due to the pressure of the gas inside the spinning cylinder. The stress in a thin-walled cylinder due to the centrifugal force is(1)

$$\sigma_{CF} = \frac{\rho(r_1\omega)^2}{g} \tag{6.114}$$

The loop stress in the cylinder wall due to the internal pressure is(1)

$$\sigma_P = \frac{P_{(r_1)}\, r_1}{t_w} \tag{6.115}$$

The radial pressure distribution in the centrifuge cylinder is shown in Section 3.3 to be

$$P_{(r)} = P_{(o)} \exp \frac{\bar{M}(\omega r)^2}{2g\underline{R}T} \tag{3.21}$$

Therefore, for a centrifuge operating in a vacuum chamber, the hoop stress due to the internal pressure is

$$\sigma_P = \frac{P_{(o)}\ (\exp \bar{M}(\omega r)^2/2g\underline{R}T}{2t_w/d} \tag{6.116}$$

The above equations show that the stress due to the centrifugal force is independent of the wall thickness while that due to the internal pressure is a function of the wall thickness. Fixing the ratio of σ_P to σ_{CF} provides a basis for determining the centrifuge wall thickness. Combining Equations (6.114) and (6.116) and solving for t_w/d gives

$$\frac{t_w}{d} = \frac{g \times p_{(o)} \; \exp \bar{M} \; (\omega r)^2/2g\underline{R}T}{2 \times \rho(\omega r)^2 \; (\sigma_P/\sigma_{CF}) \text{ design}} \qquad (6.117)$$

Based on structural stability considerations a value for σ_P/σ_{CF} of 0.05 is considered to be the minimum practical design value.

There is also an axial or longitudinal stress in the centrifuge wall due to the internal pressure on the closed ends of the cylinder This stress is(1)

$$\sigma_L = \frac{\bar{p} \; r_1}{2t} \qquad (6.118)$$

where

$$\bar{p} = \int_o^{r_1^2} p_{(r)} \; d(r^2)/r_1^2 \qquad (6.119)$$

Combining Equations(3.21) and (6.119) gives

$$\bar{p} = \frac{p_{(o)}}{r_1^2} \int_o^{r_1^2} \exp \bar{M} \; (\omega r)^2/2g\underline{R}t \; d(r^2) \qquad (6.120)$$

Integration of Equation (6.120) gives

$$\bar{p} = \frac{p_{(o)}}{(\omega r_1)^2 \; M/2gRT} \; (\exp \bar{M} \; (\omega r_1)^2/2g\underline{R}T-1) \qquad (6.121)$$

Combining Equations (6.118) and (6.121) gives

$$\sigma_L = \frac{p_{(o)} \; (\exp \bar{M} \; (\omega r_1)^2/2g\underline{R}T - 1)}{4 \; \bar{M} \; (\omega r_1)^2 \; (t_w/d_1)/2g\underline{R}T} \qquad (6.122)$$

Comparison of Equations (6.116) and (6.122) shows that σ_A is less then σ_P for all values of (ωr) greater than about 300 meters/sec. for the gas conditions pertinent to this study. Therefore, the axial stress in the centrifuge was/is considered to be negligible if (σ_P/σ_{CF}) design is 0.05. Therefore, the principle stress is the hoop stress.

$$\sigma_H = \sigma_{CF} + \sigma_P = 1.05\ \sigma_{CF} \qquad (6.123)$$

The natural frequency of the centrifuge rotor is(2)

$$\omega_n = \frac{a_n r}{\sqrt{2}\ z^2} \sqrt{\frac{Eg}{\rho}} \qquad (6.124)$$

The value of a_n is dependent on the support of the rotor. For a simply supported rotor a_n has a value of 9.87 and for a free-free situation the value is 22.4. Since it is desirable to have the natural frequency of the rotor as high as possible, the rotor support should be designed to be as nearly free-free as practicable. This is considered to be realistic with a thin-walled cylindrical rotor equipped with tilting pad journal bearings.

The prime criteria for selecting the operating speed of the centrifuge rotor is the ratio of operating speed to critical speed. The expression for operating speed is

$$N_s = (\omega r)/\pi d \qquad (6.125)$$

Equation (6.124) with $a_n = 22.4$ gives the following expression for critical speed,

$$(N_s)_{critical} = 7.156 \left(\frac{E}{\rho}\right)^{1/2} \frac{d}{z^2} \qquad (6.126)$$

Combining (6.125) and (6.126) gives

$$\frac{N_s}{N_{s\ crit}} = \frac{1}{22.47}\left(\frac{Z}{d}\right)^2 \times \left(\frac{E}{\rho}\right)^{-1/2} \times (\omega r) \tag{6.127}$$

Solving for $\frac{Z}{d}$ gives

$$\frac{Z}{d} = 4.74\left(\frac{N_s}{N_{s\ crit}}\right)^{1/2}\left(\frac{E}{\rho}\right)^{1/4}\left(\frac{1}{\omega r}\right)^{1/2} \tag{6.128}$$

Thus for a given isotropic material where the design peripheral velocity of the centrifuge is set by the material strength and the value of E/ρ is fixed, the ratio of rotor length to diameter is a function of the ratio of rotor operating to critical speeds.

In filament wound glass-resin composite materials the properties of the composite are primarily derived from the glass filament. If the filaments are wound circumferentially on a cylinder, the full strength of the glass is allocated to the resistance of hoop or tangential loads and none is available for resisting axial loads. Therefore, it is necessary to wind the filaments in a pattern so that the filament strength is available in the axial direction as well as in the circumferential direction.

One such filament winding pattern consists of alternate layers of fibers wound at an angle α to the longitudinal axis of the cylinder as shown schematically below

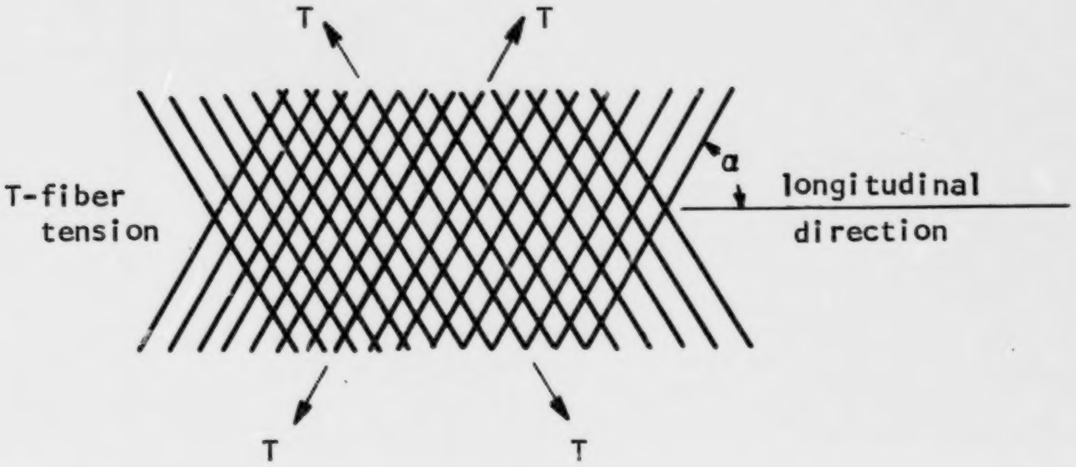

In this analysis it is assumed that the glass fibers carry all of the load and that the angle α does not change under strain.

The relationship between the glass stress and the composite stress is

$$\sigma_C = \frac{\sigma_g}{B} \tag{6.129}$$

where

σ_C = stress in the composite material in the direction of the filament

σ_g = stress in glass in the direction of the filament

B = resin bulk factor

The relationship between the circumferential stress and the stress at angle α is(3)

$$\sigma_H = \sigma_C \sin^2 \alpha \tag{6.130}$$

These relationships can be used to determine the optimum winding angle for balanced utilization of the glass fiber strength. For a cylindrical pressure vessel where $\sigma_C = \sigma_H/2$ this angle is 54.75(3). In the case of the centrifuge rotor where (σ_P/σ_{CF}) design is 0.05, the value of α for balanced stress would approach 90°. However, the requirements for longitudinal modulus of elasticity must be considered.

For isotropic materials, Equation (6.126) gives the relationship between rotor operating to critical speed ratio and the material modulus. For filament wound material the longitudinal modulus of the rotor is predominantly due to the glass so is dependent upon the winding angle α. Consideration of strains shows that $\varepsilon_f = \varepsilon_L = \varepsilon_H$ and

$$(E_C)_{long} = E_C \cos^2 \alpha \tag{6.131}$$

where

$$E_C = \frac{E_f}{B} \tag{6.132}$$

Combining Equations (6.127), (6.131) and (6.132) gives

$$\frac{N_s}{N_{s\ crit}} = \frac{1}{22.47}\left(\frac{Z}{d}\right)^2 \left(\frac{E_f \cos^2 \alpha}{B\ \rho_c}\right)^{-\ 1/2} (\omega r) \qquad (6.133)$$

Solving for the length to diameter ratio gives

$$\frac{Z}{d} = 4.74 \left(\frac{N_s}{N_{s\ crit}}\right)^{1/2} \left(\frac{E_f \cos^2 \alpha}{B\ \rho_c}\right)^{-\ 1/2} \left(\frac{1}{\omega r}\right)^{1/2} \qquad (6.134)$$

Combining Equations (6.116), (6.123), and (6.134) gives

$$\frac{Z}{d} = C \left(\frac{N_s}{N_{s\ crit}}\right)^{1/2} \left(\frac{E_f}{B\ \sigma_H}\right)^{1/4} (\cot \alpha)^{1/2} \qquad (6\ 135)$$

In view of the above it is apparent that there is no basis for determining the optimum angle for balanced stress for a centrifuge rotor. The optimum angle and $\frac{Z}{d}$ ratio must be based on economic considerations.

The above results are based on a simplified analysis. The basic assumptions in this analysis are that the fibers carry all of the load, the angle α remains constant (the fibers stretch but do not rotate), and the fibers are tightly packed. The state-of-the-art in designing filament-wound rotors is not sufficiently established to determine if this analysis is accurate or even sufficient. The number of articles being published on this subject indicates the questions still exist. (see for example, the 111 references given for Chapter 13 of Ref. 4).

Also the helically wound construction is only one of many possible construction for utilizing the fibers in both the circumferential and the longitudinal direction. For example, some layers could be wound circumferentially and the rest longitudinally. The ratio of the number of layers of each could be determined in the same manner as the helix angle. However, the above analysis based on the helically wound construction should be adequate for this feasibility study.

References

(1) Timoshenko, S., "Strength of Materials, Part I," 3rd Ed., Van Nostrad Co., New York, 1957.

(2) Den Hartog, J. P., "Mechanical Vibrations," 3rd Ed., McGraw-Hill Book Co., New York, 1947, p. 459.

(3) Rosato and Graw, "Filament Winding: Its Development, Manufacture, Applications, and Design," Interscience Publishers, New York, 1964, p. 194.

(4) Broutna, L. J. and Kroch, R. H., "Modern Composite Materials," Addison-Wesley Co., 1967.

6.4. Properties of Materials

6.4.1. Data on Glass Fibers and Resins

Glass Filament Data

	E glass	S glass	CS glass
Density-lb/in^2	0.092	0.090	0.090
Tensile Modulus (R.T.) lb/in^2	10.5x10^6	12.4x10^6	12.4x10^6
Filament Strength (R.T.) lb/in^2	500,000	665,000	665,000
Cost-$/lb	0.35	8.00	1.50

Source: Owens-Corning Fiberglas Corporation

Glass Filament Properties at Elevated Temperature

The tensile strength of S glass and E glass at elevated temperature are shown plotted in Figure 6.3. Figure 6.4 is a plot of single fiber modulus of elasticity vs. temperature. This shows that the effect of operating at 400°F is negligible.

Ultimate Glass Strength Values for Composite Materials

The Brunswick Corporation of Lincoln, Nebraska, considers the values of ultimate glass strength listed below to be realistically attainable at room temperatures with commercially available sizings. The ultimate glass strengths for composite materials do not vary significantly with the type of resin used as long as the resin and the sizing are compatible.

Glass	Ultimate Glass Strength in Composite Material at Room Temperature
E glass	260,000
S glass	360,000
CS glass	330,000

The effect of soaking at elevated temperature on the strength of a glass filament reinforced composite material is shown in Figure 6.5. This indicates that the reduction in strength due to soaking tends to become negligible after 500 to 1000 hours.

Resin Data

Dow Corning R-5071 Silicone Resin(*) R-5071 resin is a 100% solid form of 2106 resin. Bulletin 07-208 dated June 1966 states that 2106 resin is serviceable almost indefinitely at temperatures up to 500°F. The specific gravity of this resin when cured is about 1.22. Data on the tensile strength, tensile modulus, and tensile elongation for this resin are not available. However, it is described as a relatively brittle material when compared to epoxies and polyesters. Therefore, it is assumed that the percent tensile elongation of this resin is less than 1.0%. R-5071 resin can be used for filament winding applications either preimpregnated or wet wound. The 903 finish is recommended for elevated temperature applications because of its superior long-term heat aging properties.

Dow D.E.N. 439 Epoxy Novalac Resin(**)

Dow D.E.N. 439 epoxy novalac resin is widely used in commercial applications where high temperature performance is required. The physical characteristics of this resin are as follows:

Specific gravity	1.20
Tensile strength psi @ R.T.	6600
Tensile modulus - psi @ R.T.	0.44×10^6
Ultimate elongation - % @ R.T.	1.61

(*) Data received from M. Leon J. Ostrowski, Dow Corning Corporation, Midland, Michigan.

(**) Dow Bulletin No. 170-143B.

D.E.N. 439 resin with nadic methyl anhydride hardener has a heat distortion point ranging from 400 to 540°F, depending on the curing cycle used. Thermal degradation data for this resin and hardener combination are as follows:

Weight Change - %

Time-Hours Temperature-°F	100	200	500
320	-0.09	-0.04	+0.04
410	-0.35	-0.39	-1.20
500	-4.80	-9.0	---

Koppers Company High Temperature Polyester Resin(*)

The Koppers Company markets a high temperature polyester resin, Y7000-15 or M 7000-15, which is good for a maximum continuous operating temperature of 435°F. The physical characteristics of this resin are as follows:

Specific gravity	1.13
Tensile strength, PSI @ 77°F	6000-8000
Tensile modulus, PSIx10^{-6} @ 77°F	0.50-0.52
Tensile elongation, %	0.70-0.80
Weight loss, 240 hr @ 428°F, %	1 - 2
1000 hr @ 428°F, %	3 - 4

6.4.2. Data on Titanium Alloys

A prime consideration in selecting a titanium alloy for this application is weldability since the most reasonable method for fabricating a centrifuge rotor from metal is welding. Of those titanium alloys commercially available which are classified as weldable, the type which has the highest yield strength is Ti-3Al-13V-11Cr. The tensile

---

[*] Koppers Company Bulletin No. TC-317-17-5M.

yield strength of this alloy over a range of temperatures is given in Figure 6.6.

While this alloy is classified as weldable, it is weldable only in the annealed condition and even then the weld joint efficiency tends to be low. This is so because the weld metal ages at different rates than the bare metal and large grain size and microsegregation of alloying constituents develop at weld-metal grain boundaries during the fusion process. The high potential strength of this alloy might be attained by welding in a relatively thick ring with subsequent cold rolling to reduce the grain size.

The next strongest titanium alloy which is weldable is Ti-6Al-4V. This alloy has a weld joint efficiency of nearly 100% and yield strength over a temperature range as shown in Figure 6.7.

The tensile moduli of these titanium alloys is plotted in Figure 6.8 and Figure 6.9 gives values of the ratio of the centrifuge diameter to length as a function of peripheral velocity for these two alloys.

The cost of these titanium alloys are:

	Cost-$/lb
Ti-3Al-13V-11Cr	6.00[*]
Ti-6Al-4V	5.00[**]

6.4.3. Data on Maraging Steel

The tensile strength characteristics typical for 18% Ni maraging steel are shown in Figure 6.10 as a function of temperature. The effect of temperatures up to 400°F on the tensile modulus of this material is negligible. The ratio of centrifuge diameter to length for this material as a function of peripheral velocity is given in Figure 6.11. The cost of 18% Ni managing steel is $2.50/pound.

---

[*] From G. Grotke, Westinghouse Research Labs.

[**] Material Engineering - Vol. 68, No. 5.

Curve 588096-A

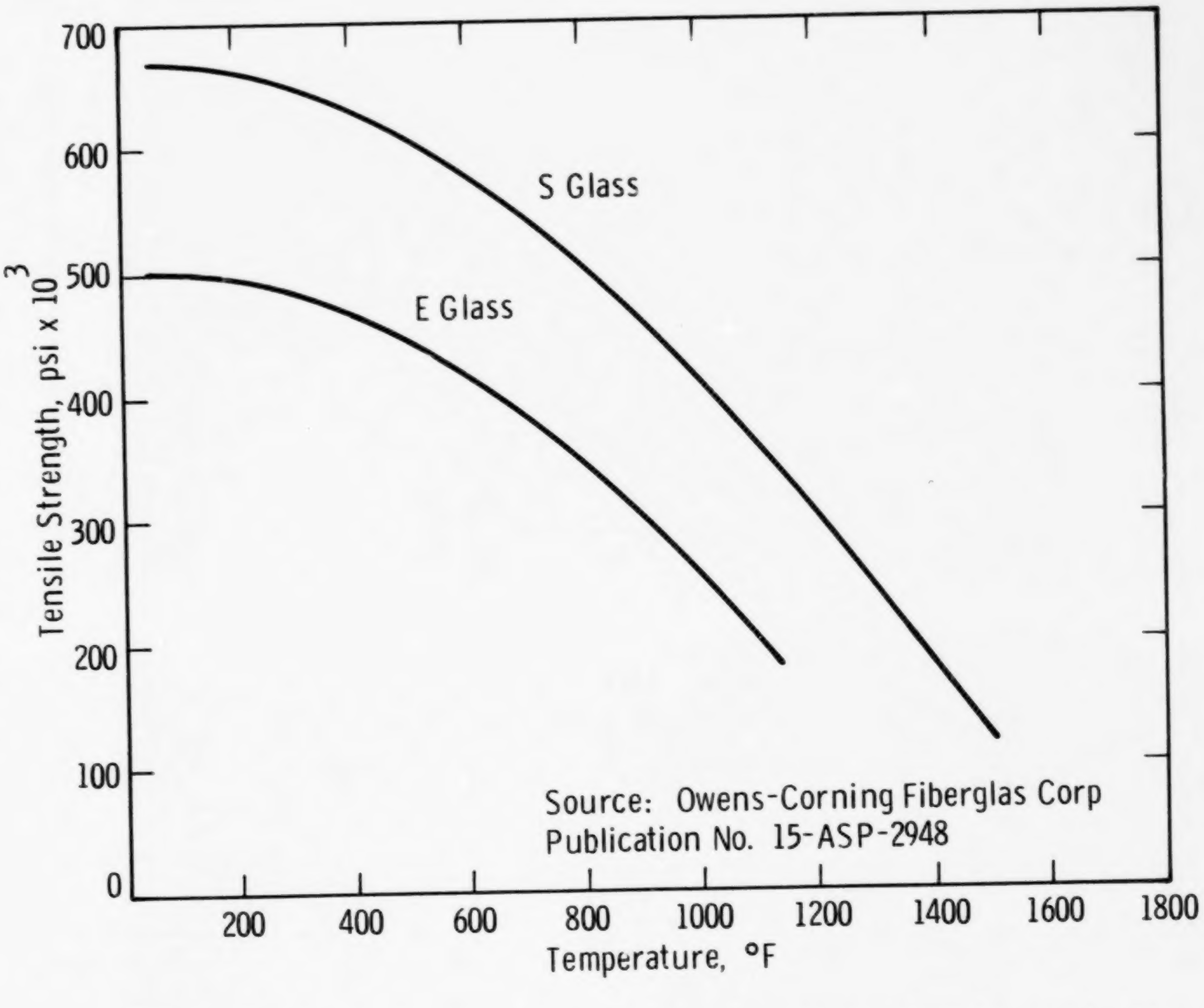

Source: Owens-Corning Fiberglas Corp Publication No. 15-ASP-2948

Fig. 6.3—Virgin glass filament tensile strengths at various temperatures

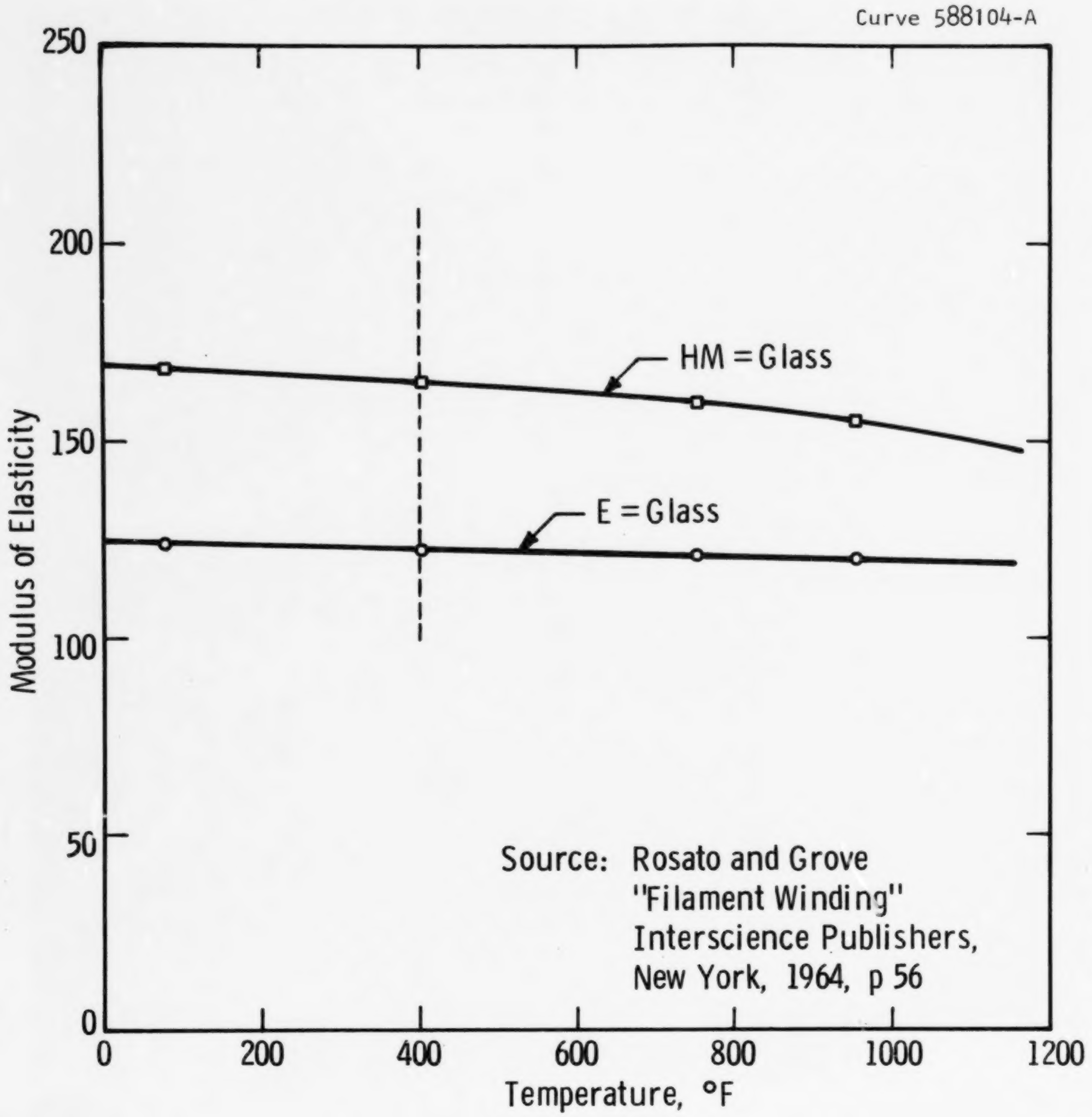

Fig. 6.4—Single glass fiber modulus of elasticity

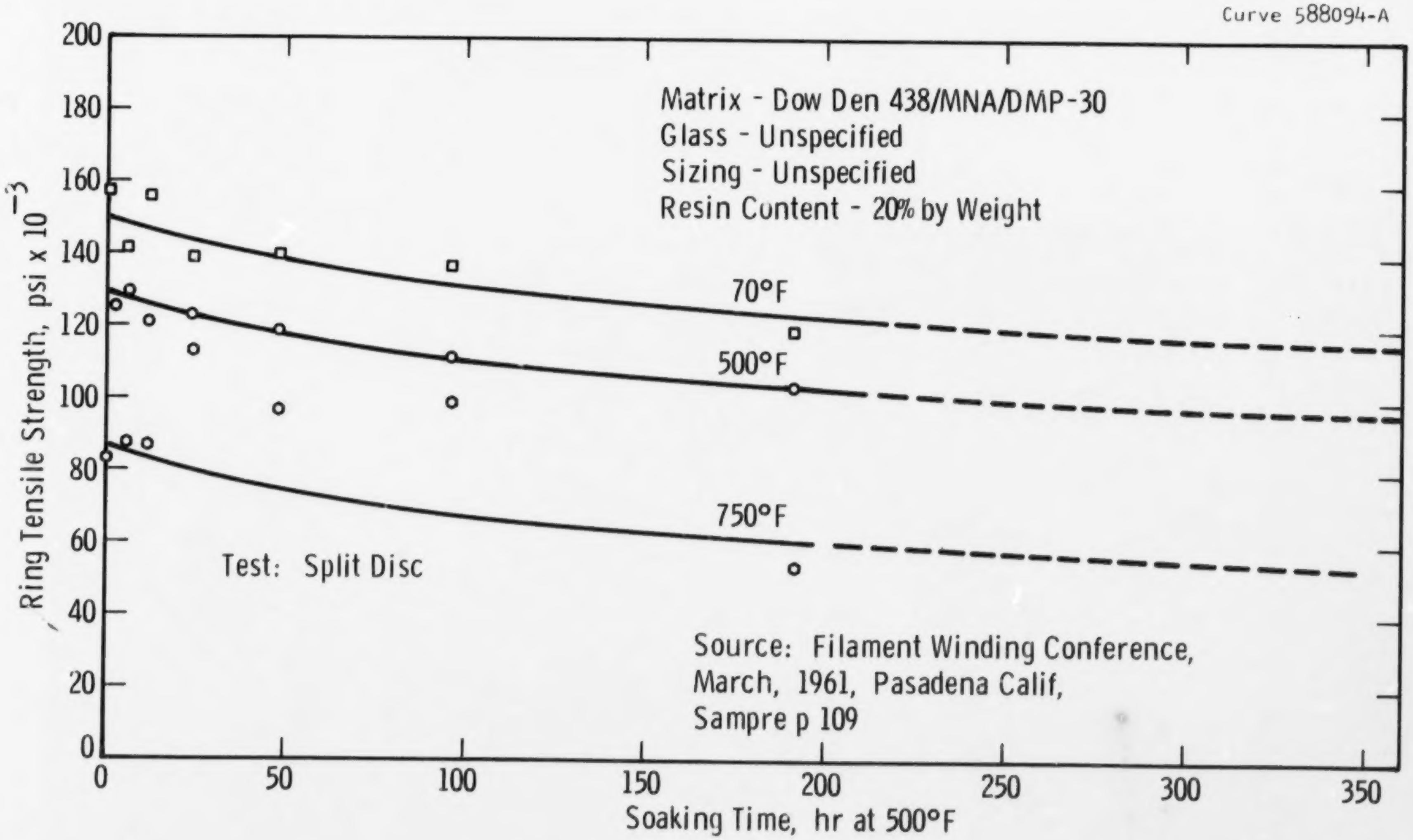

Source: Filament Winding Conference, March, 1961, Pasadena Calif, Sampre p 109

Fig. 6.5—Effect of soaking at elevated temperature on the strength of glass filament reinforced plastic composite material

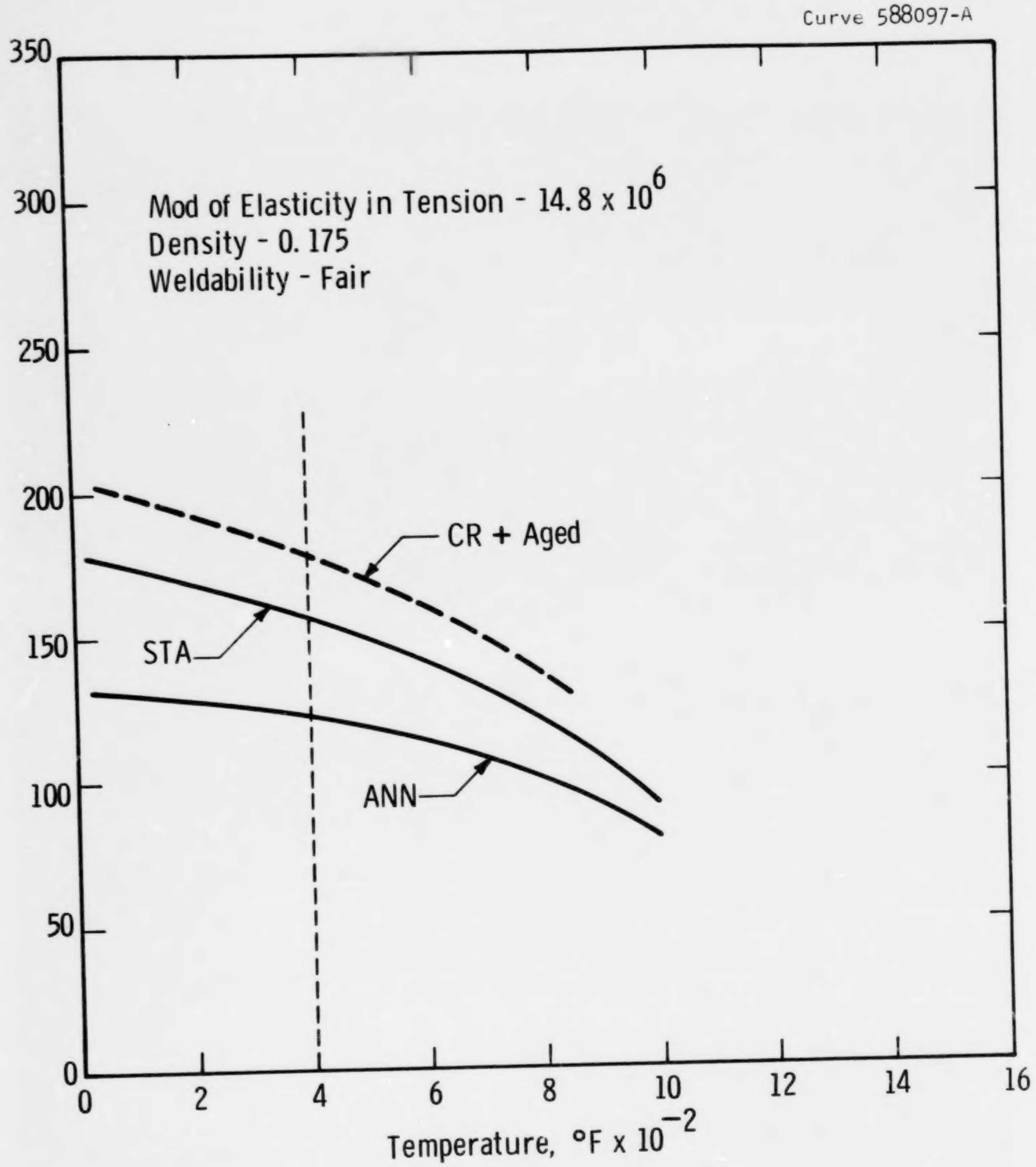

Fig. 6.6—Strength characteristics of titanium alloy Ti-13V-11Cr-3Al heat treated

Curve 588105-A

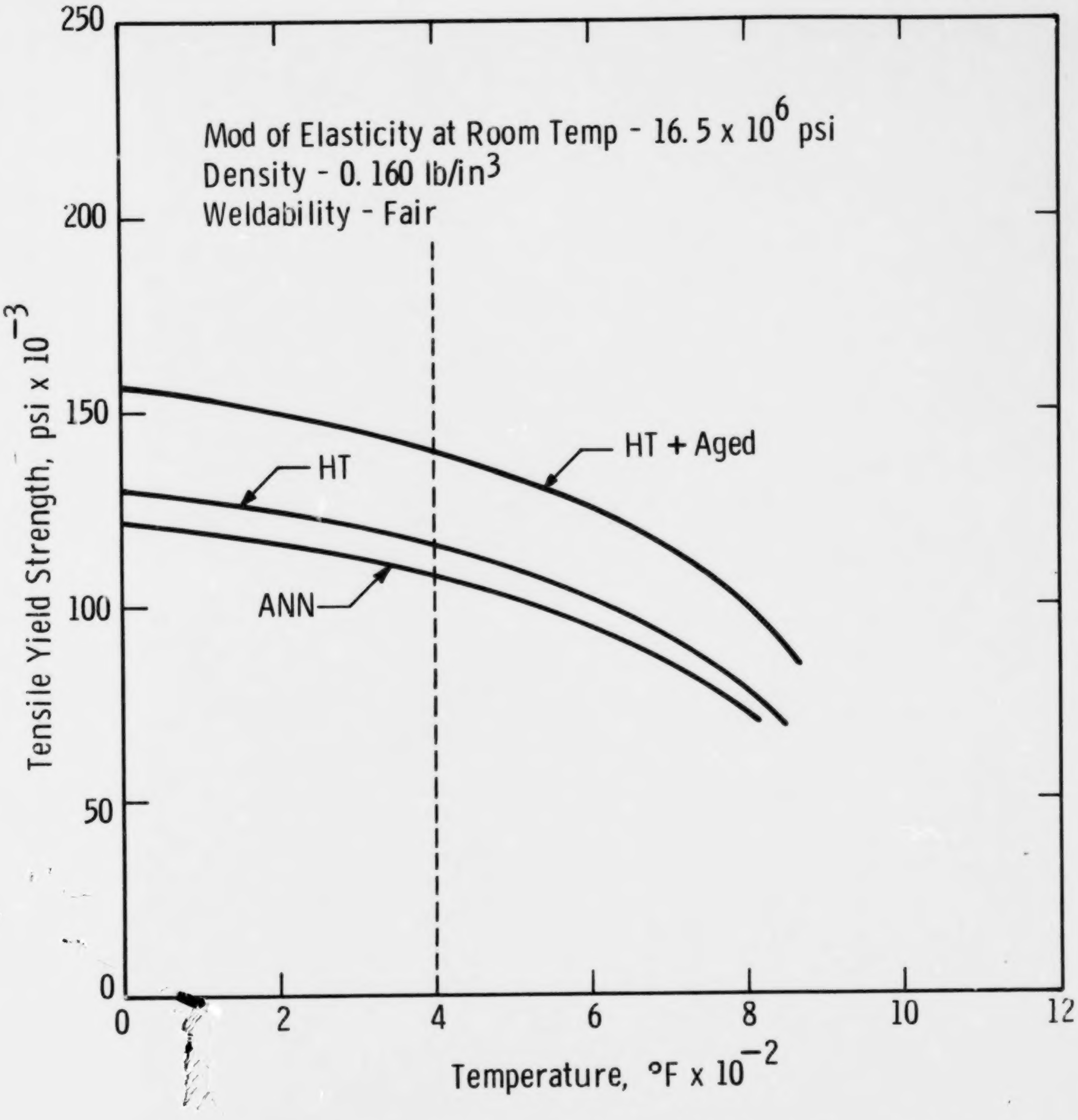

Fig. 6.7—Strength characteristics of titanium alloy Ti-6Al-4V

Curve 588133-A

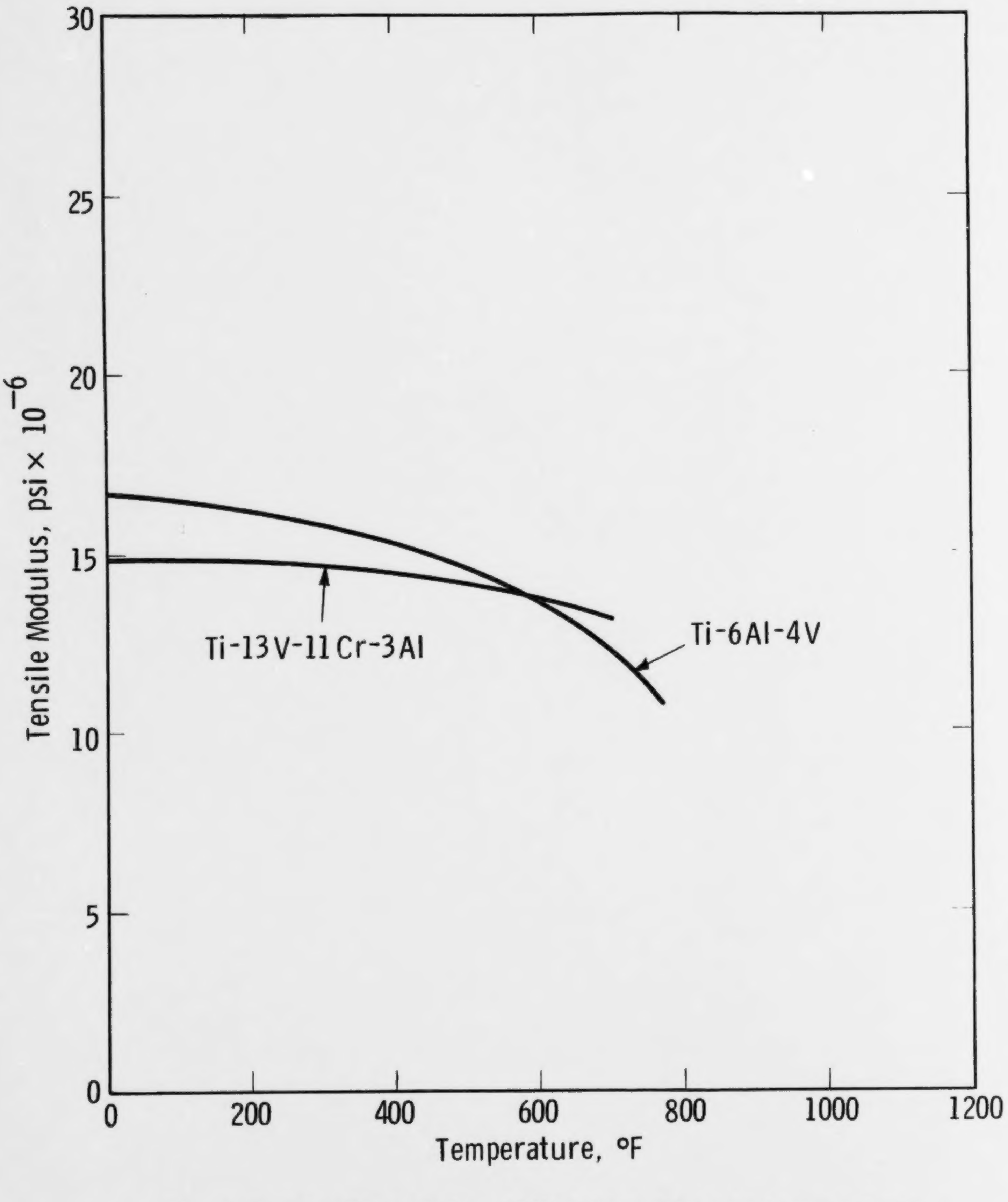

Fig. 6.8—Tensile modulus of titanium alloys vs temperature

Curve 588095-A

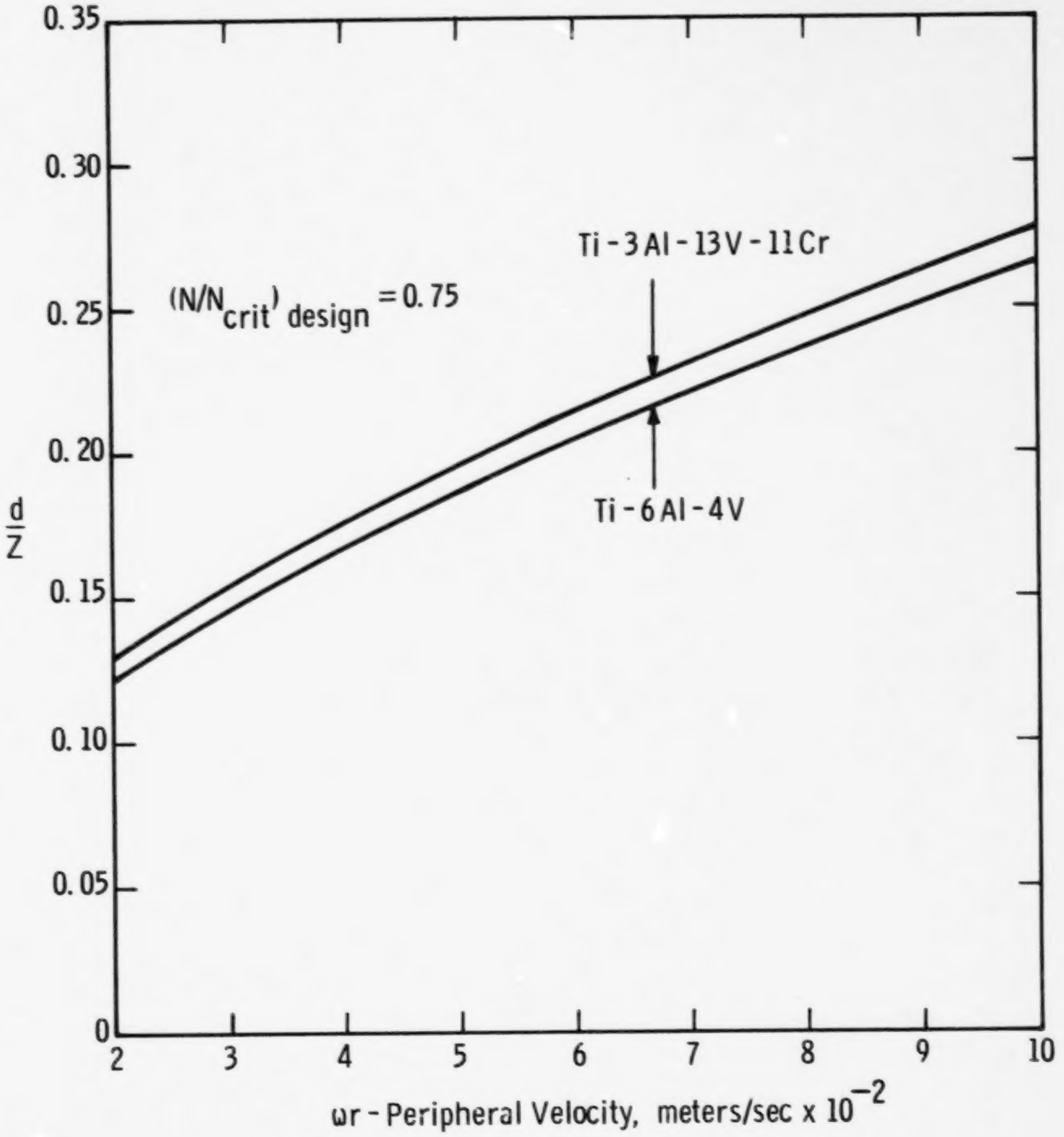

Fig. 6.9—Ratio of centrifuge diameter to length for titanium alloys

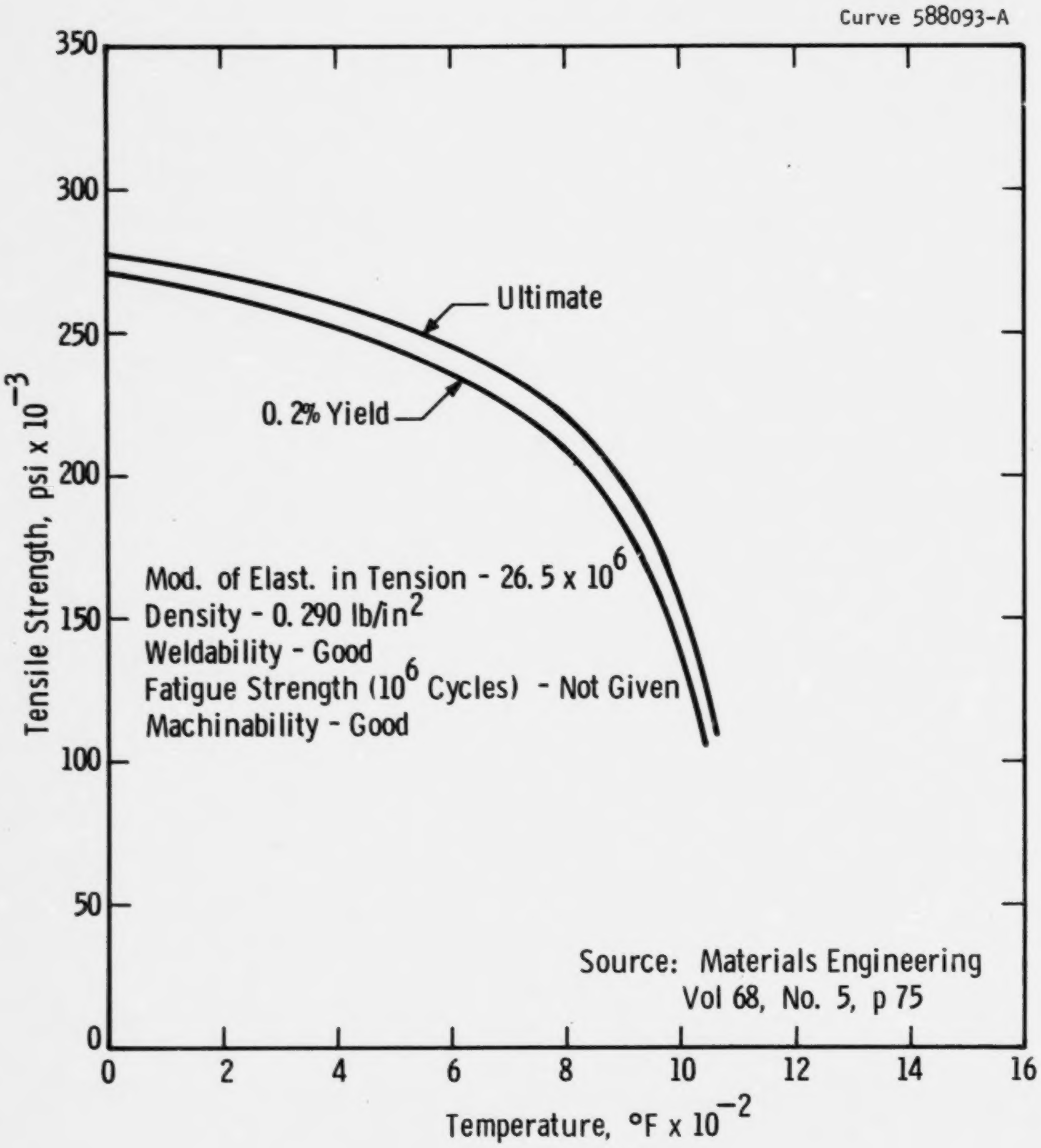

Source: Materials Engineering Vol 68, No. 5, p 75

Fig. 6.10—Ultra high strength steel
18 Ni maraging

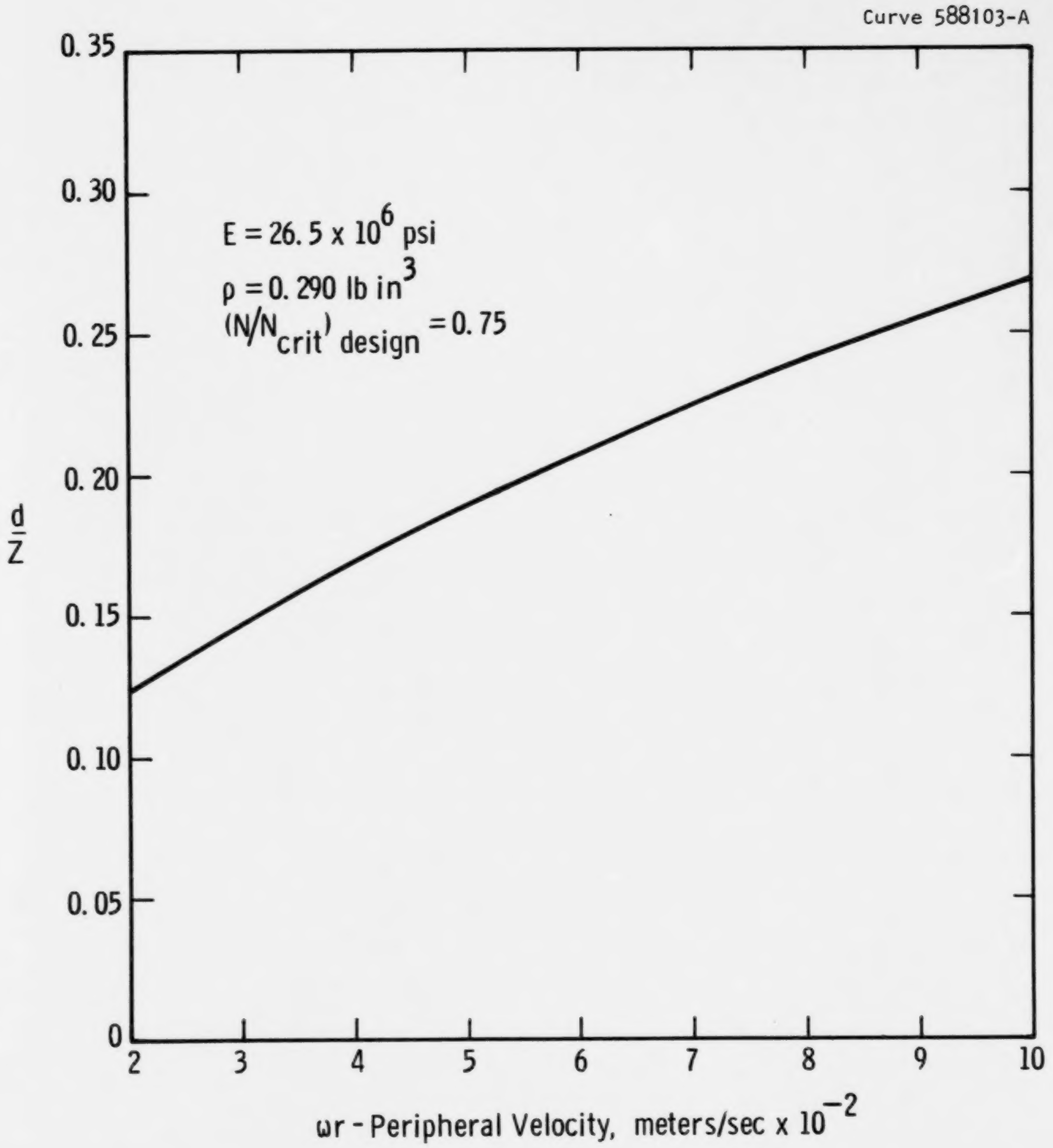

Fig. 6.11—Ratio of centrifuge diameter to length for 18% Ni maraging steel

6.5. Estimates of Certain Cost Components for Centrifuge Cascade System

6.5.1. Derivation of the Centrifuge Bearing Power Loss Equation

The power loss in a journal bearing based on straight shear of the lubricant and assuming concentricity of the shaft and the bearing is

$$P_B = \pi^3 \mu \left[\left(\frac{D_B}{c}\right) \left(\frac{L_B}{D_B}\right) \left(N_S^2\right) \left(D_B^3\right) \right] \tag{6.136}$$

where

P_B = power consumption of the bearing - in-lb/sec

μ = lubricant viscosity - Reyns - lb-sec/in^2

L_B = bearing length - inch

D_B = bearing diameter - inch

c = bearing clearance - inch

N_S = shaft rotational speed - RPS

In bearing design practice the ratios of L_B/D_B and D_B/c are constant over a wide range of bearing diameters for a given type of bearing. For the tilting pad bearings which would probably be used in the centrifuges, the values for these ratios are:

$$\frac{L_B}{D_B} \simeq 1$$

$$\frac{D_B}{c} = 500$$

and the oil which would be used in these bearings would have a viscosity of about 0.75 x 10^{-6} (lb)(sec)/in^2 at operating temperature. Hence,

$$P_B = 11.65 \times 10^{-3} (N_S^{\;2}) (D_B^{\;3}) \tag{6.137}$$

The total power consumed by the bearings in a cascade of centrifuges with two bearings per centrifuge is

$$P_B' = 2nP_B \tag{6.138}$$

where

n = number of centrifuges in a cascade

$$n = \frac{\text{total length of centrifuges}}{\text{length per centrifuge}} = \frac{\ell}{Z}$$

The total length of the centrifuges in a cascade is a function of the separative duty and of the peripheral velocity i.e. $\ell = \ell(D,\omega r)$. Hence,

$$\begin{aligned} P_B' &= 2 \times \frac{\ell(D,\omega r)}{Z} \times 11.65 \times 10^{-3} (N^2) (D_B^{\;3}) \\ &= 23.30 \times 10^{-3} \times \ell(D,\omega r) (N_S^{\;2}) (D_B^{\;3})/Z \end{aligned} \tag{6.139}$$

The flow through a centrifuge enters and leaves through hollow shafts at the ends of the centrifuge. If it assumed that the feed enters through one end and the heads and tails flows leave through the other so that the molar flows are equal, the cross section area of the shafts is:

$$A_S = \frac{L\underline{R}T}{p\ u_S} \tag{6.140}$$

where

A_S = shaft flow area - in^2

L = molar flow rate to centrifuge - moles/sec

R = universal gas constant - 1545 $\frac{\text{ft-lb}}{\text{mole °R}}$

T = temperature - °R

p = pressure - psia

u_S = velocity of gas in shaft - ft/sec

Therefore,

$$D_S = \left[\frac{4}{\pi}\,\frac{L\underline{R}T}{p\;u_S}\right]^{1/2} = \left[\frac{4}{\pi} \times \left(\frac{L}{Z}\right)\,\frac{Z\underline{R}T}{p\;u_S}\right]^{1/2} \tag{6.141}$$

Since, the bearing diameter D_B is proportional to the shaft I.D.,

$$D_B = CD_S \tag{6.142}$$

It is assumed that $D_B/D_S = 1.25$ so

$$D_B = 1.25\,\left[\frac{4}{\pi} \times \left(\frac{L}{Z}\right)\,\frac{Z\underline{R}T}{p\;u_S}\right]^{1/2} \tag{6.143}$$

If u_S is assumed to be 100 ft/sec, pressure is 1 atmosphere and temperature is 760°R. Equation (6.143) reduces to

$$D_B = 39.87\;\left[\left(\frac{L}{Z}\right)\;Z\right]^{1/2} \tag{6.144}$$

where Z has the units of feet.

The maximum separative work per foot of length of a centrifuge, as derived by Cohen(1), is shown in Section 3.3 to be

$$\frac{\delta U_{max}}{Z} = \frac{\pi c\;D_{AB}\;Z}{2}\left[\frac{(M_B - M_A)\;(\omega r)^2}{2\underline{g}RT}\right]^2 \tag{3.31}$$

From the definition of separative efficiency

$$\frac{\delta U_{exp}}{Z} = E\;\frac{\delta U_{max}}{Z} \tag{6.145}$$

Benedict and Pigford[(2)] give the following expression for the total length of centrifuges required for a given separative duty

$$\ell = \frac{2 \ \ln (r''/r')}{\pi \ D_{AB} \ \rho(\alpha-1)^2} \times D \tag{6.146}$$

For an idealized counter current centrifuge the minimum length is obtained when $\frac{r'}{r''} = 0.53$ and Equation (6.146) becomes

$$\ell = \frac{1.272 \ D}{\pi \ D_{AB} \ \rho(\alpha-1)^2} \tag{6.147}$$

By definition

$$\ell \equiv \frac{D}{\delta U_{exp}/Z} \tag{6.148}$$

Combining Equations (6.147) and (6.148) gives

$$\frac{\delta U_{exp}}{Z} = \frac{\pi \ D_{AB} \ \rho(\alpha-1)^2}{1.272} \tag{6.149}$$

Combining (6.145) and (6.149) gives $\alpha = \alpha(\omega r)$ for a specified gas composition and temperature.

For large values of α, the flow through the centrifuge L, is given by[(3)]

$$L = \delta U_{exp} \frac{\beta+1}{(\beta-1) \ \ln \beta}$$

where $\beta = \sqrt{\alpha}$. Solving for L/Z gives

$$\frac{L}{Z} = \left(\frac{\delta U_{exp}}{Z}\right) \frac{\beta+1}{(\beta-1) \ \ln\beta} \tag{6.150}$$

Substituting Equation (6,145) and $\alpha = \alpha\ (\omega r)$ into Equation (6.150) gives

$$\frac{L}{Z} = \frac{L}{Z}\ (\omega r)$$

and this relationship for the specified flue gas at a temperature of 300°F and a pressure of 1 atmosphere is shown plotted in Figure 6.12. Substituting values of $\frac{L}{Z}$ from this plot into Equation (6.144) gives

$$D_B = 39.87 \left(\frac{L}{Z}\ (\omega r)\ \times\ Z\right)^{1/2} \qquad (6.151)$$

By definition

$$N_s = \frac{(\omega r)}{\pi d} \qquad (6.152)$$

where d is the diameter of the centrifuge rotor.

Substituting Equations (6.151) and (6.152) into 6,139 gives

$$P'_B = 149.8 \times \ell(D,\omega r) \times \left(\frac{L}{Z}(\omega r)\right)^{3/2} \times (\omega r)^2 \times \left(\frac{Z}{d}\right)^2 \times \frac{1}{Z^{3/2}} \qquad (6.153)$$

For a freely support shaft, the ratio of centrifuge rotor operating speed to critical speed is shown in Appendix 6.3 to be

$$\frac{N_s}{N_{s\ crit}} = \frac{1}{22.47} \left(\frac{Z}{d}\right)^2 \times \left(\frac{E}{\rho}\right)^{-1/2} \times (\omega r) \qquad (6.154)$$

where

E = elastic modulus of centrifuge rotor in the axial direction - psf

ρ = density of rotor wall lb/ft^3

ωr = rotor peripheral velocity - ft/sec

Solving for Z/d gives

$$\frac{Z}{d} = 4.74 \left(\frac{N_s}{N_{s\ crit}}\right)^{1/2} \left(\frac{E}{\rho}\right)^{1/4} \frac{1}{(\omega r)^{1/2}} \qquad (6.155)$$

This can also be expressed as

$$\frac{Z}{d} = 2.015 \left(\frac{N_s}{N_{s\ crit}}\right)^{1/2} \left((E_C)_{long}/\sigma_{CF}\right)^{1/4}$$

In order to avoid vibration, the operating speed of the centrifuge must have a fixed relationship to the critical speed. While centrifuges have been operated at speeds greater then the first critical, this is thought to be impractical for that application. A value of 0.75 has been selected for the design ratio of $(N_s/N_{s\ crit})$. This gives

$$\frac{Z}{d} = 4.11 \times \left(\frac{E}{\rho}\right)^{1/4} \times \frac{1}{(\omega r)^{1/2}} \qquad (6.156)$$

This shows that this ratio is a function of the peripheral velocity which is dependent on the design hoop stress of the rotor as well as the rotor longitudinal modulus of elasticity and the rotor wall density. All of these are functions of the material used in constructing the rotor. Therefore, each material has a unique solution for this expression.

For power consumption in KW units Equation (6.153) becomes

$$P_B' = 1.693 \times 10^{-2} \times \ell(D,\omega r) \times \left(\frac{L}{Z}(\omega r)\right)^{3/2} \times (\omega r)^2 \times \left(\frac{Z}{d}\right)^2 \times \frac{1}{Z^{3/2}} \qquad (6.157)$$

Curve 588111-B

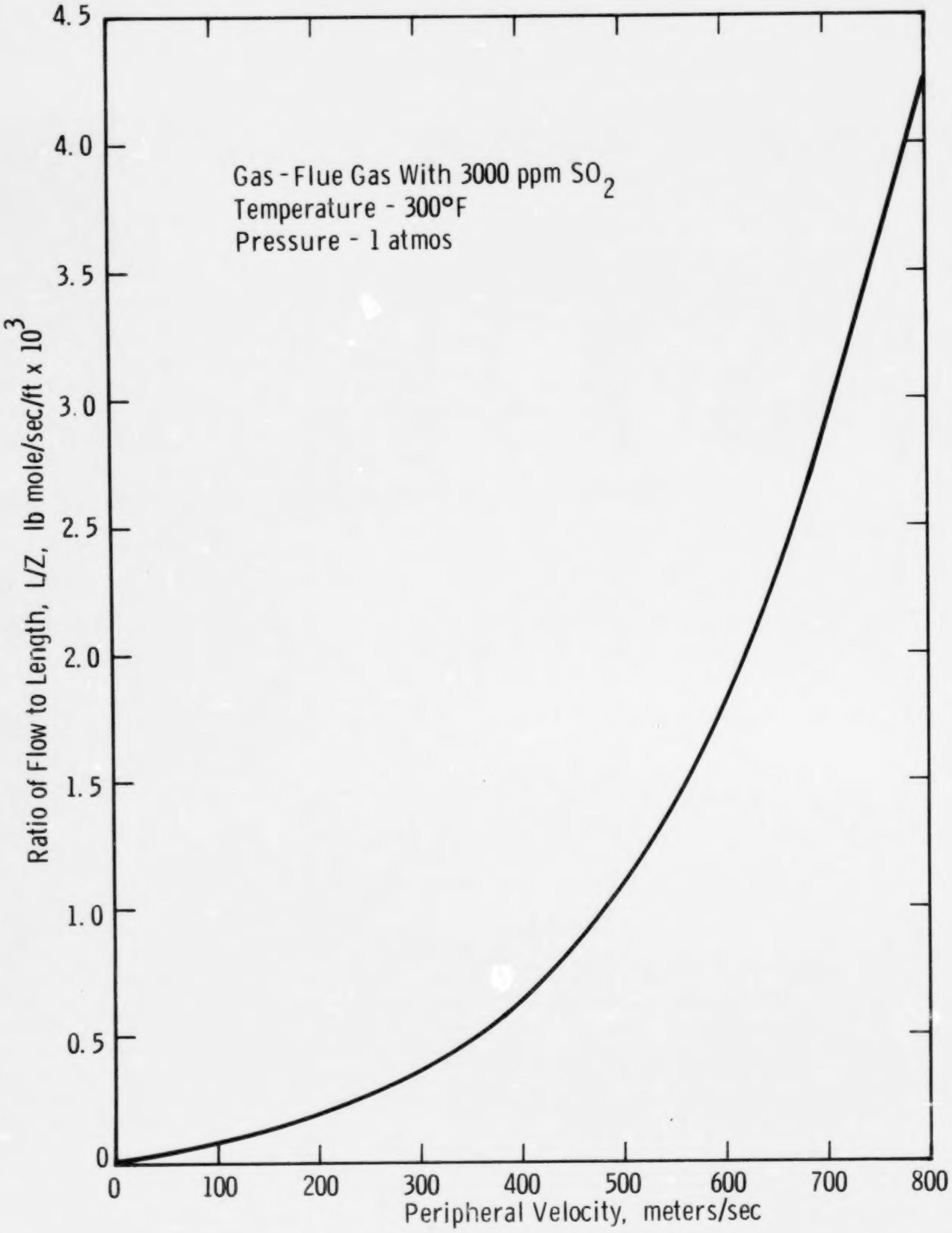

Fig. 6.12—Ratio of inlet flow to length vs peripheral velocity for centrifuge with Martin profile

References

(1) Cohen, Karl, "The Theory of Isotope Separators as Applied to the Large Scale Production of U 235," McGraw-Hill, New York, 1951.

(2) Benedict and Pigford, "Nuclear Chemical Engineering," McGraw-Hill, New York, 1957.

(3) Cohen, p. 19.

6.5.2. Estimate of Cost of Material used in Fabricating Centrifuges

The volume of material used in the fabrication of a single centrifuge rotor is

$$\begin{aligned} V_C &= Z \times \pi d \times t_w + 2 \times \frac{\pi}{4} d^2 \times t_e \\ &= \pi\, Z^2 (d/Z)\ (t_w + \frac{1}{2}\ (d/Z)\ t_e) \end{aligned} \qquad (6.158)$$

The total volume of material of construction in a cascade of n centrifuges is

$$\begin{aligned} V_T &= V_C \times n \\ &= \ell \times \pi \times d\ (t_w + \frac{1}{2} \left(\frac{d}{Z}\right) t_e) \end{aligned} \qquad (6.159)$$

If the average thickness of the ends of the centrifuge is assumed to be 25% greater than that of the cylinder walls, the total volume of material is

$$V_T = \pi \ell\ d^2 \left(\frac{t_w}{d}\right) (1 + 0.625 \left(\frac{d}{Z}\right)) \qquad (6.160)$$

The hoop stress of the centrifuge wall due to internal pressure wall is

$$(\sigma_H)_P = \frac{P_{(o)}\ \exp M(\omega r)^2/2g\underline{R}T}{2(t_w/d)} \qquad (6.161)$$

The hoop stress due to centrifugal force is

$$(\sigma_H)_{CF} = \rho(\omega r)^2/g \qquad (6.162)$$

If the ratio of the stress due to pressure to that due to centrifugal force is taken as a design parameter,

$$\left(\frac{t_w}{d}\right) = \frac{1}{2}\ \frac{g\ p_{(o)}\ \exp M(\omega r)^2/2g\underline{R}T}{\rho(\omega r)^2\ \left(\frac{(\sigma_H)_P}{(\sigma_H)_{CF}}\right) \text{design}} \tag{6.163}$$

For $p_{(o)} = 1$ atmos., $T = 760°R$, $x_P = 0.2$, and $(\sigma_H)_P/(\sigma_H)_{CF} = 0.05$, the expression reduces to

$$\left(\frac{t_w}{d}\right)_{5\%} = \frac{6.875 \times 10^5 \ \exp 0.4867 \times 10^{-6}\ (\omega r)^2}{\rho(\omega r)^2} \tag{6.164}$$

From Appendix 6.5.1 the expression for Z/d is

$$\frac{Z}{d} = 4.74 \left(\frac{N_s}{N_{s\ crit}}\right)^{1/2} \left(\frac{E}{\rho}\right)^{1/4} \left(\frac{1}{\omega r}\right)^{1/2} \tag{6.155}$$

Combining Equations (6.160), (6.164) and (6.155) gives the total quantity of material is the centrifuge cascade which when multiplied times the unit cost of the material gives the total cost of the material of construction.

6.5.3. Estimates of Cost of Bearings for Gas Separation Centrifuges

The type of bearing which is considered to be best for use in high speed gas centrifuges is the tilting pad journal bearing. The rationale used for estimating the size of the bearings for centrifuges is as follows:

The internal cross sectional area of the shaft is

$$A_S = WRT/Pu = L\underline{R}T/Pu \tag{6.165}$$

and

$$A_S = \left(\frac{\pi}{4} D_S^2\right) \tag{6.166}$$

Therefore, the inner diameter of the shaft is

$$D_S = \left(\frac{4}{\pi} A_S\right)^{1/2} = \left(\frac{4}{\pi} \frac{L\underline{R}T}{Pu}\right)^{1/2} = \left[\frac{4}{\pi} \left(\frac{L}{Z}\right) \left(\frac{Z\underline{R}T}{Pu}\right)\right]^{1/2} \tag{6.167}$$

Appendix 6.5.1 shows that $\frac{L}{Z} = \frac{L}{Z}(\omega r)$ and Figure 6.12 is a plot of this relationship. Therefore

$$D_S = \left[\frac{4}{\pi} \times \frac{L}{Z}(\omega r) \times \left(\frac{Z\underline{R}T}{Pu}\right)\right]^{1/2} \tag{6.168}$$

If it is assumed that the diameter of the bearing (D) is 25% greater than the inside diameter of the shaft,

$$D = \frac{2.5}{\sqrt{\pi}} \left[\frac{L}{Z}(\omega r) \times \left(\frac{Z\underline{R}T}{Pu}\right)\right]^{1/2} \tag{6.169}$$

For $P = 1$ atmos., $T = 760°R$ and $u = 100$ ft/sec

$$D = 3.32 \times [(Z) \times \frac{L}{Z}(\omega r)]^{1/2} \tag{6.170}$$

Figure 6.13 gives a correlation of the cost of tilting pad type journal bearings as a function of bearing diameter from Westinghouse sources. Equation (6.170), Figure 6.12, and Figure 6.13 were used to calculate the specific cost of the bearings for the gas centrifuge as a function of peripheral speed and centrifuge length. The results of these calculations are plotted on Figure 6.14. The centrifuge would have only two bearings. If the motor or turbine for driving the centrifuge were integral with the centrifuge, this bearing cost would be for both the centrifuge and the drive. If an external motor or turbine were used to drive the centrifuge, additional bearings would be required for the system.

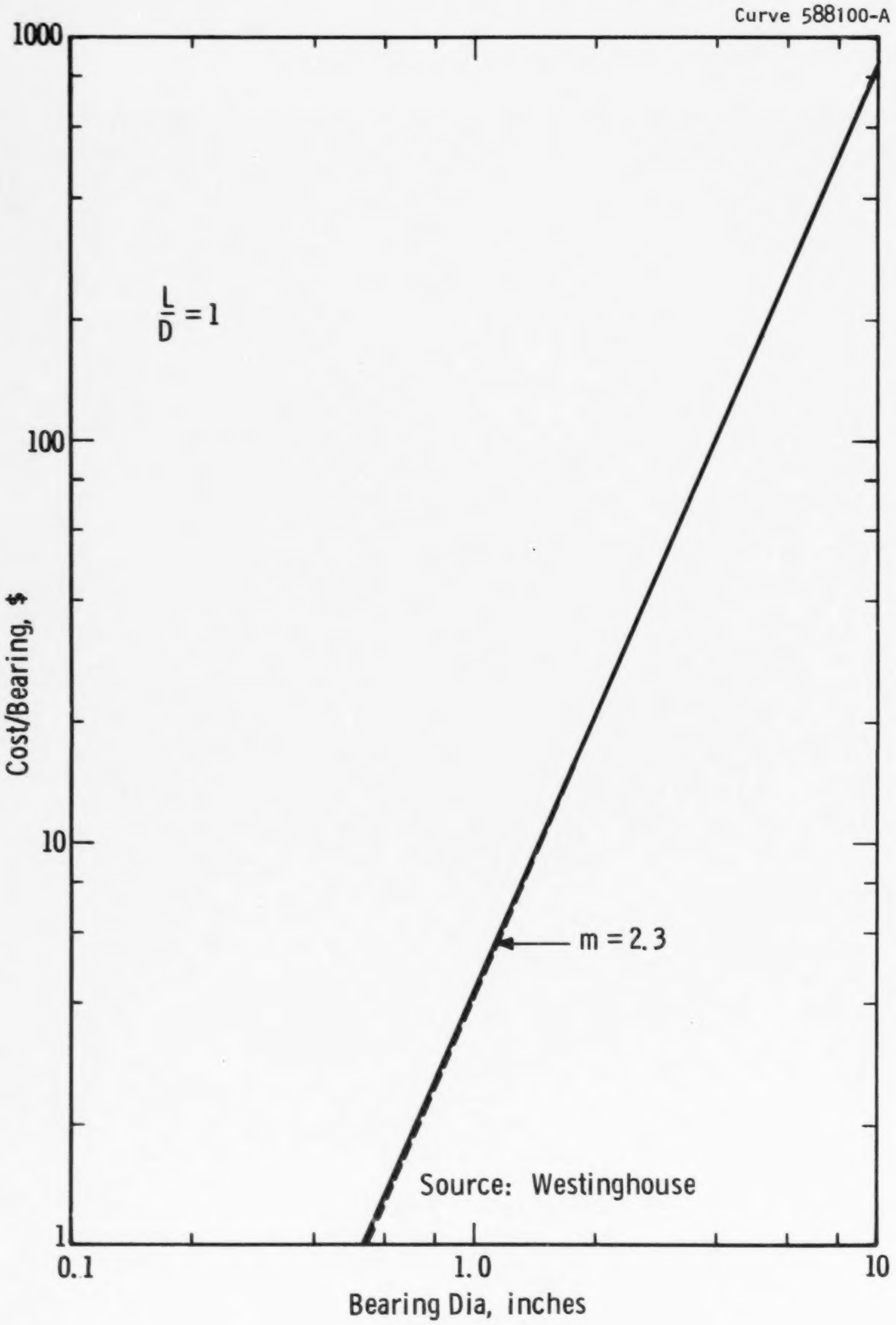
Curve 588100-A
1000
100
10
1
Cost/Bearing, $
$\frac{L}{D} = 1$
m = 2.3
Source: Westinghouse
0.1
1.0
10
Bearing Dia, inches

Curve 588098-A

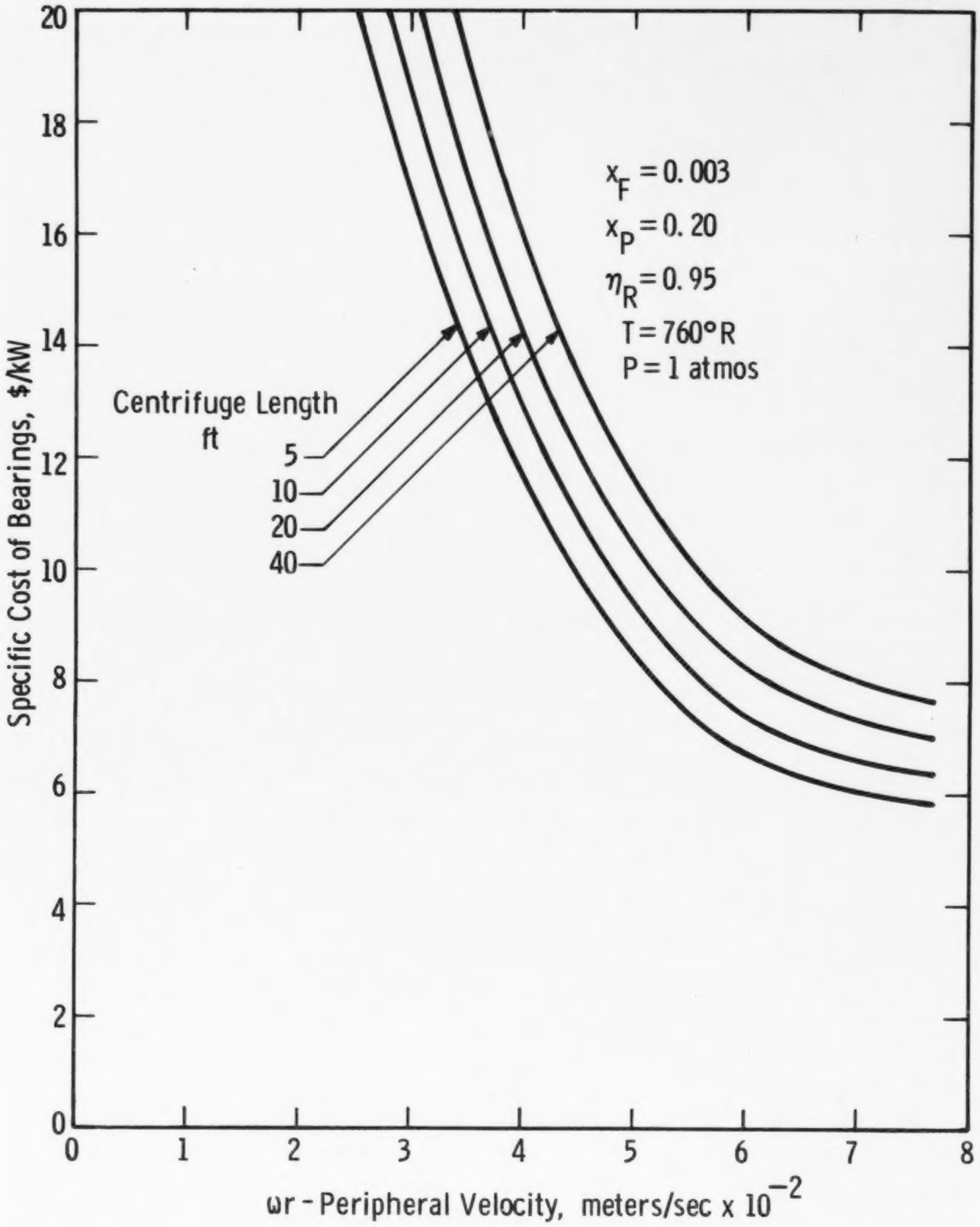

Fig. 6.14—Estimated cost of bearings for centrifuges in cascade for 500 mW power plant

6.5.4. Estimate of Vacuum Chamber Costs

It is assumed that the vacuum chambers for the individual centrifuge would be constructed of carbon steel. Either circumferential or longitudinal flanges would be necessary for assembly.

Cost data were compiled for cylindrical vessels of three types, i.e. pressure vessels, vacuum receivers, and storage tanks.

Aries and Newton,(1) p. 67 gives purchase costs for pressurized tanks.

For a cylindrical tank made of steel for pressures of 50 to 150 psig the cost as a function of volume is as follows.

Capacity gal	Volume-ft^3	Purchase Cost - $
1,000	133.7	6,500
10,000	1,337.0	16,000
100,000	13,370.0	39,000

Assume that the cost of a tank for a full vacuum is the same as for a tank with 15 psig internal pressure. This is optimistic for tank with full vacuum.

For spherical tanks the cost of a 100 psig tank is about 2 1/2 times that for a 15 psig tank.

Cost index correction (M&S index(2))

Base for 1954 - 184
Index for 3rd qtr. 1968 - 272.5
Multiplier - 272.5/184 = 1.48

Estimated costs for vacuum vessel

Volume-ft^3	Purchase Cost-$
133.7	3,840
1,337.0	9,460
13,370.0	23,100

Cost Estimate of Vacuum Chamber

Aries and Newton,(1) p. 63 gives purchase costs for vacuum receivers.

For injacketed steel vessels the 1954 cost vs capacity is as follows:

Capacity-gals	Volume-ft^3	Purchase Cost-$
30	4.45	180
100	13.37	280
1,000	133.7	950

Cost index correction (M&S index)

Base for 1954 - 184
Index for 3rd qtr. 1968 - 272.5
Multiplier - 272.5/184 = 1.48

Up-to-date cost estimates

Volume-ft^3	Purchase Cost-$
4.45	266
13.37	414
133.7	1,400

Cost of Horizontal Steel Storage Tanks

Mills(3) gives the following data for the cost of horizontal steel storage tanks.

Capacity gals	Volume ft^3	Purchase Cost-$ (M&S Index = 238.8)
10,000	1,337.	2,600
100,000	13,370.	14,000

Cost index correction (M&S index)

Base - 238.8
Index for 3rd qtr. 1968 - 272.2
Multiplier - 1.14

Up-to-date costs

Volume-ft^3	Purchase Cost-$
1,337	2,960
13,370	15,950

The cost data from each of these sources is plotted on Figure 6.15. This indicates that the extrapolated data for vacuum receivers is probably somewhat optimistic for this application. However, it will be used for estimation of centrifuge vacuum chamber costs.

References

(1) Aries and Newton, "Chemical Engineering Cost Estimation," McGraw-Hill, New York, 1955.

(2) Stevens, Robert W., "Equipment Cost Indexes for Process Industries," Chemical Engineering, Nov. 1947, p. 124-6.

(3) Mills, H. E., "Costs of Process Equipment," Chemical Engineering, March 16, 1964.

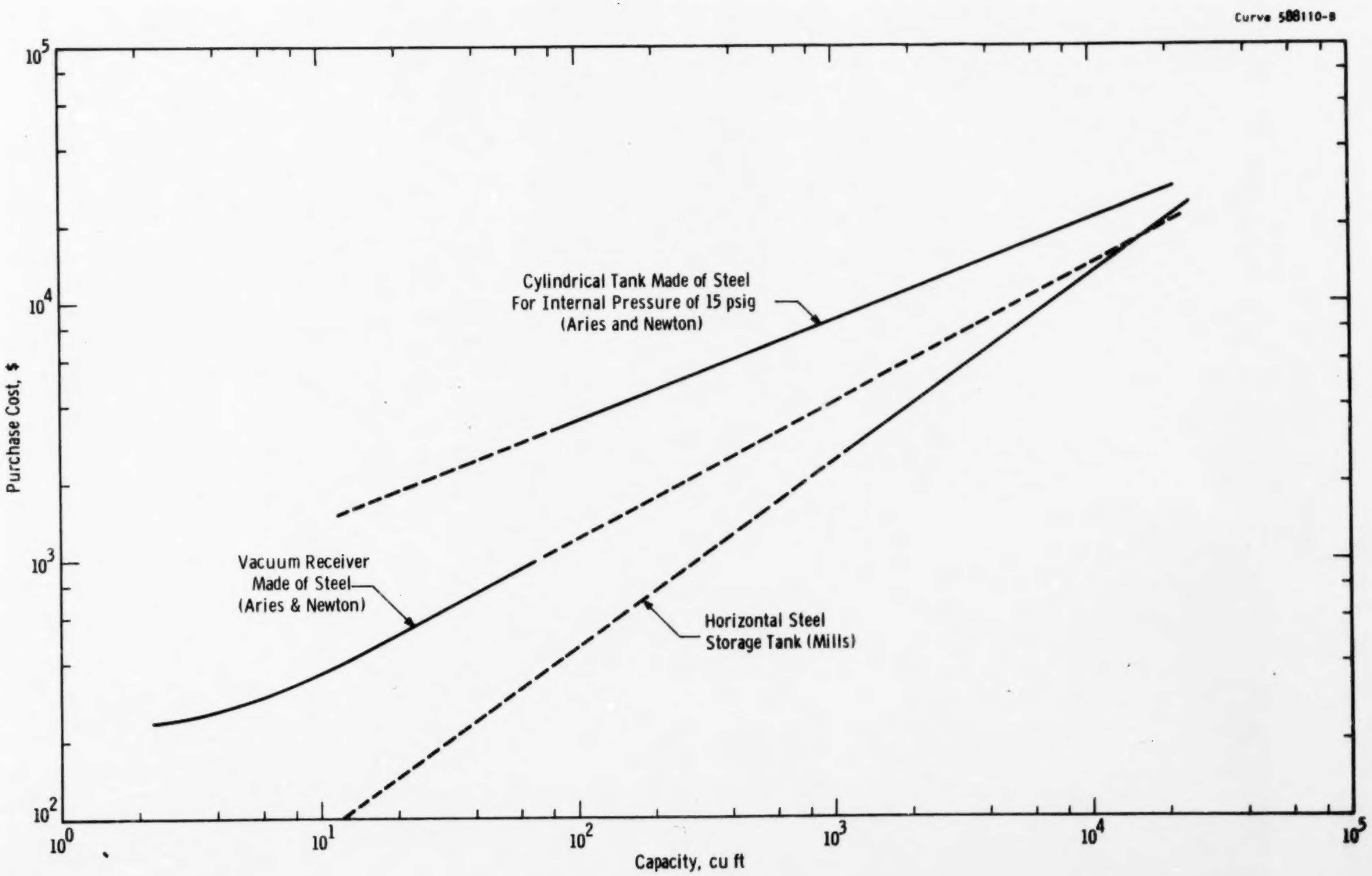

Fig. 6.15—Estimated cost of cylindrical vacuum chamber

6.6 SURVEY OF METHODS OF RECOVERY OF SULFUR AS A BY-PRODUCT

The sulfur in flue gas could be recovered and marketed in one of the following forms

Elemental sulfur
Sulfuric acid
Ammonium sulfate
Sulfur dioxide
Hydrogen sulfide

Table 6.1 gives the current prices(1) for four of these by-products.

TABLE 6.1

Market Prices of Sulfur Compounds

SULFUR		
Sulfur, coml., flour bgs., mines.	100 lbs.	3.65
dms., mines	100 lbs.	4.50
lump, bgs., mines	100 lbs.	3.55
dms., mines	100 lbs.	4.10
Sulfur, crude, dom., dark, f.o.b., vessels, Gulf ports (for U.S. and Canada)	long-ton.	41.00
Sulfur, crude, dom., dark, bulk, f.o.b. cars, mines	long-ton.	41.00
export bright, long-term contracts, f.o.b. vessels, Gulf ports	long-ton.	41.00

Domestic bright sulfur prices are $1 per long-ton higher.

TABLE 6.1 (Contd.)

Sulfur, refd., virgin block, dms., mines	100 lbs.	7.05
flour light, bgs., mines	100 lbs.	6.65
lump, bgs., mines	100 lbs.	6.35
rolls, bgs., mines	100 lbs.	6.90
salt block, bgs., mines	100 lbs.	4.55
Sulfur, refd., virgin block, dms., mines	100 lbs.	6.60
Sulfur, rubbermakers, coml., reg. bgs., mines	100 lbs.	3.75
98-100% passing through 320 mesh, bgs., mines	100 lbs.	3.85
Sulfur, refd., bgs., mines	100 lbs.	6.30
SULFURIC ACID		
Sulfuric acid 60° Be., tanks, works.	ton.	26.90
66° Be., tanks, works	ton.	32.30
Sulfuric acid, 98%, tanks, works.	ton.	33.95
Sulfuric acid, 99%, tanks, works.	ton.	34.30
100%, tanks, works	ton.	34.65
Sulfuric acid, (fuming oleum), 20% tanks, works	ton.	36.20
65%. tanks, works	ton.	53.90
Sulfuric acid, tanks, Calif., works. 100% basis	ton.	35.80

TABLE 6.1 (Contd.)

AMMONIUM SULFATE

Ammonium sulfate, large granular.		
bulk, c.l., works	ton.	25.00
bgs., c.l., works	ton.	39.00
standard, commercial, bulk, f.o.b. works	ton.	23.00
bgs., c.l., works	ton.	37.00
tech., bulk., c.l., t.l., works	ton	48.00
bgs., c.l., t.l., works	ton.	52.00

SULFUR DIOXIDE

Sulfur dioxide, liq., coml., cyls., works, frt. equald.	lb.	.11
multi-unit cars, works	lb.	.05-1/2
tanks, works	lb.	.0375

Elemental sulfur is the most marketable form of by-product. It is easy to handle and store. The largest use of sulfur is in the manufacture of sulfuric acid. However, most sulfuric acid is manufactured near the point of use because it is difficult to handle and store and expensive to transport. There is a significant market for ammonium sulfate as a fertilizer but it is a low analysis fertilizer and transportation costs tend to make it non-competitive. Pure liquid sulfur dioxide commands a high price; however, the market for this material is small. The market for hydrogen sulfide is even smaller.

Processes for Recovery of Sulfur Dioxide

In the commercial production of sulfur dioxide, the sulfur dioxide is usually prepared by burning sulfur in air. Since no excess air is required in the products, the highest possible sulfur dioxide content is desired. The stoichiometric combustion of Frasch process sulfur and air results in an SO_2 concentration in the products of about 21% by volume. In practice the concentration of SO_2 ranges from 14% to 20%.

Pyrite, FeS_2, is also used for the preparation of SO_2. With pyrite and air the theoretical maximum CO_2 of the products are about 16% and levels of 10-14% by volume are generally attained.

If the SO_2 in flue gas is concentrated to 10-20% by volume by a physical process, the same processes which are presently used for purification of the SO_2 from commercial sulfur burners could be used to recover sulfur dioxide as a by-product.

Many of the United States plants for the manufacture of liquid sulfur dioxide employ water as the absorbent in various modifications of the old Hanisch-Schroder process. The cooled products of combustion are blown into the bottom of packed towers down which water flows. The exit gas contains from 0.02 - 0.1% sulfur dioxide while the rich absorbent contains 1-2% of SO_2. The cool rich liquor is stripped to about 0.01% SO_2 by heating with low pressure steam. The gaseous mixture of sulfur dioxide and water vapor leaving the stripper is then dried with sulfuric acid and finally compressed and liquified. From 50 to 100 tons of water is required per ton of sulfur dioxide produced. Because of the large amount of water required and the high heat losses in stripping, this process is relatively expensive and is unsuited for the recovery of sulfur dioxide from waste gases.

A number of absorption processes have been developed for the recovery of SO_2 from smelter gases and other waste gases where the concentration of SO_2 is less than 8% by volume(3,4). The Lurgi "Sulfidine Process" uses a 1:1 xylidine-water mixture as the absorbent. Xylidine and water are normally immiscible; but, as sulfur dioxide reacts with the xylidine, some xylidine sulfate, which is water soluble, forms. As the concentration of sulfur dioxide approaches 100 g/l, the mixture becomes homogeneous. Sodium carbonate (soda ash) solution is added to convert the xylidine sulfate formed to sodium sulfate, and the sodium sulfate is stripped off in a column heated to 95 - 100°C. This sulfur dioxide, with some xylidine, is washed to produce pure sulfur dioxide. Some dilute sulfuric acid is used to recover xylidine vapors from the exhaust gases. When a gas containing 8% SO_2 is used, the concentration after scrubbing is reduced to 0.05 - 0.10% sulfur dioxide. With low sulfur dioxide concentrations the process is not economical because of the losses of xylidine. A flow sheet is given in Figure 6.16.

The ASARCO process, developed by the American Smelting and Refining Company, uses dimethylanaline as the absorbent. Particulates are first removed from the gases by means of an electrostatic precipitator. Then the gases are scrubbed with pure dimethylanaline. The waste gases are scrubbed with sodium carbonate to remove traces of sulfur dioxide and dimethylanaline, and also with dilute sulfuric acid to absorb the last traces of dimethylanaline. The sulfur dioxide rich absorbent is passed through a steam distillation column which strips the sulfur dioxide from the liquors. The gases are then passed to a scrubber to remove the dimethylanaline and a drying tower to remove moisture. A flow sheet of this process is given in Figure 6.17.

The COMINCO process, developed by the Consolidated Mining and Smelting Company, uses ammonia. As shown in Figure 6.18, the gases are passed through a two-stage column filled with packing of wooden slats. The absorption is carried out in a dilute ammonium sulfate solution to which ammonia is added. The sulfur dioxide is stripped from the ammonium sulfite by adding concentrated (93 per cent) sulfuric acid, producing sulfur dioxide and ammonium sulfate.

Processes for the Recovery of Sulfuric Acid

There are two well known processes for manufacturing sulfuric acid which are applicable to sulfur burner products, roaster gas or smelter gas(5,6,7). The older process is the chamber process which is shown in Figure 6·19. A more recent development is the contact process which is shown in Figure 6·20. The contact process uses either platinum or vanadium catalysts to convert the SO_2 to SO_3. Details of these processes are widely available in the literature(5,6,7). In sulfuric acid production the percent excess air for the sulfur burner is adjusted to give about the same concentration of SO_2 and air which is in the range of 8-11%.

Processes for the Recovery of Ammonium Sulfate

Production of ammonium sulfate can be attained by injecting ammonia into a stream of gas containing H_2SO_4 at a suitable temperature level. Therefore, a process for producing ammonium sulfate can be a modified sulfuric acid process. The Kiyoura- T.I.T. process(8) is a modified catalytic oxidation process for application to low concentration streams, i.e., flue gas. Processes which produce ammonia sulfate in combination with other sulfur compounds are discussed in other sections of this survey.

Processes for the Recovery of H_2S

Sulfur dioxide can be reacted with hydrogen with the assistance of a catalyst to form a mixture of sulfur dioxide, hydrogen sulfide and sulfur as follows:(9)

$$2SO_2 + 4H_2 = S_2 + 4H_2O$$

$$2H_2 + S_2 = 2H_2S$$

Any water vapor present in the gas stream plus the water formed above will react with free sulfur

$$3/2S_2 + 2H_2O = 2H_2S + SO_2$$

Nickel or nickel sulfide are effective catalysts at temperatures of 400° to 450°C. Gel catalysts consisting of ferric and aluminum oxides and pretreated with hydrogen sulfide to convert the iron oxide to sulfide are particularly valuable for reducing sulfur dioxide with hydrogen. These catalysts may be used at temperatures as low as 325°C. For higher temperatures less active catalysts, such as iron sulfide and various aluminas, can be used.

Because of the availability of hydrogen sulfide from other sources, no commercial applications of this process appear to have been made.

Processes for the Recovery of Elemental Sulfur

A two-stage process for converting sulfur dioxide to sulfur has been proposed(9). In the first stage, part of the gas stream containing sulfur dioxide would be mixed with hydrogen and passed through a catalyst bed to convert the SO_2 to H_2S as described in the section on H_2S recovery. In the second stage the balance of the stream would be mixed with the first part and the mixture stream would be passed over activated alumina at 100 - 200°C to form elemental sulfur. This is a variation of the Claus process for converting H_2S to sulfur.

Sulfur dioxide can be reduced to elemental sulfur by use of carbon monoxide, methane or carbon(9). The reaction, $2SO_2 + 4CO = 4CO_2 + S_2$, proceeds very slowly without a catalyst even at temperatures as high as 800°C. At this temperature nearly any hot surface will be effective, and there are a number of materials which are capable of catalyzing the reaction at lower temperatures.

The rate of reaction between sulfur dioxide and methane is substantially smaller than that with carbon monoxide so reduction with methane requires higher temperature. In the reduction process carbonyl sulfide is first formed along with the elemental sulfur

$$2CH_4 + 3SO_2 = 2COS + 1/2S_2 + 4H_2O$$

The carbonyl sulfide decomposes

$$2COS = S_2 + 2CO$$

$$2COS = CS_2 + CO_2$$

The carbon monoxide thus formed reduces some of the sulfur dioxide

$$2SO_2 + 4CO = 4CO_2 + S_2$$

Moisture free sulfur dioxide reacts with carbon in the temperature range of 500° to 1200°C to form a mixture of carbon disulfide, carbonyl sulfide, sulfur, carbon monoxide, and carbon dioxide. The composition of the product varies with the temperature of the reaction and the type of carbon used. If moisture is present, hydrogen sulfide is also produced. In the reduction of sulfur dioxide by carbon, the simultaneous reduction of carbon dioxide occurs as follows

$$SO_2 + C = CO_2 + 1/2S_2$$

$$CO_2 + C = 2CO$$

Comparison of the kinetics of these two reactions with experimental results indicates that a third reaction takes place, i.e.,

$$SO_2 + 2CO = 2CO_2 + 1/2S_2$$

In laboratory studies dry sulfur dioxide was passed through calcined metallurgical coke. Almost complete reduction of sulfur dioxide to sulfur was obtained in the temperature range of 850 to 1200°C.

There are several commercial processes which utilize the above reactions either alone or in combination(9). The Bolidens process was developed in Sweden for converting the sulfur dioxide from a copper smelter gas containing 5 percent sulfur dioxide. In this process a reducing gas is prepared by a method similar to the production of producer gas. A portion of the smelter gas is diluted with air and blown through red hot coke. The remainder of the raw gas is added and the total stream is passed over a catalyst to obtain elemental sulfur. The Bolidens process was operated for several years prior to 1943, but was discontinued when the price of coke became uneconomic.

The Trail process first reduces the sulfur dioxide by coke and then uses carbon monoxide reduction in the final cleanup. The exit gas from the coke reduction furnace is cooled to about 500°C then passed through an electrostatic precipitator to remove the dust which would foul the catalyst. Alumina catalysts are used to convert the SO_2 and intermediates to S_2. The last step in the process consists of condensing the sulfur vapor and removing the mist by electrostatic or other means.

The ASARCO process uses natural gas to reduce the sulfur dioxide in smelter gases. Figure 6-21 shows a simplified flow sheet of the process. The process is applicable to the treatment of gases containing 5 to 8% sulfur dioxide by volume. A 5 ton/day pilot plant has been operated which produced a high purity (99.99 percent) sulfur.

The alkalized alumina process(10) being developed by the U.S. Bureau of Mines, for removal of sulfur dioxide from flue gas could be applied to the recovery of sulfur dioxide from streams concentrated by physical processes. In this process (see Figure 6-22) the sulfur dioxide bearing gas is fed to an absorber where the SO_2 and SO_3 are absorbed by alkalized alumina spheres, 1/16 inch in diameter, in free fall. Absorption will occur over a temperature range of 265 to 625°F. A recycle to fresh solids feed ratio of 10 is used. The spent absorbent is transported to the regenerator, heated to 1200°F, and then treated with producer gas.

The absorbed sulfur oxides react with the hydrogen in the producer gas to give H_2S. This H_2S plus that originally in the producer gas are then converted to elemental sulfur in a Claus unit.

There are a number of other processes which might be applied to the recovery of by-product sulfur from gas streams that have been concentrated by physical processes. Examples of these are the Fulham-Simon-Carves ammoniacal liquid process and the regenerative sodium sulfite process(11).

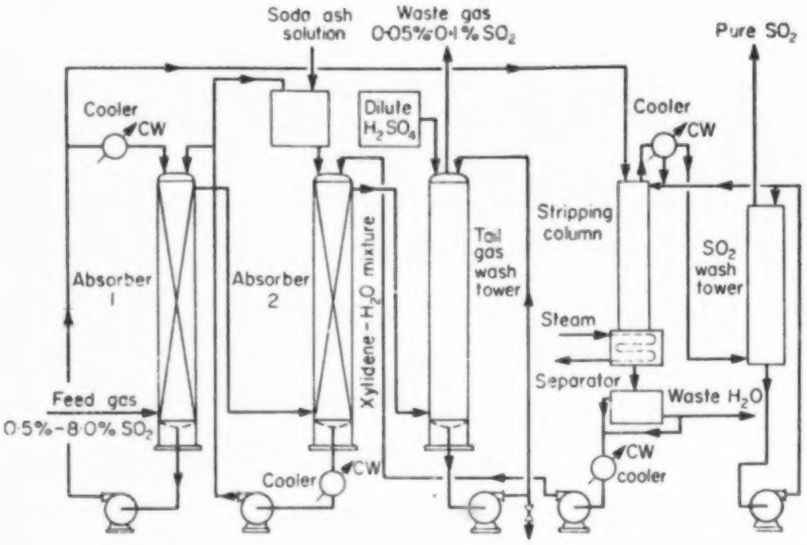
Soda ash solution
Waste gas 0·05%–0·1% SO_2
Pure SO_2
Cooler
CW
Dilute H_2SO_4
Cooler
CW
Stripping column
Absorber 1
Absorber 2
Xylidene - H_2O mixture
Tail gas wash tower
SO_2 wash tower
Steam
Separator
Feed gas 0·5%–8·0% SO_2
Waste H_2O
Cooler
CW
CW cooler

FIG. 6.16. Flow sheet of sulphidine process: absorption of sulphur dioxide in xylidine-water mixtures.

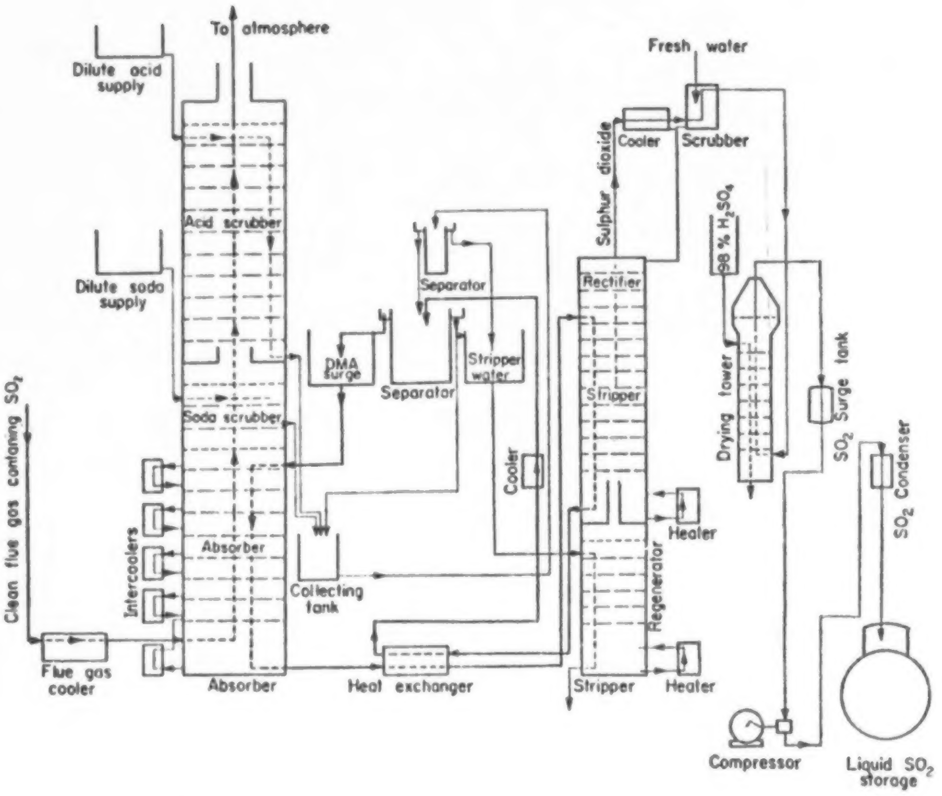
To atmosphere
Dilute acid supply
Fresh water
Cooler
Scrubber
Sulphur dioxide
Acid scrubber
98 % H_2SO_4
Dilute soda supply
Separator
Rectifier
DMA surge
Separator
Stripper water
Stripper
Drying tower
SO_2 Surge tank
Clean flue gas containing SO_2
Soda scrubber
SO_2 Condenser
Cooler
Heater
Intercoolers
Absorber
Collecting tank
Regenerator
Flue gas cooler
Absorber
Heat exchanger
Stripper
Heater
Compressor
Liquid SO_2 storage

FIG. 6.17. Flow sheet of ASARCO process: absorption of sulphur dioxide in dimethylaniline solution.

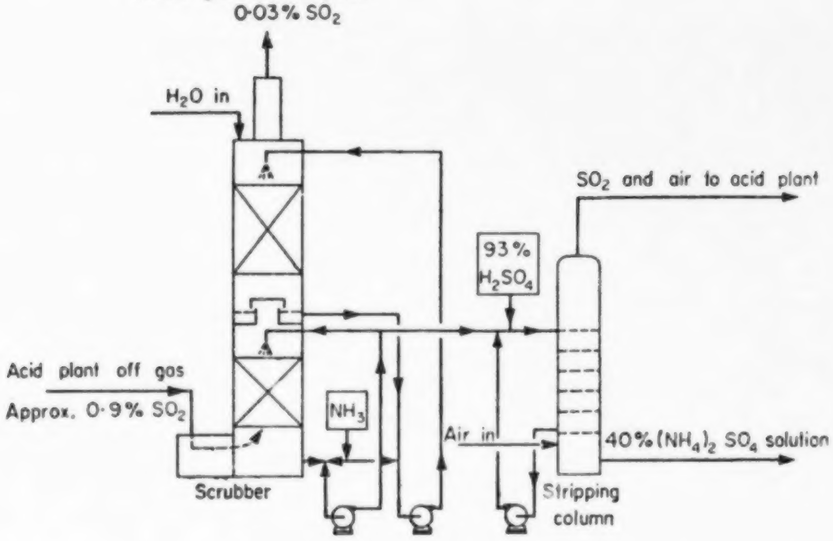
Waste gas to atmosphere
0·03% SO_2
H_2O in
SO_2 and air to acid plant
93% H_2SO_4
Acid plant off gas
Approx. 0·9% SO_2
NH_3
Air in
40% $(NH_4)_2SO_4$ solution
Scrubber
Stripping column

FIG. 6·18. Flow sheet of COMINCO process: absorption of sulphur dioxide in ammonia solution.

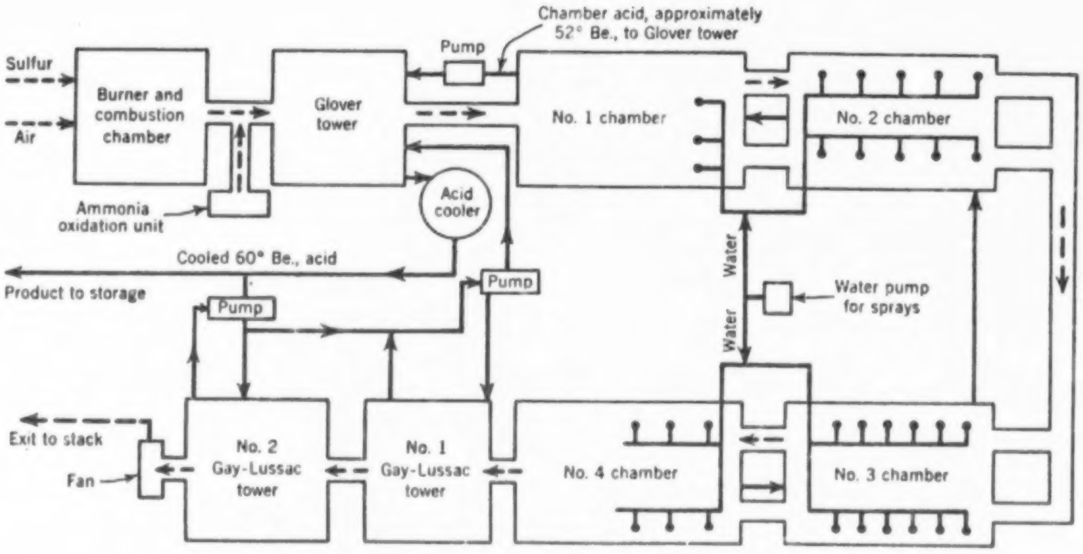
Chamber acid, approximately 52° Be., to Glover tower
Pump
Sulfur
Air
Burner and combustion chamber
Glover tower
No. 1 chamber
No. 2 chamber
Ammonia oxidation unit
Acid cooler
Cooled 60° Be., acid
Product to storage
Pump
Pump
Water
Water
Water pump for sprays
Exit to stack
Fan
No. 2 Gay-Lussac tower
No. 1 Gay-Lussac tower
No. 4 chamber
No. 3 chamber

FIG. 6. 19. Original chamber process.

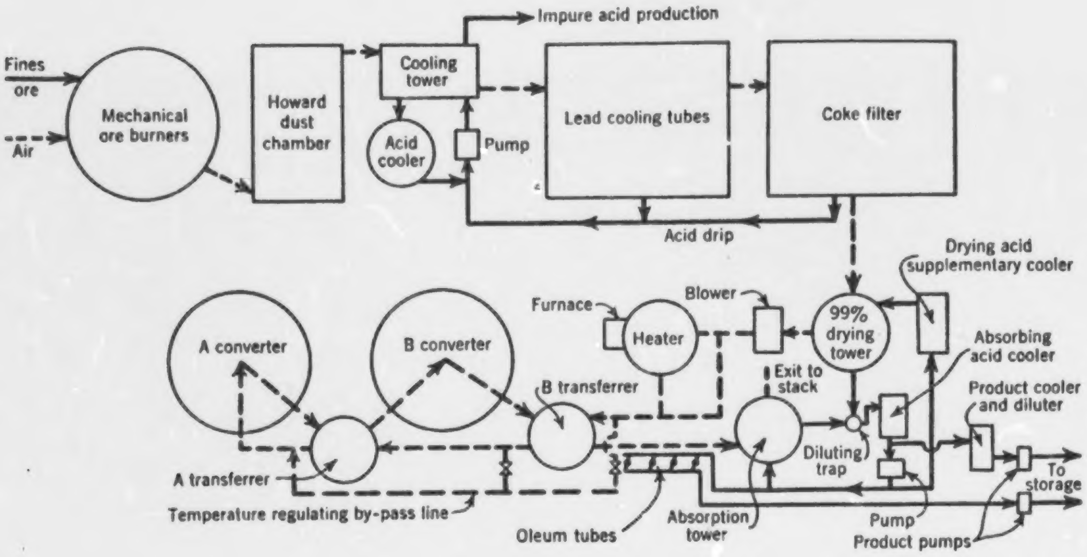
Impure acid production
Fines ore
Air
Mechanical ore burners
Howard dust chamber
Cooling tower
Acid cooler
Pump
Lead cooling tubes
Coke filter
Acid drip
Drying acid supplementary cooler
Blower
Furnace
Heater
99% drying tower
A converter
B converter
B transferrer
Exit to stack
Absorbing acid cooler
Product cooler and diluter
Diluting trap
To storage
A transferrer
Temperature regulating by-pass line
Oleum tubes
Absorption tower
Pump
Product pumps

Figure 6.20 - American Type Badische Contact Unit

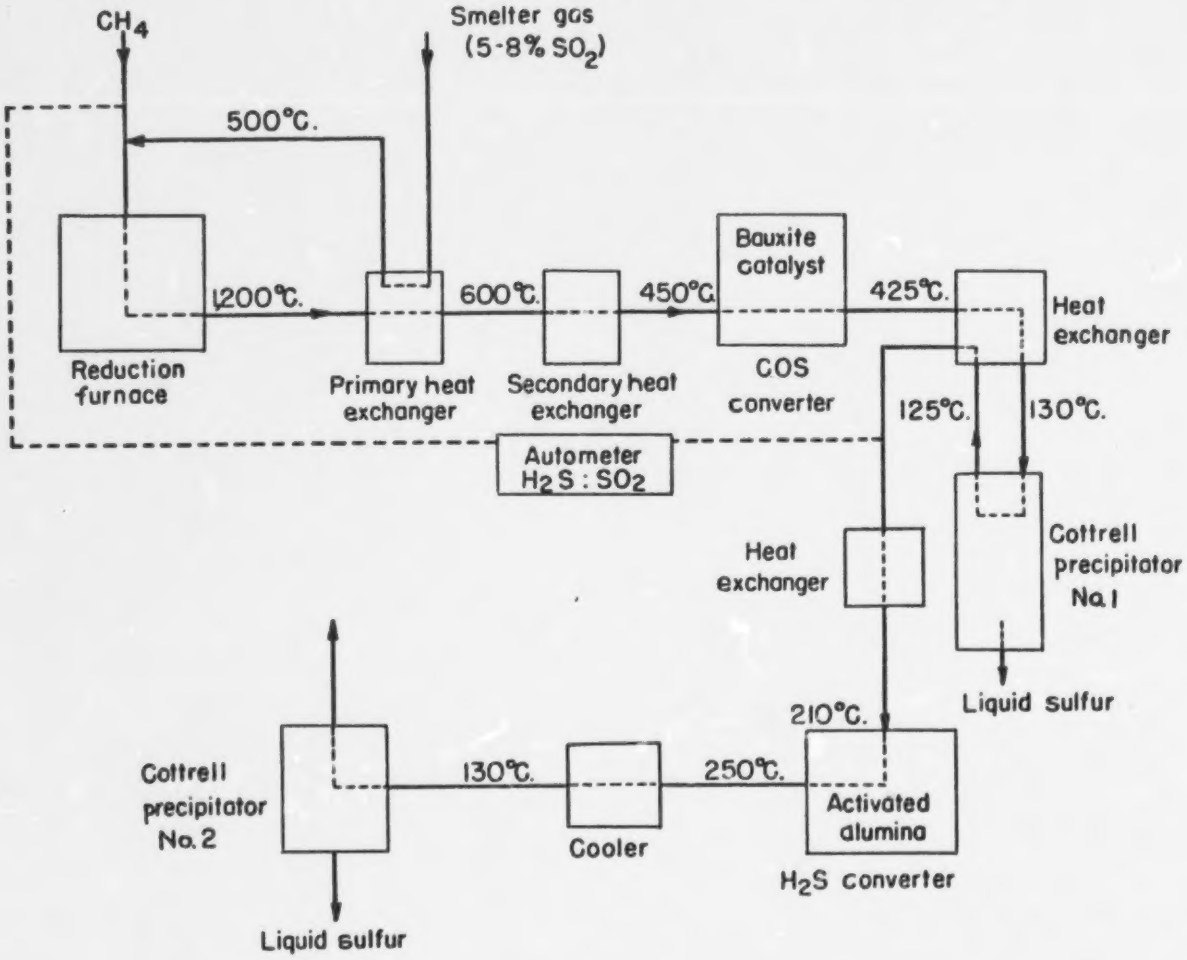
CH4
Smelter gas (5-8% SO2)
500°C.
1200°C.
600°C.
450°C.
Bauxite catalyst
425°C.
Heat exchanger
Reduction furnace
Primary heat exchanger
Secondary heat exchanger
COS converter
125°C.
130°C.
Autometer H2S : SO2
Heat exchanger
Cottrell precipitator No. 1
Liquid sulfur
210°C.
Cottrell precipitator No. 2
130°C.
250°C.
Cooler
Activated alumina
H2S converter
Liquid sulfur

Figure 6.21 - Simplified Flow Diagram of Asarco Process

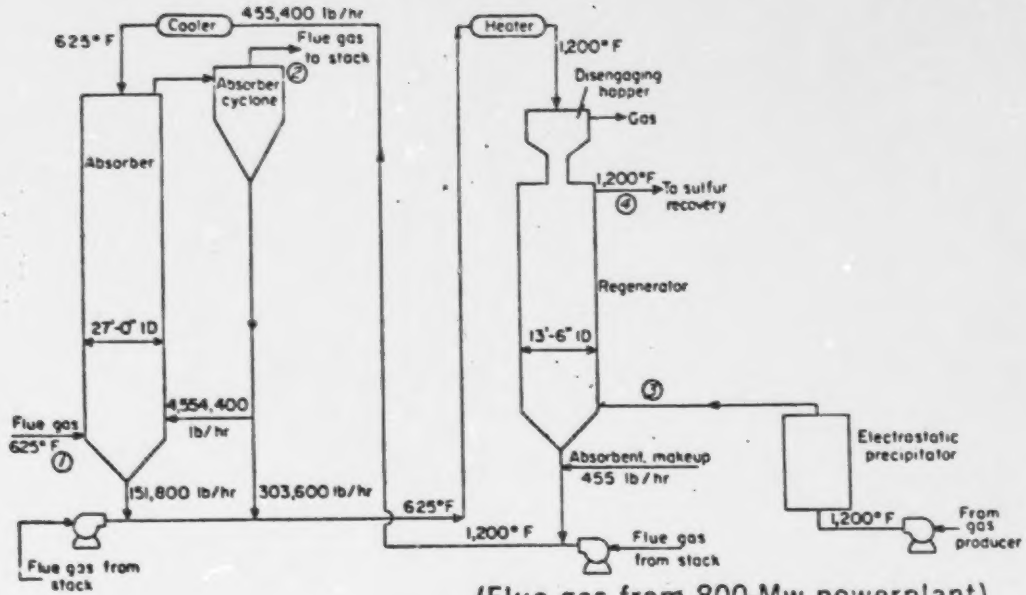
625° F
Cooler
455,400 lb/hr
Flue gas to stack
②
Absorber cyclone
Absorber
27'-0" ID
4,554,400 lb/hr
Flue gas 625° F
①
151,800 lb/hr
303,600 lb/hr
Flue gas from stack
625°F
Heater
1,200° F
Disengaging hopper
Gas
1,200°F
To sulfur recovery
④
Regenerator
13'-6" ID
③
Electrostatic precipitator
Absorbent. makeup 455 lb/hr
1,200° F
Flue gas from stack
1,200° F
From gas producer

(Flue gas from 800-Mw powerplant)
Amounts of solids flow are total for 6 units.

Figure 6.22 - Alkalized Alumina Process Flowsheet

REFERENCES

1. Oil, Paint and Drug Reporter, August 12, 1968.
2. Kirk-Othmer, "Encyclopedia of Chemical Technology - 1st Ed.", Vol. 13, Interscience Publishers, New York, 1954, p. 458.
3. Strauss, W., "Industrial Gas Cleaning", Pergamon Press, New York, 1966.
4. Kohl and Riesenfeld, "Gas Purification", McGraw-Hill Book Co., New York, 1960.
5. Kirk-Othmer, "Encyclopedia of Chemical Technology - 1st Ed.", Vol. 13, Interscience Publishers, New York, 1954, p. 472.
6. Fairlie, Andrew M., "Sulfuric Acid Manufacture", Reinhold Publishing Co., New York, 1936.
7. Drucker, Werner W. and West, James R., "The Manufacture of Sulfuric Acid", Reinhold Publishing Co., New York, 1959.
8. Kiyoura, R., "Studies on the Removal of Sulfur Dioxide from Hot Flue Gases to Prevent Air Pollution", J. of A.P.C.A., Vol. 16, No. 9, September 1966, pp. 488-9.
9. Bienstock, Brunn, Murphy and Benson, "Sulfur Dioxide - Its Chemistry and Removal from Industrial Waste Gases", Bureau of Mines Information Circular 7836, 1958.
10. Bienstock, D., Field, J.H., and Myers, J.G., "Removal of Sulfur Oxide from Flue Gas with Alkalized Alumina at Elevated Temperatures", J. Eng. for Power, Trans. ASME, Series A, Vol. 86, No. 3, pp. 353-360, (1964).
11. Field, Brunn, Hayner and Benson, "Cost Estimates of Liquid Scrubbing Processes", U.S.B.M. R. of I. 5469, 1959.

APPENDIX 6.7

OAK RIDGE NATIONAL LABORATORY
OPERATED BY
UNION CARBIDE CORPORATION
NUCLEAR DIVISION
UNION CARBIDE
POST OFFICE BOX X
OAK RIDGE, TENNESSEE 37830

September 27, 1968

Mr. J. R. Hamm
Westinghouse Electric Corporation
Research and Development Center
Churchill Boro.
Pittsburgh, Pennsylvania 15235

Dear Mr. Hamm:

This is in reply to your letter of August 14 requesting design and cost data on the separation of SO_2 from flue gases by use of permselective membranes and porous barriers. I was on vacation when your letter came, and I apologize for not being able to give you an earlier reply.

The cascade design and cost calculations were made by Mr. Sam Blumkin of the Oak Ridge Gaseous Diffusion Plant using computer programs that he developed for treating similar stagewise operations. The computations were based on a dry flue gas composition derived from your letter of June 24 to Dr. E. Von Halle. This composition is:

N_2	80.8 vol %
CO_2	15.9
O_2	3.0
SO_2	0.3

The target of the calculation was to reduce the SO_2 concentration in the treated flue gas to a value in the range of 300 ppm and to concentrate the SO_2 in the non-disposable stream to about 50 vol %. The results of the calculations are shown in Table 1 for both a permselective membrane plant and a barrier plant to treat 1,000,000 scfm of flue gas. This volume of flue gas is about that produced in a 600 Mw(e) power plant.

The results clearly indicate that neither of these plants is economically suitable for removing SO_2 from such large volumes of flue gas. In fact, the $80-million cost of the membrane plant, which is considerably more favorable than the barrier plant, is probably equivalent to the capital cost of the remainder of the power station. Chemical methods of removing SO_2 should be significantly more economical, and it is unlikely that sufficient improvements can be made in either of the above physical separation methods to make either one competitive with chemical methods.

In regard to your later question about the effect of reducing the SO_2 enrichment target from 50 to 20%, our intuitive qualitative answer is that the cost reduction would be relatively small and insufficient to make either process economically competitive. However, we will examine this question more closely, and furnish you with a quantitative result at a later date.

I hope that these data are helpful in your evaluation of physical separations methods. Please communicate with us if we can be of further help.

Very truly yours,

William L. Carter

W. L. Carter
Process Design Section
Chemical Technology Division

WLC:ram

Attachment

cc: D. E. Ferguson
W. E. Unger
S. Blumkin
S. Levin
E. Von Halle
R. H. Rainey
R. E. Blanco
J. T. Long

Table 1. Design and Cost Data for the Separation of SO_2 from Flue Gas Using Permselective Membranes and Porous Barriers

	Permselective Membrane Plant	Porous Barrier Plant
Flue gas feed rate, scfm	1,000,000	1,000,000
SO_2 Concentration		
Feed, ppm by vol	3,000	3,000
Cleaned gas, ppm by vol	120*	340*
Enriched stream, mole %	53*	49*
Design Data		
Number of stages	5	53
Membrane or barrier area, ft^2	45,000,000	94,000,000
Total interstage flow, scfm	750,000	106,000,000
Power requirement, Mw	321	12,300
Compression ratio	11	5
Δ P across element, atm	10	0.8
Area of largest stage, ft^2	10,000,000	5,500,000
Power for largest stage, hp	87,000	1,000,000
Flow in largest stage, scfm	350,000	6,000,000
Enriched stream rate, scfm	5,400	5,400
Estimated Cost		
Capital, $	80,000,000	390,000,000
Power, $/year	13,000,000	490,000,000

*These values were obtained with the concentrations of CO_2 and O_2 in the flue gas inadvertently interchanged. The correct values for the SO_2 concentrations for the membrane plant should be 370 ppm in the stripped stream and 49 mole % for the enriched stream. The net effect of this error, therefore, is that the table above describes cascades and costs for a lesser separation job than indicated by it.

APPENDIX 6.8

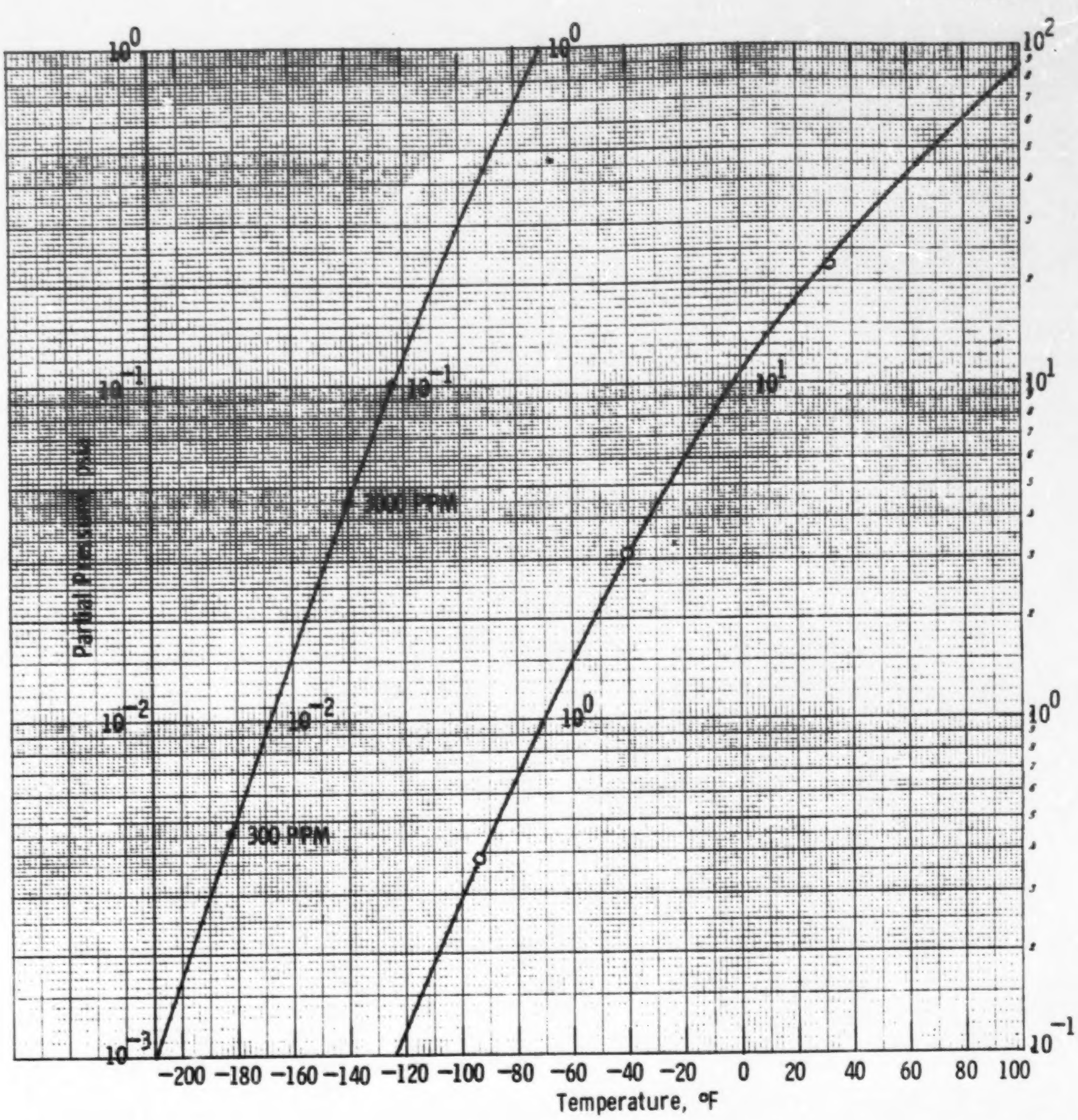

FIG. 6-23 - Saturation Pr. α Temperature For SO_2
From International Critical Tables

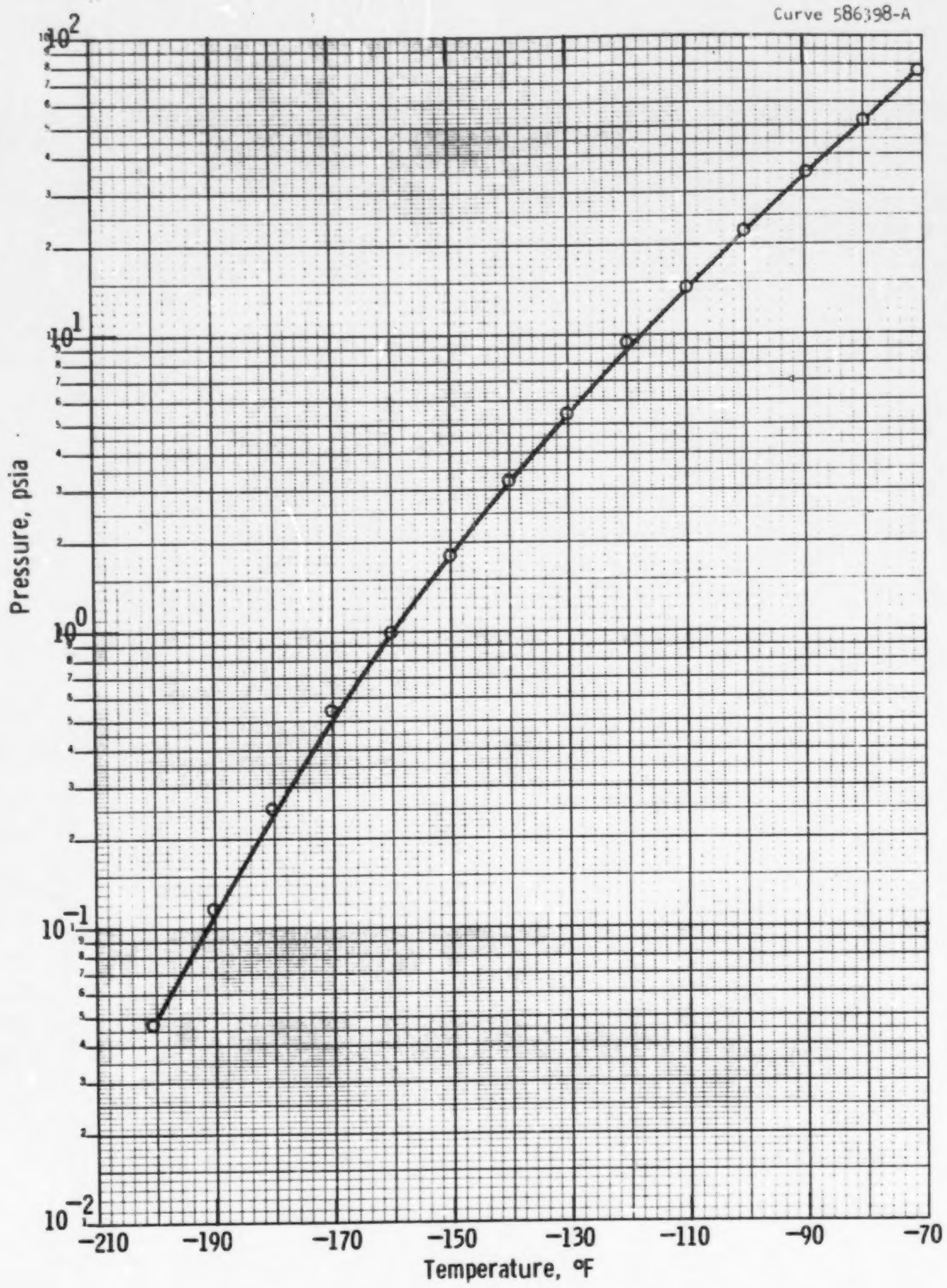

FIG. 6-24 - Saturation Pr. α Temperature For CO_2

From Canjar, L.N. and Manning, F.S.
"Thermodynamic Properties and
Reduced Correlations for Gases",
Houston, Texas, Gulf 1967